The Biogeochemical Cycling of Dissolved Organic Carbon in the Iberian Margin Upwelling System (NE Atlantic Ocean)

by

GEORGINA SPYRES

A thesis submitted to the University of Plymouth in partial fulfilment for the degree of

DOCTOR OF PHILOSOPHY

Department of Environmental Sciences
Faculty of Science

In collaboration with
Plymouth Marine Laboratory

December 2001

The Biogeochemical Cycling of Dissolved Organic Carbon in the Iberian Margin Upwelling System (NE Atlantic Ocean).

Georgina Spyres

Abstract

Dissolved organic carbon (DOC) is the quantitatively most important organic carbon reservoir in the world's oceans and its determination at ocean margins, where the exchange of terrestrial and oceanic organic matter occurs, is important for estimating cross-slope fluxes to deep waters. With the increased accuracy and precision (~1%) of analytical methodologies, small changes in the DOC pool can be detected (i.e. 1-2μM-C).

This study investigated the biogeochemical cycling of DOC at the Iberian Margin upwelling system (42-43°N, ~9–10°W), where contrasting seasonal hydrologic phenomena occur (e.g. summer upwelling, winter poleward current). Spatial and temporal DOC distributions were determined using high temperature catalytic oxidation (HTCO) techniques. DOC concentrations generally decreased with distance from the continental shelf and with increasing depth, although localised accumulation was observed in surface as well as in deep waters with a mean excess of up to 16 μM-C over background concentrations (57 μM-C). DOC concentrations in surface waters were closely associated with bacterial productivity and dissolved organic nitrogen (DON) production was facilitated by photosynthetic extra-cellular release from phytoplankton. There was no marked difference in DOC concentrations between the summer and winter seasons due to increased mineralization during the summer and lateral inputs during the winter.

DOC production exceeded removal rates in summer upwelled surface waters following enhanced biological activity, in the winter surface poleward current and in deep waters that contained high levels of suspended particulates. DOC from terrestrial run-off was recycled rapidly at the coast before it could be exported to the shelf. Cross-slope export of accumulated DOC was generally hindered by the net on-shore velocity component during both winter and summer seasons and by the presence of water masses travelling along-slope.

List of Contents

List of Figures

Appendix 1

Appendix 2

Appendix 3

Appendix 4

List of Tables

Acknowledgements

I would like to thank my directors of study Dr. Malcolm Nimmo and Dr. Axel E.J. Miller. I was very lucky to be supervised by Axel and Malcolm. Young-spirited and enthusiastic about marine chemistry, with strong dedication to education, and yielding sound advice and warmth they were always there for me. I hope to be in personal and scientific correspondence with them for many years to come. Many thanks to Dr. Eric P. Achterberg for the insightful discussions on HTCO techniques and Professor Paul Worsfold for advice on analytical issues.

I am grateful to Professor R. Fauzi C. Mantoura who showed great interest in my work and provided me with many other research opportunities such as the CYCLOPS project. "Obrigado" to Paulo Gardolinski who taught me to use the nutrient autoanalyser among other things. All the staff at the Plymouth Marine Laboratory were very supportive and made me feel a part of the team. This study was a part of the EU MAST Ocean Margin Exchange II-II programme (contract no: MAS3-CT07-0076) and was partly funded by the University of Plymouth and the Plymouth Marine Laboratory.

I could never have undertaken such a research project if my parents had not supported me. Completing my thesis is not an issue of making them proud. Nor are achievements a requisite for love. Whatever I may do, my parents keep things in perspective: health and happiness comes first.

Αριστειδη και Μαριανθη Σπυρη,
το Τζωρτζινακι σας εγινε δοκτορ.
Σας ευχαριστω απο τα βαθη της καρδιας μου!

Author's Declaration

At no time during the registration for the degree of Doctor of Philosophy has the author been registered for any other University award.

Publications

Sharp J.H., K.R. Rinker, K.B. Savidge, T.W. Walsh, J. Merriam, N. Kaumeyer, M.D. Doval, K. Johnson, G. Cauwet, N. Morley, C. Hopkinson, K. Nagel, **G. Spyres** et al., (subm.) A preliminary methods comparison for measurement of dissolved organic nitrogen in seawater. Marine Chemistry.

Thingstad F., N. Kress, B. Herut, T. Zohary, P. Pitta, S. Psarra, T. Polychronaki, **G. Spyres**, F. Mantoura, T. Tanaka, F. Rassoulzadegan, M. Krom (2001) Mixed indications of mineral nutrient limitation in a microcosm experiment using eastern Mediterranean surface water. CIESM 2001 proceedings.

Spyres G., M. Nimmo, A.E.J. Miller, P.J. Worsfold and E.P. Achterberg (2000) Determination of dissolved organic carbon in seawater using high temperature catalytic oxidation techniques. trends in analytical chemistry (TrAC), vol. 19, no. 8, 498-506

Spyres, G. and Miller, A.E.J. (2000). Final Report: The Cycling of Dissolved Organic Matter (DOM) at the Iberian Margin, October, 2000, EU MAST OMEX grant no. MAS3-CT97-0076, 13 pp.

Spyres G. (2000) The Determination of DOC and DON using high temperature catalytic oxidation. In: DECOS/OMEX II, Cruise No.43, 25.Nov.1998 – 14.Jan.1999, Meteor-Berichte by H.-U. Schminke and G. Graf. Universitat Hamburg, 00-2, 99pp.

Spyres G., and A.E.J. Miller (1998) Determination of dissolved organic carbon and nitrogen. In: RRS Charles Darwin – Cruise CD110B Iberian Shelf Seas by A.E.J. Miller, 61p. Plymouth Marine Laboratory – N.E.R.C. Publications.

Presentations and Conferences Attended

12-16th Feb.2001: American Society for Limnology and Oceanography (ASLO) Aquatic Sciences Meeting, New Mexico, USA. Carbon Fluxes at Ocean and Large Lake Margins (oral) "*Dynamics of DOM in the Iberian upwelling system-NE Atlantic Ocean Margin*" by Spyres G., A.E.J. Miller and M. Nimmo

14-16th Jan.2001: Cycling of Phosphorus in the Mediterranean (CYCLOPS) 2nd workshop at Institute of Marine Biology of Crete, Heraclion, Greece (oral) "*Results from the CYCLOPS microcosm experiment: DOC and DON*" by Spyres G. and F. Mantoura

8-13th May.2000: Ocean Margin Exchange Programme (OMEX) II-II Final Workshop 'The Carbon Cycle at the Iberian Margin' in conjunction with the 32nd International Liege Colloquium on Ocean Hydrodynamics 'Exchange Processes at the Ocean Margins' Liege, Belgium. (oral) "*Seasonal and spatial distribution of DOM at the Iberian Margin*" by Spyres G., A.E.J. Miller and M. Nimmo (recipient of a Liege Young Scientist grant)

24-29th Apr.2000: European Geophysical Society (EGS) , Nice, France 2000 "The dynamics of DOM in marine systems" (attended & gave an announcement on the new HTCO website)

19th Apr.2000: Earth System Science Presentations, Plymouth Marine Laboratory, U.K. (oral) "*The role of the ocean in global carbon fluxes*" by Spyres, G.

21st Jan.2000: Marine and Fluid Interactions Group, Univ. of Plymouth, U.K. (oral) "*A seasonal comparison of DOC at the Iberian margin*" by Spyres G., A.E.J. Miller and M. Nimmo

30th Sept. – 1st Oct.1999: New Directions in Marine Science, Dunstaffnage Marine Laboratory, Oban, U.K. (oral) "*A seasonal comparison of DOC vertical distributions at the Iberian margin*" by Spyres G., A.E.J. Miller and M. Nimmo

9-10th Sept.1999: Progress in Chemical Oceanography (PICO), Univ. of Plymouth, U.K. (poster) "*Seasonal DOC vertical distributions at the Iberian Margin*" by Spyres G., A.E.J. Miller and M. Nimmo

25-27th Apr.1999: OMEX II-II Annual Workshop 'The Carbon Cycle at the Iberian Margin', Plymouth, U.K. 1.(poster) "*Seasonal DOC vertical distributions at the Iberian Margin*" by Spyres G., A.E.J. Miller and M. Nimmo 2. (oral) "*Preliminary DOC/ N results from the OMEX II-II project*" by Spyres G.

23-24th Feb.1999: Postgraduate Research in Marine Sciences (PRMES) 1999, London, U.K. (oral) "*DOC in an upwelling region of the Iberian coast*" by Spyres G., A.E.J. Miller and M. Nimmo

Signature 

The biogeochemical cycling of dissolved organic carbon in the Iberian Margin upwelling system (NE Atlantic Ocean)

by

Georgina Spyres

Chapter 1

1. INTRODUCTION

1.1 The Global Carbon Cycle

The anthropogenically-induced increase of greenhouse gases (e.g. CO_2) in the atmosphere has triggered what is now widely recognised as the "global warming" effect. Due to the adverse climatic conditions and potential social problems associated with global warming, scientific research in the past decade has increasingly been focused on the global carbon cycle and the quantification of net fluxes of atmospheric CO_2 at various global interfaces (e.g. atmosphere-ocean). However, there are discrepancies in the estimates of carbon reservoirs and fluxes between these reservoirs (Figure 1) (Siegenthaler & Sarmiento, 1993 and references therein; Williams et al., 1993). Further studies of global carbon cycling are necessary, especially for the identification and accurate quantification of net carbon sinks.

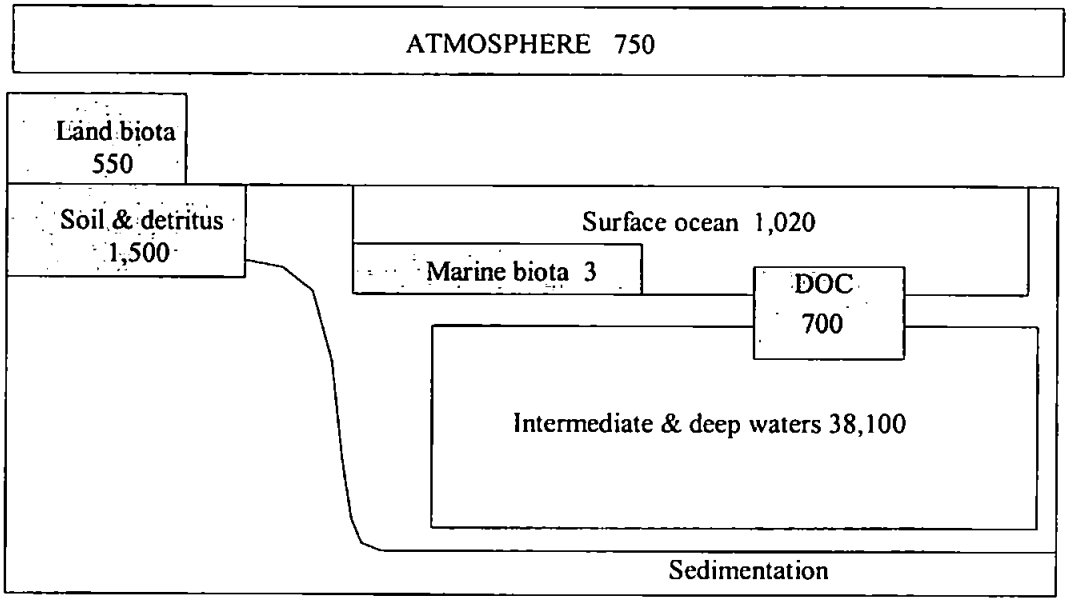

Figure 1. The global carbon pools (Gt-C). After Siegenthaler & Sarmiento, 1993. Note: shaded boxes indicative of organic carbon reservoirs.

The atmospheric pool of CO_2 is estimated to hold approximately 660Gt-C (Gt = 10^{15} g) with more recent estimates being in the order of 750 Gt-C (Figure 1), compared to the estimated ~600 Gt-C in pre-industrial times (Siegenthaler & Sarmiento, 1993 and references therein).

Global carbon reservoirs of significance include the land biota, soil humus, surface marine sediments and the ocean (Hedges, 1992). The quantitatively most important carbon reservoir at the Earth's surface is the dissolved inorganic carbon (DIC) pool in the ocean ("Intermediate and Deep water" reservoir in Figure 1), estimated to hold approximately 38,000 Gt-C (Siegenthaler and Sarmiento, 1993).

1.2 The Role of the Oceans

The ocean is considered a significant sink for anthropogenically-produced atmospheric CO_2, taking up approximately ~2.0±0.6Gt-C.yr^{-1}. The dynamics of uptake are mainly determined by the rate of transport of surface water that is rich in CO_2 to depth (Siegenthaler & Sarmiento, 1993). The autotrophic biota at the surface of the ocean play an important role in the marine carbon cycle by fixing carbon from dissolved CO_2 *via* photosynthesis and consequently producing organic matter (OM).

The OM produced by the photosynthesising organisms can be in an assimilated form as particulate biomass (i.e. particulate organic matter, POM) and/or released as dissolved exudates (i.e. dissolved organic matter, DOM). The separation between particulate and dissolved matter is determined practically, according to the nominal cut-off size of the filtration system used (i.e. typically 0.7 - 0.2μm). The operational classification of aquatic carbon species is shown in Figure 2.

Once produced, OM is subject to a series of complex biogeochemical and hydrological processes which collectively act to either transport OM to the deep ocean for burial in the sediments and/or remineralise and recycle OM back into the upper ocean *via* advective mixing and upwelling processes. A simplified schematic of the biogeochemical cycling of OM in the ocean is presented in Figure 3.

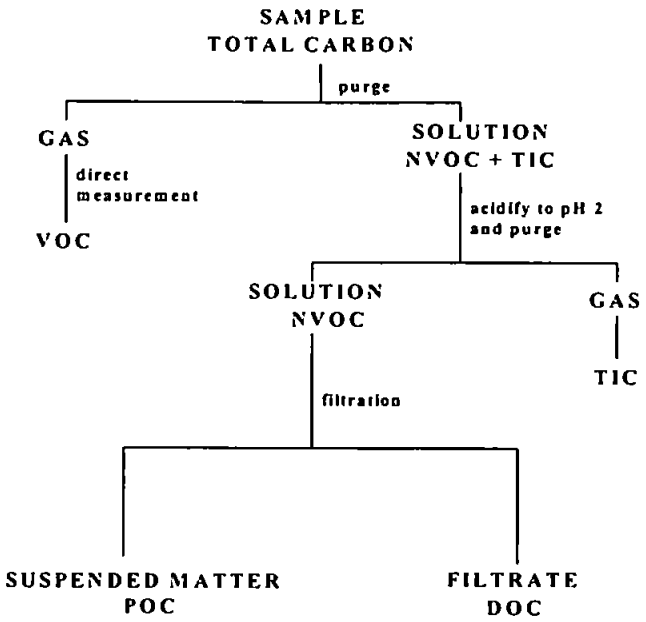

Figure 2. An operational classification of aquatic carbon species. After Robards, et al., 1994. Note: VOC- volatile organic carbon, NVOC- non-volatile organic carbon, TIC- total inorganic carbon, POC- particulate organic carbon, DOC- dissolved organic carbon.

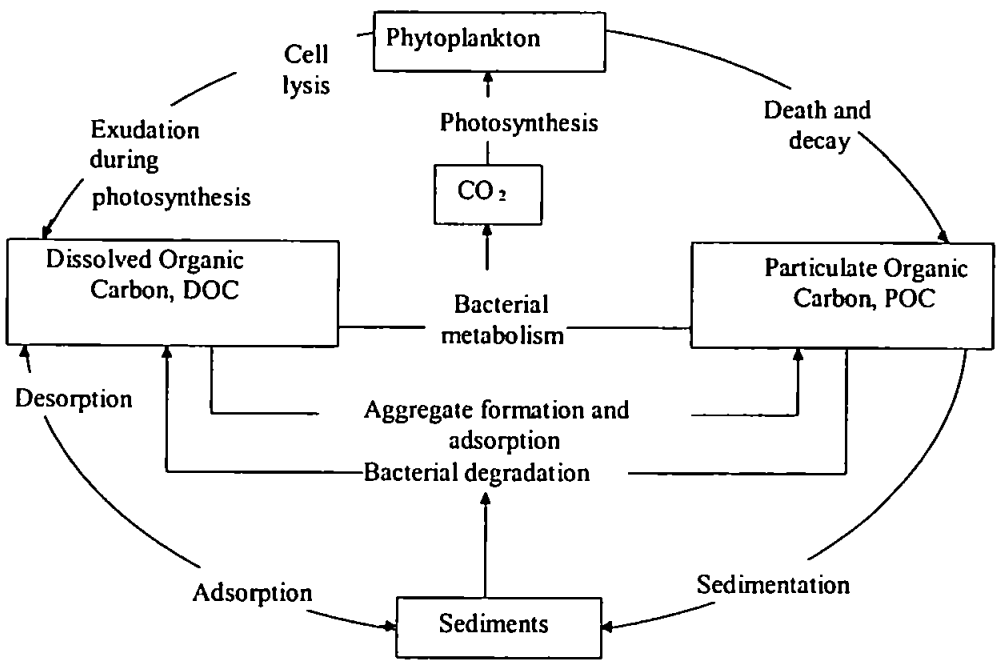

Figure 3. The organic carbon cycle in the marine environment. After Chester, 1990.

Recent estimates of global ocean primary production (i.e. the amount of OM synthesised as phytoplankton biomass from inorganic carbon; Lalli and Parsons, 1993) typically range from 45 to 51 Gt-C.yr^{-1} (Longhurst et al., 1995 and references therein). POC export from the surface ocean, as estimated from studies of sinking particulate matter, is typically <5-10% of the primary production in open ocean areas (Buesseler, 1998a and references therein). Higher values (e.g. 37%) have been reported for near shore and shelf waters (Fernandez et al., 1995; Buesseler et al., 1998b; Hall et al., 2000) (Table 1). The export of carbon from the upper ocean to the deep mainly occurs *via* the sinking, mixing and advection of OM products from senescing (i.e. lysing and decaying) biomass (Shaffer, 1996 and references therein). On a localised scale, phytoplankton biomass is mainly subject to dissolution (e.g. hydrolytic process) (Smith et al., 1992) and remineralisation transforming it to DOM and inorganic nutrients (Azam et al., 1983); a very small amount of the sinking flux is eventually buried in the deep ocean sediments (see section 1.7.3). Even in the deep ocean, sedimented OM is subject to resuspension and physical processes that may be significant in introducing it back into the water column for further remineralisation (Burdige and Homstead, 1994).

Table 1. Estimates of POC flux (g-C m^{-2} y^{-1}) from different oceanic regions.

Author	Method	POC flux	Notes
Jeandell et al., 2000	Barium	1.6±0.4 – 12.0±4.0	Tropical N.E. Atlantic
Dehairs et al., 2000	Barium	7 – 18	Bay of Biscay – N. Atlantic
Hall et al., 2000	Th^{234}/U^{238}	0.4 – 23.1*	Iberian Margin – N. Atlantic
Buesseler et al., 1998b	Th^{234}	0.4 - 10.9*	Arabian Sea & Eq. Pacific
Moran et al., 1997	Th^{234}	1.3±0.9*	Central Arctic Ocean
Piskaln et al., 1996	Sediment traps	4 – 44*	Coastal upwelling – North Pacific
Fernandez et al., 1995	Sediment traps	63 – 86*	S. Bay of Biscay – Atlantic

*Converted units to g-C m^{-2} yr^{-1} from literature

1.3 The Importance of Oceanic DOM

The DOC pool in the oceans, the major component of DOM (>50% by mass; Hedges and Farrington, 1993), represents the quantitatively most important organic carbon reservoir in the

oceans and it is equivalent to that of atmospheric CO_2 (Hedges & Farrington, 1993). It has recently been estimated to hold approximately 1000 Gt-C (McCarthy et al., 1996) compared to ~30 Gt-C in the POC pool and is fundamental to many oceanic processes (i.e. nutrient and trace element cycling) (Toggweiler, 1990). The contribution of the DOC pool to the annual downward flux of organic material from the ocean surface is considered quantitatively significant (i.e. >25% of the total downward flux, Noji et al., 1999; 20%, Alldredge, 2000) and could be equivalent to the measured flux of particulate matter (Carlson et al., 1994; Guo et al., 1995). An important mechanism that can instigate significant DOM downward export is hydrolytic dissolution of sinking particles that are colonised by bacteria (Smith et al., 1992, Alldredge, 2000). In addition, seasonally accumulated DOM that is typically observed in productive marine waters (Williams, 1995) may be subject to vertical transportation. However, Williams and Druffel (1987) estimated that the amount of photosynthetically fixed C entering the deep ocean as DOC only represents up to 3% of the sinking POM flux. These estimates are important for mass-budget calculations for the vertical flux of carbon but there is still little known in terms of the mechanisms of the biogeochemical cycling of DOM and its composition.

The measurement of DOM in seawater has been a difficult and often controversial procedure. There has been uncertainty in the accuracy of past and current methods used (Hansell, 1993), which has resulted in limited and questionable information on the distribution of DOM in the global ocean, its spatial and temporal variability, and reactivity in the marine environment (Hopkinson *et al.*, 1997).

As measured by historical methods (*i.e.* wet chemical oxidation (WCO) techniques) vertical distributions of DOC in the oceans were shown to be relatively homogeneous and it was presumed that the material was of a refractory nature. In 1988, Sugimura and Suzuki presented the high temperature catalytic oxidation (HTCO) method as a rapid and precise technique (± 1-2%) for the determination of non-volatile DOC in seawater (Sugimura and Suzuki, 1988). The authors found 2 to 3 times higher concentrations of DOC (180-280μM-C) than had been previously reported by WCO methods and total dissolved nitrogen concentrations of approximately 40μM-N (Suzuki *et al.*, 1985; Sugimura and Suzuki, 1988) in surface oceanic waters. Large vertical gradients of DOC in the upper water column, and a strong inverse correlation with apparent oxygen utilisation (AOU) were observed. In 1993, in a special issue of Marine Chemistry, Suzuki issued a statement retracting the results from the 1988 paper (Suzuki, 1993). However, their findings had instigated the critical re-evaluation of the relative importance of marine DOC in the global carbon cycle.

Although not precisely reproduced, vertical gradients of DOC concentrations in the upper water column are oceanographically consistent and can generally exhibit a ~50% decrease according to Miller (1996). A consensus on DON and DOP distribution in the marine water column has not yet been achieved. The range of DOC concentrations reported for the oceanic environment can be large and variable (~50 – 500μM-C; Miller, 1996) but typically falls within 40 – 80μM-C (Williams, 2000). DOC concentrations are usually higher in more productive areas and decrease towards the open ocean and with increasing depth. Deep water DOC concentrations, as measured consistently by both WCO and HTCO methods, are typically 40 – 50μM-C (Sharp et al., 1995), their distribution is homogeneous and the pool is mainly of a refractory nature (Sharp, 1997). Reported deep-water values of the north-west Mediterranean, north-west Atlantic, and equatorial Atlantic are in the range of 50 – 58, 50 – 55 and 46±7μM-C, respectively (Copin-Montegut and Avril, 1993; Thomas et al., 1995; Chen et al., 1996c).

Current work is centred on producing contemporary estimates of oceanic DOC and DON distributions in order to create more accurate biogeochemical models of marine carbon fluxes. By combining HTCO with other analytical techniques (i.e. ultrafiltration, isotope mass spectrometry) it should be possible to define the chemical nature and further understand the biogeochemistry of DOM and elucidate the mechanisms associated with DOM production and degradation in the marine environment.

1.4 The Composition of DOM

The DOM pool is composed of a great variety of organic molecules from simple hydrocarbons to complex polymers that are exchanged biogeochemically within the marine environment. However, the majority of the component molecules have not yet been identified (Hedges, 1992). This is a major drawback in understanding the bio-reactivity (i.e. biological availability or lability) of the marine DOM pool considering that molecules of different composition and molecular weight may be selectively utilised by the marine microbial community (Williams, 2000). Amon and Benner (1996) suggest that the bioreactivity of OM decreases along a continuum of size (from large to small) and diagenetic state (from fresh to old).

The principal fractions of DOM consist of hydrocarbons, carbohydrates, lipids, fatty acids, amino acids, and nucleic acids (Figure 4; Libes, 1992). A detailed explanation of the above groups of compounds is beyond the scope of this discussion and to the author's knowledge there is no sufficiently comprehensive review of the composition of DOM. This is probably due to the lack of identification of the complex compounds that the majority of DOM is composed of. However, certain compounds merit emphasis as they may be indicators of specific species and

processes occurring in the marine environment at a given space and time. For example, complex lipids like phospholipids are used in the construction of bacterial cell walls and the potential release of inorganic P from their mineralisation may be important in areas where P is a limiting nutrient. However, recent experiments have revealed that OM associated with such lipids are protected from rapid enzymatic attack in seawater; thus, their production (e.g. *via* bacterivory and viral-lysis) may be an important source of refractory material to the DOM pool (Nagata, 2000). Carbohydrates are important cellular reservoirs of chemical energy for marine organisms. The simple carbohydrates are usually single sugar molecules like glucose, which are excreted by phytoplankton (Libes, 1992) and can be easily taken up by bacteria (Doetsch and Cook, 1973), whereas complex carbohydrates like cellulose and lignin are chemically inert. Lignin-derived molecules have been successfully used as markers for terrestrial components of oceanic DOM (Meyers-Schulte and Hedges, 1986). Radioactively labelled glucose is commonly used in tracer studies to study the microbial ingestion rates of DOM.

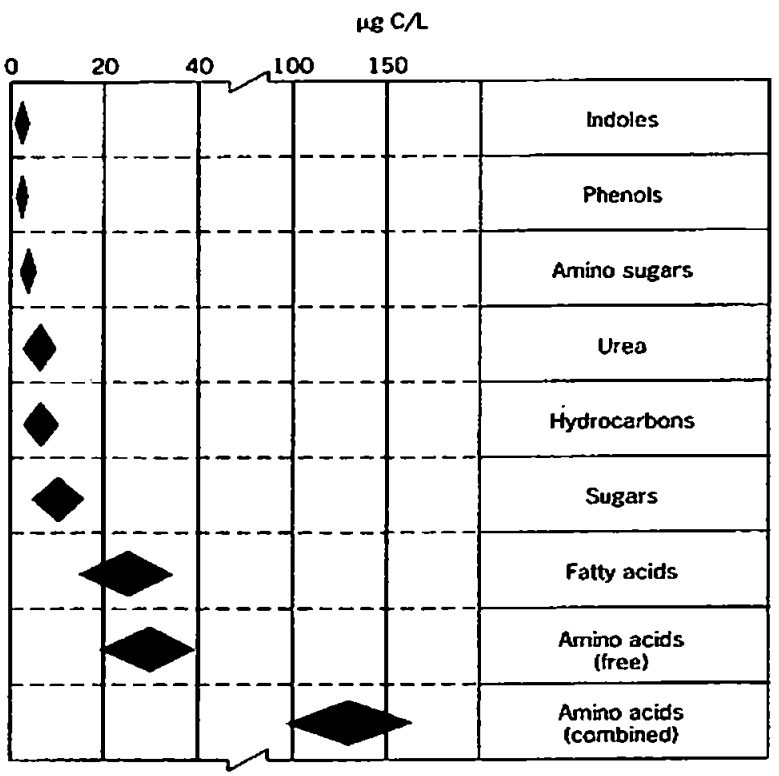

Figure 4. Range of concentrations of various types of DOC. After Degens, 1970 in Libes, 1992.

In addition to the identification of individual DOM components, several perhaps more generic approaches for investigating the biogeochemical nature of marine DOM include:

- the determination of the major elemental components (i.e. C, N and P),
- the separation of the different size fractions by filtration techniques,
- the determination of the isotopic composition (e.g. ^{12}C, ^{13}C),
- the use of radioactively labelled materials (e.g. ^{14}C, ^{15}N),
- and the determination of the optical properties.

1.4.1 Major Elemental Composition

The DOM pool is a significant store of (fixed) nutrients for use in the marine microbial community, and the relative cycling of its components can have major implications in defining the link between OC export and the import of inorganic nutrients for oceanic new production (Williams, 1995). Therefore, it is important to accurately determine its major elemental composition (i.e. C, N and P). The composition of organic matter generally follows the Redfield ratio (i.e. C:N = ~6.6; Redfield et al., 1963). However, several studies have established that the C:N ratio of DOM in the marine environment can significantly deviate from 6.6, varying spatially and temporally (see Table 2; Kirchman et al., 1991; Kortzinger et al., 2001, Kahler and Koeve, 2001) and ranging from below the Redfield ratio to infinity (Sondergaard et al., 2000). The C and N content of DOM may differ depending on its source (Guo and Santschi, 1997) and fate. In the oceans, it has been found that DOC:DON and DOC:DOP ratios typically increase with depth, possibly due to the preferential mineralisation of N and P relative to C (Hopkinson et al., 1997). However, the input of dissolved compounds that are C-rich to surface waters (e.g. terrestrial sources, Meyers-Schulte and Hedges, 1986; exudation of C-rich DOM, Sondergaard et al., 2000) and the presence of high nitrate concentrations in deep waters[1] can counteract this trend. Such observations indicate that the DOC, DON and DOP pools can cycle on different time scales. Although evidence of preferential mineralisation of DON and DOP from the DOM pool has been produced, inferring biological lability of DOM from C:N ratios should be approached with caution because the mechanisms of DOM production and the relationship of its major elemental components are still unclear.

[1] High nitrate concentrations present in deep water samples may cause irregular total-N recovery in the HTCO analytical methodology (Kahler and Koeve, 2001).

Table 2. Estimated C:N ratios for total and fractionated (i.e. HMW and LMW) DOM at different areas in the marine environment and from laboratory cultures.

Author	Area	C:N	Notes
	N.E. Atlantic Ocean		
Doval et al., 1997	Coastal embayment	~15	
Alvarez-Salgado et al., 1999	Shelf waters	12.0±0.7	
	N.W. Atlantic Ocean		
Guo & Santschi, 1997		13 – 17	Colloidal OM
Hopkinson et al., 1997	Surface water	11 – 15	
	Deeper water	14 – 20	
	Pacific Ocean		
Clark et al., 1998		~16.8	
McCarthy et al., 1997		15.6 – 18.4	HMW DOM
	N.W. Mediterranean		
Doval et al., 1999		15.5±0.4	
	Southern Ocean		
Ogawa et al., 1999	Surface water	2.7 – 5.0	
	Other		
Williams, 1995	English Channel, Coastal Pacific Ocean, North Sea, and Strait of Georgia samples	~15	average
McCarthy et al., 1996	North Pacific Ocean, Gulf of Mexico and Sargasso Sea samples	13.4 – 22.5	HMW DOM
Biddanda and Benner, 1997	DOM produced from cultures	4.1 – 14.1	Initial growth
		21	HMW DOM
		6	LMW DOM
Sondergaard et al., 2000	Excreted DOM produced from cultures	infinite[2]	Initial growth
		11	Stationary
		20	Decaying

[2] This is due to non-detectable DON values.

1.4.2 Size Classification

For analytical convenience, DOM is generally classified as the fraction passing through a filter with a given pore size or nominal cut-off (typically ranges from ~0.7 to 0.2μm). However, in the last decade, it became apparent that traditional filtration procedures attempting to separate the dissolved and particulate phases of a seawater sample do not distinguish between true solutes and the smaller colloidal phases (Buesseler et al., 1996). Studies indicate that a significant fraction of the DOC pool is within the colloidal size range (i.e. 1-2nm to ~1μm; Koike et al., 1990; Wells and Goldberg, 1991; Benner et al., 1992). Marine colloids have high aggregation rates (Wells, 1998) and have been investigated extensively due to their potentially important role as reactive particles that scavenge trace metals and hydrophobic organic compounds (Buesseler et al, 1996).

Cross-flow filtration (CFF), also known as tangential flow filtration or ultrafiltration (UF), is a technique widely used in the marine community for separating the colloidal fraction from the truly dissolved (special issue Marine Chemistry vol. 55). The cut-off point of the CFF membrane is determined by its ability to retain standard molecules of a known nominal molecular weight (1,000 nominal molecular weight = 1 kiloDalton = 1 kD = ~1 nm). DOM passing through a 1kD cut-off membrane is typically classified as low molecular weight (LMW) material (Buesseler, et al., 1996) (i.e. true solutes).

LMW compounds comprise 65-80% of the DOM pool (Benner et al., 1992) and range from carboxylic acids which are abundant in marine organisms (Libes, 1992) to simple sugars like glucose. A significant fraction of photosynthetically excreted material (>68% below 10kD; Ridal and Moore, 1993) is N-rich LMW compounds (C:N ratio is ~6; Biddanda and Benner, 1997) with small turnover times (<days) but this fraction is said to be less than 1% of total DOM (Carlson and Ducklow, 1995). The high molecular weight (HMW) pool has a high carbohydrate content (25-50%) and it typically comprises 20-35% of the oceanic DOM pool (Carlson et al., 1985; Benner et al., 1992; Amon and Benner, 1994; Aluwihare et al., 1997). HMW compounds are mainly composed of highly complex polymeric substances that are collectively known as humics. They are said to be formed during the linking of relatively LMW compounds *via* abiotic processes such as condensation, polymerisation, oxidation and reduction (Libes, 1992). Due to its chemical nature (i.e. higher aromatic content and chemical refractivity; Erhardt, 1977) it was commonly believed that HMW DOM is relatively inert and refractory to bacterial attack (Ogura, 1977). However, investigations on the relative bioavailability of DOM from seawater samples collected during bloom conditions show that bacterial growth and respiration in the presence of HMW DOM can be three and six times

higher than with LMW DOM (Amon and Benner, 1994). In addition, recent evidence (Aluwihare et al., 1997) suggests that a large fraction of macromolecular DOC in surface seawaters is not the complex, heterogeneous polymeric material expected from abiotic geopolymerization of simple biomolecules. In fact, as much as 70% of the HMW material in surface seawater may have been produced by direct biosynthesis. McCarthy et al., (1997) found that most HMW DON is amides, also biosynthesised directly from degradation-resistant biomolecules. The above information suggests that the HMW fraction may be a recycled product from biological processes and may contribute significantly to the bioavailable, or labile, pool of DOM.

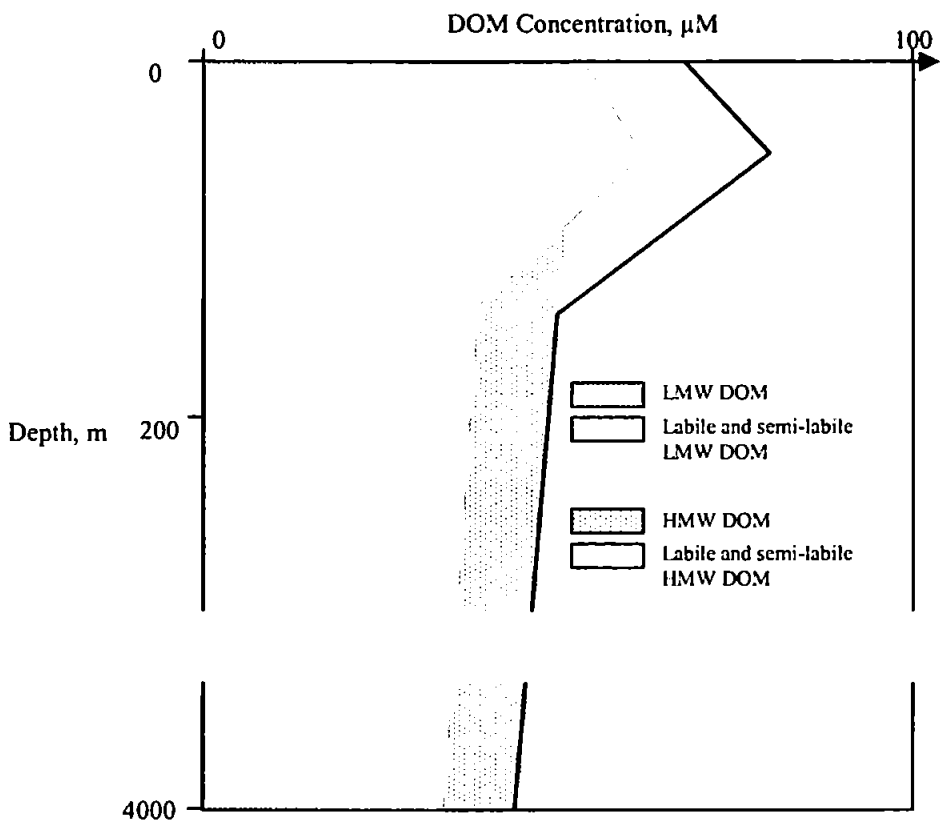

Figure 5. Generalised oceanic profile of DOM (solid line) and its molecular fractions Adapted from Williams, 2000.

Thus, the conventional view that LMW DOM cycles faster and is more bioavailable to the microbial community due to its apparent higher nitrogen content is being re-evaluated. It is

most likely that a small fraction of LMW DOM does turn over rapidly but the remaining material is largely refractory and cycles at slower rates (see Figure 5; Williams, 2000).

1.4.3 Isotopic Composition

The determination of the stable carbon and nitrogen isotope ratios ($\delta^{13}C$ and $\delta^{15}N$) of marine DOM can help identify its sources. Marine humics have a heavier isotopic composition ($\delta^{13}C$ -20‰ to -23‰; $\delta^{15}N$ +9‰) than terrestrially derived humic material ($\delta^{13}C$ -25‰ to -28‰; $\delta^{15}N$ +2‰) (Libes, 1992). Guo and Santschi (1997) investigated the origin of DOM in coastal areas (Galveston and Chesapeake Bays, N.E. Atlantic) sampling both terrestrial and marine waters (salinity = 0 – 35). They found that the $\delta^{13}C$ of HMW DOM remained almost constant between salinities 0 and 22 (-28.5‰), increasing in marine waters with higher salinity, showing that terrestrially-derived DOM did not cycle conservatively to the ocean but was subject to short time-scale removal processes at the estuarine mixing zone. The origin of HMW DOM in different oceanic regions was investigated by Benner et al. (1997); the isotopic composition ($\delta^{13}C$ -21.7‰) did not vary significantly between regions indicating a predominantly marine origin for the material sampled. Mitra et al. (2000), using a combination of stable isotopic values, C:N ratios and radiocarbon ages, detected terrestrially derived HMW DOM in deep waters of the Atlantic Ocean that may have been transported there *via* diffusion and/or desorption of DOM from resuspended weathered shelf and slope sediments. The use of stable carbon isotope determination for different molecular weight fractions and compound classes of DOM can provide a more detailed and thorough investigation of the different biogeochemical pathways of fractionated DOM components.

1.4.4 Radioactively labelled DOM

Radioactive carbon (^{14}C) and nitrogen (^{15}N) can be used to investigate rates and mechanisms of DOM production and consumption (Bronk and Glibert, 1991; Slawyk et al., 1998; references in Table 3). Radiotracer experiments, whereby a radioactively labelled compound is introduced to a seawater sample and its fate monitored periodically, have shown release and uptake rates varying greatly from hours to years (Chen and Wangersky, 1996b). This indicates that the DOM pool consists of material with varying degrees of lability and refractivity (Hansell et al., 1995). However, estimates produced from such studies can be inaccurate to some extent as the conditions under which the biota are observed are artificial compared to those in the marine environment (for a critical review on microbial studies see Hobbie and Williams, 1984). In addition, the experiments typically employed for investigating the metabolic consumption or

production of DOM usually describe the flux of the labile fraction of DOM and omit the refractory fraction due to their short duration (Williams, 2000).

^{14}C can be measured in fractions of the DOM pool to determine its apparent age. Williams and Druffel, (1987) and Bauer et al., (1992), using radiocarbon measurements ($\Delta^{14}C$), estimated the mean turnover rate of deep water DOC in the Pacific and Atlantic Oceans to be ~6,000 years. Surface ocean DOC was estimated to have a mean turnover rate of 1,300 – 3,100 years. However, this includes fractions which cycle faster (one to two hundred years, Lee and Wakeham, 1992; Yamanaka and Tajika, 1997) as suggested by the observed rapid decrease in oceanic DOC concentrations with depth (Guo et al., 1995; Thomas et al., 1995; Wiebinga and deBaar, 1998). Williams and Druffel (1987) estimated that in the surface mixed layer of the central North Pacific Ocean, ~44% of the DOC pool was recycled deep-water DOC that was resistant to rapid microbial utilisation and ~56% represented the labile or bio-available fraction.

1.4.5 Optical properties of DOM

Absorbance and fluorescence properties of the DOM pool (e.g. protein- or humic-type fluorescence spectra, Mopper and Schultz, 1993) can now be used to identify sources and sinks of DOM. The fraction of the marine DOM pool that absorbs light is termed chromophoric DOM (CDOM) and the fraction of CDOM that re-emits absorbed light at longer wavelengths is termed fluorophoric DOM (FDOM) (Mopper et al., 1996). Components that are terrestrially derived (i.e. old humic material) contain more aromatic and ketonic structures and have an increased potential for absorbing light whereas algal-derived DOM contains mostly aliphatic carbons with little or no absorbance (Aiken et al., 1996). High-resolution fluorescence can also be used to study DOM fluxes in coastal waters and off continental margins. For a detailed review see Chen, 1999.

1.5 Sources of DOM

Studies show that the majority of DOM in the marine environment is autochthonous (i.e. produced from internal sources) with a small contribution from allochthonous sources (i.e. terrestrial, atmospheric and benthic inputs). For a schematic of the main factors affecting OM distribution in the marine environment refer to Figure 6.

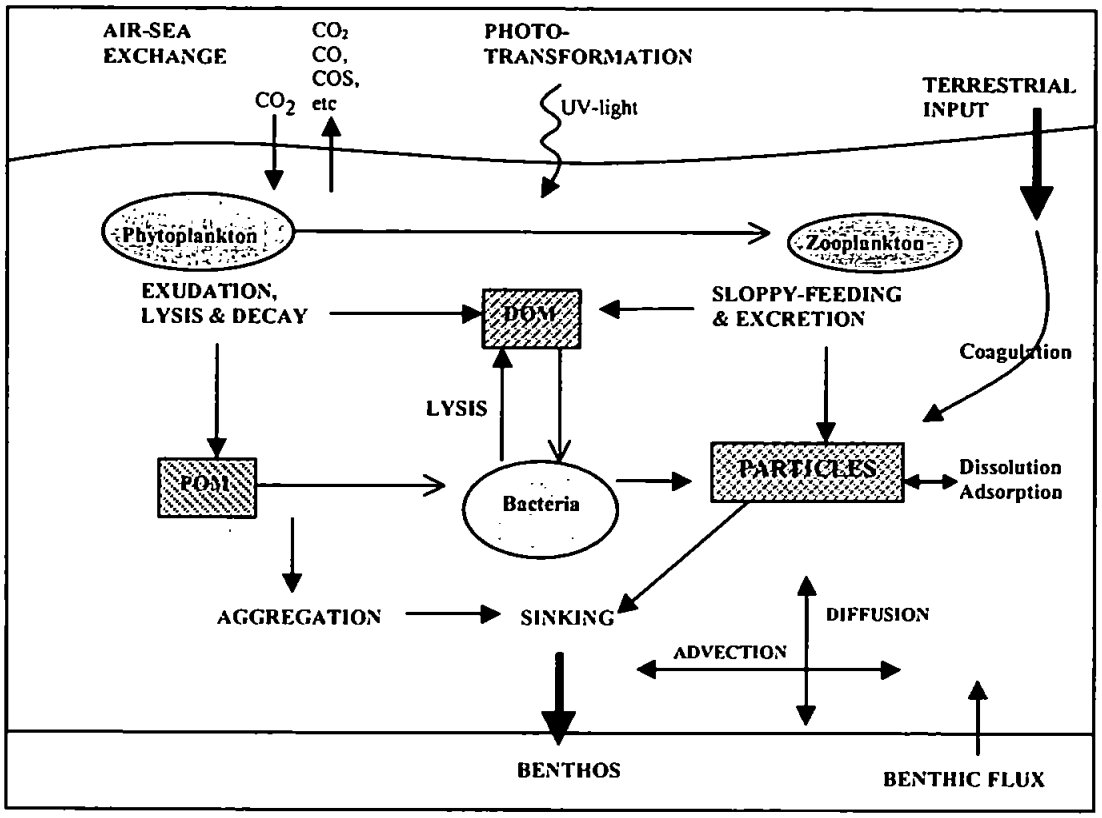

Figure 6. Factors affecting the distribution of organic matter in the oceans. Note: Unfilled arrowheads - ingestion

1.5.1 Autochthonous Sources

The largest source of marine DOM is *in-situ* biological activity (i.e. phytoplankton exudation & viral induced cell lysis, zooplankton grazing & excretion and microbial degradation of POM) (Williams, 1995).

1.5.1.1 Phytoplankton exudation & viral-induced cell lysis

The proportion of photosynthetically fixed carbon that is released as DOC *via* exudation is typically 3-32% of total carbon fixation rates (e.g. Verity et al., 1988; Baines and Pace, 1991; Lee and Henrichs, 1993 and references therein; Biddanda and Benner, 1997). However, estimates of >40% have been observed (Ridal and Moore, 1993). Many studies have been performed to elucidate the mechanisms, rates of exudation and qualitative characteristics of the DOM released by different phytoplankton communities (Chen and Wangersky, 1996a, Chen and Wangersky, 1996b, Lara and Thomas, 1995; Kepkay et al., 1997), which have resulted in variable information.

Table 3. Estimates of DOC production *via* phytoplankton exudation.

Author - year	Method summary	PER of P.P. (%)	Notes
Verity et al., 1988	^{14}C labelling	4 - 13%	As light ↑, PER ↑
Hagstrom et al., 1988	^{14}C labelling	11%	
Baines and Pace, 1991	^{14}C labelling	13%	As P.P. ↑, PER ↑
Ridal and Moore, 1993	^{14}C labelling	8 - 45%	Most of DOM was LMW
Lara and Thomas, 1995	^{14}C labelling	20%	On day 20 of culture
Obernosterer and Herndl, 1995	DOC concentration change	15 - 39%	P-limited, PER ↑
Biddanda and Benner, 1997	DOC concentration change	10 - 32%	During growth phase

PER of P.P. (%) = Percent photosynthetic extra-cellular release of primary productivity.

The rate of photosynthetic extra-cellular release (PER) of DOM from phytoplankton in the marine environment is likely to be influenced by many factors including the phytoplankton community (e.g. algal species and physiology) and environmental conditions (e.g. light irradiance, nutrient availability). A study investigating the excretion rates of DOC by marine phytoplankton of different sizes (Malinsky-Rushansky and Legrand, 1996) found that the percentage PER for larger algal cells was lower compared to that of pico-eukaryotes. Further studies (Verity et al., 1988, Obernosterer and Herndl, 1995) found that DOC exudation was highest in samples exposed to higher irradiance and was inversely related to ambient inorganic nutrient concentrations. This suggests that cells that were 'stressed' (i.e. unable to divide but still able to photo-assimilate) or nutrient limited (i.e. N:P ratio significantly different to 16), excreted more DOC. The above findings have been confirmed by other studies (Ridal and Moore, 1993; Norrman et al., 1995) which observed an increase in the release of DOC by algae that were in their declining or stationary growth phases.

Viruses can be a significant cause of mortality for phytoplankton and bacteria and thus may be a potentially large contributor to the release of DOC in marine waters *via* cell lysis and breakage (Nagata, 2000 and references therein). Weinbauer and Hofle (1998) found that the contribution to the DOM pool *via* viral-lysis in a eutrophic lake was low, but may have the potential to significantly stimulate bacterial production. However, the production of complex biopolymers like peptidoglycans (i.e. a remnant of bacterial cell wall components) thought to be a result of

viral lysis rather than bacterial-grazing (i.e. because grazers tend to digest components rather than release them) is considered to contribute to the refractory pool of DOM (Stoderegger and Herndl, 1998 & 1999; Fuhrman, 2000). Further studies in the marine environment are necessary to quantify the contribution of organic matter released *via* viral cell-lysis to the DOM pool and how bioreactive the components are.

1.5.1.2 Zooplankton grazing & excretion

Grazing (i.e. cell breakage) on phytoplankton by heterotrophs is an established mechanism for inducing the release of DOM to the surrounding water. This process may play a key role in providing substrates for use by the bacterial community in different marine environments (Bianchi et al., 1995; Moller and Nielsen, 2000). Studies have shown that as heterotrophic processes (i.e. grazing inducing release of DOM *via* "sloppy feeding") dominate, the quantitative importance of PER decreases (Bronk and Glibert, 1991; Slawyk et al., 1998). It was found that 16-37% of algal carbon content can be released as DOC during grazing in comparison to 3-7% DOC released *via* direct exudation by the phytoplankton present (Strom et al., 1997). This suggests that grazing is in fact a more significant mechanism for producing DOM than direct phytoplankton exudation.

The possibility of zooplankton significantly contributing to DOM production *via* direct excretion (i.e. urea and amino acids, dissolution of faecal pellets) has recently been examined. Otsuki et al. (2000) suggested that the enhanced total DOC production rates they observed were mainly attributable to excretion by small zooplankton (<100μm). Another study (Steinberg et al., 1998) showed that on average, the excretion of DOC by zooplankton made up 24% of the total carbon metabolized (excreted and respired); this could be a major contribution to DOC production and moreover, implicates the diel vertical migration of zooplankton in DOC vertical export.

1.5.1.3 Microbial degradation of POM

Sinking marine aggregates are mostly interstitial fluid that is colonised by bacteria and are subject to both solubilisation and mineralisation processes in surface and deep waters (Smith et al., 1992). In a study by Alldredge (2000), interstitial DOC concentrations were found to be one to two orders of magnitude higher than ambient DOC concentrations probably due to the hydrolytic activity of bacterial exo-enzymes that solubilise the POM of the aggregates. However, the estimated cumulative interstitial DOC in the aggregates contributed less than 2.5% to the total DOC in the water column. Although this value may seem insignificant,

Alldredge (2000) estimated that, on average, 20% of the total organic matter of marine aggregates undergoing sedimentation is DOC. Therefore, the sinking carbon flux as determined from particulate matter alone is significantly underestimated. In a particle dissolution study by Smith et al. (1992) it was found that the amino acids of particles were hydrolysed rapidly with very little of the hydrolysate being taken up by the attached bacteria. 'Uncoupled' hydrolysis is a biochemical mechanism for large-scale transfer of OM from sinking particles to the dissolved phase, and this may supply a slowly degradable fraction of DOM for downward export (Smith et al., 1992) but essentially reduces the total sinking carbon flux (Azam, 1998).

1.5.2 Allochthonous Sources

Other sources of DOM to the marine environment include terrestrial, atmospheric and benthic inputs. These were historically considered to be a relatively small percentage of the total marine pool.

1.5.2.1 Fluvial Inputs

On a global scale, the riverine DOC discharge into the ocean is approximately 0.2 Gt-C yr^{-1} (Meybeck, 1982). DOC concentrations of riverine and lake waters can be 10 times higher than those of marine waters. However, the terrestrially derived DOC component of the total marine DOC pool typically does not exceed a value of ~10% (Meyers-Schulte and Hedges, 1986; Williams and Druffel, 1987). The exact removal mechanisms of terrestrially-derived DOM are not known but particle scavenging and aggregation processes are suggested to play a key role. This is probably because between 40 – 80% of freshwater DOC is humic material, which tends to undergo reactions with suspended particles and may thus be scavenged or precipitated out of solution in the estuarine environment (Chester, 1990) before it reaches the ocean. The remaining material includes fulvic acids, which remain soluble in waters with acidic pH (Libes, 1992) and it is suggested that this fraction enters the marine environment (Ertel, 1986).

1.5.2.2 Atmospheric Inputs

There is very little quantitative information on OM flux to the water column *via* the atmosphere. The organic carbon fraction of aerosols (i.e. a suspension of solid and liquid material in a gaseous medium; Chester, 1990) can originate from vegetation, soils, the marine and freshwater biomass, anthropogenic activities (e.g. forest burning, industry), and some in situ production of organics in the atmosphere itself. Aerosols can be transported over several thousand kilometers (Blank et al., 1985) and this long-range transport can be significant for OM input to the

oligotrophic open ocean areas. The main mechanisms by which this might occur are dry and wet deposition (Chester, 1990). Duce and Duursma (1977) estimated a dry and wet deposition flux of OM to the oceans as ~0.006 Gt-C yr^{-1} and ~1 Gt-C yr^{-1}, respectively. However, there can be significant errors associated with these estimates due to the practical difficulties in determining source and sink of the marine aerosols near the air-water interface. More recently, Willey et al. (2000) found that marine rain (23 μM-DOC) is a significant source of DOC to surface seawater (0.09 Gt-C yr^{-1}) contributing a global rainwater DOC flux of 0.43±0.15 Gt-C yr^{-1}. However, more research is required to better quantitatively define both atmospheric wet and dry inputs.

1.5.2.3 Benthic Inputs

DOC concentrations in pore waters of surficial sediments have been found to be higher than those in the overlying water column (references in Burdige and Homstead, 1994; Bauer and Druffel, 1998). Burdige et al., (1992) made a lower-limit estimate of the globally integrated benthic DOC flux from marine sediments ($0.1 - 0.9 \times 10^{14}$ g-C yr^{-1}) indicating that it is comparable in magnitude to processes such as riverine inputs of DOC and POC to the oceans. This suggests that benthic fluxes from sediments and pore waters may play a significant role in the oceanic carbon cycle. The processes involved in the production and consumption of DOM in sediments are not clearly understood, but an imbalance between the rates of production and consumption may result in DOM accumulation and a subsequent benthic flux of sedimentary DOM to the overlying waters. Diffusion of porewater DOM (pDOM) into overlying waters may occur as a result of resuspension events caused by episodic winter storms and/or bioturbation from macrofauna (Burdige and Homstead, 1994 and references therein). The pool of pDOM is likely to be intermediate products in the remineralisation process of sedimentary OM. Thimsen and Keil (1998) found that less than 40% of pDOM was surface-reactive and that it undergoes exchange with the surface-bound pool of OM. Hydrolytic processes may be more important in remineralising organic material at the sediment water interface than respiration processes (Burdige and Gardner, 1998). Further work is required to elucidate the factors controlling benthic fluxes of DOM from marine sediments.

1.6 Sinks of DOM

The mechanisms of DOM removal in the water column are not well known, however the main processes are considered to be bacterial mineralisation to inorganic nutrients, adsorption onto particles (i.e. aggregation) and photochemical degradation, the latter being a less direct sink of DOM.

1.6.1 Bacterial Mineralisation

Bacterial interactions with organic matter are complex and poorly understood. In a broad sense, DOM released by phytoplankton is returned to the main food chain *via* a 'microbial loop' (see Figure 7) of bacteria-flagellates-microzooplankton. It is estimated that, on average, one-half of the oceanic primary production may be channelled *via* DOC and bacteria into this 'microbial loop' (Azam et al., 1983; Smith et al., 1995). However, the fraction of primary production utilised changes temporally and spatially, and this introduces a high variation in estimating the flux of OM fractions through the 'microbial loop'.

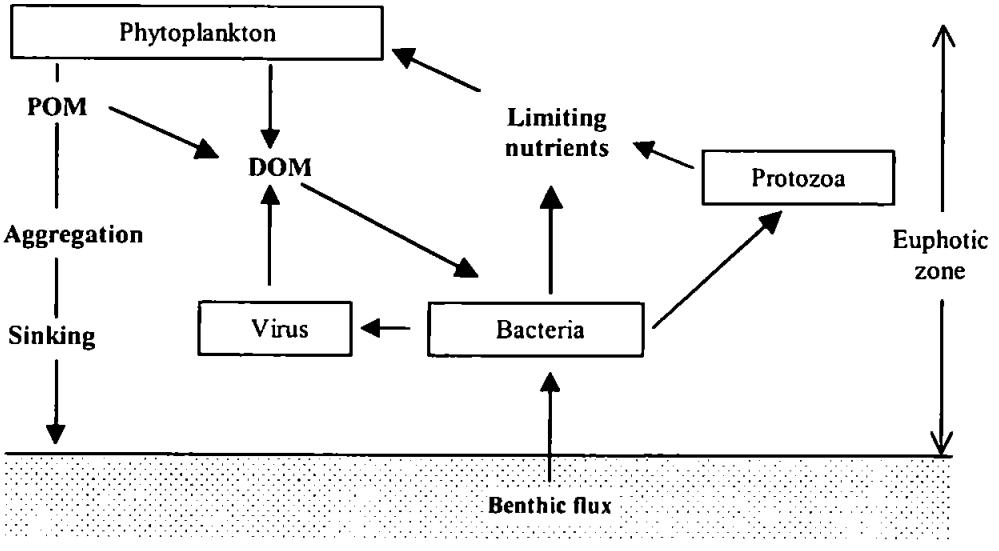

Figure 7. A simple schematic of the microbial loop. After Azam, 1998. Note: POM- particulate organic matter; DOM- dissolved organic matter.

Organic matter must be in LMW form for heterotrophic bacteria to directly transport it across their membrane. HMW DOM such as polysaccharides and proteins can be taken up only after hydrolysis to smaller molecules *via* the use of extracellular enzymes associated with the bacterial cell surface (Sherr and Sherr, 2000). Thus, photosynthetically exuded LMW DOM, having a higher N content (Biddanda and Benner, 1997) and being more energy-efficient for

bacterial uptake, should be preferentially mineralised. However, to the author's knowledge, there is no direct evidence showing the preferential use of LMW DOM by bacteria. One study showed that bacterial uptake rates of glucose in surface waters of the Gulf of Mexico decreased when HMW DOM was added (Skoog et al., 1999). There is a serious lack of understanding of DOM uptake mechanisms by heterotrophic bacteria. New evidence has revealed that several groups of bacteria can be responsible for degrading different fractions of DOM (Cottrell and Kirchman, 2000). Further work is necessary to establish which molecular fractions are available to bacteria and what the primary metabolic processes are.

Some recent estimates of bacterial uptake (i.e. assimilation and respiration) of labile and semi-labile DOM, expressed as %, are listed in Table 4. The wide range of values produced are likely a result of the different methodologies (i.e. rates estimated from radiotracer experiments, DOC concentration changes, bacterial respiration and growth rate measurements) used in the studies for quantifying labile and semi-labile DOM and its subsequent uptake. Given that their growth efficiencies are lower than 50%, heterotrophic bacteria are most likely a net sink of organic matter rather than a net "link" in the microbial loop and thus mineralise >50% of the DOM flux to inorganic nutrients (Kirchman and Williams, 2000).

Table 4. Estimates of uptake rates of DOM by bacteria.

Author	**Rate**	**Notes**
Obernosterer and Herndl, 1995	~46%	*C. affinis*
Sondergaard and Middelboe, 1995	19%	Grazer-free cultures
Amon and Benner, 1996	0.5 – 23%	Per day
Malinsky-Rushansky and Legrand, 1996	18 – 70%	Marine nanoplankton

Note: Rate - % assimilated and respired of total labile DOM.

Interestingly, Amon and Benner (1994) observed nitrogen regeneration when bacteria utilised newly produced LMW DOM compared to a net uptake of inorganic nitrogen when HMW DOM was utilised. This information may suggest that the higher nitrogen content of LMW DOM is sufficient to sustain growth whereas inorganic nutrients are required for assimilation of low-N HMW DOM. In addition, the observed uptake of inorganic nutrients by bacteria follows the now established theory that heterotrophic bacteria consume inorganic nutrients (i.e. N, P and Fe) in order to grow and can be in direct competition with the autotrophs.

1.6.2 Limitations to the bacterial uptake of DOM:

The production of DOM and its uptake are not always tightly coupled resulting in its accumulation, especially in the photic zone of the ocean during the productive season (Copin-Montegut and Avril, 1993; Carlson et al., 1994). This phenomenon is thought to be due to an inability of bacteria to assimilate the DOM. Bacterial uptake rates of DOM could be influenced by several parameters but the main controls are thought to be bacterial mortality by viral-lysis and protozoan grazing (i.e. top-down controls) and organic- and nutrient-limitation (i.e. bottom-up controls).

Historically, it was thought that the generally homogeneous distribution of bacterial biomass in the world's oceans is due to a lack of substrate inhibiting growth. It is now known that predatory control by bacterivorous flagellate grazing and viral-lysis are the main processes keeping bacterial biomass in check. Mesocosm studies (i.e. isolated experimental systems) of the marine microbial community, with and without bacterial grazers, demonstrate the significant influence of protozoan grazers on the magnitude of bacterial production and hence population growth (Caron et al., 2000). In a recent study investigating microbial community dynamics in Mediterranean seawater, it was found that although the bacterial community positively responded to additions of nutrients, their biomass was rapidly controlled by grazing (Lebaron et al., 2001). Viral lysis is thought to play a significant role in bacterial mortality (i.e. 5 – 40%) and thus may be an important control on heterotrophic activity (see review of Fuhrman, 2000). The presence of bacterivores in a natural community creates a dynamic flow of energy (i.e. nutrients/OM → bacteria → grazers/viruses) which seems to induce higher carbon mineralisation by bacteria (Johnson and Ward, 1997; Fuhrman, 1999).

In the deep ocean where inorganic nutrients are in abundance, the main limiting factor on bacterial growth seems to be the inability to assimilate DOC (organic-limitation). One of the main suggestions as to why DOC is not degraded is that it is largely refractory. Generally, deep ocean DOC concentrations (35 – 45 μM-C) represent mainly "background" refractory material that has a long turnover time but the nature of its resistance to decomposition has not been fully ascertained. For detailed reviews on the basis of biological stability and resistance of the DOM pool see Nagata (2000) and Williams (2000). DOC concentrations in excess of the "background" are considered to be labile and semi-labile material with a faster turnover rate. As much as 50% of the DOC in the photic zone is biologically degradable with 19% as an average (Sondergaard and Middelboe, 1995). The extent of the accumulated labile and semi-labile DOC varies spatially and temporally and is likely to be a combination of the production

of refractory DOM and a deficiency in DOM removal mechanisms (e.g. inhibition of bacterial activity).

In the surface ocean, where bacteria may be in competition with phytoplankton for inorganic nutrients, nitrogen and phosphorus can become limiting factors to bacterial growth (e.g. Pomeroy et al., 1995; Thingstad et al., 1998). Mineral nutrient limitation of bacteria was suggested when the addition of inorganic nutrients to water samples from different marine areas stimulated bacterial growth (Zweifel et al., 1993; Pomeroy et al., 1995). Recent experimental studies (e.g. dose-response mesocosms) where inorganic nutrients alone or complemented by organic compounds were added to a natural marine sample are listed in Table 5.

Table 5. Dose-response studies in different marine regions testing organic- and nutrient-limitation scenarios. After Williams, 2000.

Author	Location	Addition	Limitation	Notes
Zweifel et al., 1995	Bothnian Sea	PO_4, PO_4+NH_3	nutrient	Extra N had no effect
Kirchman & Rich, 1996	Eq. Pacific	Glu, Glu+NH_3, a.a., NH_3	organic	N important for growth
Cherrier et al., 1996	N.E. Pacific	Algal extract, NH_3, Glu, Glu+NH_3, PO_4, a.a., Urea	partially organic	Glu, a.a., & algal extract: small effect on growth
Carlson & Ducklow, 1996	Sargasso Sea	Glu, NH_3, a.a.	organic	NH_3 had no effect
Thingstad et al., 1998	N.W. Med.	PO_4, NO_3, Glu	nutrient	Phytoplankton & bacteria P-limited
Thingstad et al., 1999	Fjord	PO_4, Glycine	nutrient	
Thingstad et al, 2001	E. Med.	PO_4, NO_3, Glu,	nutrient	Mixed signals of N or P limitation

Note: a.a. – amino acids; Glu – glucose.

The information from dose-response studies thus far has not been able to provide the marine community with any definite conclusions. Co-limitation of inorganic nutrients may be possible (Thingstad et al., 2001) and microbial community nutrient-limitation could also switch from one nutrient (N or P) to another depending on nutrient supply rates. The combined lack of information on the production mechanisms of refractory DOM and the processes inhibiting the use of DOM by bacteria provides us with many challenging questions for future research.

1.6.3 POM-DOM partitioning and OC burial

Organic matter in seawater is subject to recycling by heterotrophic organisms and/or export to the deep ocean (Figure 3). The dynamics of the particle-dissolved partitioning of organic components are currently being extensively investigated in order to determine whether DOM is net adsorbed/coagulated onto particles and exported to the deep ocean or net desorbed/hydrolysed from the particulate phase and re-introduced to the water column. Evidence shows that less than 10% of DOM can be directly adsorbed or aggregated to particles (e.g. Chin et al., 1998 and references therein). Similar results (<10%) were found in a study performed in brackish estuarine waters (4 – 6 salinity) (Forsgren et al., 1996). It has been suggested that the adsorption (i.e. abiotic complexation) of labile organic compounds onto existing marine DOM produces complexes that have a slower turnover rate (Keil and Kirchman, 1994; Nagata and Kirchman, 1996). Thus, adsorption may be an important mechanism that temporarily stores labile DOM into a less labile pool that is available for subsequent export and/or mineralisation. Additional mechanisms resulting in the formation of particulate matter from marine DOM include spontaneous assembly into polymer gels (Chin et al., 1998) and coagulation of DOM components into transparent exopolymeric particles (TEP, 3 to 100s of micrometres) (Passow et al., 1994; Mari and Burd, 1998; Stoderegger and Herndl, 1999). The formation of TEP is suggested to be an important mechanism for diatom aggregation, and hence vertical export (Smith et al., 1995). The above processes that result in the abiotic complexation of DOM to POM in the marine water column are thought to be generally reversible as they are continuously subject to dissolution and bacterial degradation processes. Williams and Keil (1997) demonstrated that carbohydrate compounds underwent both aggregation with natural DOM and degradation by heterotrophic organisms. They found that less than 70% of the carbohydrate compounds were assimilated by heterotrophic bacteria and the rest were released to the seawater. The dissolution and mineralisation of sinking marine aggregates was discussed in section 1.6.1.3.

A very small percentage of the DOC produced at the surface ocean actually reaches the deep ocean (~3% of sinking POM flux; Williams and Druffel, 1987). Hedges et al. (2001)

characterised the chemical structure of sinking organic matter from surface ocean waters; their results suggest that the bulk organic composition of the material that eventually reaches the sea floor is preserved within the inorganic matrix of the sinking particles despite extensive biodegradation (>98%). Once organic matter reaches the benthic sediments it is either accumulated, buried and/or remineralised. Organic carbon accumulation and burial rates from recent studies are listed in Table 6. Few studies have calculated DOC burial rates, but the estimates produced suggest that DOM fluxes to sediments might be a quantitatively significant component of the local carbon budget. Further studies are necessary to determine the relative contribution of benthic DOM to organic matter preservation and degradation in sediments.

Table 6. Organic carbon burial rates (g-C m^{-2} yr^{-1}) from different marine regions.

Author	Location	Burial Rate	Notes
Anderson et al., 1994	Mid-Atlantic Bight	2.2 – 8.8 *	sediment traps
de Haas et al., 1997	North Sea	0.2 *	shelf sea
Hulth et al., 1997	Antarctica, Weddell Sea	2.0 – 8.5 *	accumulation rate; 78% recycling efficiency of DOC
Thunell et al., 2000	Cariaco Basin, Carribean Sea	2.9 – 4.4 *	accumulation rate
Schluter et al., 2000	Norwegian & Greenland Seas	0.6 – 0.65	deep basins
Holcombe et al., 2001	North-western Mexican margin	0.09 – 0.14 *	sediment DOC flux (~8% of sedimentary C-input)

*Converted units to g-C m^{-2} yr^{-1} from literature

1.6.4 Photochemical degradation of DOM

Photochemical processes in the marine environment are currently a topic of intense investigation because of the potentially detrimental effects of increasing UV radiation reaching the ocean surface due to ozone depletion. The biogeochemistry of marine ecosystems has been shown to be significantly affected by photoreactions, especially due to the photochemical alteration of DOM (e.g. Miller and Moran, 1997). The pool of seawater DOM is the most important component contributing to the absorption of UV radiation reaching the ocean surface (Moran and Zepp, 2000). Apart from playing a major role in the diffusion and attenuation of

UV and visible light in the marine environment, DOM can be mineralised by UV radiation to DIC (i.e. CO_2, HCO^-_3, CO^{2-}_3, CO; Mopper et al., 1991), nutrients (e.g. NH_4; Bushaw et al., 1996) and/or different organic molecules of increased biological lability or refractivity (Moran and Zepp, 1997; Miller and Moran, 1997; Kieber et al., 1997).

In the mixed layer of coastal and shelf waters, ~10% of the DOC pool may be directly converted photochemically to DIC (Vodacek et al., 1997; Andrews et al., 2000). The direct photochemical mineralisation of DOM from surface waters is in the order of 12 - 16 Gt-C yr^{-1} as estimated by Moran and Zepp, (1997). Thus photochemical degradation may represent a significant DOM sink, equivalent or even exceeding that of bacterial mineralisation. An estimated 20% increase from terrestrial N is expected to be available to micro-organisms in coastal areas due to the photochemical release of biologically labile N from humic substances (Bushaw et al., 1996). The increased availability of substrates for use in the microbial loop can cause dynamic changes in carbon fluxes, especially in organic- and nutrient-limited marine ecosystems. However, there is some evidence that suggests that labile DOM components may be incorporated into a more refractory humic DOM pool by photochemical alterations, thereby quenching DOM degradation (Kieber et al., 1997; Whitehead et al., 2000). Furthermore, a recent study in a lagoon showed that photochemical processes had no significant effect on the cycling of DOM, suggesting that their ecological significance in aquatic systems is largely dependent on the initial photo- and bio-reactivity of the DOM (Ziegler and Benner, 2000). A thorough quantification of which fractions of DOM are photochemically altered to inorganic, biologically labile and refractory compounds would allow a better evaluation of the effects of increased UV radiation to the marine DOM pool.

1.7 Ocean Margins and Coastal Upwelling

Ocean margins comprise of estuaries, coastal embayments, coastal, shelf and shelf-edge components, and are a critical land-ocean interface controlling the anthropogenic and terrestrial fluxes of chemicals and biological production to and from the open ocean. Ocean margins comprise only ~10% of the global ocean's surface area and ~0.5% of the volume, but account for approximately 25% of global ocean productivity due to the supply of nutrients from terrestrial sources and upwelling of deep waters (Mantoura et al., 1991).

Coastal upwelling occurs at sub- and tropical latitudes on the eastern ocean margins where trade winds with an equatorward component drive surface waters towards the equator and offshore (Figure 8). Along the margins, the cross-shelf flow of surface waters travelling towards the open ocean causes deeper waters to travel landwards. In addition, equatorward surface flow

gives way to poleward subsurface flow, its magnitude depending on the presence and strength of the coast-parallel winds. The front that is created between the coastal upwelling and the open ocean may be distorted by eddies, plumes, and filaments extending out to hundreds of kilometres. Because upwelling is largely wind-driven, it is both temporally and spatially variable. This makes the biogeochemical systems in upwelling systems often very complex and thus poorly understood as they are often driven by physical mechanisms.

Upwelling regions which exist at the Eastern Atlantic and Pacific Ocean margins represent the most productive marine systems. The upwelling of deeper nutrient-rich waters is thought to supply nitrate for an estimated 11% of the global new production (Chavez and Toggweiler, 1995).

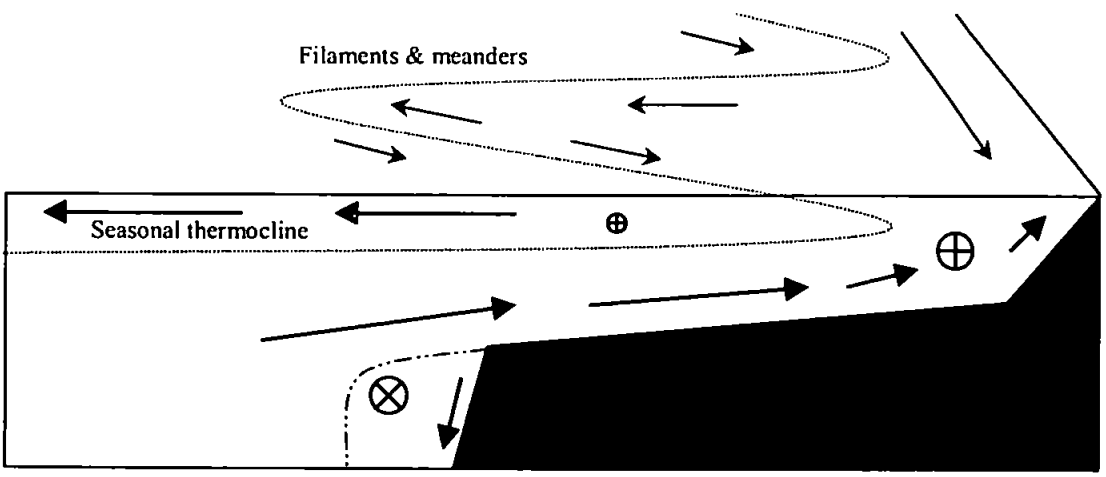

Figure 8. Rough schematic diagram of shelf-edge coastal upwelling with flow direction. Adapted from OMEX II – Phase II proposal. Note: ⊗ - flow into the paper away from reader, ⊕ - flow out of the paper towards reader.

In addition to receiving oceanic water and material from beyond the continental shelf/slope, ocean margins receive dissolved and particulate matter from rivers, the atmosphere, bottom sediments and groundwater with fluxes varying both temporally and spatially (Liss et al., 1991). Estuaries and coastal zones are highly productive, resulting in enhanced sedimentation of organic biomass in such regions. Due to the decreasing magnitude of productivity towards the open ocean, the vertical flux of OC from surface to deep open-ocean waters is found to be lower than that in coastal waters. However, OC (e.g. as DOC and suspended particulate matter) can be exchanged across the continental margin to the deep for sequestration into the abyssal sediments (Bauer and Druffel, 1998). But cross-margin exchange of OC is poorly quantified and

the influence of physical, chemical and biological parameters on the exchange processes, are not thoroughly understood (Wollast, 1991). Nevertheless, it is thought that productive ocean margins have a large potential for sequestering carbon from the atmosphere and thus, the extent to which they exchange and trap terrestrial and marine carbon has significant implications to the global carbon mass balance and future climatic changes (Mantoura, 1991). Therefore, our understanding of these systems is essential in accurately defining global carbon fluxes.

1.7.1 Ocean Margin Exchange (OMEX) Project

The Ocean Margin Exchange Project (OMEX) was established within the European Commission's Marine Science and Technology Programme (MAST) to investigate specific problems associated with understanding the physical, biological, chemical and sedimentological processes occurring along the European shelf break facing the North-East Atlantic Ocean. The main objective of the project was to quantify exchange processes at the ocean margin as a basis for developing global models to predict the impact of environmental changes on the oceanic system and especially on the coastal zone. Specific aims of the OMEX programme were to characterise the flux of organic carbon, nutrients and other trace elements between the open ocean and the coastal seas. Due to the complexity of the biogeochemical processes occurring at ocean margins, it was necessary to implement an interdisciplinary and integrated approach. The project engaged the expertise of over 100 scientists (40 principal investigators) from 10 European countries and focused on two areas: the Goban Spur (1 June 1993 to 31 May 1997: OMEX I, MAS3-CT93-0069) and the Iberian Margin (1 June 1997 to 31 May 2000: OMEX II-II, MAS3-CT97-0076). The author participated in the second phase of the project, which was focused on the upwelling region of the Iberian coast.

1.7.2 The Iberian Margin

The Iberian margin faces the North Atlantic Ocean and extends along the NW Iberian Peninsula, occupying the northern boundary (41° to 43°N) of the NW Africa upwelling system (Figure 9).

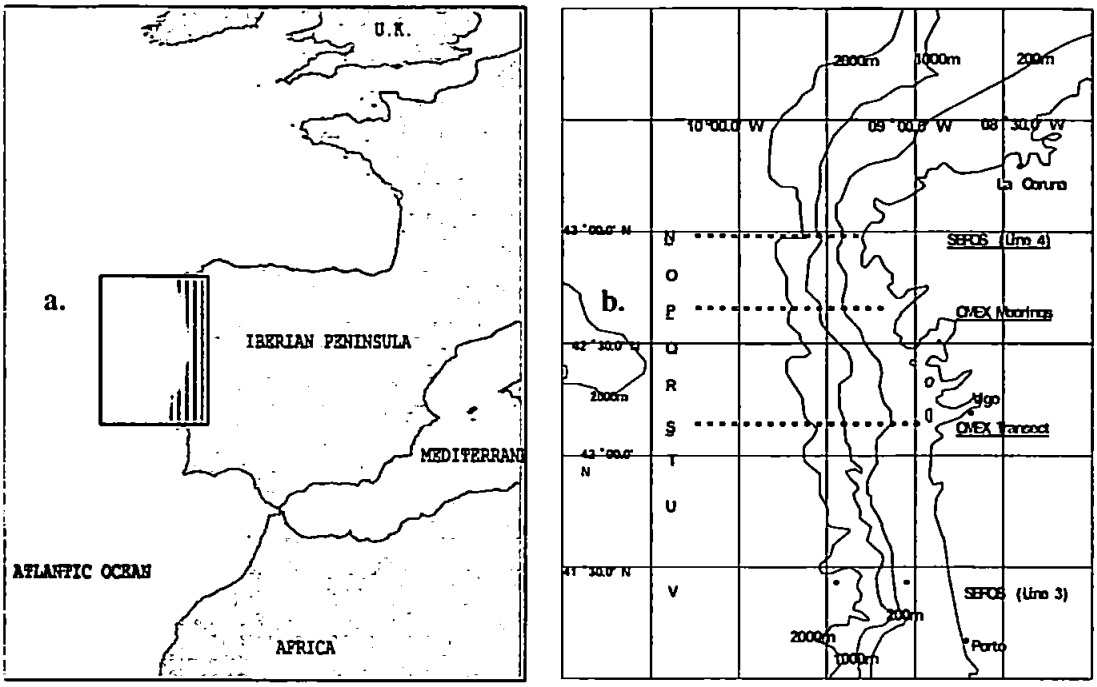

Figure 9a. Chart of the North-East Atlantic Continental Margin and the OMEX II – Phase II study area (light box). 9b. Chart of study area with depth contours and sampling transects N to V. Note: dashed lines represent transects sampled for DOM in this study.

The Iberian margin is a relatively narrow shelf with a steep slope. Coastal upwelling events typically predominate from June to September (Alvarez-Salgado *et al.*, 1993; Roson *et al.*, 1997) with associated offshore advective filaments (Haynes *et al.*, 1993). The upwelling intensity is subject to variable wind patterns which may result in periods of upwelling-relaxation or downwelling, especially during winter, causing current directions to reverse. A warm northward current along the slope (Haynes and Barton, 1990) with associated eddies is also observed during the winter period.

During the summer season, with the onset of the Portuguese trade winds, the Azores high pressure cell is located in the central North Atlantic ocean and the Greenland low pressure cell is diminished in intensity. The resulting atmospheric pressure field forces northerly winds along the Galician coast and cause upwelling. Cold, nutrient-rich Eastern North Atlantic Central Water (ENACW) is upwelled from 150-200m depth to above 50m (Alvarez-Salgado *et al.*, 1993). A narrow band of colder water is subsequently produced along much of the coast (Haynes *et al.*, 1993) as a result of the combined effects of the upwelling, the interacting subsurface waters and the Galician coastline (Castro *et al.*, 1994); see Figure 10.

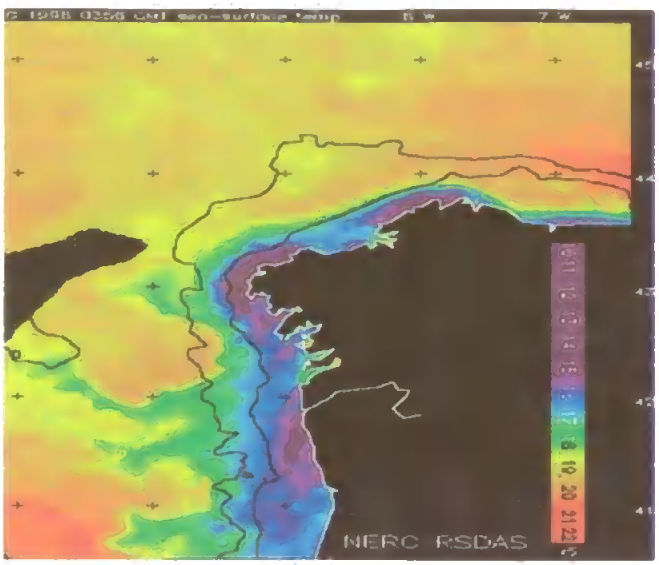

Figure 10. SeaWifs satellite image of the sea surface temperature (°C) off NW Iberian Peninsula on 05-Aug-1998 Courtesy of RSDAS, U.K. Note: the upwelling of colder waters is depicted in blue/violet and associated offshore filaments are in green.

This band appears to consist of narrow filaments of cool water that extend seaward. Filaments usually recur yearly at approximately the same sites at the Iberian coast and may extend 200-250km offshore. The filaments potentially export significant quantities of organic matter produced on the continental shelf, resulting in a seasonally intense cross-slope flux (OMEX II-Phase II Proposal). After upwelled water travels to the surface of the water column carrying nutrient-rich ENACW, productivity increases resulting in rapid growth and succession of biota. The surface water in the upwelling region becomes progressively modified with age as it moves away from the source due to exposure to light and following biological production. As upwelling is largely wind-driven, it is complex in both space and time, making it difficult to understand and model the system. Depending on the wind action, the duration and intensity of the upwelling events can vary, resulting in complex hydrological scenarios which can either enhance or lower primary production.

During the winter period, the Azores high-pressure cell is located off the north-western African coast, and the Greenland low-pressure cell has deepened and is located off the south-eastern coast of Greenland. The pressure gradient between the two systems results in an on-shore wind with a strong southerly component. Southerly winds create conditions for downwelling, forcing shelf waters into the coastal embayments (Rias) of the Iberian coast (Doval *et al.*, 1998) and generally preclude shelf-edge exchange (Castro *et al.*, 1997). Over the slope, a distinct northward warm and saline current (10 – 40 km wide; pers. obs.; Frouin *et al.*, 1990) extends from the surface down to about 200m (Figure 11). Below the surface mixed layer, ENACW

predominates until it mixes with Mediterranean Sea Outflow Water (MSOW) below 500m. MSOW extends northwards along the slope, parallel to the west coast of the Iberian Peninsula. Below 2500m, Labrador Sea Water (LSW) is transported northwards on the deep eastern boundary.

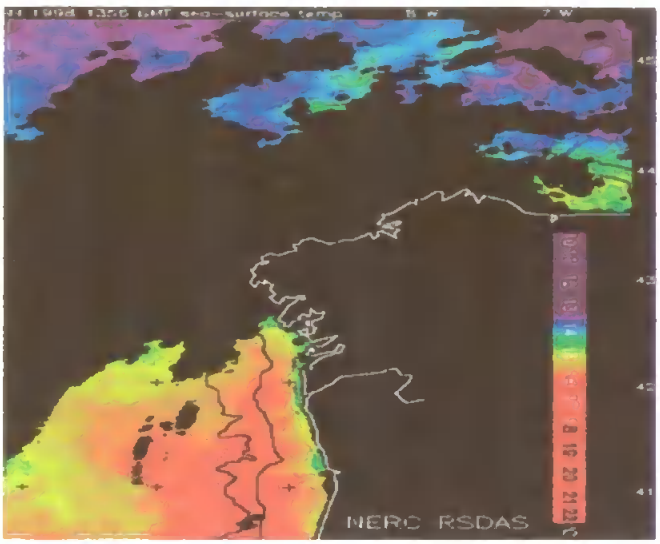

Figure 11. SeaWifs satellite image of the sea-surface temperature (°C) off the north-west coast of the Iberian Peninsula on 08-Jan-1998. Courtesy of RSDAS, U.K. Note: black colour is cloud coverage and land.

The incident warm and salty surface current hinders shelf to ocean exchange and evokes trapping of colder, fresh water from the Rias at the coast, resulting in nutrient enhancement and consequently higher biological activity. When the slope current reaches the north-west corner of Spain, it turns eastward and follows the coastline (Frouin *et al.*, 1990). Anticyclonic warm slope-water eddies (SWODDIES) that have been associated with this flow are located in the Bay of Biscay (OMEX II-Phase II Proposal), possibly exporting organic matter from the shelf to the open ocean, but estimates of exchange rates are lacking. The aforementioned processes that are characteristic of the Iberian margin upwelling system generally occur on a seasonal scale and are summarised in Figure 12.

OM exchange on a localised and regional scale at the Iberian margin may thus be facilitated by ocean margin phenomena such as seasonal upwelling and filaments, terrestrial water input at the coast, vertical flux of biomass from the surface ocean and the creation of intermediate and benthic nepheloid layers that extend offshore (see Figure 13). OM exchange may equally be hindered by the presence of different dynamic water masses such as the winter surface current at the slope and the Mediterranean Outflow water mass.

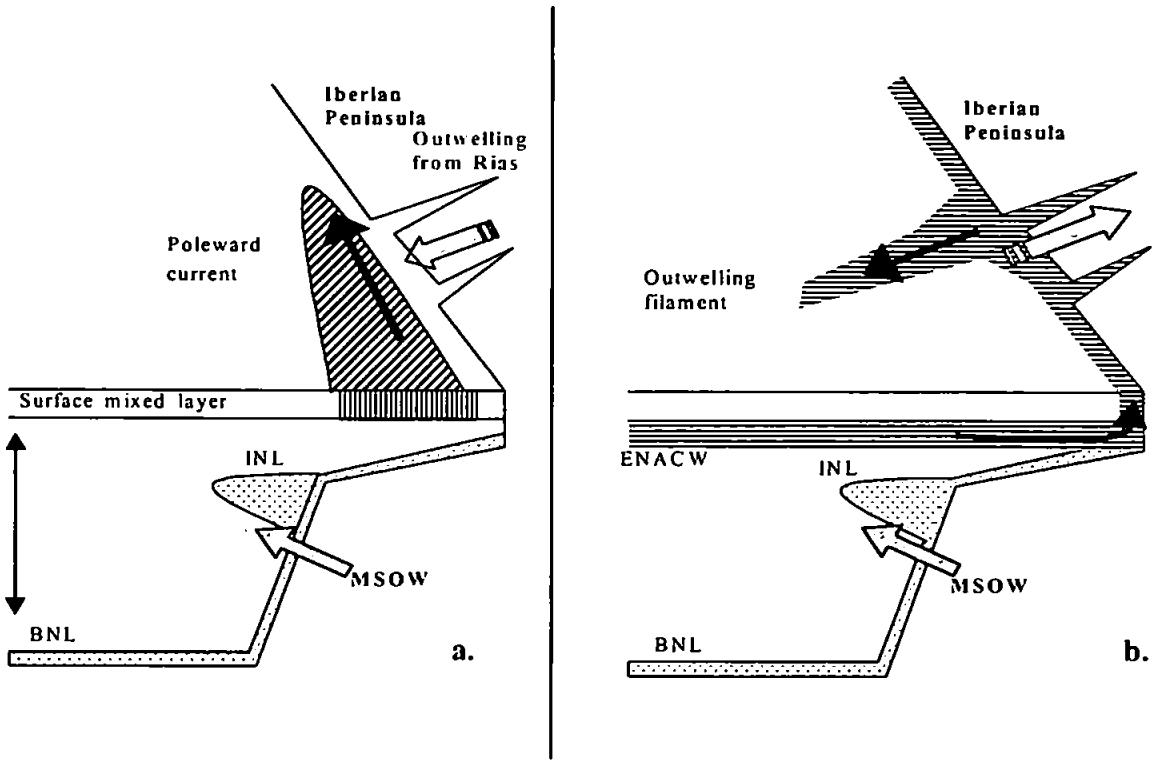

Figure 12. A schematic of the Iberian margin with characteristic physical processes that occur during the winter (a.) and summer (b.) seasons. INL – Intermediate nepheloid layer; MSOW – Mediterranean Sea Outflow Water; ENACW – Eastern North Atlantic Central Water; BNL – Benthic Nepheloid Layer. Note: Not to scale.

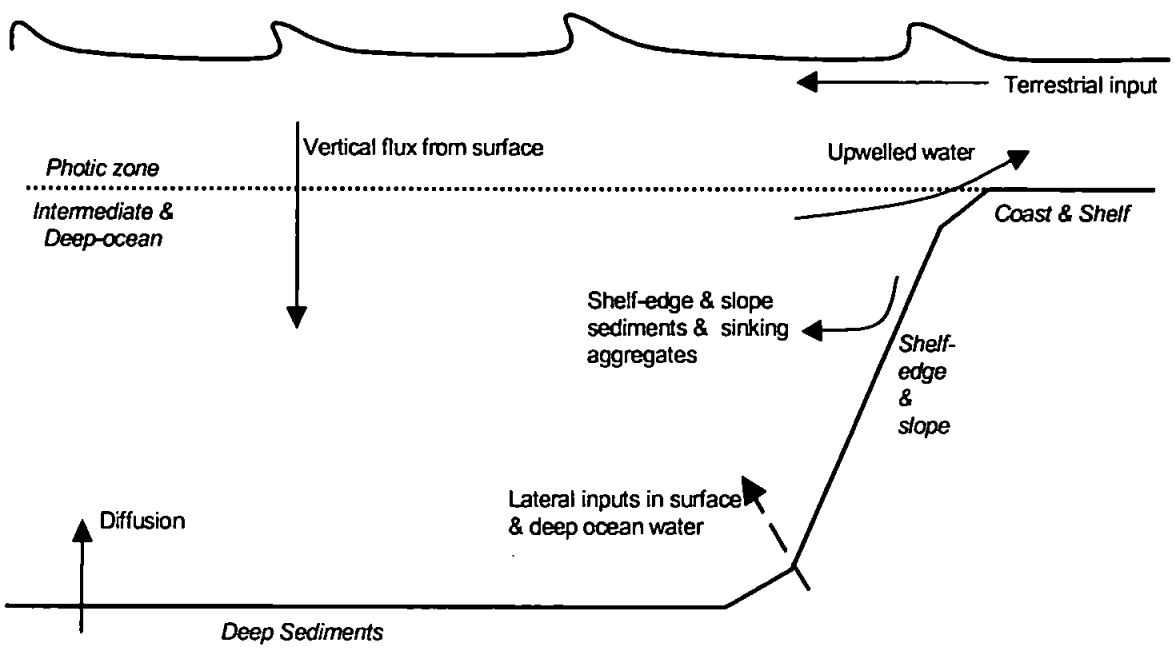

Figure 13. Schematic diagram representing physical processes that may facilitate OM exchange at the Iberian margin.

1.8 DOC at Ocean Margins and Upwelling Areas

Recent investigations across continental shelves have shown the seasonal accumulation of DOC in the mixed layer and localised concentration enhancement in bottom nepheloid layers (Miller, pers. comm.). However, the fate of this material and the driving mechanisms behind its biogeochemical cycling are not well known. Table 7 summarises published DOC concentrations and associated key findings at ocean margins.

Table 7. Summary of DOC concentrations at ocean margin regions.

Author	Area	DOC (μM-C)	Notes
Suzuki and Tanoue, 1991	Delaware Estuary	240 – 480	DOC recycled at front between continental shelf & open sea
	East China Sea	255 – 427	
Guo et al., 1995	Gulf of Mexico	45 - 80	Lowest DOC found in deeper waters (>600m)
Zweifel et al., 1995	Bothnian Sea	250 - 400	DOC accumulation due to P-limitation
Winter et al., 1996	Swartkops estuary, South Africa	Typically ~83 - ~333	DOC outwelled from estuary
Doval et al., 1997; 1998	Ria de Vigo, Spain	<70 - >100	Extreme concentrations during upwelling season
Bauer and Druffel, 1998	West N. Atlantic		More input from margins than from recent surface production.
	Surface slope:	~91	
	300 – 1000m:	~52	
	East N. Pacific		
	Surface slope:	~83	
	300 – 1000m:	~51	
Dafner et al., 1999	Gulf of Cadiz		*NASW* – N. Atlantic Surface Water; *NACW* – N. Atlantic Central Water; *MSOW* – Mediterranean Sea Outflow Water located at ~350m depth.
	Shelf Water:	61 – 89	
	NASW:	48 – 64	
	NACW:	49 – 55	
	MSOW:	52 – 58	
Scott et al., 2000	Antarctic coastal site	30 – 260	July to October

The primary objectives of this project were to identify and understand the processes controlling the biogeochemical cycling of DOC in cross-margin exchange at the Iberian upwelling region. The project thus aims a.) to define seasonal and spatial patterns of DOC in relation to hydrodynamic and biological processes and b) to determine its fate (e.g. fluxes) at the Iberian ocean margin. This was achieved by near-real-time on board ship determination of DOC and DON[3] in surface waters and through vertical sections across the shelf, coupled to hydrodynamic and biological data. DOC and DON distributions at the Iberian slope and offshore waters have not been measured before and thus the data produced is original.

[3] DON concentrations in this study were used as a complementary parameter to the DOC measurements

Chapter 2

2. THE ANALYTICAL DETERMINATION OF DOM USING HTCO

2.1 Introduction

The composition of dissolved organic matter (DOM) is complex and largely uncharacterised, making the development of a single method for its determination very difficult. The favoured approach to measure DOM has been to determine bulk dissolved organic carbon (DOC), comprising approximately 50% of DOM as a proxy. DOC is oxidised to a single product (typically CO_2) which can be measured with higher sensitivity, accuracy and precision (Miller, 1996)

Historically, the measurement of DOC in seawater has been a challenging and often controversial procedure (Hopkinson et al., 1997). There was uncertainty in the accuracy of past (wet chemical oxidation, WCO) and current methods used (Hansell, 1993). This has resulted in limited and questionable information on the distribution of DOC in the global ocean, its spatial and temporal variability, and reactivity in the marine environment (Hopkinson et al., 1997). Current methodologies for the determination of dissolved organic carbon and nitrogen in seawater samples have been well documented and critically assessed by Cauwet (1999) and Spyres et al., (2000).

As measured by historical methods (e.g. WCO techniques), vertical distributions of DOC in the oceans were shown to be relatively homogeneous and it was presumed that the material was of a refractory nature. In 1988, Sugimura and Suzuki presented the high temperature catalytic oxidation (HTCO) method as a rapid and precise technique (± 1-2%) for the determination of non-volatile DOC in seawater. Their measurements exhibited 2 to 10 times higher concentrations of DOC (180-280 μM) and DON (10-45 μM) in surface oceanic waters than previously reported with WCO methods. These new findings instigated the re-evaluation of the marine DOC pool and its role in global carbon cycling. Following studies focused on verifying the technique's capability to oxidise previously undetected oceanic DOC (Suzuki and Tanoue, 1991; Kepkay and Wells, 1992; Martin and Fitzwater, 1992; Ogawa and Ogura, 1992; Tanoue, 1992). Analysts using similar HTCO instrumentation were largely unable to reproduce Sugimura and Suzuki's results (Sharp, *et al.*, 1993; Sharp, 1997). Suzuki (1993) later issued a statement retracting the Sugimura and Suzuki (1988) data.

---

for the further elucidation of the main biological processes occuring at the Iberian ocean margin.

Controversy surrounding the technique's reliability led to an organised DOC/DON Workshop from 15th –19th July 1991 in Seattle, Washington, USA. Leading analysts gathered to clarify some of the problems with HTCO methods and to recommend appropriate HTCO methodologies (Fitzwater and Martin, 1993). Investigations were aimed at developing a standard methodology for the determination of DOC and DON using appropriate HTCO instrumentation. From such studies, HTCO techniques were improved and it is now possible to routinely measure DOC and TDN both accurately and precisely (Sharp, 1997).

The high temperature catalytic oxidation-discrete injection (HTCO-DI) method for liquid samples is currently the preferred analytical technique for the determination of DOC in natural water samples and is recommended in the Joint Global Ocean Flux Study (JGOFS) Protocols manual (1994). It is recognised as the most efficient analytical technique for the oxidation of DOM in seawater (Hedges et al., 1993). This approach yields equivalent or greater amounts of DOC than wet chemical oxidation (WCO) methods, is suitable for routine analyses and is stable for shipboard determinations. The application of HTCO for the determination of DOC presents a number of interesting analytical challenges. However, with appropriate use, HTCO determinations can be rapid and of high precision allowing the analyst to accurately evaluate the size of the DOM pool and detect small changes in concentration (~1μM-C) that may result from marine biogeochemical processes.

The procedure for the determination of DOC in natural water samples by HTCO consists of several distinct stages: (i) sampling, (ii) preservation (*i.e.* filtration, acidification and cold storage), (iii) decarbonation (*i.e.* removal of dissolved inorganic carbon, DIC) and (iv) analysis. These are discussed in more detail in the following sections. Carbon can be classified into several operationally defined fractions (e.g. particulate and dissolved organic carbon). For the different classes of DOC and other aquatic carbon species, see Figure 2.

2.2 Sampling

Sample collection protocols should be designed to minimise changes in sample composition resulting from contamination, sorption onto container walls, biological and flocculation processes (Sharp, 1993). Due to the low background concentrations of DOC (40-50 μM C) in marine waters (Alvarez-Salgado & Miller, 1998), seawater samples can easily be contaminated *via*: (i) the atmosphere (e.g. engine exhaust fume aerosols), (ii) sampling bottles (i.e. incomplete cleaning, leaching of organic substances from new plastic components), and (iii) careless handling (i.e. not wearing gloves, dirty laboratory working environment). *Niskin* ™and *Go-Flo* ™

bottles are commonly used for sampling the seawater column; they are designed to minimise contamination and *Go-Flo™* can pass the air/sea interface closed. This avoids contamination from the sea-surface micro-layer where surface-active organic materials are present in high concentrations (Liss and Duce, 1997; Kuznetsova and Lee, 2001). Glass and plastic containers (e.g. polysulphone, polycarbonate) that have been thoroughly cleaned and 'aged' (i.e. all leachable components removed *via* soaking in carbon-free water) are used as temporary storage bottles (Sharp, 1993; Wangersky, 1993; Miller, 1996). Sorption of DOC onto the container walls is reported to be negligible (Hedges et al., 1993; Tanoue, 1993; Tupas et al., 1994).

The sampling procedure used in the current study was that based on recommendations of Miller (1996) and references therein. A rigorous protocol was adhered to for sample compatibility and various precautions were taken to ensure the minimisation of contamination. Polythene (powder-free) gloves were worn throughout handling procedures. The sample collection bottles were either all-glass or glass-with-*Teflon™*-cap 250ml bottles that had been pre-cleaned. The sample was pressure filtered (high-purity oxygen) through pre-combusted glass fibre filters (*Whatman*, GFF) in a pre-cleaned (see Section 2.1 for cleaning procedure) all-glass filtration system. The samples were collected in pre-combusted 10ml glass ampoules, acidified with high-quality phosphoric acid and flame sealed. All reagents used were of high quality (*e.g.* ultra high purity-UHP oxygen, *Aristar™* chemicals). UV-irradiated *Milli-Q™* water (*Millipore*) was used for rinsing glassware and preparing standard solutions.

2.2.1. Pre-sampling preparation

Glassware used for the collection and filtration of the sample was soaked overnight in a 2% *Decon-90™* (detergent) solution, and subsequently rinsed with copious amounts of UV-irradiated *Milli-Q™*. The efficiency of the washing/rinsing procedure used was investigated. Two 250ml glass bottles that were used for sampling were soaked in the *Decon-90™* solution overnight and subsequently rinsed with *R/O™* and *Milli-Q™* water. Results (Figure 14) showed that contaminants and any residual detergent were effectively removed from the glassware after rinsing. Note that the last measurements of *Milli-Q™* rinse water were negative, this being a result of the subtraction of the analytical system blank. Nevertheless, the final concentration is not significantly different from zero (i.e. $\pm 2\sigma$).

Further inspection (06/05/99) of the washing procedure on quartz tubes (50ml) showed that there was a decrease in detectable remnants of the *Decon-90™* solution after rinsing with *Milli-Q™* water (i.e. DOC concentration of *Milli-Q™* water in quartz tube before rinsing: 10±3μM-C

and after rinsing: 7±5μM-C). The high standard errors of the measurements are most likely due to operation near the analytical system's limit of detection (see section 2.5.5.).

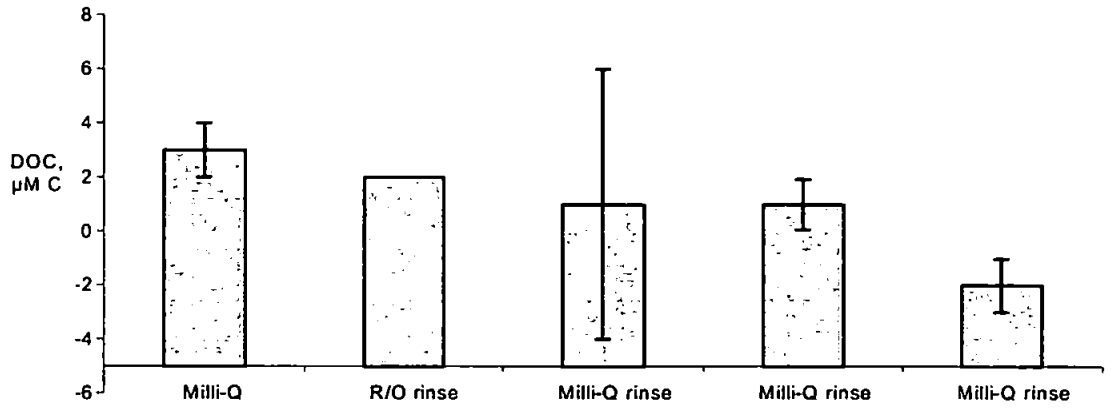

Figure 14. Mean DOC concentration (n = 3 - 5) in Milli-Q rinse-water depicting residual carbon contamination from a 250ml glass bottle. Note: analytical system blank was subtracted from values (see section 2.6.2.); error bars = standard deviation.

Glassware was subsequently placed in a closed drying oven until completely dry. To minimise contamination from the atmosphere, the openings of the glassware were covered with ashed (450°C, 4 hrs) aluminium foil and stored in a cupboard for that purpose. Glass ampoules, glass fibre filters and any other small glass components used in the sample collection and handling were combusted in a furnace (*Gallenkamp* ™ Muffle Furnace) at 450°C for >4 hrs to remove all potential organic contaminants.

2.2.2 Sample collection

To sample the water column, *Niskin* ™ bottles (10L) mounted on a CTD rosette were 'fired' at the specified depth of the water column. For surface (~1-3m depth) sampling underway, the on-board non-toxic supply system was used. Water was drawn at the earliest opportunity (*i.e.* after water collection for gases) into 250ml glass bottles without it coming into contact with the *Niskin* ™ bottle spout. The glass bottle was rinsed with the sample water three times before retention of the sample for subsequent filtration, acidification and storage (Figure 15).

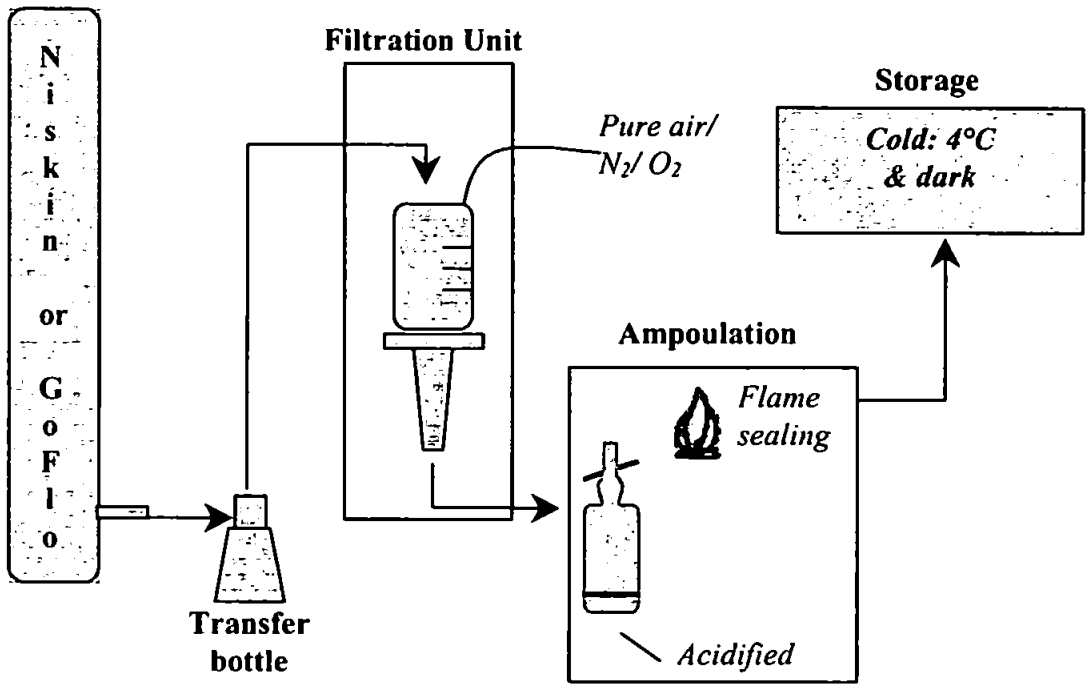

Figure 15. Schematic representation of the DOC sampling and preservation process (not to scale).

Samples were collected for the determination of DOC and TDN and some were analysed on-board OMEX II-II cruises CD110B (R.R.S. Charles Darwin; 06 to19-Jan-98), ST0898 (R.V. *Prof. Shtokman*; 01 to 12-Aug-98), M43/2 (R.V. *Meteor*; 28-Dec-98 to 14-Jan-99) and BG9919 (R.V. *Belgica*; 04 to 18-Sep-99) (Table 8). Three main transects in total (i.e. N, P and S; Figure 16) were sampled on a seasonal and inter-annual scale during the OMEX II-II cruises that the author participated in. It was not possible to sample all the designated stations on each cruise due to poor weather conditions encountered during the winter cruises (i.e. CD110B – Jan'98 and M43/2 – Jan'99).

Table 8 Summary of samples collected during OMEX II-II cruises.

Cruise	Transect	No. Stations	Co-ordinates	Depth range, m	No. Samples
CD110B	V	2	41°25N	8 – 1926	21
	P	4	42°40N	7 – 2820	42
	Surface	Underway		1	47
ST0898	N	7	43°00N	5 – 3000	65
	P	6	42°40N	5 – 2000	58
	S	6	42°10N	5 – 2000	34

Table 8 cont.

Cruise	Transect	No. Stations	Co-ordinates	Depth range, m	No. Samples
M43/2	S	8	42°10N	10 – 2700	92
	Bottom Lander	1	42°10N, 09°35W	1900	1
M43/2	Canyon 1	1	39°30N, 09°55W	10 – 3500	21
	Canyon 2	1	39°34N, 10°09W	20 – 4000	7
	Cadiz Bay	1	36°33N, 08°30W	10 – 2000	20
	Surface	Underway		3	27
BG9919	N	5	43°00N	5 – 1750	62
	P	8	42°40N	5 – 1750	94
	S	6	42°10N	5 – 1728	65
	Cape Finisterre	1	43°12N, 09°15W	5 – 80	5
	Surface	Underway		3	37
TOTAL					**698**

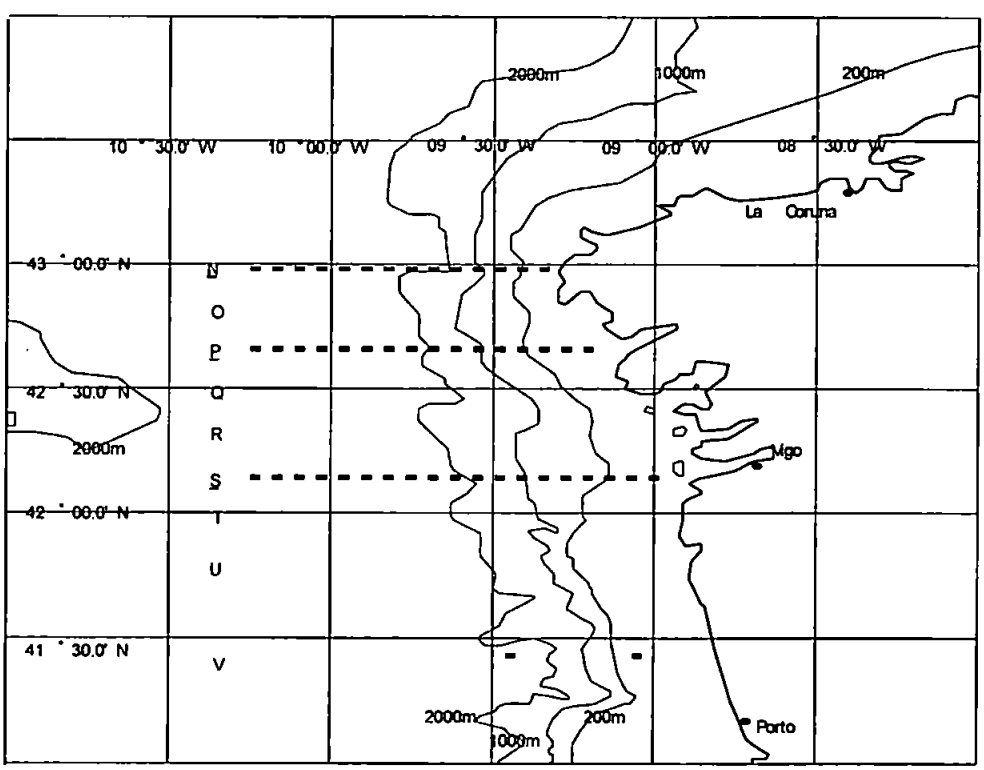

Figure 16 . Map of the OMEX II-II sampling region with cross-slope transects sampled for DOC/TDN marked with a dashed line (reference transects are underlined).

2.3 Preservation

2.3.1 Filtration

Filtration, immediately after sample collection, is recommended since biological processes occurring within the sample could result in a net increase (i.e. release from any organisms present) or decrease of DOC (i.e. microbial consumption) within hours of collection. Particulate organic carbon (POC) and the majority of organisms present in the sample can be removed by filtration; the nominal cut-off commonly used ranges from 0.2 to 0.7 μm. Contamination by carbon leaching from filters with plastic components may be significant and should be removed by thorough cleaning.

Glass fibre filters (e.g. GFF, nominal cut-off is 0.7 μm) are robust and are easily cleaned in a furnace by combustion at high temperatures (e.g. 450°C for >4 hours). Negligible contamination from GFF filters has been observed (Tanoue, 1992), although they allow passage of some particles (e.g. bacteria and viruses) (Norrman, 1993). However, the fraction of the POC in the filtrate is considered to be negligible (i.e. ~1 μM-C) compared to the DOC and is lost in the precision error of the analysis. Moran *et al.* (1999) recently investigated DOC adsorption onto GFF filters. Their results indicate that there was some adsorption of DOC (~2-5μM C) onto the filter when used for filtering seawater for POC analysis. However, with increasing sensitivity and precision of HTCO analytical systems (i.e. ~1 - 2% coefficient of variation, CV; Sharp, 1997) it is essential that filtration artefacts are quantified and accounted for in sample analyses.

Alternative filters with a smaller cut-off and defined pore size (0.2 μm) include polycarbonate and polysulphone filters. However, investigations have shown that these filters can significantly contaminate the sample by leaching carbon from their matrix (e.g. up to ~20μM-C excess, Norrman, 1993; Hansell et al., 1995). Cleaning filters with an organic matrix is a very time-consuming process. A promising alternative is the *Anopore™* Al_2O_3 (inorganic matrix) filter with pore sizes ranging from 0.02 to 0.7 μm. Investigations have shown that, with the use of *Anopore™* filters, there is little quantifiable effect on DOC concentrations in water samples (Williams et al., 1993). However, their rapid clogging presents a problem when filtering highly productive and turbid waters (i.e. waters with high concentrations of phytoplanktonic organisms). Clogging reduces the flow rate, may reduce the effective pore size of the filter, and increases the back-pressure with time causing DOC from cell lysis to leach into the filtrate

(Mopper and Qian, 1998). In oligotrophic waters where the particle loading is minimal (<1% of total organic carbon, TOC) the filtration step may be omitted (Wangersky, 1993).

For the OMEX II-II programme, a pre-cleaned all-glass filtration system fitted with a combusted glass fibre filter (GFF, 47mm ∅) was used. Although the nominal cut-off of the GFF is 0.7μm effectively allowing bacteria through (Norrman, 1993) they are commonly used for practical & comparative reasons (Fitzwater and Martin, 1993; Hansell, 1993; Hedges *et al.*, 1993; Cauwet, 1994; Thomas *et al.*, 1995; Miller, 1996; Hopkinson *et al.*, 1997). The filtration system (Figure 18) works as a positive pressure system (<5psi); oxygen is purged *via* a gas line delivered through a pressure regulator to a narrow vent on top of the lid of the filtration unit.

An investigation comparing the use of GFF with the *Anopore™*(0.2μm pore size, 47mm ∅) was carried out on estuarine samples (salinity 0 – 35; Tamar Estuary) in October, 1998. Four stations along the Tamar Estuary were sampled filtering one aliquot through a GFF filter and a replicate aliquot through an *Anopore™* filter mounted on a GFF. The combined GFF with *Anopore™* was done for greater stability because the latter are fragile and can break easily. The results showed that in three out of four stations, DOC concentrations were higher when filtered through the *Anopore™* filter (Figure 17).

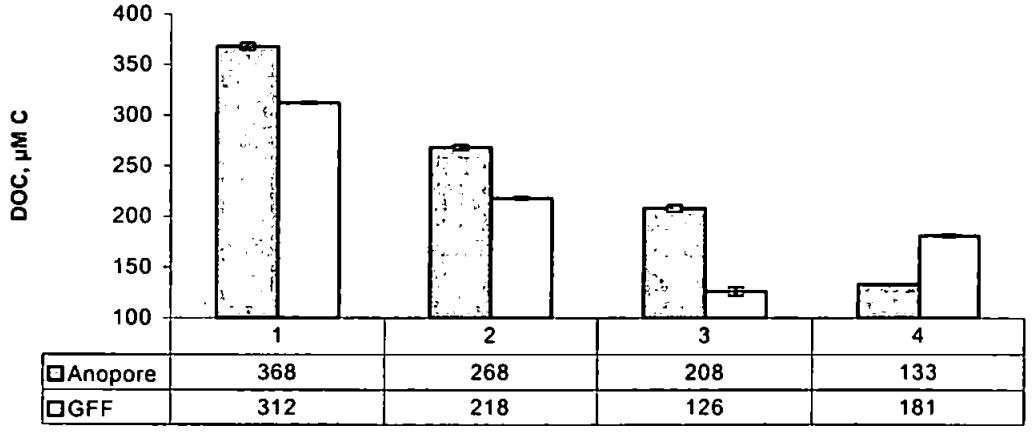

Figure 17. A comparison of DOC concentrations (μM C) in estuarine samples 1-4 after filtration with an Anopore™ filter and a GFF filter.

The filter blank for the *Anopore™* was found to be within analytical error, suggesting that the filtration apparatus (i.e. filters and glass units) was not releasing carbon-contaminants. Previous investigations have shown little alteration in DOC analysis due to the *Anopore™* (Williams *et al.*, 1993), however their small pore size effectively reduces the flow rate and causes quick clogging when filtering highly productive and turbid waters (pers. obs.). This may induce higher

pressure in the filtration process causing the breakage of cells and subsequent release of DOM into the filtrate. This could account for the relatively high DOC concentrations in samples filtered using an *Anopore™*.

Analyses of *Milli-Q™* filtered through disposable GFF filter devices (25mm ∅, polypropylene housing) resulted in a random filtration blank (3 - 23μM C) rendering them inappropriate for DOC measurements.

2.3.2. Acidification

When immediate analysis is not possible, preservation of the samples is necessary (*i.e.* acidification and cold storage). Sample acidification to pH 2 - 3 is performed to remove DIC and to arrest biological processes. Mercuric chloride had been used until it was suggested that it might deactivate the catalyst (Wangersky, 1993; Bauer et al., 1993). Although both hydrochloric acid (HCl) and orthophosphoric acid (H_3PO_4) are used, H_3PO_4 is preferred to HCl because the Cl^- ion may corrode the infrared gas detector cell (Sharp, 1993). High purity orthophosphoric acid is commercially available and does not contribute significantly to the procedural blank (Sugimura and Suzuki, 1988; Norrman, 1993; Tupas et al., 1994; Miller, 1996). It is also possible to acidify seawater samples with a smaller volume of H_3PO_4 than HCl of the same concentration as H_3PO_4 is tri-protonated (i.e. $3H^+$).

The samples were acidified to pH <3 by adding 30μl H_3PO_4 (85% v/v, *Aristar* or high-grade orthophosphoric acid) to approximately 10ml of sample, using a high-precision dispenser (*Volac*) with a glass tip. Potential effects of acidification include the production of volatile products from hydrolysis of organic matter, precipitation of macromolecules and for DON, absorption of atmospheric ammonia and volatile organic amines (Sharp, 1993) but these are unlikely to be quantitatively significant. However, no studies on such acidification effects have been reported.

2.3.3. Storage

After acidification, the glass ampoules containing the sample were flame-sealed (butane gas) and when immediate analysis was not possible they were stored cold (~4°C) in the dark. Common methods of storage of acidified samples include quick freezing to –20°C, and cold storage at 4°C. Tupas *et al.* (1994) found that there were insignificant differences between freezing and cold storage when samples are acidified. However, cold storage alone (*i.e.* without

acidification) is not an appropriate preservation method (Tupas *et al.*, 1994). It is recommended that airtight glass ampoules should be used for the storage of samples as plastic containers can leach organic substances and contaminate the sample over time (Fry et al., 1996).

The maximum storage time for some samples from the Jan'98 and Aug'98 cruises was 11 months. It has been shown that acidification (H_3PO_4) and subsequent cold storage (5°C) up to 15 months does not have a significant effect on the stability of the water sample (Wiebinga and de Baar, 1998).

2.4 Decarbonation

DIC concentration is 10-20 times the DOC concentration in seawater and therefore it must be removed before analysis. This was achieved by purging the acidified sample with CO_2-free gas (i.e. ultra high purity (UHP) oxygen) passed through a hydrocarbon trap and molecular sieve (*Fissons*, UK) to remove any remaining CO_2 and drying trap to remove moisture (Bauer et al., 1993). The sample was purged for approximately 20minutes at a rate of ~100ml.min^{-1} through a pre-combusted glass Pasteur pipette. A constant purging time for all samples was followed to ensure reproducibility. Contamination from UHP gas is not significant (Miller, 1996), but purging removes organic volatiles from the sample. The volatile organic carbon (VOC) fraction lost is usually minor (<1% of total organic carbon), thus the error introduced is generally insignificant (Mopper and Qian, 1998).

The success of the DIC removal largely depends on the gas flow rate, the duration of the flow, the pH of the sample and its volume. It is suggested that for small volume samples (<40ml) a flow rate of 100 - 120 ml min^{-1} for 6 - 8 minutes is found to be sufficient for complete removal of DIC (JGOFS, 1994). Some commercial total organic carbon (TOC) analysers (e.g. *Shimadzu TOC-5000™*) are able to measure DOC and DIC, thus presenting a practical way to determine the purging specifications. A simple decarbonation test was thus performed by analysing a reference seawater sample of known TOC concentration (approx. 45 µM-C) at 5 minute intervals of continuous purging with high purity oxygen gas at a steady flow-rate for a total of 35 minutes. The results (Figure 18) showed that for a 10ml seawater sample purged at a flow rate of 150 ml min^{-1}, at least 15 minutes were necessary for complete removal of DIC. This agrees with the findings of Peltzer and Brewer (1993) who determined that for a 100 ml seawater sample purged at 175 ml min^{-1} flow rate, more than 20 minutes were needed for complete removal of IC. The differences observed between JGOFS recommended purging

times and the results from this study could be due to a number of factors including the initial amount of inorganic carbon.

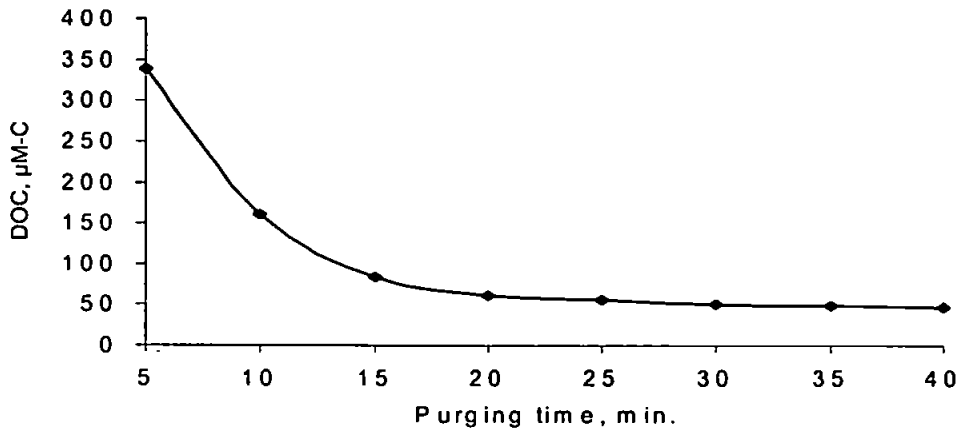

Figure 18. A time-series plot from a decarbonation test (i.e. purging of CO_2 from a deep-oceanic seawater sample).

Coagulation of colloidal matter on the bubbles (Kepkay and Johnson, 1989), flocculation and precipitation processes during purging could result in heterogeneity of the sample and therefore further mixing of the sample prior to analysis may be necessary (Sharp, 1993).

2.5 Analysis

The determination of DOC involves the complete oxidation of organic matter in a sample to CO_2 through the interaction with a catalyst, usually impregnated with platinum (Pt), maintained at high temperatures (>680°C). The gas produced is subsequently measured with a CO_2-specific detector.

2.5.1 Principle of Operation

There are two types of HTCO methods: (i) dry combustion and (ii) direct aqueous injection. The dry combustion method involves acidification and drying of the sample, and subsequent combustion of the residue in a sealed tube usually in the presence of a catalyst; copper oxide or platinum-based catalysts are commonly used. Following combustion, the gas stream is passed through a number of purifiers and traps. After purification, the CO_2 gas produced is quantified using an infrared gas analyser (IRGA). There are some major disadvantages associated with this technique that limit its use, including the high susceptibility to contamination (Fry et al.,

1996) and the labour-intensive analytical procedure. In addition, the analytical system cannot be automated and is restricted to laboratory use only (i.e. not suitable for ship-board fieldwork). Dry combustion is usually used in stable isotope analysis of DOC, because it can analyse relatively large samples, providing a sufficiently high analytical signal (Mopper and Qian, 1998).

Direct injection of aqueous solution is the preferred technique in the measurement of DOC in seawater samples and this technique was used here. Such systems operate on the principle of high temperature catalytic oxidation of organic carbon compounds in aqueous samples and the subsequent quantification of the generated CO_2 by an IRGA. An aliquot (e.g. 200 µl typical volume) of each sample is manually or automatically injected onto the oxidation column filled with catalyst (e.g. platinum on aluminium oxide, cobalt oxide, copper oxide) at 600-900°C in a carbon-free, pure gas atmosphere (e.g. oxygen, nitrogen). The organic matter present in the sample is oxidised on the catalyst to CO_2. The stream of gas products is dried using a dehumidifier (e.g. electronic dehumidifier, magnesium perchlorate) and purified by means of gas scrubbers (e.g. halogen and halide scrubbers) and particle filters before final determination with the IRGA. The signal (voltage) from the IRGA is recorded using a data collection/integration system; the peak area is used to calculate the amount of carbon present in the sample. The system is calibrated using a carbon compound (e.g. potassium hydrogen phthalate, sulphathiazole, sodium bicarbonate, sucrose) diluted in low-carbon water (LCW). A schematic of a typical HTCO-discrete injection (HTCO-DI) system is presented in Figure 19.

2.5.2 Analytical System

The HTCO system used here is the one described by Alvarez-Salgado and Miller (1998). The instrumentation used for the analysis of DOC in the samples was a *Shimadzu TOC-5000™* analyser (Fig 20) coupled to an *Antek 705D™* nitrogen-specific chemiluminescence detector for the detection of total dissolved nitrogen (TDN). Dissolved inorganic nitrogen (DIN) data is subsequently subtracted from TDN to estimate dissolved organic nitrogen (DON). A *LiCor Li6252™* solid-state infrared gas analyser (IRGA) is incorporated for precise measurements of CO_2 during shipboard determination when vibrations can critically affect the *Shimadzu TOC-5000™* IRGA by significantly reducing the precision and accuracy of the measurements (Figure 20). The *Li6252™* and *TOC-5000™* detectors compared well when both used on land (paired *t*-test; P=0.05).

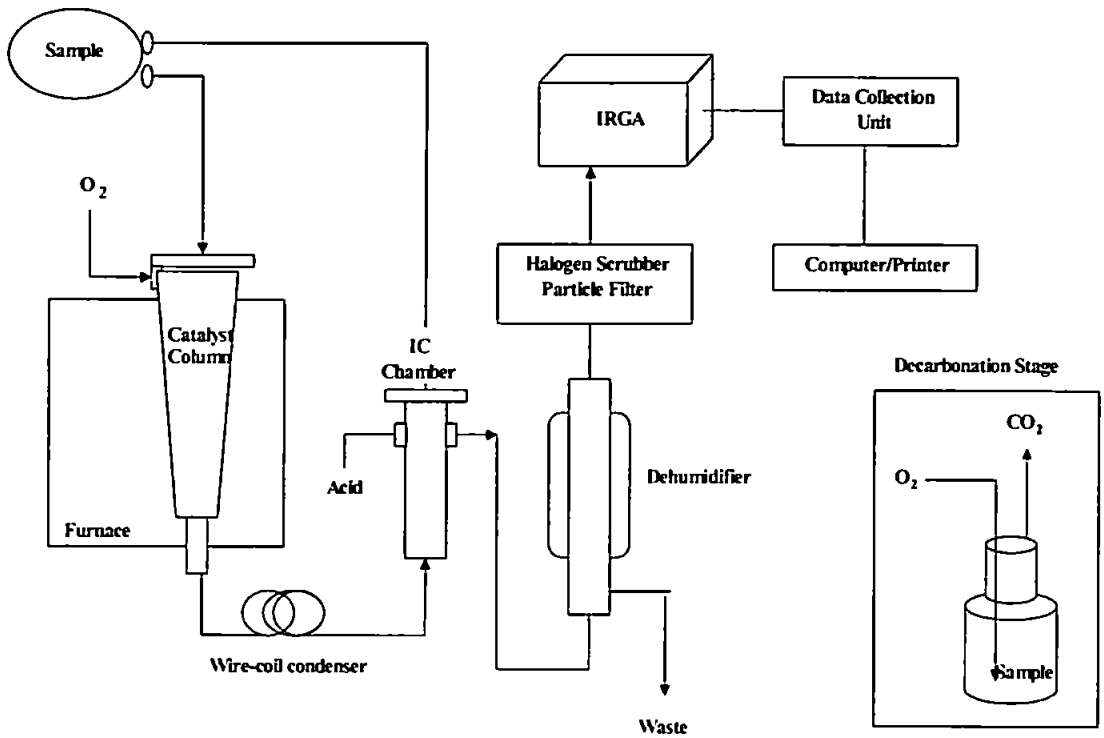

Figure 19. A simple schematic diagram of the Shimadzu TOC-5000™ high temperature catalytic oxidation – discrete injection (HTCO-DI) system for the analysis of DOC (not to scale) Note: IC - inorganic carbon; IRGA - infrared gas analyser

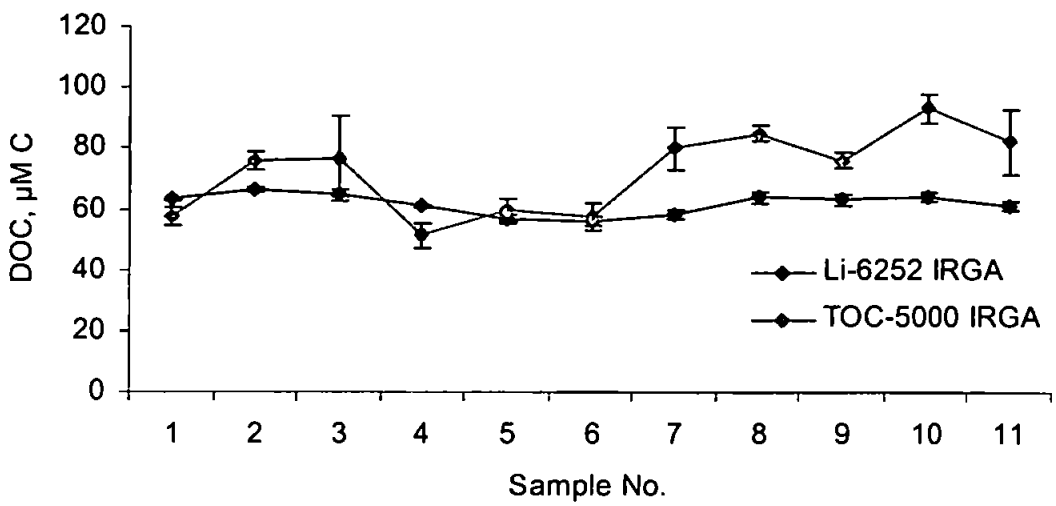

Figure 20. DOC concentrations (µM-C) measured at sea with the Li6252™ and TOC-5000™ IRGA simultaneously.

Oxygen passed through a hydrocarbon and organics trap (Fissons, UK) and a moisture trap (Drierite™) is delivered to the Shimadzu TOC-5000™ instrument and the Antek 705D™ [4] using a pressure regulator to maintain a constant flow rate of 150ml.min^{-1}.

The sample is automatically injected (200µl) into the TOC-5000™ catalyst column, held in the furnace (680°C). The sample is combusted in the column which consists of a quartz tube filled with a conditioned Shimadzu catalyst (0.5% Pt on Al_2O_3). Platinum (Pt) has over 98% efficiency in converting total hydrocarbons and CO to CO_2 under net oxidising conditions, and over 95% efficiency in converting inorganic nitrogen to NO (Bauer et al., 1993). However, no single amount, distribution or formulation of Pt or temperature has been found to be optimal for all applications (Bauer et al., 1993 & references therein). In addition, Miller (1996) found that the use of several catalysts (0.5%Pt-Al_2O_3, 100%Pt, and 3%Pt-Al_2O_3) did not significantly influence the recovery of caffeine-C.

The combustion products (CO_2; •NO, i.e. nitric oxide radicals; H_2O; etc.) are passed through a 25% H_3PO_4 solution (IC reaction vessel) which prevents CO_2 from dissolving into the water vapour. The gas stream is passed through an electronic dehumidifier, a halogen scrubber and a particle filter (20mm Ø, sub-micron membrane) before it enters the Li6252™ where CO_2 is quantitatively measured. The signal output is recorded by a PC-based integration software package (ProGC™, ATi Unicam). The stream then enters the Shimadzu IRGA where the CO_2 is measured and is recorded using a built-in integration system.

The gas stream is subsequently routed to the Antek 705D™ analyser (Figure 21) through additional particle filters and a charcoal/Drierite™ (water trap) trap to remove any particles, organic halides and water. 25% of the total flow from the Shimadzu is purged into the atmosphere so that back-pressure effects are eliminated. A vacuum pump is used to lower the pressure in the ozone reaction chamber; this increases the sensitivity and reduces background noise. In the reaction chamber, •NO reacts with O_3 to produce excited NO_2 that emits quantifiable light energy detected by a photo-multiplier tube and recorded onto the integration software package.

[4] The supply of oxygen to the Antek 705D™ ozone generator is 150 ml min^{-1}

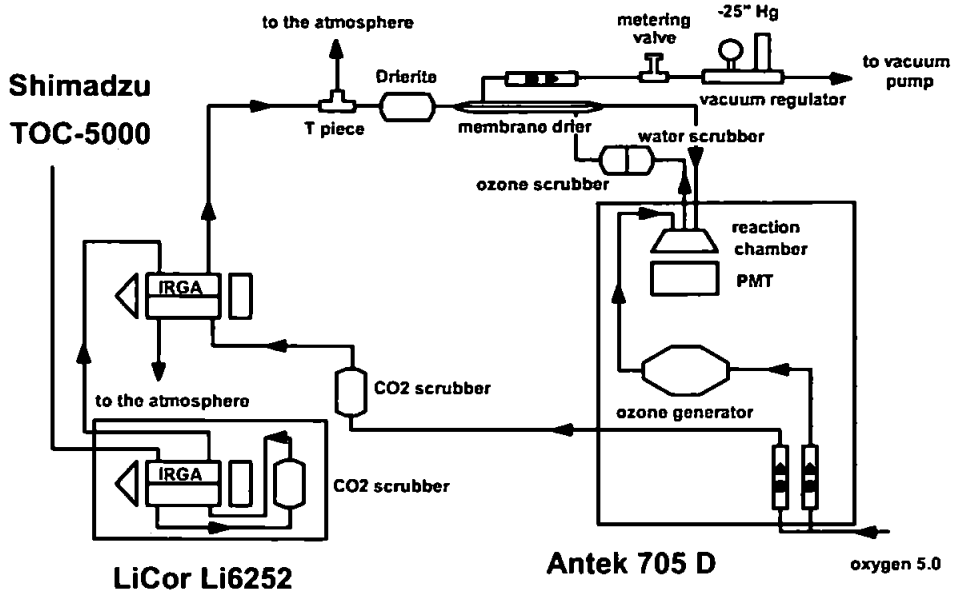

Figure 21. Schematic of HTCO equipment set-up detailing the interfacing of the LiCor Li6252™ IRGA detector to the Shimadzu TOC-5000™ and Antek 705D™ analysers. After Alvarez-Salgado & Miller, 1998

2.5.3 Calibration

All detectors of the analytical system used here were calibrated between sample batches and/or daily. The *LiCor Li6252™* IRGA detector is calibrated between sample batches by using a CO_2 gas standard (53ppm in N_2 gas). The *Shimadzu* and *Antek705D™* detectors were calibrated daily by the method of standard addition. It was determined that the analytical system gave a linear response (R^2 = >0.99) for concentrations up to 700μM-C.

A mixed stock solution was made with potassium hydrogen phthalate (KHP, $C_8H_5O_4K$) for the calibration of the DOC analyser and glycine (NH_2CH_2COOH) for the calibration of the TDN analyser. Five standards (approximate concentrations were 0, +25, +50, +100, +150 μM-C and 0, +3.125, +6.25, +12.5, +18.75 μM-N) were made daily by spiking *Milli-Q™* water with known amounts of stock solution. The stock solution was kept cold (~4°C) in the dark and was used for sample batches. New stock solutions were prepared for each batch analysis (i.e. used for a period of 1-2 months and then replaced). However, stock solution that was prepared as far back as 22-Aug-00, acidified and stored in the dark at 4°C, gave a response factor not significantly different (±2σ) to a fresh stock solution prepared on the day (22-Mar-01).

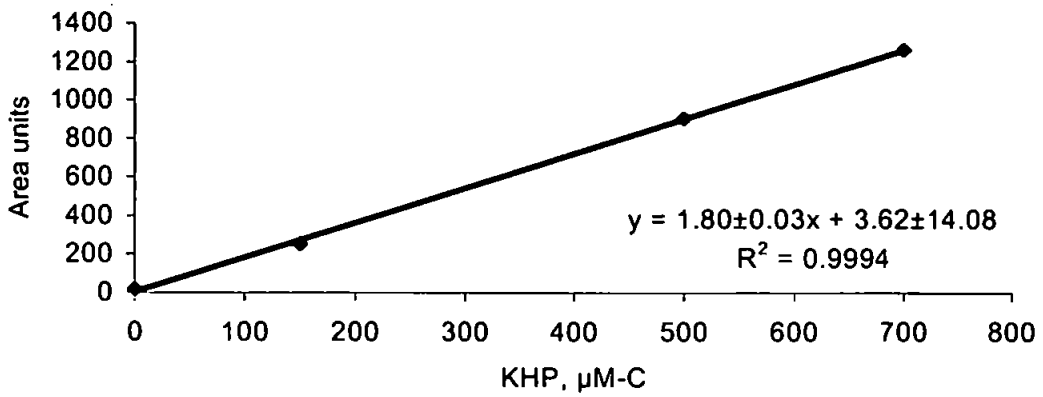

Figure 22. A linear regression plot of calibration standards (n=4) spiked with KHP-C; date of analysis 05-May-99.

Linear regressions (R^2=>0.99) were plotted for each daily calibration (Figure 22). The DOC concentration of each sample was defined by the mean peak area of replicate sample injections (n= 3 - 5), divided by the slope of the calibration curve. The slopes of each daily calibration plotted against time gave an indication of changes in sensitivity (Miller and Miller, 1993). It was demonstrated that for the measurement of DOC the HTCO system remained fairly stable throughout weekly analytical runs (Figure 23).

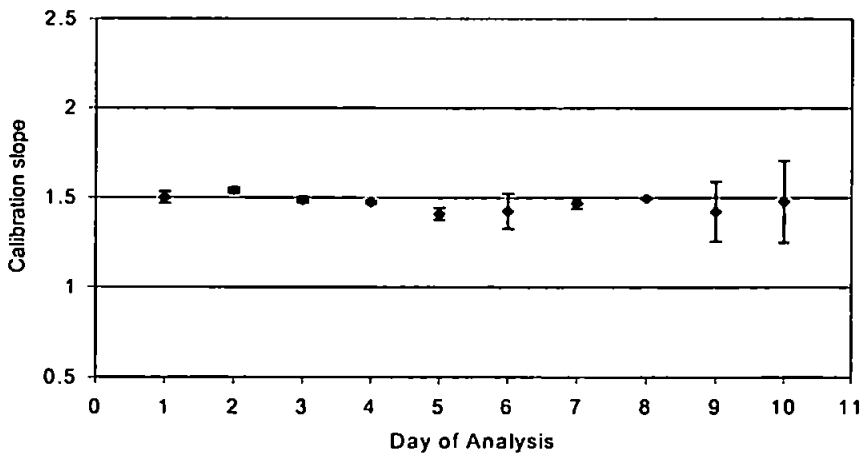

Figure 23. An example of the sensitivity of the Li6252™ IRGA detector; error bars = 2σ (daily calibration slopes on 08th until 17th Jan 1998).

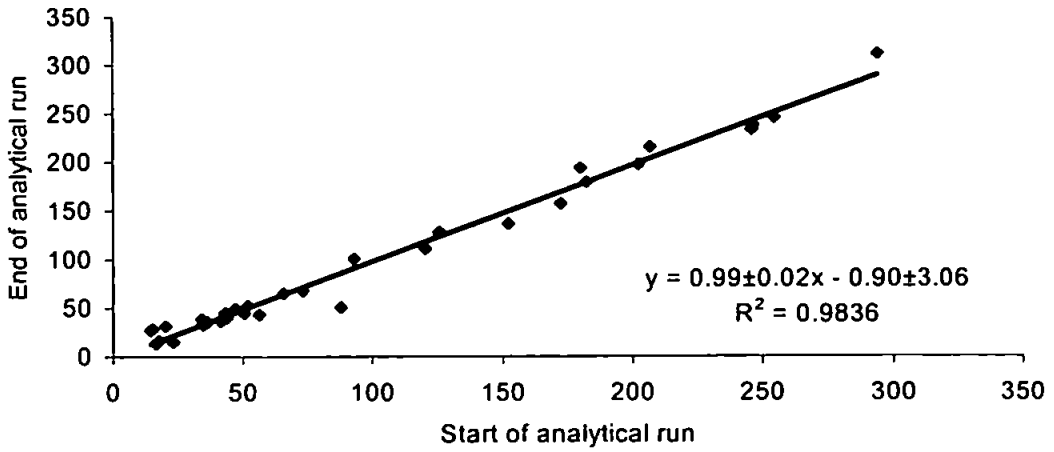

Figure 24. A regression plot of samples (n=32) analysed at the start and end of daily analytical runs (units are area units of the Li6252™ IRGA detector).

To determine whether on a daily analytical run there was any drift to the system response, calibration standards and samples were occasionally re-analysed at the start and end of a run. Results showed that there was no statistically significant drift to the daily response factor of the instrument.

A linear regression of the results (i.e. samples analysed at the start and end of daily analytical runs between 19/07/98 to 19/05/00) (Figure 24) produced a slope not significantly different from one (1) and a y-intercept not significantly different from zero (0), indicating that the analytical system was not subject to systematic drift.

2.5.4 Data handling

The signal output of the *LiCor Li6252™* IRGA detector and *Antek 705D™* chemiluminescence detector were recorded as signal output (peaks) (Figure 25) using the *ATi Unicam PROGC™* software package. The *PROGC™* software detects peaks and integrates the area under each peak from baseline (start of peak) to baseline (end of peak). Each trace/output was examined carefully for integration errors. In some cases, the 'integration baseline' under each peak had to be manually adjusted to cover the area of the peak from "baseline to baseline" in order to correct integration errors made by the software package.

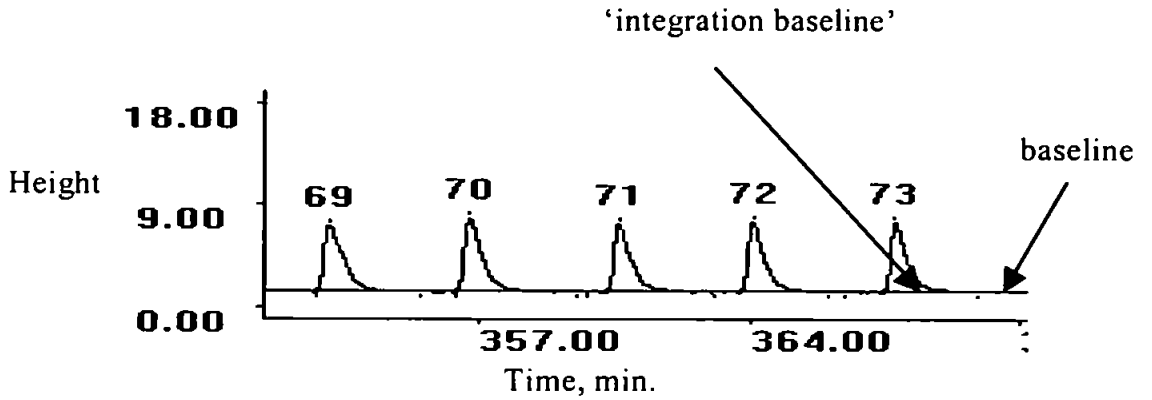

Figure 25. Example of a typical signal output trace with replicate peak injections, baseline and integration baseline.

The *Shimadzu TOC-5000™* detector output signal is recorded by a built-in *Shimadzu* integration system which does not allow correction of the 'integration baseline'.

Peak areas were tabulated on *Microsoft Excel'97* spreadsheets. The values were tabulated indicating:

- Analyser and detector used
- Catalyst used and the day it was installed
- Date of the analysis
- File name corresponding to the data
- Whether the analysis was shipboard or land-based
- Sample name (i.e. cruise, CTD cast, station and depth)
- Mean and standard deviation of each sample:
    - using all replicate injections for each sample
    - if appropriate, using the values remaining after the outlier rejection process

2.5.4.1 Outlier rejection criteria

To ensure quality control of data, each trace/ouput and values produced from the measurement of samples were examined for outliers. Among many, the following are very likely causes of outliers: sudden perturbations to the gas flow of the analytical system causing an abrupt flow-rate fluctuation, a gas-bubble being accidentally injected by the sample syringe onto the catalyst, a piece of salt or particle passing through the analytical system, electrical interference causing distortion to the baseline and peaks, etc. The main criteria for the rejection of peaks were:

- To reject odd-shaped peaks
- To use Dixon's Q-test for the detection of outliers.

A way of assessing a suspect measurement within a set of replicate injections, is to compare the difference between it and the measurement nearest to it in size, with the difference between the highest and lowest measurements. The ratio of these differences is known as Dixon's Q (Miller and Miller, 1993).

$$Q = [\text{suspect value} - \text{nearest value}] \div (\text{largest value} - \text{smallest value}) \qquad \textit{(Equation 1.)}$$

The critical values of Q for P=0.05 (i.e. 95% confidence) and P=0.01 (i.e. 99% confidence) are supplied in Table A.4 in Miller and Miller (1993). If the obtained value of Q exceeds the critical value, then the suspected outlier is rejected.

Carbon carry-over between samples (i.e. residual carbon remaining within the analytical system from a sample with a high concentration may contribute to subsequent measurements) occasionally occurred when a sample analysed was either contaminated or had a high carbon concentration (typically over 400μM-C). As a precautionary measure, the first couple of measurements from a set of 5-6 replicate injections of the next sample analysed were rejected as outliers.

Suspicious oceanic samples (>200μM-DOC and/or >25μM-TDN) were identified in the data set and depending on their oceanographic consistency (i.e. near-sample concentrations and published data), were excluded from the final data analysis. It is unlikely that samples exhibiting the above DOC and TDN concentrations are representative of the marine environment at the Iberian margin. This is because even during the highly productive upwelling season the Ria de Vigo waters at the Iberian margin typically exhibit >100μM-C (Doval et al., 1998). In addition, deep oceanic waters with a high total nitrogen content rarely exhibit TDN concentrations over 25μM-N (International Methods Comparison for DON, see section 2.7.2; Alvarez-Salgado, pers.comm.).

2.5.4.2 Equations used to process analytical datasets

The DOC concentration (C) of the analyte (μM-C) was calculated by dividing the mean peak area (x) of replicate sample injections by the analytical response factor, m (i.e. slope of the calibration curve) (Miller, 1996):

$$C = x \div m \qquad \textit{(Equation 2.)}$$

The standard deviation (σ) was calculated to define a degree of spread around the mean value (Miller and Miller, 1993):

$$\sigma = \sqrt{\frac{\Sigma\, x_i^{\,2}}{(n-1)} - \frac{(\Sigma\, x_i)^2}{n(n-1)}} \qquad \textit{(Equation 3.)}$$

2.5.5 Analytical Figures of Merit

Current HTCO techniques can provide highly precise (± 1 - 2%) data (see review: Spyres et al., 2000). The typical precision of the HTCO system used here was ±1 - 3% for DOC and TDN measurements with a concentration range of 36 - 208μM-C and 0.2 - 24μM-N, respectively. These values included all measurements performed between November 1997 and February 2001. The results compared well with those reported by Alvarez-Salgado and Miller (1998) (Table 9).

Table 9. A comparison of analytical figures of merit of the HTCO analytical system.

	Alvarez-Salgado & Miller, 1998		*This study*	
Analytical parameter	DOC	TDN	DOC	TDN
Typical precision (%)	*1 – 2*	*1 – 2*	*1 – 3*	*1 – 3*
C.V. of calibration slopes (%)	*<1*	*<1*	*1-2*	*1-3*
System blanks[5] (μM)	*5 – 10*	*<0.3*	*2 – 10*	*b.l.d.[6]*

In general, the limit of detection (LOD) of an analyte may be described as that concentration which gives an instrument signal (y) significantly different from the 'background signal' (i.e. system blank). A commonly used definition of LOD is the analyte concentration giving a signal equal to the blank signal (y_B) plus two standard deviations of the blank (s_B). Recent guidelines from public bodies suggest that the criterion should be (Miller and Miller, 1993):

[5]*System blank estimates obtained when the catalyst used in the HTCO process was suitably conditioned.*

$$y - y_B = 3\, s_B \qquad \text{(Equation 4.)}$$

The system used here had a mean limit of detection of 4μM-C and 2.3μM-N, calculated as the average for all daily analyses. However, due to a lack of truly carbon-free water, there is some uncertainty in its determination using equation above. The limit of detection of HTCO analytical systems is not often reported in publications of peer-reviewed journals.

2.6 Sources of Error in HTCO Techniques

Quantitatively, the most significant sources of error are: (i) mechanical effects associated with HTCO techniques (e.g. sample injection, salt deposition, memory effects) (Alvarez-Salgado and Miller, 1998; Wiebinga and De Baar, 1998; Qian and Mopper, 1996), (ii) the estimation of the system blank (i.e. carbon emission from the catalyst and components of the analytical hardware), and (iii) the oxidation efficiency. If not identified and resolved, these problems can significantly compromise the quality of analyses.

2.6.1 Mechanical Effects

The design of HTCO systems is crucial in minimising mechanical effects that may interfere with the DOC analysis. Sample injection mechanisms and the combustion column are important design aspects. The decision to use a manual or automated injection system depends on the analytical chemist and the laboratory budget. Automated injection systems comprising of a sliding metallic or *PTFE™ (or Teflon™)* plate and valve may cause problems during the analyses of saline samples because of their susceptibility to salt abrasion with time. However, salt abrasion problems can be effectively eliminated with regular and careful cleaning of the slide-plate and its replacement after a number of injections (e.g. >1,500 injections). Manual injection of samples is more labour intensive, and can be highly susceptible to contamination and difficult to reproduce. Variations in the injection time and interval between injections could also lead to gas flow disturbances (Mopper and Qian, 1998). These problems are less likely to occur with the use of an automated system.

As the liquid sample is introduced onto the catalyst at high temperatures, it subsequently expands causing a pressure pulse higher than the void space of the column (Skoog et al., 1997). A cold zone at the head-space of the column may result, causing the deposition of

[6] The signal was below the limit of detection (b.l.d.).

salt/carbonaceous residues (Mopper and Qian, 1998). This causes clogging of the column head with time, and may result in incomplete combustion of the organic compounds and/or a memory effect (i.e. carry-over between samples). Skoog *et al.* (1997) found that there were no significant remnants on the catalyst surface after the injection of ^{14}C-labelled organic material (500μM C). However, salt/carbonaceous residue at the column head could randomly flush through during injection of water samples, resulting in reduced accuracy and precision. This random interference is difficult to eliminate; preventative methods include flushing copious amounts of LCW through the system in order to remove any salt residue, or replacing the catalyst. Qian and Mopper (1996) greatly decreased the dead volume at the top of their catalyst column, virtually eliminating memory effects. This modification cannot be applied to some commercial HTCO analysers (e.g. Shimadzu TOC-5000) because they may not be able to physically contain the pressure pulse created by the sample expansion in the catalyst column without a head-space.

When the precision of the analytical system used here deteriorated to <2 - 3% (C.V.), the catalyst column was taken out and any salt residues were removed from the top of the column. Occasionally, the catalyst beads were damaged (i.e. broken) and had to be replaced. After regeneration of the catalyst column, the analytical system had to be stabilised by injecting copious amounts of LCW to reduce the blank signal sufficiently enough to resume analyses. In addition, a blank check on the catalyst would be performed to determine the carbon contribution of the catalyst and the system components.

2.6.2 System blank

Sample concentrations (μM-C) as measured by the analytical system reflect the organic carbon dissolved in the sample plus the carbon derived from the analytical components (i.e. system blank). Therefore, it is necessary to quantify the system blank in order to accurately determine the sample DOC concentration. The catalyst is considered to be the major source of carbon contamination in the system (Benner and Strom, 1993). The correct quantification of the system blank is a difficult process. Carbon contamination can vary between catalysts (e.g. alumina has a higher adsorption capacity for CO_2 than silica) (Benner and Strom, 1993, Cauwet, 1994) and there is lack of a completely carbon-free water to calculate the carbon contamination from the system components alone.

It is possible with some commercially available TOC analysers (e.g. *Shimadzu TOC- 5000™*) to condition the catalyst (Skoog et al., 1997) and measure the system blank by running a 'blank-check' programme. This programme involves the injection of LCW onto the catalyst where it is combusted and collected downstream as pyrolysed water (i.e. theoretically C-free water). The

latter is subsequently re-injected to determine the system blank (Alvarez-Salgado and Miller, 1998). This closed-loop injection system currently appears to be the most effective (Benner and Strom, 1993). A common alternative when such a programme is not available is the subtraction of an average of LCW injections (i.e. system plus water blank) from the sample measurements (Qian and Mopper, 1996; Wiebinga and De Baar, 1998). However, this blank-correction method may result in an underestimation of the DOC concentration in seawater samples. Recently reported blank concentrations are consistently below 10μM C after rigorous cleaning/conditioning of the catalyst (Qian and Mopper, 1996; Doval et al., 1997; Alvarez-Salgado and Miller, 1998; Dai et al., 1998; Wiebinga and De Baar, 1998; Alvarez-Salgado et al., 1999); however some workers have reported values as high as 30μM C (Wheeler et al., 1997). A common protocol for blank estimation and correction has yet to be accepted, therefore reporting the method used for blank estimations in the determination of DOC is essential.

The automated 'blank check' programme of the *TOC-5000™* analyser used here was employed to determine the system blank when the catalyst was replaced. Pyrolised (theoretically C-free) water was collected as a product of previously oxidised *Milli-Q™* water and was subsequently re-injected through the catalyst column in sets of 5 replicate injections in "TC blank-check" mode. A gradual decrease in the DOC concentration was observed, indicating that the catalyst was being cleaned and conditioned (Figure 26).

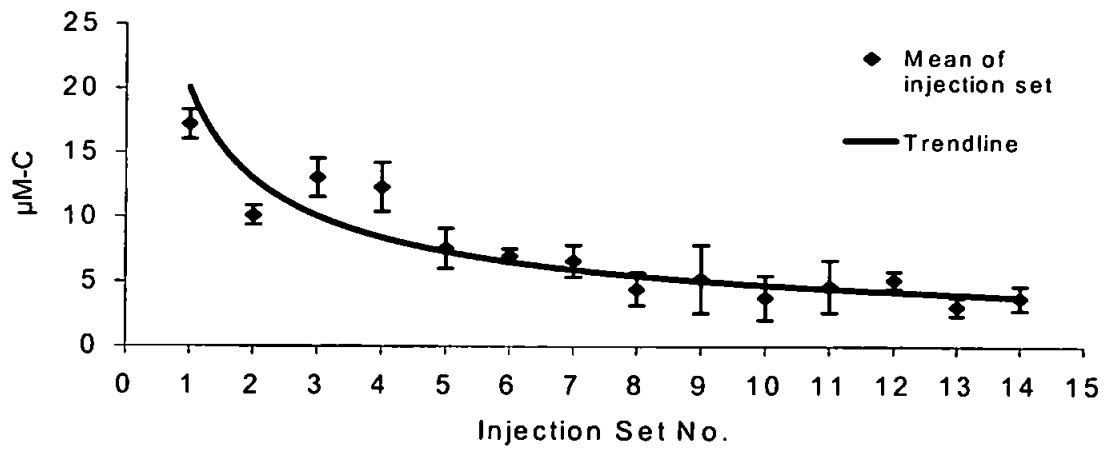

Figure 26. The average DOC concentration (μM-C; n=4-5) of pyrolysed water with increasing sets of injections during conditioning of a catalyst (TOC-5000™ blank check programme).

When the mean DOC concentrations of the last sets of pyrolysed water injections were not significantly different (±2σ) (usually after 50 x 2.5ml injections) the catalyst was considered stable and the average of the last two sets of injections was used as the system blank. This

value was subtracted from the DOC measurements analysed with that particular catalyst. The system blank estimates obtained during this project are listed in Table 10.

Table 10. Date of TOC-5000™ blank-check programme and system blank estimate produced

Date of blank-check	*System blank (µM-C)*
07-01-98	*7±0*
09-06-98	*2±0*
10-07-98	*7±1*
01-05-99	*10±1*
21-10-99	*7±1*
09-02-00	*22±5*
16-05-00	*32±1*
20-05-00	*19±1*

It is essential to ensure that the catalyst is sufficiently cleaned and conditioned when running the "blank-check programme" of the TOC-5000™. If the catalyst is not thoroughly cleaned and stable, then the "blank-check programme" will give unreliable estimates of the system blank. After considerable use of the TOC-5000™ system and consultation with HTCO experts, it was decided that the catalyst is considered cleaned and stabilised when the system blank average value was equal to or less than 2000 area units (of the Shimadzu TOC-5000™) for an injection volume of 200µl. Low-carbon water samples (i.e. Milli-Q™ water and LCW reference samples) were analysed daily to give estimates of the total blank (i.e. system blank plus the Milli-Q™ or LCW carbon). If the system blank was significantly higher than the total blank on a daily run, then the latter was used to correct the samples analysed on that run.

Sample concentrations (µM-C) that were determined during eight analytical runs between 14-Feb-00 and 16-Mar-00, were used to compare the two methods (total blank vs. system blank) used for the correction of the final sample concentrations by plotting them as a regression (Figure 27).

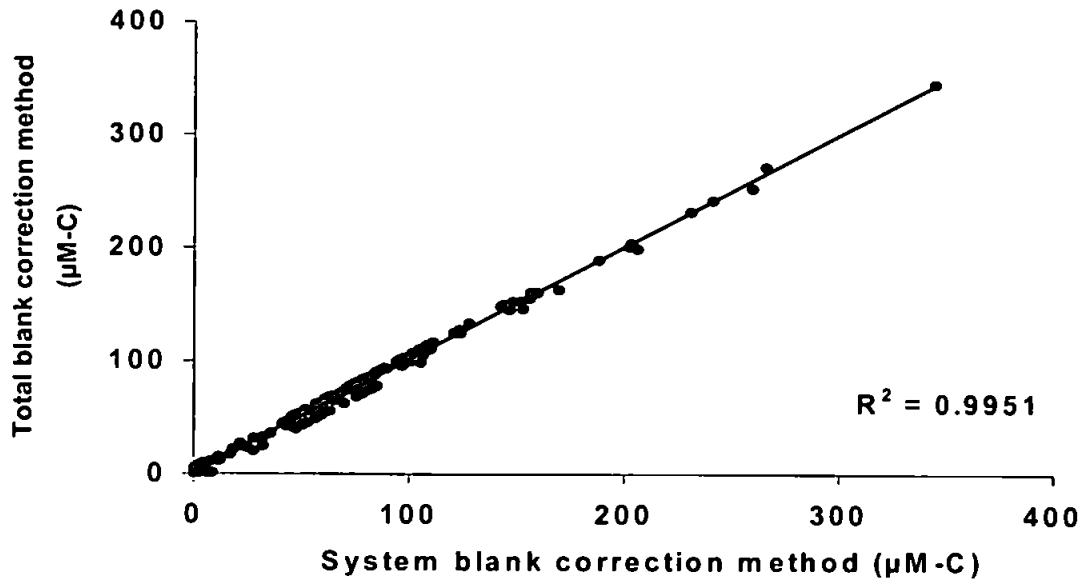

Figure 27. Linear regression plot of sample concentrations (µM-C) corrected by the daily total blank versus the automated blank-estimation programme of the TOC-5000™.

The linear regression above shows >99% agreement between the two blank correction methods (slope: 0.992±0.005; Y-int: 2±1). The y-intercept suggests that the total blank correction method may underestimate the final sample concentrations by approximately 2±1µM-C. This value is typically within ±2σ of the sample concentrations therefore it is not considered a significant underestimation but may be worth noting in studies that require high precision (±1σ). Thus, when the system blank cannot be accurately determined it is possible to use the total blank estimate instead.

2.6.3 Oxidation efficiency

Oxidation efficiency of the HTCO technique is likely to be a function of the refractivity of the organic material in the analysed sample (Alperin and Martens, 1993). Since the chemical character of dissolved organic matter is largely unknown, it is not possible be 100% confident that standard solutions represent naturally occurring organic matter. This has limited our understanding of the mechanism of HTCO and the combustion mechanism. Nevertheless, efforts to evaluate the oxidation efficiency of HTCO have been made using various compounds with different degrees of refractivity (i.e. caffeine, antipyrine, thiourea, graphite, diamond) (Miller, 1996; Verardo et al., 1990). Recent studies investigating the percentage recovery for current HTCO techniques quote >94% (Mopper and Qian, 1998; Fry et al., 1996; Qian and Mopper, 1996), although a direct comparison between techniques is not often possible due to the use of different catalysts and reference compounds. A summary of analytical figures of

merit from recent studies on the oxidation efficiency of HTCO systems is given in Spyres et al (2000). Some studies have shown that complete oxidation can be achieved without a catalyst (e.g. using pure quartz beads) Williams et al., 1993; Qian and Mopper, 1996) and using a carrier gas that does not include oxygen (Skoog et al., 1997), bringing into question the combustion mechanism occurring in HTCO systems. It is recommended that a set of compounds of different refractivity, each at varying concentrations, should be injected to test the ability of the system to oxidise organic matter efficiently. Oxidation efficiency should be determined on each day of analysis until constant percent recovery patterns can be established for each method and/or instrument, after which periodic assessment is sufficient (Hopkinson and Cifuentes, 1993). A measure of oxidative efficiency of the analytical system used here was determined daily by analysing 'certified reference materials'.

2.6.4 Accuracy and reference materials

Analyses of DOC in seawater samples by HTCO techniques can display unreliability on a daily basis (Sharp, 1997). Certified reference materials (CRMs) are essential for checking the performance of the HTCO techniques and for the quantitative validation of the measurement (i.e. a measure of oxidation efficiency) but they are not readily available. In the past five years an international intercomparison exercise for DOC analysis has been carried out (Sharp, 1997). A deep ocean sample and a deep ocean sample spiked with glucose were distributed and subsequently analysed by 47 laboratories. The majority of the results were within ±10% of the expected value for the two samples. This international effort was a major advance in determining accuracy but it is necessary to achieve an agreement of ±1-2% to allow rigorous comparison and interpretation of different environmental data sets (Sharp, 1997).

A further inter-laboratory study was recently co-ordinated by J. Sharp (Uni. of Delaware) and D. Hansell (Bermuda Biological Station for Research, BBSR) to produce CRMs for the international community. Two sets of reference samples, a low-C water (LCW) and a deep water (DW) set, were supplied as part of an international 'certified reference material' programme supported by the U.S. National Science Foundation (NSF). The LCW was collected directly from a Millipore™ TOC+ water system, and the DW sample was collected from the Sargasso Sea at ~2000m depth.

The first part of the programme (May 1997 - November 1999) was organised by J. Sharp and D. Hansell. After preparation of the reference materials at the Uni. of Delaware, a batch of ampoulated CRMs were analysed in three separate laboratories (i.e. Woods Hole Oceanographic Institute, Uni. of Delaware and BBSR). The analyses verified that there was no significant

variation between batches prepared on separate days and also provided an estimate of the DOC content in the ampoules (i.e. LCW: 0.0 ±1.5μM-C; DW: 44.0 ±1.5μM-C).

The second part of the programme (i.e. November 1999 – ongoing) was organised by D. Hansell and W. Chen (BBSR). Both LCW (2μM-C) and DW (44-45μM-C) samples were certified for DOC concentrations by the laboratories of Drs. Jim Bauer, Ron Benner, Yngve Borsheim, Gus Cauwet, Bob Chen, Dennis Hansell, Chuck Hopkinson, Ken Mopper/Jianguo Qian and Yoshimi Suzuki. For information on the supply and suggested use of the CRMs visit the following webpage http://www.pml.ac.uk/gs/News/news.htm.

The reference materials supplied were used as a daily monitor on the consistency of the analyses and a check that the instrument was giving an accurate response to a known concentration of DOC in a natural seawater matrix. The objective was to analyse a set of CRMs on each daily run, although sometimes this was not possible due to shortage. The DOC concentrations of CRMs analysed between January 1998 and March 2000 (Figure 28) showed that the analytical methodology employed was historically reliable. The mean DOC concentrations of the CRMs analysed (LCW = 4±3 μM-C; DW = 48±4 μM-C) were not significantly different (±2σ) to the certified values.

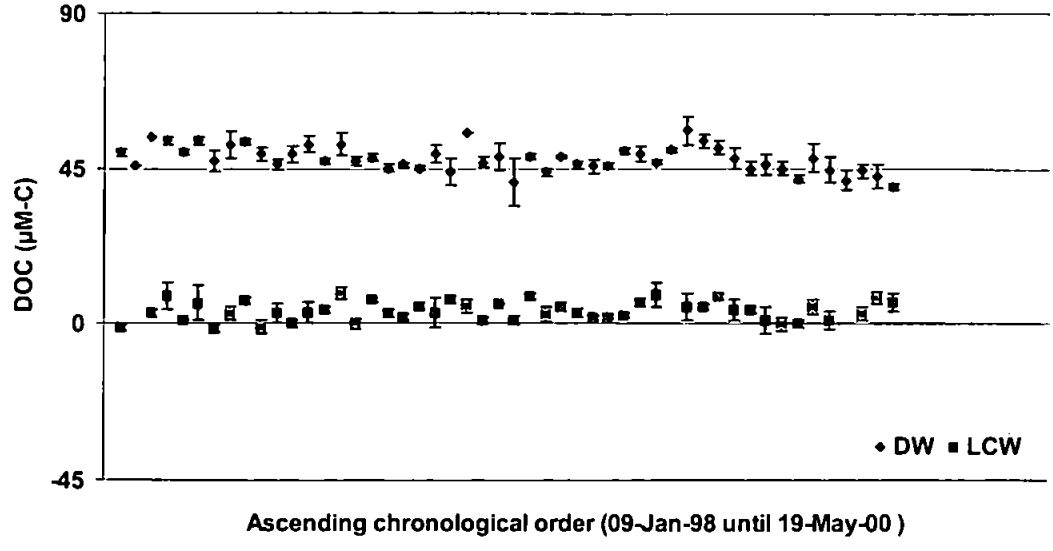

Figure 28. Time series plot (n=50) of the CRMs (μM-C) measured on daily analytical runs during the period between 09-Jan-98 and 19-May-00.

Occasionally some ampoules of CRMs gave significantly different DOC concentrations from the expected, in which case, replicate ampoules were analysed immediately following or soon

after, and always on the same daily analytical run. The results (Table 11) suggest that some ampoules may have been slightly or heavily contaminated. This reinforces the suggestion that the CRMs supplied should only be used as an indicator of instrument performance by checking the results of the individual analyst against the international community of DOC analysts (Hansell, pers.com.). With the wider distribution of reference materials it is hoped that the analyses of DOC and the environmental interpretation of results can be carried out with greater certainty.

Table 11. DOC concentrations (μM-C; n= 3 - 5) of replicate CRMs analysed on the same daily analytical run.

Date of Analysis	*CRM Sample Type*	*Replicate 1*	*Replicate 2*
		μM-C (±1σ)	*μM-C (±1σ)*
27-Feb-1998	*LCW*	*16±2*	*6±2*
05-Mar-1999	*DW*	*66±2*	*50±1*
14-Feb-00	*DW*	*62±2*	*50±1*
20-Feb-00	*DW*	*53±5*	*48±3*
09-Mar-00	*DW*	*199±2*	*46±3*

2.7 Intercalibration Exercises

The main aim of the intercalibration exercises performed was to compare and co-ordinate the analytical systems and methodologies employed here with those of internationally recognised laboratories and to check for overall consistency of results. The author participated in two main intercalibration 'programmes', collaborating with X.A. Alvarez-Salgado's group at the Instituto de Investigaciones Marinas, Spain an OMEX II-II partner laboratory, and J. Sharp's group at the University of Delaware, USA for DOC and TDN measurements.

2.7.1 OMEX II-II DOC and TDN intercalibration exercise

The Instituto de Investigaciones Marinas (IIM) was a partner in the OMEX II-II programme responsible for nutrient analyses. Inorganic nutrient data from IIM was used to calculate DON from the TDN results, therefore it was essential to perform several intercalibration exercises to ensure consistency between data sets. Both analytical systems follow the coupled DOC/TDN configuration described by Alvarez-Salgado and Miller (1998), therefore both DOC and TDN intercalibrations were performed. Replicate samples from the vertical profile of a deep station (typically over 1000m) were collected from each of four cruises by the author and a set of

samples was distributed to IIM for analysis. In addition, standards (Milli-Q and seawater spiked with KHP/glycine) were prepared by both laboratories and distributed to check the accuracy of standards and to investigate the catalyst efficiency for standards in low-carbon-water (i.e. *Milli-Q™*) and seawater diluents.

The intercalibration results from all exercises were pooled and plotted (linear regression) with the trend-line forced through the origin (Figure 29) in order to investigate whether they agree well (i.e. slope should not be significantly different from one (1), Miller and Miller, 1993). The two laboratory methods for measuring DOC agree well (correlation coefficient, R^2 =0.94) when suspicious and/or contaminated samples are excluded (Figure 29a). When all samples are included in the regression plot there is more scatter about the best-fit line and the correlation coefficient is lower (R^2 = 0.66), although the slope was not statistically significant from one ($\pm 2\sigma$). Various methodological and analytical problems may explain the scatter observed in Figure 29b; these are discussed in more detail below.

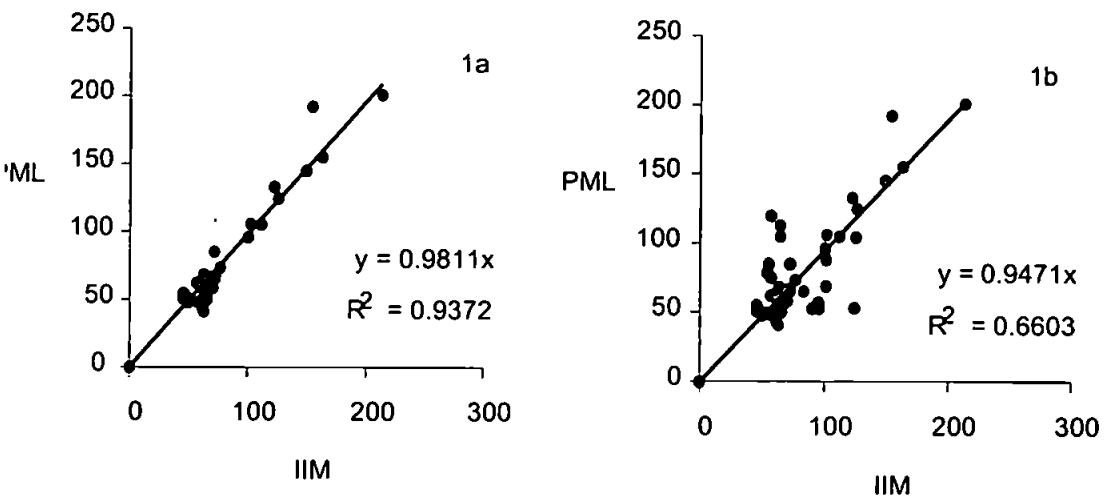

Figure 29 a. Linear regression plot of DOC (μM-C) of intercalibration samples, n=35[7]; b. Linear regression plot of DOC (μM-C) of intercalibration samples, n=50[8].

[7] Samples that were 'suspicious', i.e. not oceanographically consistent, were excluded

2.7.1.1 CD110B Cruise Intercalibration Exercise

The following sections (2.7.1.1 – 2.7.1.6) present the results from each intercalibration exercise performed. A set of seawater samples (n=12) was collected on the 14-Jan-98 during cruise CD110B and was analysed at the PML and IIM (Table 12).

Concentrations generally agreed with the exception of three samples analysed by IIM which had comparatively high concentrations. The cause of this was probably due to sample contamination occurring after sample collection and the sealing of ampoules, as such elevated DOC levels were not observed in replicates (Figure 30). Due to the high carbon concentrations observed at the time of analysis, the 'suspicious' samples were re-analysed by IIM at the end of the run to check whether the source of contamination was from the analytical system or within the sample itself. The re-analyses gave similarly high values, and the reference samples and *Milli-Q™* water analysed on that run indicated that the analytical system was stable and precise (Alvarez-Salgado, pers.com.). This evidence suggests sample contamination between the sealing process and analysis.

2.7.1.2 OMEX0898 Cruise Intercalibration Exercise

For the intercalibration exercise during the second sampling campaign, a set of seawater samples (n=9) was collected on 06-Aug-98 and subsequently analysed by PML and IIM (Table 13) for comparison.

The vertical profiles showed similar trends (Figure 31), but a systematic mean difference of approximately 14μM-C was observed between profiles. The most probable cause of this 'offset' is a difference in the system blank estimation and the correction procedures between the two participating laboratories.

Both PML and IIM use Milli-Q and CRMs (see section 2.6.4) as indicators of stability and to estimate the system blank contribution to the measured concentrations. Considering that IIM's CRM concentrations were within the certified values and PML had no available CRMs to analyse on the date, it is suggested that the blank correction of PML may have underestimated the sample concentrations. However, for methodological consistency, it was decided not to change the blank correction procedures (see Section 2.6.2) for the remainder of the samples

[8] Only clearly contaminated samples, n=7, were excluded

analysed in that batch. Notably, the deep water concentrations as measured by PML, are oceanographically consistent (i.e. ~40-45μM-C for deep ocean waters).

2.7.1.3 M43-2 Cruise Intercalibration Exercise

A further intercalibration exercise was performed for sampling campaign M43-2 (January 1999). The majority of the intercalibration samples analysed by both laboratories were contaminated causing disagreement between the data sets. The source of error was identified as a problem with the ampoule sealing technique. The sealing system (i.e. a newly-acquired mini gas-torch, *RS Components*®) caused delayed cracking of the glass ampoule tips - probably during storage and transportation - often with salt accumulation there. This resulted in the random contamination of ampoules.

Due to the small number of samples that were oceanographically consistent (i.e. not contaminated, 50% in this intercalibration exercise), results from both partners (Table 14) for this intercalibration exercise were combined in order to plot a vertical profile of DOC concentration for that station. The resulting vertical profile (Figure 32) is oceanographically consistent; DOC concentration decreases with increasing depth. In addition, the top 100m of the water column at the station exhibit homogeneous distribution of DOC concentrations.

For all other contaminated samples of the M43-2 research cruise, replicate ampoules that were intact were analysed. Overall, over a quarter of the M43-2 data set (i.e. 32 from a total 92 samples) was excluded on grounds of clear contamination and oceanographic inconsistency.

2.7.1.4 BG9919 Cruise Intercalibration Exercise

Duplicate sets of seawater samples (n=8) that were collected on 07-Sept-99 were analysed by PML and IIM (Table 15). The vertical profiles produced by the two laboratories generally agreed. Significant differences observed between replicate samples may have been due to contamination introduced during any stage of the sampling and subsequent analysis. Results from the two laboratories are presented in Figure 33.

2.7.1.5 Spiked Seawater Standards

Four replicate sets of spiked seawater samples (Table 16) were prepared by the author for analysis by PML and IIM. The objective of this exercise was to test the accuracy of standards and to check the percentage recovery of the analyte by the analytical systems.

Seawater stock was made from ~2000m Sargasso sea water that was collected on the 04-15-Feb-99 by D. Hansell's laboratory (BBSR) and shipped to PML on the 16-Feb-99. The seawater was neither filtered, nor acidified and was stored in small 50ml polycarbonate bottles in the dark at 4°C. It was subsequently pooled in a 500ml clean flask for homogeneity on the 01-Feb-00 and acidified with 1.5ml H_3PO_4 (85% v/v) to pH ~2 and stored in the dark at 4°C. On the 02-Feb-00, four standards were made with stock seawater and KHP/glycine solution in 100ml clean glass flasks. Ampoules were then filled by pipetting seawater-standard solution and were subsequently flame-sealed and stored in the dark at 4°C. Two replicate sets of ampoules were sent to IIM for analysis. Each laboratory analysed two sets of spiked standards on different days (Table 17).

Linear regressions were produced by plotting the measured concentrations against the spiked KHP-C concentrations (Figure 34). All measured concentrations (μM-C ±2σ) were consistent with the known spiked concentrations (Table 16), with the exception of four samples. Two samples were significantly higher than the expected concentrations, probably due to contamination during the various stages of the methodology and/or an error in the manual addition of KHP/glycine to the standards. The other two samples were significantly lower than the expected concentrations suggesting that an error was made during the manual addition of the KHP/glycine stock and/or the analytical systems of IIM and PML were not efficiently oxidising the carbon in the standards. The latter hypothesis is less likely because both analytical systems were stable during the daily run (see IIM1 and PML2 in Table 17) and the other standards analysed on that day were fully recovered.

Percentage recoveries (derived from the slopes of the regressions in Figure 35) for each replicate set of standards analysed ranged from 81 to 110% (Table 18), although all slopes were not significantly different (±2σ) to one (1). The high percentage recovery (>100%) observed could be due to random contamination arising from any stage of the methodology and/or error in the spiked addition although this could not be verified. The small number of standards (n=4) in the regressions could account for the large range observed.

2.7.1.6 Additional Spiked Seawater and Milli-Q Standards

During discussions between the author and analysts from IIM regarding the results produced from the spiked seawater standards exercise, the possibility of a saltwater matrix effect on the oxidation efficiency was suggested. It was therefore decided to investigate the oxidation efficiencies of the analytical systems when analysing samples with and without a saltwater

matrix. Six replicates of spiked *Milli-Q™* and seawater samples (Table 19) were prepared by IIM and distributed to both laboratories to be analysed.

A batch of standards (n=8) were prepared in 100ml clean glass flasks by spiking KHP/glycine standard solution in seawater (surface seawater from the 'Ria de Vigo') (M, M1, M2 and M3) and in *Milli-Q™* (A, A1, A2, and A3). Ampoules were filled, acidified to pH ~2, flame-sealed and stored in the dark at 4°C. Two replicate sets were sent to PML for analysis; each laboratory analysed one replicate set of samples. The results plotted against the spiked KHP/glycine concentrations are presented in Figure 36.

Results from both laboratories (slope±2σ) indicate that there was no significant difference between the recovered KHP/glycine spiked carbon (μM-C) in *Milli-Q™* and in seawater solution (Table 21). In addition, there was no significant difference (±2σ) in the measured concentrations between laboratories. Percentage recoveries (derived from the slopes of regressions in Figure 36) for each replicate set of standards analysed ranged from 97 to 101%.

Table 12. Summary of the CD110B intercalibration sample analyses. Note: R^2: regression coefficient; Y-int: y intercept

	PML	IIM
Analyst	G. Spyres	X.A. Alvarez-Salgado
Analysis date	18-Jan-98	11-Jun-98
Blank correction (µM-C)	7.3±0.3	10
R^2	0.9882	0.9996
Y-int (µM-C)	1±7	12.2
LCW (µM-C)	7±1	3.3±1.3
DW (µM-C)	53±1	44.4±0.4

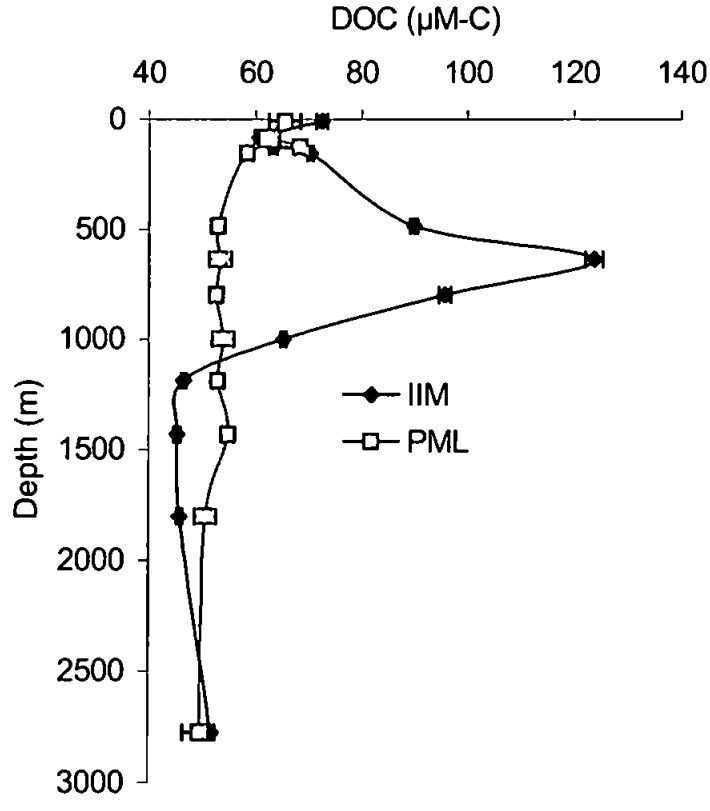

Figure 30. Vertical DOC profiles of replicate samples of CTD49 (CD110B cruise) analysed by PML and IIM.

Table 13. Summary of the OMEX0898 intercalibration sample analyses.

	PML	IIM
Analyst	G. Spyres	M. D. Doval
Analysis date	20-Aug-99	19-Nov-99
Blank correction (μM C)	18±2	11.5
R^2	0.9959	0.9999
Y-int (μM-C)	21±3	10.9±0.2
LCW (μM-C)	(Milli-Q) 2±3	0.5±0.2
DW (μM-C)	None available (N/A)	44.8±1.4

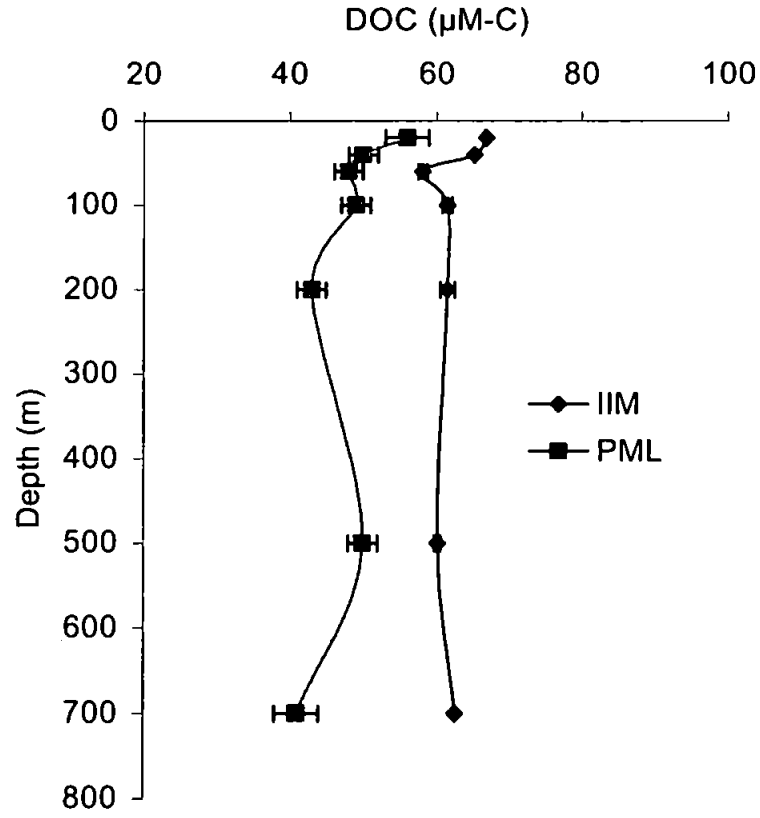

Figure 31. Vertical DOC profiles of replicate samples of CTD13 (OMEX0898 cruise) analysed by PML and IIM Note: clearly contaminated samples were excluded from either profile, n=4).

Table 14. Summary of the M43-2 intercalibration sample analyses.

	PML	IIM
Analyst	G. Spyres	M.D. Doval
Analysis date	02-Nov-99	10-Feb-00
Blank correction (μM-C)	6.9±0.7	9.0
R^2	0.9962	0.9999
Y-int (μM-C)	8±4	8.1±0.5
LCW (μM-C)	N/A	0.5±0.2
DW (μM-C)	N/A	44.1±1.5

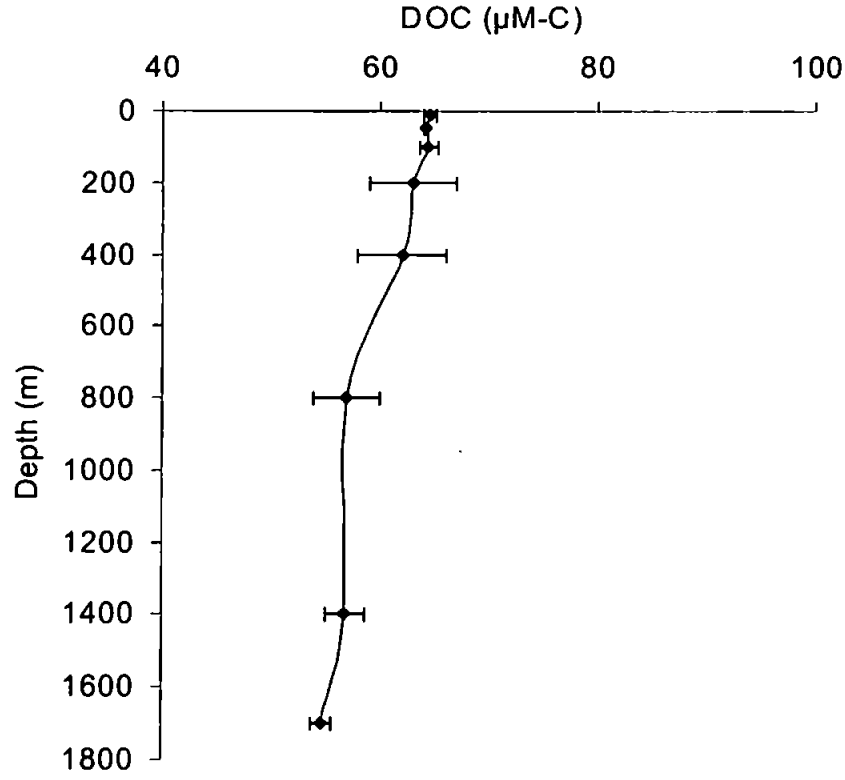

Figure 32. Vertical profile of DOC (μM-C) at station S2000 (M43-2 cruise). Note: samples analysed by either IIM or PML.

Table 15. Details of analyses of BG9919 intercalibration samples.

	PML	IIM
Analyst	G. Spyres	M.D. Doval
Analysis date	21-Feb-00	09-Mar-00
Blank correction (μM-C)	6.5±0.9	10
R^2	0.9996	N/A
Y-int (μM-C)	7.7±1.0	N/A
LCW (μM-C)	4±1	0.0±1.0
DW (μM-C)	45±2	45.0±1.8

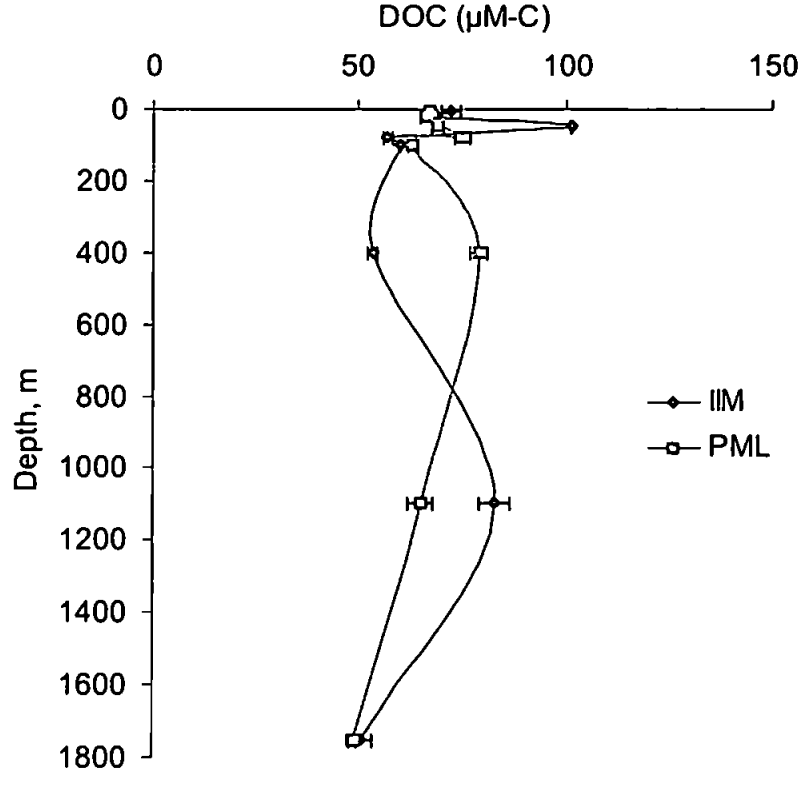

Figure 33. Vertical DOC profiles of replicate samples from station P2000 (BG9919 cruise) analysed by PML and IIM.

Table 16. A description of the four spiked seawater standards prepared by PML

Sample	Description
A	Seawater alone
B	Seawater spiked with 98.8 µM C and 12.5 µM N
C	Seawater spiked with 49.4 µM C and 6.26 µM N
D	Seawater spiked with 24.7 µM C and 3.13 µM N

Table 17. Summary of the KHP/glycine intercalibration standard analyses.

	PML 1	IIM 1	PML 2	IIM 2
Analyst	G.Spyres	M.D. Doval	G.Spyres	M.D. Doval
Analysis date	10-Feb-00	11-Feb-00	21-Feb-00	10-Mar-00
Blank correction (µM-C)	15±2	9.0	6.5±0.9	11.0
R^2	0.9994	0.9999	0.9996	0.9999
Y-int (µM-C)	13±3	8.0±0.5	8±1	7.5±0.5
LCW (µM-C)	N/A	0.5±0.2	4±1	0.0±0.4
DW (µM-C)	N/A	44.1±1.5	45±2	44.2±3.2

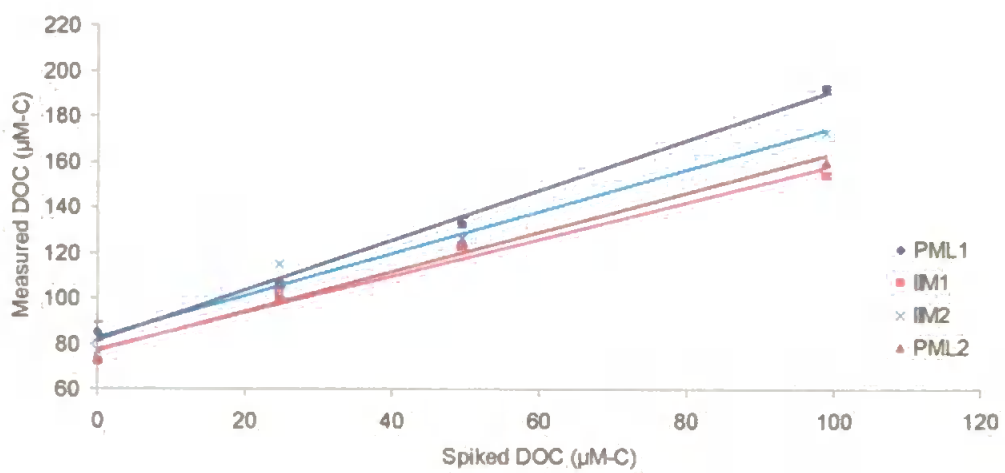

Figure 34. Linear regression plot of the measured DOC in the spiked sea water samples against the added carbon standards.

Table 18. Regression parameters from the KHP/glycine-spiked replicate sets of standards analysed by IIM and PML

	PML 1	±2σ	PML 2	±2σ	IIM 1	±2σ	IIM 2	±2σ
Slope	1.10	0.10	0.87	0.14	0.81	0.18	0.93	0.22
Y-int (μM-C)	82	6	77	8	78	10	83	12
R^2	0.9952		0.9889		0.9767		0.9731	

Table 19. A description of the seawater and freshwater standards prepared by IIM

Sample	Description
A	*Milli-Q™* alone
A1	*Milli-Q™* spiked with 49.6μM-C and 6.2μM-N
A2	*Milli-Q™* spiked with 99.3μM-C and 12.4μM-N
A3	*Milli-Q™* spiked with 148.9μM-C and 18.6μM-N
M	Seawater alone
M1	Seawater spiked with 49.6μM-C and 6.2μM-N
M2	Seawater spiked with 99.3μM-C and 12.4μM-N
M3	Seawater spiked with 148.9μM-C and 18.6μM-N

Table 20. Details of daily calibration and analysis of KHP/glycine spiked standards.

	PML	IIM
Analyst	G.Spyres	M.D. Doval
Analysis date	16-Mar-00	10-Mar-00
Blank correction (μM-C)	11±1	11.0±0.2
R^2	0.9996	0.9999
Y-int (μM-C)	10±1	7.5±0.5
LCW (μM-C)	0±1	0.0±0.4
DW (μM-C)	42±1	44.2±3.2

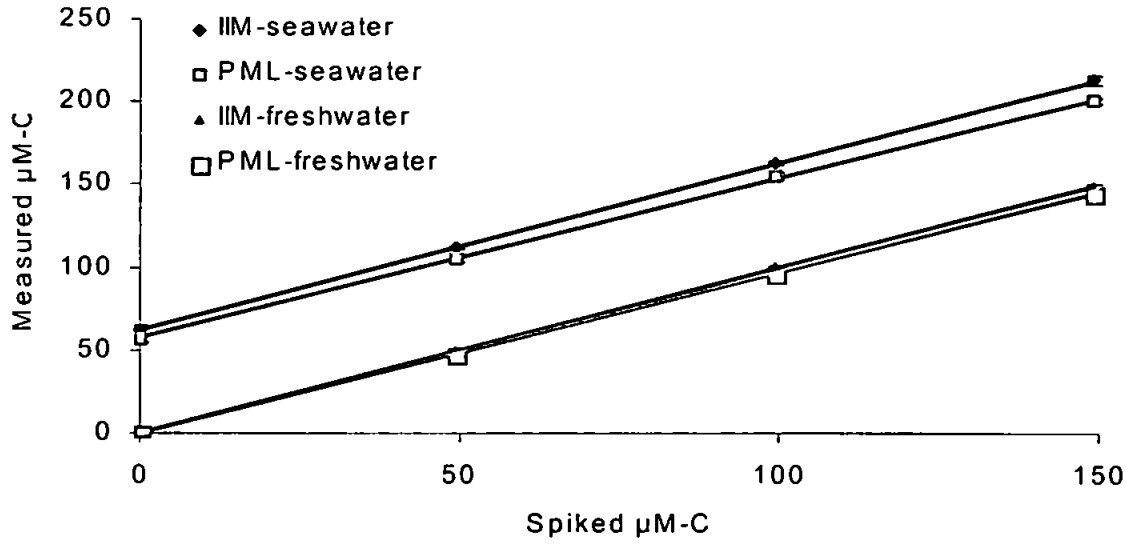

Figure 35. Regression plots of measured DOC (µM-C) by IIM and PML against spiked concentrations.

Table 21. Regression results from the seawater & freshwater standards analysed by IIM and PML. Note: sw - seawater standards, fw - freshwater standards

	PML-sw	±2σ	**PML-fw**	±2σ	**IIM-sw**	±2σ	**IIM-fw**	±2σ
Slope	0.97	0.02	0.97	0.00	1.01	0.02	1.00	0.02
Y-int (µM-C)	57	2	-0.2	0.6	62.1	1.2	0.5	1.0
R^2	0.9998		1		0.9999		0.9999	

2.7.1.7 TDN Results

Total dissolved nitrogen results were produced for only four out of the six intercalibration exercises performed by IIM and PML due to technical limitations experienced by both PML and IIM (i.e. unable to use TDN analyser). The results were pooled and plotted as a linear regression plot (see Figure 36).

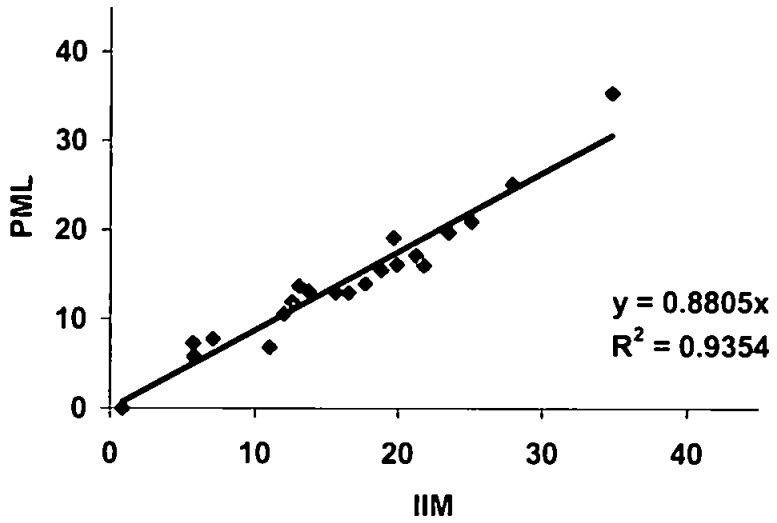

Figure 36. Linear regression plot of TDN (μM-N) of all intercalibration samples, n=21. Note: only clearly contaminated samples, n=12, were excluded.

The two laboratory methods for measuring TDN agree well (correlation coefficient, R^2 =0.94) when suspicious and/or contaminated samples are excluded (Figure 36). When all samples are included in the regression plot there is more scatter about the best-fit line and the correlation coefficient is lower (0.78). Most of the contaminated samples observed were from the M43/2 cruise intercalibration exercise. The contamination of the M43/2 cruise intercalibration samples may have contributed to the significantly (±2σ) lower than 1 slope (0.88±0.02) of the regression plot (i.e. some samples analysed by IIM were of higher TDN content than those analysed by PML). The regression slope also suggests that the analytical system of PML may have been less efficient in measuring the TDN present in the samples. In either case, we are not able to clearly ascertain the reasons for the value of the slope.

There are concerns that HTCO analytical techniques may not completely recover NO_2^- (Sharp, to be subm.), however results (see section 2.7.2) showed that there was good agreement of TDN recovery (DON plus added NO_2^- in a seawater sample) between HTC methods and other techniques (i.e. UV and persulphate) with 8 – 28% agreement (i.e. % c.v. of all results).

2.7.2 International Methods Comparison for Measurement of DON in Seawater

The author participated (18-Feb-00) in an international community methods comparison for the measurement of TDN headed by Jonathan Sharp of the University of Delaware, U.S.A. This

exercise served as a preliminary test of the comparison of the families of methods being used in various laboratories around the world. It also served as a comparison of the relative performance of the analytical system of PML with other laboratories that routinely measure TDN. The data was collated by J. Sharp and a manuscript was produced with all participants (Table 22) as co-authors (Sharp et al., to be publ.).

Five seawater samples from estuarine, coastal, and surface and deep ocean environments were used in the exercise. Most samples were aged for several months to allow oxidation of reduced inorganic ions (NH_4^+ and NO_2^-) to NO_3^- and decomposition of labile dissolved organic matter. The ageing was done in 5-gallon glass carboys closed with silicone rubber stoppers. The purpose of the ageing was to render the samples stable for the period of time necessary to include a large number of analysts (about six months). The samples were collected by J. Sharp and aged in his laboratory. Samples were collected in 1998 and 1999 and were monitored during ageing to verify that the reduced inorganic ion concentrations were decreasing and NO_3^- was increasing.

For the comparison, 50 ml aliquots were sealed in glass ampoules. Ampoules were prepared by ashing overnight in an oven at 450°C. They were then filled from an aspirator bottle with silicone rubber tubing in a fashion similar to that used for the DOC intercalibration samples (Sharp et al, in prep.). One of the aged samples was spiked before preparing ampoules to give it relatively high NO_2^- and NH_4^+ concentrations. All ampoules of that sample and the comparatively fresh estuarine sample were autoclaved to inhibit further microbial oxidation. Ampoules were filled and shipped to analysts in January 2000. The five samples are shown in Table 23.

To compare the author's results to those of the intercalibration community a two-tailed t-test ($P = 0.05$) was used with the author's TDN concentrations as one variable and the averaged TDN concentrations of the whole community as the second variable. There was no statistically significant difference between the two variables indicating that the analytical system of PML compared well with the rest of the participant laboratories, even with different methodologies employed. Likewise, there was no statistically significant difference when comparing the TDN results of the author with those of the participants using only HTC methodologies, and again when comparing DOC concentrations with those produced by J. Sharp (Table 23).

Table 22. Information on participating laboratories for the DON methods comparison.

Laboratory	Analyst(s)	Institution
X. A. Alvarez-Salgado	M. Doval	Instituto de Investigaciones Marinas, Vigo, Spain
J. Y. Benaim	C. Le Poupon	Université Toulon, France
D. Bronk	M. Sanderson	Univ. of Georgia, USA
D. Burdige	K. Gardner	Old Dominion Univ., USA
G. Cauwet	M. Pujo-Pay, L. Oriol	Laboratoire Arago, Banyuls sur Mer, France
S. Emerson	J. Abell	Univ. of Washington, USA
D. Hansell	W. Chen	BBSR, Bermuda
C. Hopkinson	A. Nowlin, B.N. Weston	M.B.L., Woods Hole, MA, USA
G. Kattner	C. Hartmann	Alfred Wegener Institute, Germany
N. Kaumeyer		Univ. of Maryland, USA
W. McDowell	J. Merrimam	Univ. of New Hampshire, USA
K. McGlathery	K. Russell, A. C. Tyler	Univ. of Virginia, USA
A.E.J. Miller	G. Spyres	Plymouth Marine Laboratory, U.K.
N. Morley		Southampton Ocean Center, U.K.
K. Nagel	A.-M. Welz, O. Primm	Institut für Ostseeforschung Warnemünde, Rostock, Germany
H. Ogawa		Ocean Research Institute, Univ. of Tokyo, Japan
C. Pollard		VIMS Analytical Laboratory, USA
P. Raimbault		Centre d'Oceanologie de Marseille, France
R. Sambrotto		Lamont Doherty Earth Observatory, Columbia Univ., USA
S. Seitzinger	R. Styles	Rutgers Univ., USA
J. Sharp	K. Rinker	Univ. of Delaware, USA
F. Tirendi	J. WuWon	Australian Institute of Marine Science, Australia
W. Ullman	K. Savidge	Univ. of Delaware, USA
T. Walsh		Univ. of Hawaii, USA
C.S. Wong	K. Johnson	Institute of Ocean Sciences, British Columbia, Canada

Table 23. DOC and TDN concentrations (μM-C and μM-N, respectively) of intercalibration samples from the international DON comparison exercise.

Sample	DOC* G. Spyres	DOC J. Sharp	TDN* G. Spyres	TDN Intercal. community[9]
CSW: central shelf water	85 ± 1	88	6.3 ± 0.5	6.4 ± 0.7
SBW: shelf-break water	112 ± 5	93	13.4 ± 0.3	14.7 ± 1.1
DSS: deep Sargasso Sea	67 ± 1	64	20.3 ± 0.3	22.6 ± 1.7
CPN: shelf water plus N	115 ± 1	103	19.7 ± 0.2	17.7 ± 1.5
FHW: fresh lower estuary water	276 ± 2	254	20.8 ± 0.4	22.6 ± 1.2

*The Dixon's Q-test for outliers was not applied.

2.8 Conclusions

It is now established that HTC methods compare well with historical methods such as WCO and the broad marine community is measuring similar concentrations of DOC in the marine environment. Analysts are able to achieve high precision, rapidly, allowing the evaluation of the size of the DOM pool and the detection of small changes in concentration (~1μM-C) resulting from biogeochemical processes (Sharp, 1997). HTC methods are thus commonly used and are the preferred analytical technique for the measurement of DOC in natural waters. However, there are still many mechanical hindrances (e.g. salt deposition, estimation of the system blank) that must be alleviated to ultimately achieve accurate and more precise measurements.

The broad community in the last decade, has been working towards solving such problems *via* individual studies on aspects of the HTC methodology (e.g. Cauwet, 1994; Skoog et al., 1997; Alvarez-Salgado and Miller, 1998; Mopper and Qian, 1998), participation in intercalibration exercises (e.g. Sharp et al., 2001; Sharp et al., unpubl) and the exchange of practical information between analysts (e.g. *via* a world-wide-web open forum on HTCO created by the author).

[9] TDN average (μM-N) from all participating laboratories that used HTC methodologies.

Several issues fundamental to the accurate determination of DOC and TDN by HTCO were highlighted by the intercalibration exercises performed in this study:

- There is great risk of sample contamination at several stages of the methodology and it is necessary that 'clean' sampling and handling protocols are followed meticulously. Replicate sampling can, to a certain extent, alleviate this problem.
- Errors in the preparation of standards (e.g. volumetric measurement errors) can influence the calibration of the analytical system. This problem can be avoided by careful and appropriate handling and by ensuring that the apparatus used is accurate.
- A difference in blank correction procedures between laboratories can result in significant 'offsets' in the measured concentrations. This problem is difficult to alleviate without the use of CRMs. An appropriate blank correction procedure is still to be established in the HTCO-DOM community.
- Low oxidation efficiency can produce inaccurate measurements. The efficiency of a an analytical system can be determined by measuring percentage recoveries of a suite of reference materials.

Overall, there was generally good agreement between PML and other laboratories for the measurement of DOC and DON. However, the analytical system of PML measured lower TDN than IIM and it cannot be ascertained what the cause of this was. As highlighted by the international DON comparison (section 2.7.2), HTC analyses for the measurement of TDN are diverse and there may be significant differences in the HTC methods that could contribute to variability and ultimately to the HTC method underestimating the TDN. However, the PML results were not statistically significantly different to those of the HTC community in this exercise and the HTC systems did not measure significantly lower TDN than UV and persulphate methodologies. Further inter-laboratory studies may help to resolve such differences and to establish appropriate criteria for the accurate measurement of TDN by HTC.

The critical assessment of the methodology and analytical technique employed in this study, regular use of reference materials and participation in intercomparison exercises have been used to ensure that the author routinely measured DOC and TDN concentrations in seawater precisely (1-3%) and as accurately as possible.

Chapter 3

3. RESULTS AND DISCUSSION

3.1 Introduction

This chapter presents combined data sets from the four cruises: CD110B (Jan.98), ST0898 (Aug.98), M43/2 (Jan.99) and BG9919 (Sep.99). Three main cross-slope transects in the OMEX II-II sampling grid (41°00'N – 43°00'N and 8°30'W – 10°30'W) were sampled seasonally and inter-annually (see Figure 17 and Table 8 in section 2.2.2). A number of samples (approximately 20% of the total collected) were analysed on-board during the cruises whilst the remainder were transported back to the land-based laboratory for subsequent analysis. In this chapter, vertical DOC and DON distributions from transects N, P and S are presented and discussed for each cruise. Salinity, temperature and other hydrographic parameters including oxygen and transmittance has allowed the identification of the dominant water masses present at the Iberian margin. Hypotheses on the main physical and biological processes driving the DOC vertical and cross-margin distributions are discussed based on the dominant seasonal hydrographic characteristics and from statistical comparisons of DOC with complementary data (e.g. DON, inorganic nutrients, primary production, bacterial production).

3.2 RRS Charles Darwin Cruise CD110B

Cruise 110 Leg B on the RRS Charles Darwin (CD110B) was one of several focusing on the NW Iberian continental shelf and slope for the OMEX II-II programme. The cruise aimed to systematically map water properties along several cross-shelf transects covering coastal and oceanic environments, at the surface and throughout the water column. However, this was only achieved along transect P (Table 8 in section 2.2.2) due to the persistent, extremely poor weather conditions hampering the deployment of the CTD (i.e. conductivity, temperature, depth sensors) and bottles for water collection and hydrological measurements. For further detailed information on cruise CD110B refer to Miller (1998).

3.2.1 General Hydrography

Near the coast, a plume of fresher, colder water (i.e. <35, ~14°C) was observed (Figure 37). This plume was constrained by a poleward surface current travelling along the coastline, which effectively traps terrestrial-derived waters at the coast and/or within the associated Rias. The

warm and saline waters (14.5 - 16.0°C, >35.8 salinity) of the poleward current are thought to originate from the Gulf of Cadiz (Frouin et al., 1990) and when the current reaches the Spanish coastline it is mainly depleted of nutrients (Castro et al., 1997).

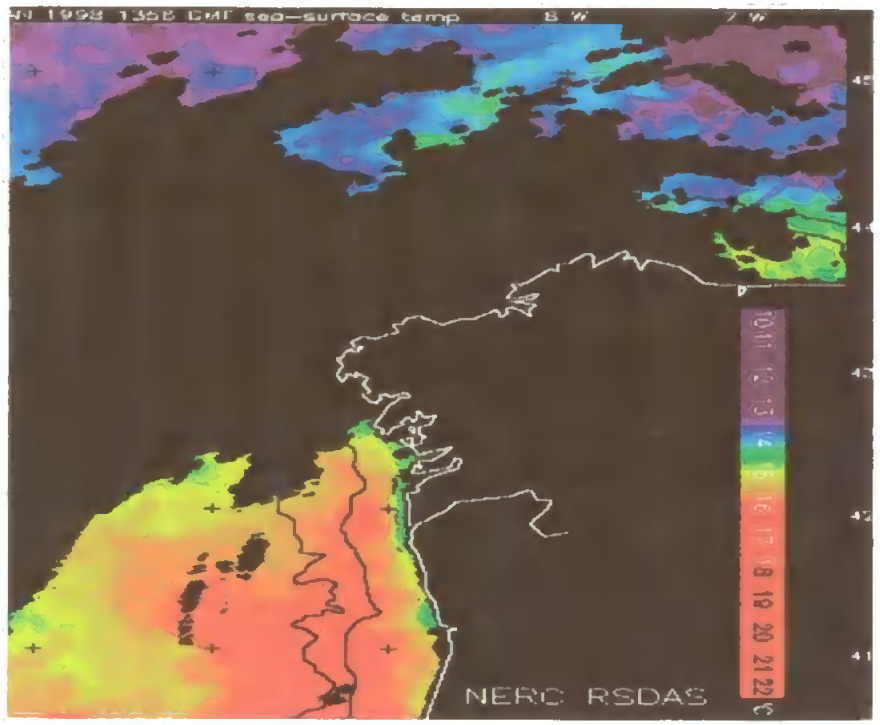

Figure 37. SeaWifs satellite image of the sea-surface temperature (SST) off the north-west coast of the Iberian Peninsula (08-Jan-1998). Courtesy of RSG, PML, U.K. Note: Black colour to the east is cloud coverage

3.2.2 Transect P (42°40'N) Salinity and Temperature

The water column displayed an upper mixed layer (see Figures 38 and 39) which varied from 75 to 140m depth. This layer was bounded below by a pycnocline that was present in water columns of 150m or more depth. Below the surface mixed layer, Eastern North Atlantic Central Water (ENACW) predominated (Figure 40). This water mass was mixed at intermediate depths with Mediterranean Sea Outflow Water (MSW: 12.01°C, 36.5; van Aken, 2000b) that was largely located between 800 - 1200m. Labrador Sea Water (LSW: 3.43°C, 34.9; van Aken, 2000a) is usually present in depths over ~1800m as suggested by the enhanced dissolved oxygen levels (Figure 41; 279µmol kg^{-1}, van Aken, 2000a). Hinrichsen et al. (1993) carried out hydrographic observations at the Iberian margin to demonstrate the variability of water masses (i.e. ENACW, MSW and LSW) in upper and intermediate layers (Figure 42). T-S plots

produced from this study (e.g. Figure 43) agree well with those from the same area produced by Hinrichsen and his co-workers (Hinrichsen et al., 1993).

A T - S plot (i.e. temperature and salinity) along transect P throughout the water column shows the presence and mixing of distinct water masses (Figure 43). Freshwater (FW) from terrestrial sources near the coast had the lowest salinity (~33) but was warm (~14°C) due to its presence at the surface. This mixed with the poleward current (PC) which had slightly higher temperature (~15°C) due to its subtropical origin. ENACW was colder (~11°C) and of slightly lower salinity (35.5) than the poleward current. MSW was of approximately the same temperature as ENACW but had distinctively higher salinity (>36). LSW was the coldest water mass present (<4°C) at the Iberian margin and was of lower salinity (~35).

At some stations (e.g. P200), especially those at the shelf break, optical backscatter increased near the bottom and was coupled with reduced light transmittance (Figure 44), suggesting possible resuspension of sediments. This has been observed elsewhere on the shelf and has been associated with the remineralisation of OM (Alvarez-Salgado et al., 1999).

3.2.3 CD110B (42°40'N) Dissolved Organic Matter

Seawater samples were collected from four stations along 42°40'N during winter survey cruise CD110B (see Table 24): a coastal station (P100), two stations on the slope, which sampled the pole-ward current (P200, P1000), and an offshore station (P2800).

Table 24. Co-ordinates, maximum depth and number of samples from CD110B transect P stations.

Station	Cast	Latitude	Longitude	Maximum depth	No. samples
P100	52	42°40'N	09°12'W	~100m	5
P200	50, 51	42°40'N	09°30'W	~200m	7
P1000	54, 55	42°40'N	09°36'W	~1000m	12
P2800	49	42°40'N	10°18'W	~2800m	12

DOC and DON concentrations measured along the water column at transect P ranged from 46 – 85 μM-C and 0 – 10.4 μM-N (see Table 25 for individual stations) [10]. C:N ratios of DOM

[10] Zero DON concentration denotes that all of the TDN was inorganic nitrogen; DON was calculated by subtracting NO_2 and NO_3 from TDN. Inorganic nutrient data was obtained from IIM-CSIC in Vigo, Spain, IEO in La Coruna, Spain and University of Plymouth in Plymouth, U.K.

ranged from 6 to infinity suggesting that there were various sources of carbon and nitrogen to the DOM pool at the Iberian margin and that the rates of cycling of the two pools were different.

Table 25. DOC and DON concentration ranges from CD110B stations.

Station	Range of DOC, μM-C	Range of DON, μM-N	C:N ratios
P100	60 – 68	n.d. – 4.7	14
P200	59 – 85	2.8 – 10.4	(13) 6 – 17
P1000	46 – 82	1.7 – 8.3	(14) 9 – 30
P2800	50 – 68	n.d. – 4.9	14

Note: values in parentheses = mean; n.d. = non-detectable levels.

C:N ratios decreased with depth in the shelf stations (P100 and P200) whereas they generally increased in the offshore stations (P1000 and P2800). This and high inorganic nutrient concentrations of surface coastal waters (Figure 46) suggests enhanced DOC contribution from terrestrial sources. DOC:DON ratios near the Redfield value (i.e. C:N = ~6.6; Redfield et al., 1963) were observed in bottom waters of the shelf-break station (P200). The presence of deep water N-rich DOM may result from the quality of organic material diffused from sediment pore waters or remineralised from suspended particles (Alvarez-Salgado et al., 1999).

DOC concentrations were significantly higher (ANOVA; $F_{1,40} = 4.25$, $P = 0.046$) [11] in the upper 100m (mean: 72 μM-C) than those in deeper waters (mean: 65 μM-C) along transect P. Surface DON concentrations (mean: 5.0 μM-N) were also generally higher than those in deeper waters (mean: 3.6 μM-N) but there was no statistically significant difference between upper and deep-water column DON concentrations.

Vertical profiles of DOC at stations sampled along transect N show generally homogeneous concentrations in the upper 100m with small elevations (~10 - 20 μM-C) at near-bottom waters at the shelf-break (P200) and between 100 – 150m depth in offshore stations (Figure 46). Elevated DOC concentrations of similar magnitude were also observed in near-bottom waters of station P1000 on the continental slope (Figure 48). Elevations of such magnitude have been previously observed and may reflect a zone of enhanced organic carbon deposition (Miller et al., 1997). Deep-water background concentrations were as low as 46 μM-C. This value is in agreement with previously measured concentrations in deep Atlantic waters (46±7 μM-C,

[11] ANOVA tests whether the difference between the sample means is too great to be explained by random error (Miller and Miller, 1993).

Thomas et al., 1995; ~50 - 55 μM-C, Chen et al., 1996c). DON concentrations at bottom waters of stations P200 and P1000 were also elevated (~2 – 5 μM-N excess) (Figures 49 and 50).

To aid in the determination of any discernible trends in DOM concentrations across the Iberian margin, contour diagrams (*Surfer®*) of DOC and DON concentrations were created. For a higher resolution, and hence more representative contour plot, it was necessary to interpolate concentrations between stations and depths, whereby a mean estimate was calculated between any two consecutive measurements. However, it is important to use caution when interpreting results from contour plots as the software (*Surfer®*) sometimes contrives features when there is lack of sufficient data points and/or high variability in the dataset. A combined use of vertical profiles and contour plots is thus necessary to retain objectivity and accuracy in the interpretation of results.

Figures 50 and 51 illustrates the DOC and DON distribution at a vertical cross-section of the Iberian margin along transect P. DOC and DON concentrations in the pole-ward current (upper 100m) were elevated (range: 65 – 82 μM-C and 4.6 - 8.3 μM-N) compared to the coastal and oceanic stations (range: 62 - 70μM-C and n.d. – 5.0 μM-N). In deeper waters (>100m), DOM concentrations progressively decreased away from the coast.

3.2.4 Transect P (42°40'N) Summary

In summary, there were several main features of the DOC and DON distributions along transect P of the Iberian margin during January 1998. These included:

- Higher DOM (i.e. DOC and DON) concentrations in the upper 100m of the water column compared to deeper waters
- Higher DOC concentrations in the poleward current compared to surface coastal and offshore waters
- Higher DOM concentrations in bottom waters of the shelf-break and slope stations
- A progressive decrease in DOM concentrations away from the continental shelf and slope

To elucidate some of the dominant physical and biological factors influencing vertical DOC and DON distributions cross-margin and at each station along 42°40'N, salinity, temperature (°C), NO_2 + NO_3 (μM-N), NH_4 (μM-N), and chlorophyll-a (mg m^{-3}) were selected as the key parameters against which to regress DOC and DON in a correlation matrix analyses using Pearson's product-moment correlations and Anova to test their significance. Primary

production (mg-C m^{-3} hr^{-1}) and maximum photosynthetic yield (PmB) were also used in correlation matrices with DOC and DON to study the relationship between phytoplankton production and DOM. Regression plots showing best-fit lines and the square of regression coefficients (R^2) are presented in the Appendices.

The negative correlation of inorganic nutrients with DON (-0.76; n = 38; P<0.05; Figure 1 in Appendix 1) suggests that as nutrients were utilised by the phytoplankton community in the photic zone, DON was released (Biddanda and Benner, 1997). DON was also strongly correlated with PmB (0.93; n = 4; P<0.001; Figure 2 in Appendix 1) and primary production (0.84; n = 4; P<0.001; Figure 3 in Appendix 1) at the shelf station (P200), further supporting the suggestion that N-rich DOM was being released from the phytoplankton biomass. A strong correlation was obtained for both DOC and DON with PmB at station P1000 (0.62; n = 4; P<0.001; Figure 4 in Appendix 1 and 0.92; n = 4; P<0.001; Figure 5 in Appendix 1, respectively). In deeper waters DON was most likely taken up by bacteria and nitrified to inorganic nutrients (Kirchman and Williams, 2000).

Higher DOM concentrations are commonly found in surface oceanic waters and within the photic zone where DOM production by the active biota is high (Williams, 1995). Biological activity was higher in the surface waters of the Iberian margin as observed by measurements of primary productivity (Figure 52). At the offshore station (P2800), DOC and DON correlated well with chlorophyll-a (0.70; n = 4; P<0.001; Figure 6 in Appendix 1 and 0.98; n = 4; P<0.001; Figure 7 in Appendix 1, respectively) indicating that as phytoplankton biomass decreased with depth, so did DOC and DON concentrations. Most surface DOM is mineralised or incorporated into POM in the upper 200m of the water column (Lee and Wakeham, 1992) leaving a background DOM pool in the deep waters containing mainly refractory material.

A contour diagram of light transmission along transect P (Figure 53) illustrates trends of increasing transmission from coastal surface water toward offshore surface waters. In addition, an area of lower transmission in the bottom waters of the slope at approximately 1000 - 1200m was observed. Reduced transmission suggests the presence of suspended particulate material (i.e. biomass, detritus, sediments) in the water column (Bartz et al., 1978; McCave et al., 2001).

The transmission distribution along transect P corresponded closely to DOC distribution and this suggests that DOM source mechanisms from POM (i.e. PER [12] and lysis from biomass and detritus, disaggregation and remineralisation) are playing an important role in the

[12] PER – photosynthetic extra-cellular release

biogeochemical cycling of DOM in surface waters and bottom waters of the slope (Azam, 1998).

Despite the enhanced particle loading near the coast (Figure 53), DOC concentrations were lower there than in the poleward current. In addition, DOC correlated well with nitrates (0.60; n = 5; P<0.001; Figure 8 in Appendix 1) and ammonia (0.78; n = 5; P<0.001; Figure 9 in Appendix 1) at station P100 suggesting that DOC near the coast has a large terrestrial component. It is thus suggested that the removal rate of DOC at the coast was higher than further on the shelf; this is supported by observations of higher bacterial activity near the coast (Dr. H. Galvao, pers.com.).

It is likely that near the bottom waters of the slope around 1000m, the northward movement of the MSW along the continental slope (current velocity: 0.1 m s^{-1}; Huthnance et al., in press) creates disturbance of the overlying sediments (i.e. *via* slow advection and turbulent diffusion; Richardson and Mooney, 1975) and causes sediment resuspension. The suspended particles may mix out of the bottom layer into the water column to create an intermediate nepheloid layer (INL) (McCave et al., 2001). DOM may subsequently be enhanced within the waters of the INL due to particle dissolution and remineralisation processes (Smith et al., 1992; Miller et al., 1997).

The progressive decrease of DOM concentrations away from the continental shelf and slope is probably a result of the decreasing influence from sources such as sediment pore waters and an increasing degree of mixing with deep water masses that contain lower DOM.

In summary, during the winter CD110B cruise, conditions of a poleward current and terrestrial water runoff were observed in surface waters of the Iberian margin. DOC distribution was relatively homogeneous in the upper mixed layer, with concentrations decreasing with depth. The poleward current had elevated DOC concentrations compared to coastal and offshore waters. Within the water column, several distinct water masses occupied specific depths. The use of complementary data suggested the following main processes occurring:

- the input of C-rich DOM from terrestrial sources but enhanced uptake rate of DOM at the coast.
- the release and accumulation of DOM from primary producers (*via* PER, lysis, grazing) in the photic zone and its subsequent removal in deeper waters.
- the re-introduction and accumulation of N-rich DOM from remineralisation of suspended particles and diffusion from sediment pore-waters at depth.

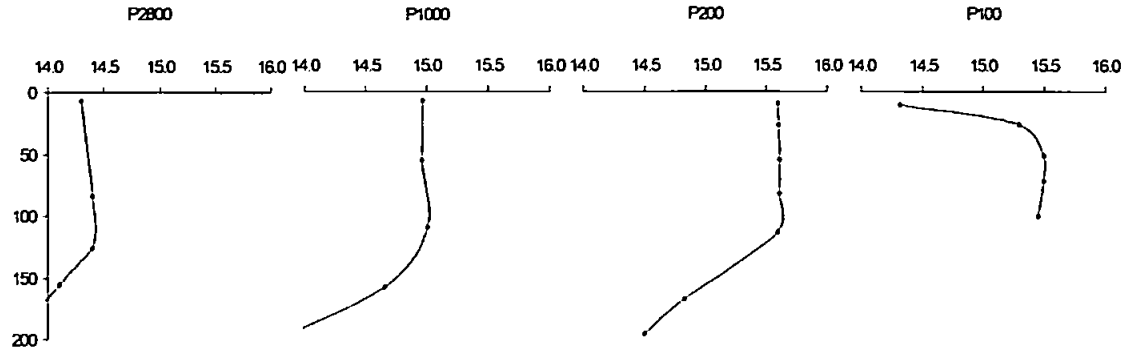

Figure 38. Vertical profiles of temperature (°C) in the upper 200m of CD110B transect P. Note: y-axis is depth (m).

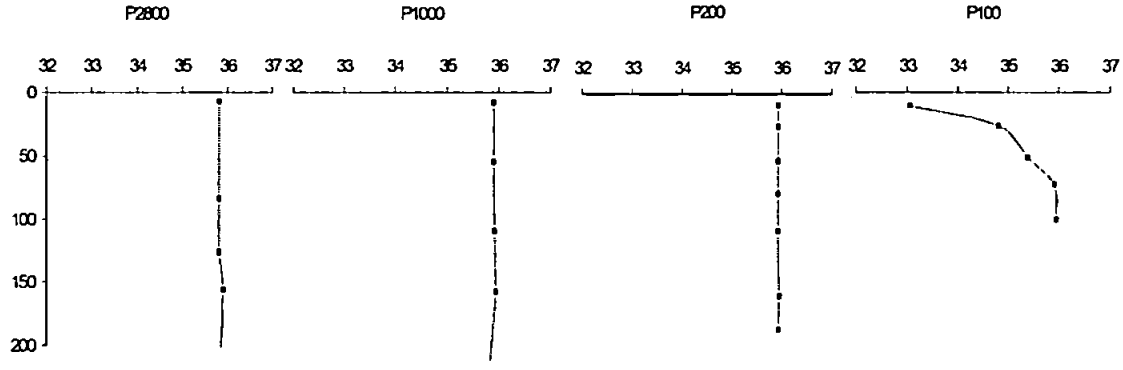

Figure 39. Vertical profiles of salinity in the upper 200m of CD110B transect P. Note: y-axis is depth (m).

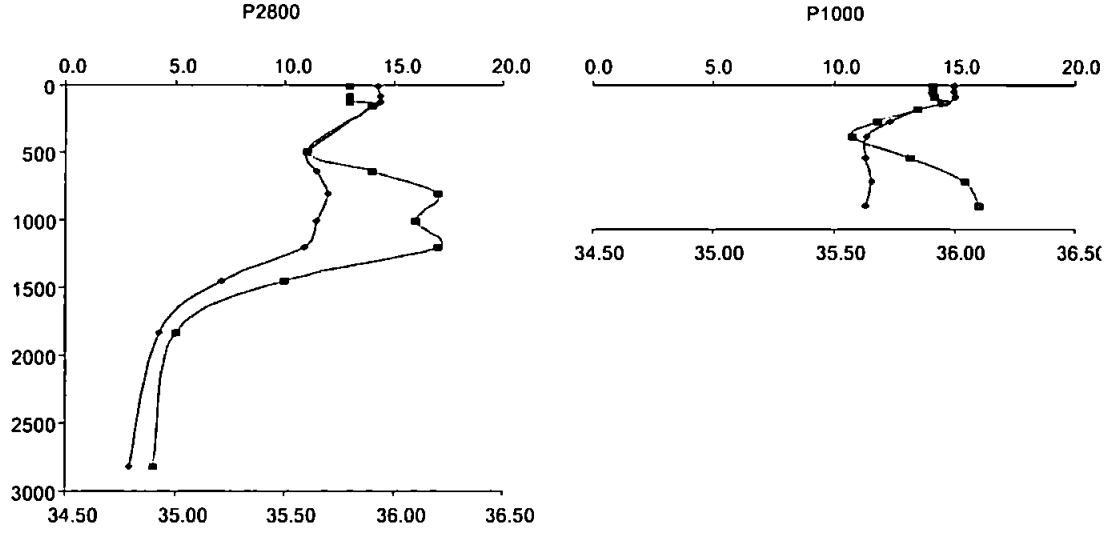

Figure 40. Vertical profiles of salinity and temperature (°C) at CD110B offshore stations P1000 and P2800. Note: ♦ - temperature, – salinity; y-axis is depth (m).

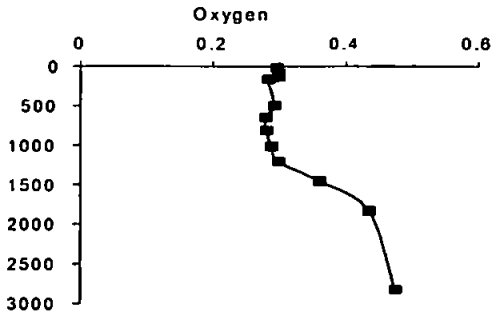

Figure 41. Vertical profile of oxygen (mM) at CD110B station P2800. Note: y-axis is depth (m).

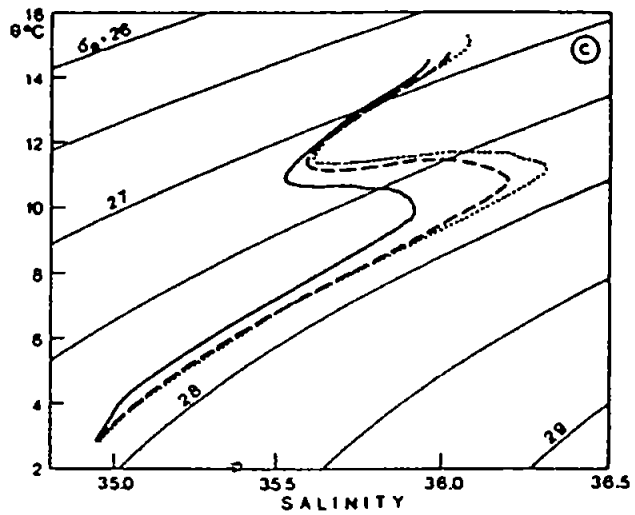

Figure 42. T-S plot for stations at the Iberian Margin east of 15°W (dashed line), west of 15°W (solid line) and for stations with intermediate salinity maxima >36.25 (dotted line)[13]. Taken from Hinrichsen et al., 1993.

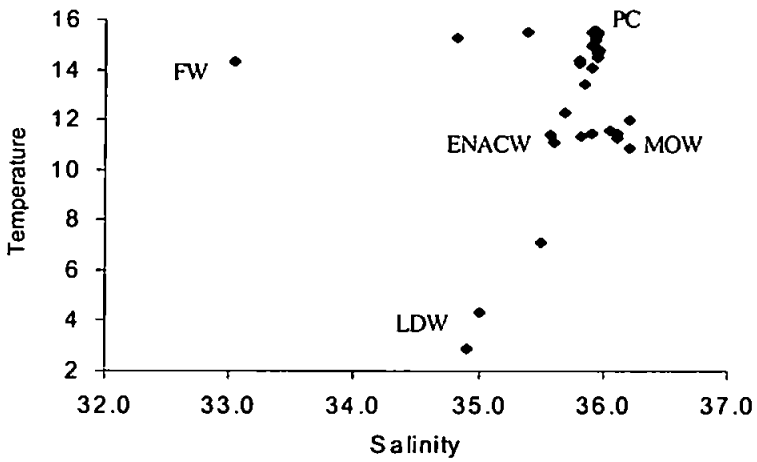

Figure 43. T - S plot of the water column along CD110B transect P.

[13] The latter (dots) is representative for the highly saline Mediterranean core layer.

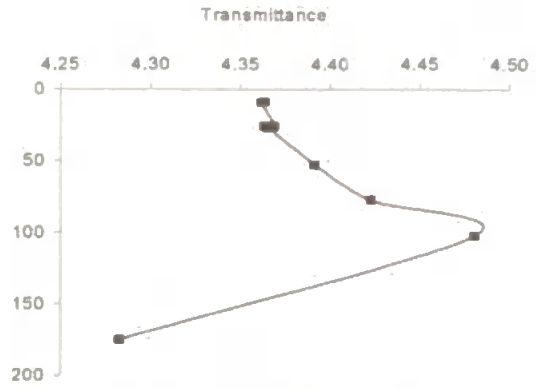

Figure 44. Vertical profile of light transmittance at CD110B station P200. Note: y-axis is depth (m).

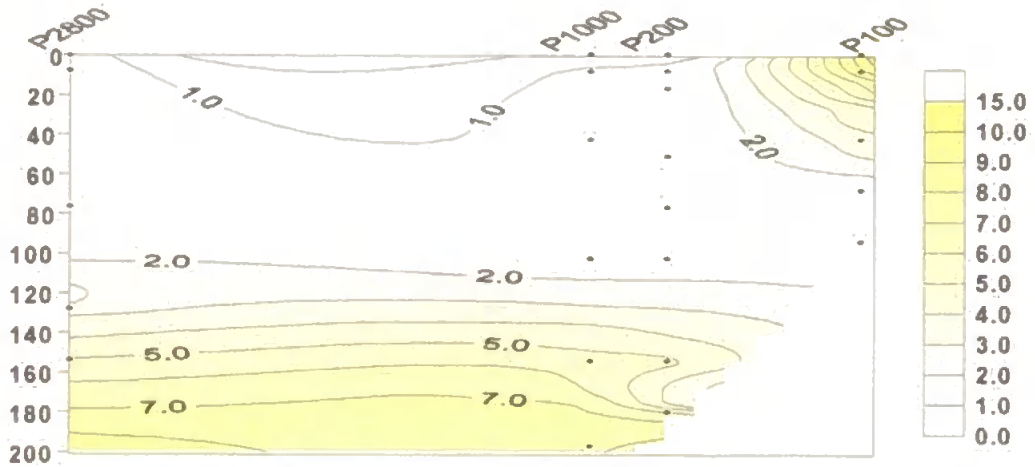

Figure 45. Contour plot of NO_2 and NO_3 concentrations along CD110B transect P. Data from IIM-CSIC, Vigo, Spain. Note: colour scale is µM-N; y-axis is depth (m).

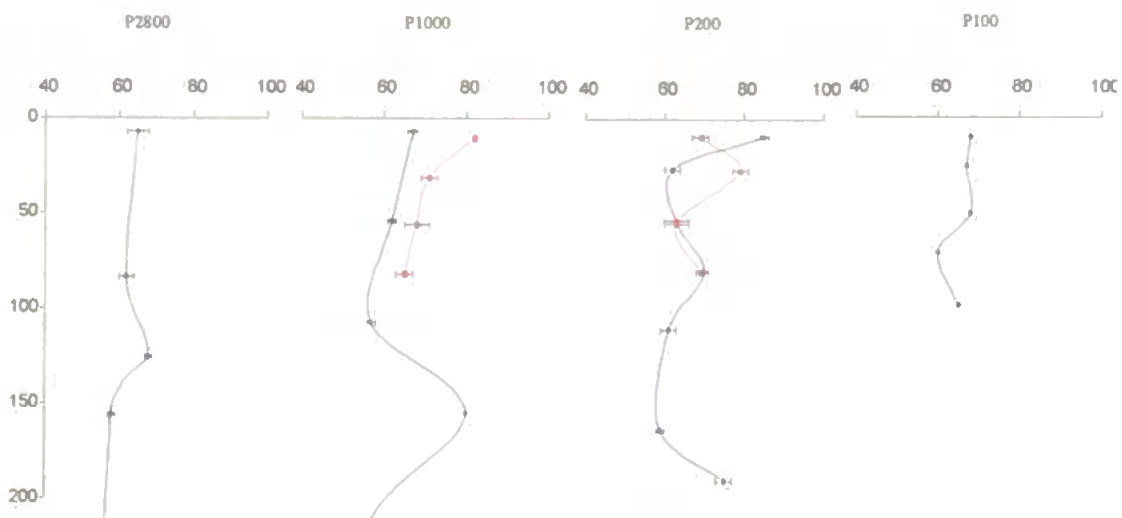

Figure 46. Vertical profiles of DOC concentrations (µM-C) in the upper 200m of CD110B transect P. Note: ♦ - first CTD cast, ■ - extra CTD cast; y-axis is depth (m).

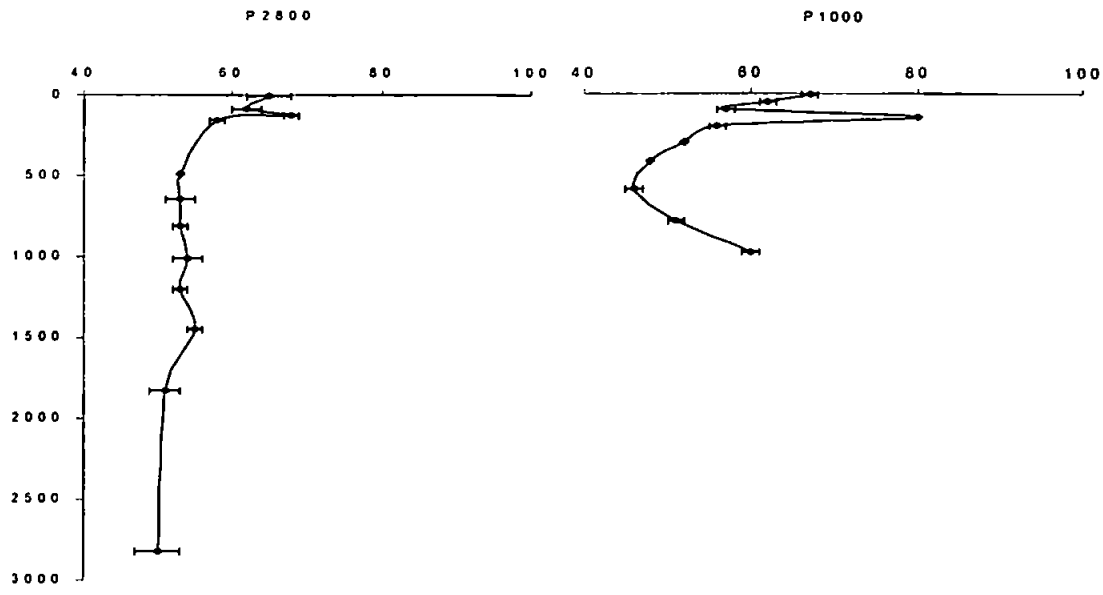

Figure 47. Full vertical profiles of DOC concentrations (μM-C) at CD110B offshore stations P1000 and P2800. Note: y-axis is depth (m).

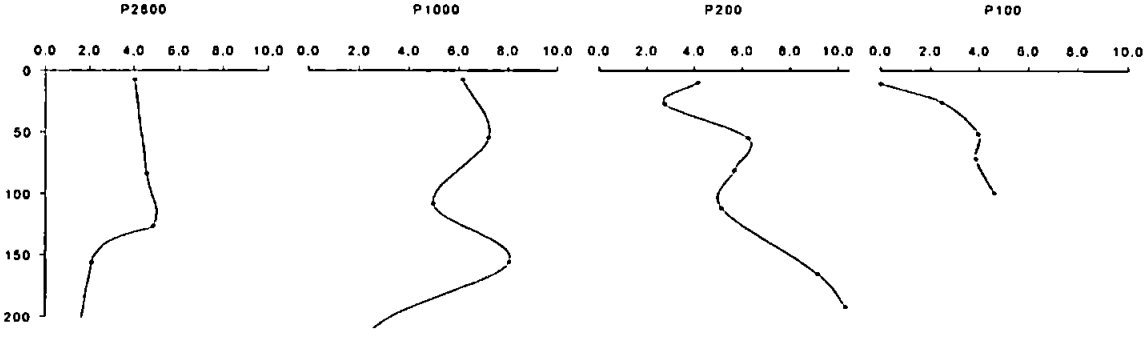

Figure 48. Vertical profiles of DON concentrations (μM-N) in the upper 200m of CD110B transect P. Note: y-axis is depth (m).

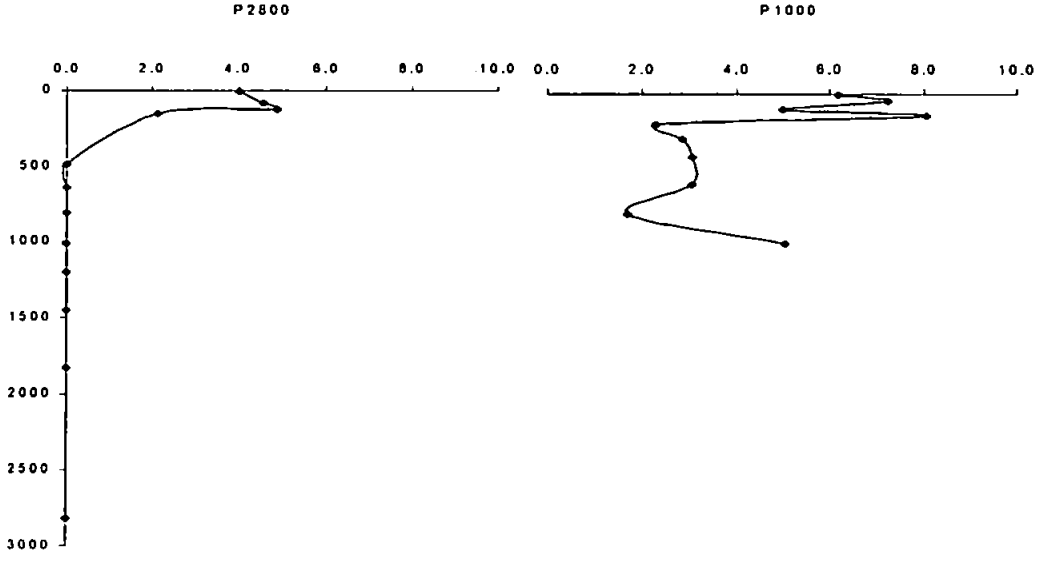

Figure 49. Full vertical profiles of DON concentrations (μM-N) at CD110B offshore stations P1000 and P2800. Note: y-axis is depth (m).

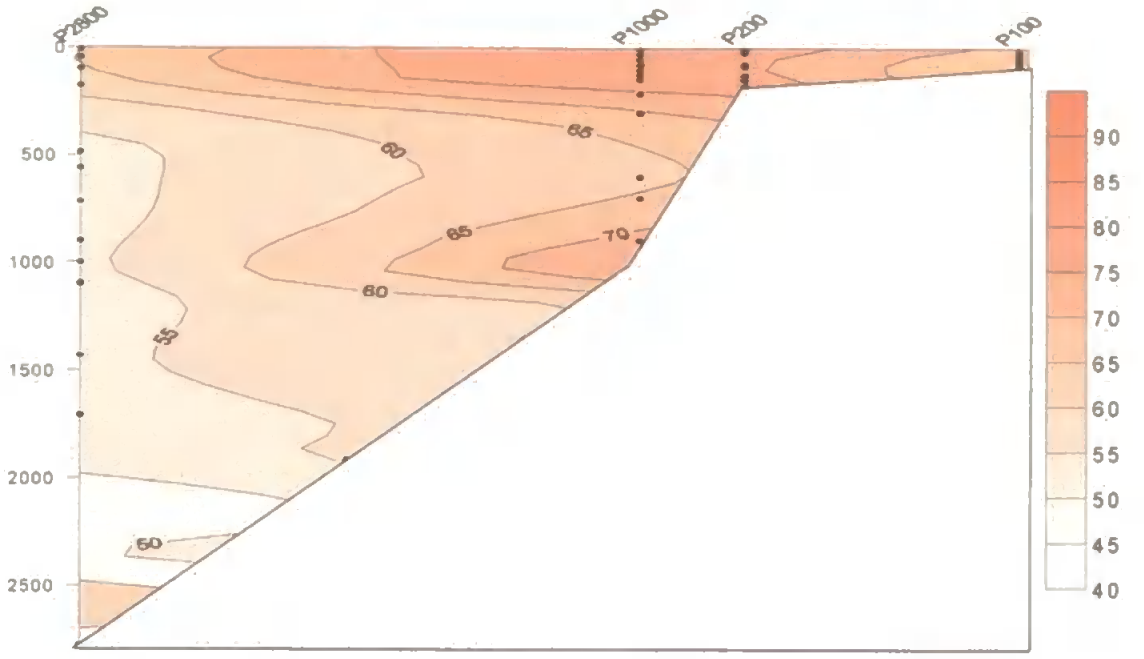

Figure 50. Contour plot of DOC concentrations along CD110B transect P. Note: colour scale is µM-C; y-axis is depth (m).

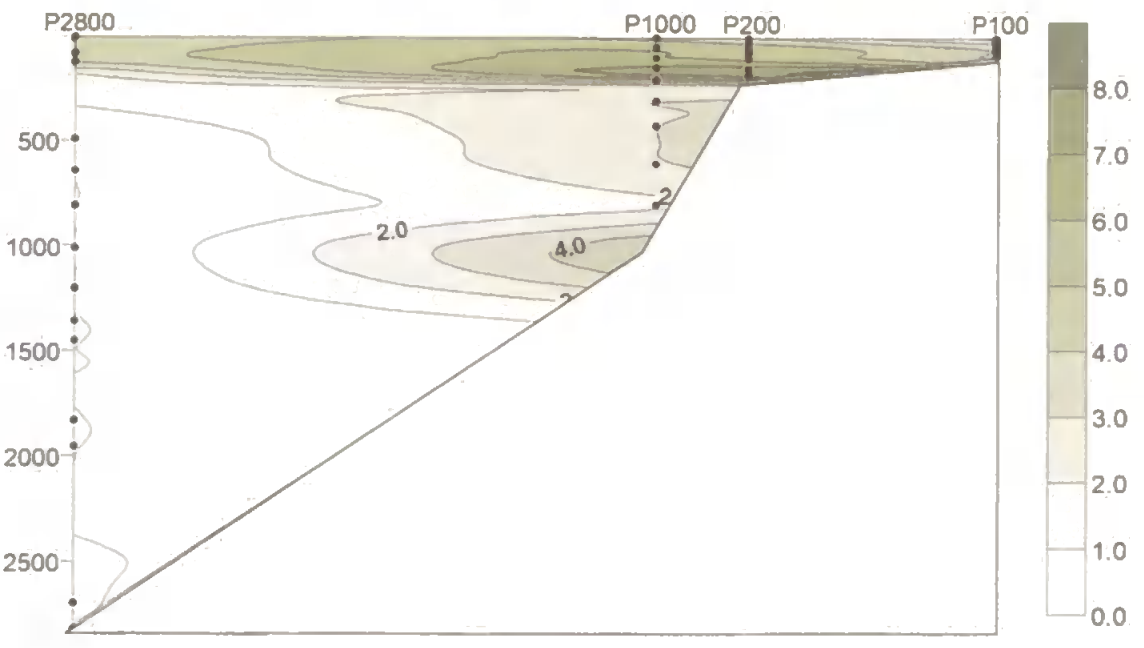

Figure 51. Contour plot of DON distribution along CD110B transect P. Note: colour scale is µM-N; y-axis is depth (m).

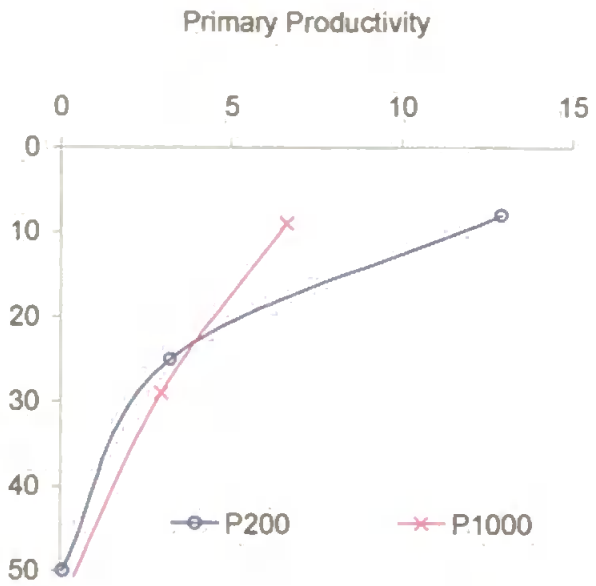

Figure 52. Vertical profiles of primary productivity (mg-C m^{-3} d^{-1}) in the upper 50m of CD110B stations P200 and P1000. Data from IIM-CSIC, Vigo, Spain. Note: y-axis is depth (m).

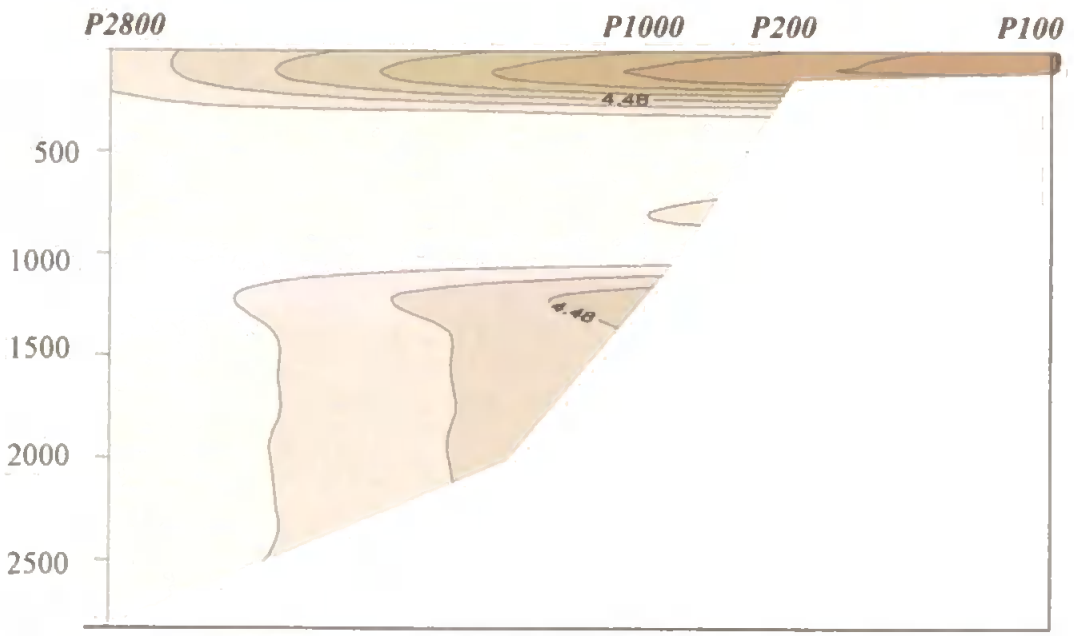

Figure 53. Contour plot of light transmission along CD110B transect P. Note: darker colour indicates lower light transmission; y-axis is depth (m).

3.3 R/V Prof. Shtokman Cruise OMEX0898

Cruise OMEX0898 on the R/V Professor Shtokman aimed to systematically map water properties along the main OMEX cross-shelf transects (N, P & S; see Figure 16 in section 2.2.2) across the Iberian margin during upwelling conditions. The weather conditions during OMEX0898 were generally favourable allowing extensive sampling of transects (Table 8 in section 2.2.2). For further detailed information of activities of cruise OMEX0898 refer to Bode (1998).

3.3.1 General Hydrography

Cruise OMEX0898 took place during 1st – 11th August 1998 during the summer period at the Iberian Margin, when upwelling conditions generally prevailed. SST Satellite images (Figure 54) and *in situ* temperature measurements showed that surface shelf waters were cooler than surface waters offshore. Minimum surface temperatures (<15°C) were observed off Cape Finisterre in the north and the River Minho south of the Ria de Vigo, where upwelling intensity has previously been reported to be high (Castro *et al.*, 1994). Colder water filaments were observed at the sampling region extending from the coast to the open ocean with the longest filament located south of the Ria de Vigo (42°00'N). Such filaments have been previously detected (Haynes et al., 1993). These conditions were generally maintained through the duration of the cruise.

3.3.2 Transect N (43°00'N) Salinity and Temperature

Temperature and salinity profiles in the upper 200m of the water column of stations on transect N (Figure 55 and 56) show upwelling of colder and more saline ENACW from ~100m to the surface [14]. It is evident from the increasing temperature of surface waters towards offshore regions (Figure 55) that near the coast ENACW was recently upwelled. Moving offshore, the surface temperature increased as a result of solar radiation. The upper 100m along transect N exhibited a weak thermocline across the margin with the exception of the offshore station (N3300), where a surface mixed layer was observed in the upper 50m bounded below by the thermocline. The upper 50m of the shelf and slope stations (N30, N220 and N1600) were slightly less saline than the subsurface and offshore waters, resulting in some vertical heterogeneity (Figure 56). Combined salinity and temperature profiles at the offshore stations

[14] Several stations were chosen for depiction of temperature and salinity properties based on their distance from other stations and the number of samples collected from each.

(Figure 57) illustrate the presence of the ENACW and MSW cores at ~500m and ~1100m, respectively.

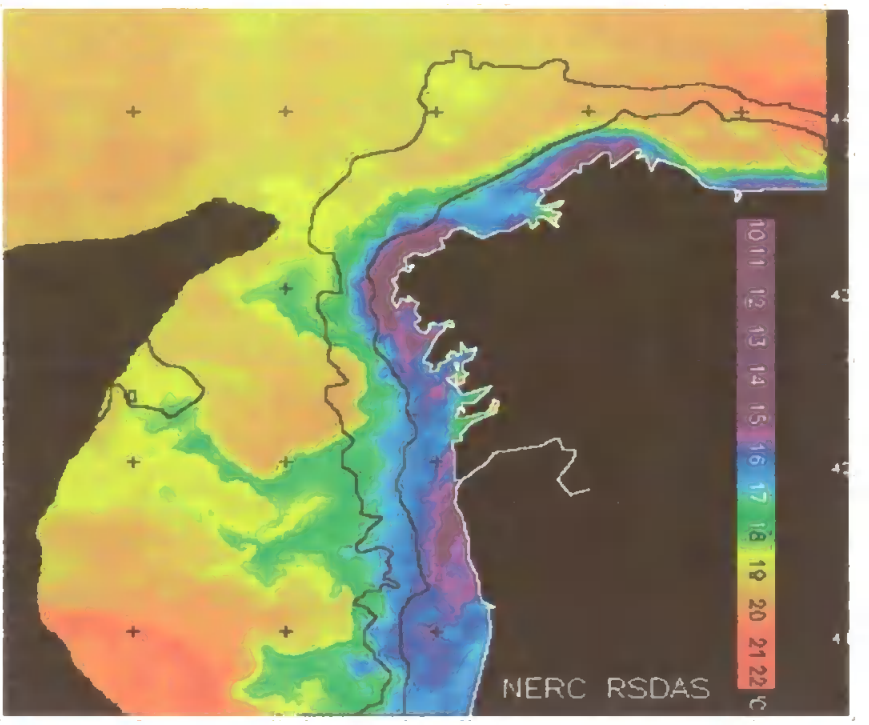

Figure 54. SeaWifs satellite image of the sea-surface temperature (SST) off the north-west coast of the Iberian Peninsula (08-Aug-1998). Courtesy of RSG, PML, U.K. Note: Black colour to the east is cloud coverage.

Four main water masses were present along transect N during the summer survey (Figure 58). Warm and saline surface water (SW; 19°C, 35.9) was found at offshore stations. The second defined water mass, ENACW, which had a fairly constant salinity (35.7 – 35.9), exhibited a large temperature range (10 – 18°C) due to it being upwelled from 100 - 150m to the surface where it was heated by the solar radiation. In contrast, MSW exhibited a wider salinity range (35.9 – 36.3) and smaller range of temperature (8 – 11°C), probably due to its mixing and subsequent dilution with less-saline offshore deep waters. Labrador Sea Water (LSW; ~35.2, ~4°C) was present at stations with depths of over ~2000m.

3.3.3 Transect N (43°00'N) Dissolved Organic Matter

Seven stations were sampled for DOC and TDN along 43°00'N during cruise OMEX0898: a coastal station (N30), a shelf station (N100), a shelf-break station (N220), two slope stations (N1600, N2300) and two offshore stations (N3000, N3300). Details of the sampling stations are presented in Table 26.

Table 26. Co-ordinates, maximum depth and number of samples collected at OMEX0898 transect N stations for DOM measurements.

Station	Cast	Latitude	Longitude	Maximum depth	No. samples
N30	22	43°00'N	09°18'W	~30m	7
N100	N/A	43°00'N	09°24'W	~100m	10
N220	19	43°00'N	09°31'W	~220m	8
N1600	21	43°00'N	09°39'W	~1600m	10
N2300	20	43°00'N	09°43'W	~2300m	11
N3000	18	43°00'N	10°01'W	~3100m	9
N3300	17	43°00'N	10°18'W	~3300m	12

DOC and DON concentrations sampled along transect N ranged from 42 – 151 μM-C and n.d.–14.3 μM-N (see Table 27 for individual stations). There were no significant trends in C:N ratios either with depth at each station or across the margin. C:N ratios varied from ~6 (i.e. near Redfield) to infinity in deep oceanic waters (>1000m) where DON concentrations were very low (i.e. 0.n.d.- 0.9 μM-N). This indicates that during the summer along transect N the input and removal rates of the main elemental components to the DOM pool were different (Williams, 1995).

Table 27. DOC and DON concentration ranges at OMEX0898 transect N stations.

Station	Range of DOC, μM-C	Range of DON, μM-N	C:N ratios
N30	69 - 151	n.d. – 8.6	9
N100	54 – 86	2.9 – 14.3	(12) 6 – 22
N220	59 – 78	2.2 – 5.4	(19) 12 – 28
N1600	43 – 57	0.2 – 5.2	(21) 10 – 33
N2300	57 – 105	2.0 – 5.9	(18) 13 – 37
N3000	51 – 70	n.d. – 5.3	13
N3300	42 – 74	1.7 – 7.5	(12) 7 – 28

Note: values in parentheses = mean; n.d. = non-detectable levels.

DOC concentrations in the upper 100m along transect N (mean: 72 μM-C) were significantly higher (ANOVA; $F_{1,58}$ = 15.08, P = 0.0003) than those in deeper waters (mean: 55 μM-C). DON concentrations were also significantly higher (ANOVA; $F_{1,59}$ = 12.00, P = 0.001) in surface (mean: 5.34 μM-N) than in the deeper waters (mean: 3.13 μM-N).

The vertical distributions of DOC in the coastal and shelf stations (Figure 59) varied between 54 – 151 μM-C. Higher DOC concentrations were found at the coastal station compared to those further offshore along the shelf, with a maximum of 151 μM-C close to coastal bottom waters. This generally corresponds to the progressively decreasing phytoplankton biomass with depth and away from the coast, as indicated by chlorophyll-a measurements (range: 0.0 – 2.5 mg m^{-3}; Figure 60). Deepening of the chlorophyll-a maximum was exemplified along transect N by increasing in situ fluorescence readings with increasing distance from the coast (Figure 61).

In the upper 200m of the slope and offshore stations (Figure 62) DOC vertical profiles exhibited fairly homogeneous distributions with slight elevations (i.e. ~10 – 30 μM-C excess) in the upper 100m (i.e. photic zone). Overall, surface DOC concentrations decreased towards offshore stations.

In the slope and offshore stations below 200m (Figure 63), DOC concentrations generally decreased to background values of 42 – 57 μM-C. There were large variations in the DOC distribution in deep waters along transect N with occasional localised DOC enhancement (i.e. ~10 – 25 μM-C excess). It is possible that the samples exhibiting enhanced DOC concentrations could be a result of random contamination (see Chapter 2 for a discussion of sources of contamination).

DON concentrations in the upper 200m along transect N varied greatly (Figures 65 and 66). Higher concentrations were observed near surface waters (<10m) in all stations with elevations of 1.5 – 9.5 μM-N over background concentrations [15]. However, surface waters of the coastal and shelf-break stations (N30 and N220) had relatively lower concentrations (<5 μM-N) which increased in sub-surface waters. Due to the large variation in DON vertical distributions at each station along transect N (Figures 64 – 66) it was difficult to detect and define any trends.

Figure 67 shows elevated DOC concentrations in surface waters compared to background deep-water concentrations. DOC accumulation was also observed at approximately 1000m depth where the MSW was present. Figure 68 depicts a DIN minimum between 1000 - 2000m generally corresponding with the DOC deep maximum. The MSW water mass is a combination of Eastern North Atlantic Central Water (ENACW), Eastern North Atlantic Deep Water (ENADW) and Gibraltar outflow from the sub-surface north-west Mediterranean Sea and enters the North Atlantic *via* the Straits of Gibraltar (Hinrichsen et al., 1993). The MSW water mass was perhaps depleted of inorganic nutrients by the time it reached the north-west Spanish

[15] Calculated mean DON in waters >20m at stations N30, N100 & N220.

coastline. The above correspondence between DOC accumulation and DIN depletion may suggest a nutrient-limitation scenario (Thingstad et al., 1998). Close to the continental slope, inorganic nutrients were enhanced, possibly due to OM mineralisation from suspended sediments (Burdige and Homstead, 1994). These processes can have a significant effect on the flux of DOM from benthic sources.

3.3.4 Transect N (43°00'N) Summary

- DOC and DON concentrations were significantly higher in surface waters (upper 100m) than deeper waters.
- There were no C:N ratio trends observed, reflecting the different rates of cycling of DOC and DON pools.
- There was enhancement of DOC in deeper waters corresponding to the location of the MSW

Correlation matrices between DOC, DON and other variables (e.g. salinity, temperature, nutrients, chlorophyll-a) along transect N showed a relatively strong correlation between DON and inorganic nutrients (-0.51; n = 59; $P<0.001$; Figure 10 in Appendix 2). In the deep waters of the offshore stations (N3000 and N3300) DOC and salinity had very strong correlations: 0.92; n = 3; $P<0.05$; Figure 11 in Appendix 2 and 0.89; n = 5; $P<0.001$; Figure 12 in Appendix 2, respectively. This relates to the suggestion that the MSW contains C-rich DOM and that with increasing depth, DON is mineralised to inorganic nutrients (Richards, 1984).

Some bacterial production (i.e. leucine uptake rate; pmol L^{-1} hr^{-1}) and biomass measurements (mg-C m^{-3}) concurrent with DOM measurements (i.e. at similar sampling depths) were performed along transect N by the University of Algarve, Portugal. DOC correlation with leucine incorporation at station N2300 gives a strong positive relationship (0.80; n = 5; $P<0.001$; Figure 13 in Appendix 2). This correlation was unexpected since bacterial production has been found to be negatively related with DOC (i.e. DOM is a food source for bacteria and hence their production; Azam et al., 1983). This shows the complexity of DOM biogeochemical dynamics at the Iberian margin.

It is suggested that:

- The DOC increase near the coast was due to increased phytoplankton productivity and N-rich DOM was present in subsurface waters across the margin in relation to the chlorophyll-a maximum.

- DOM was consumed at depth as a result of remineralisation to nutrients but the MSW may have brought in C-rich DOM and nitrogen-depleted waters.
- There was great spatial heterogeneity observed in DOM distributions due to upwelling dynamics.
- Bacterial biomass and production may have contributed to the production of DOM by facilitating its release from phytoplankton biomass and particles *via* enzymatic attack.

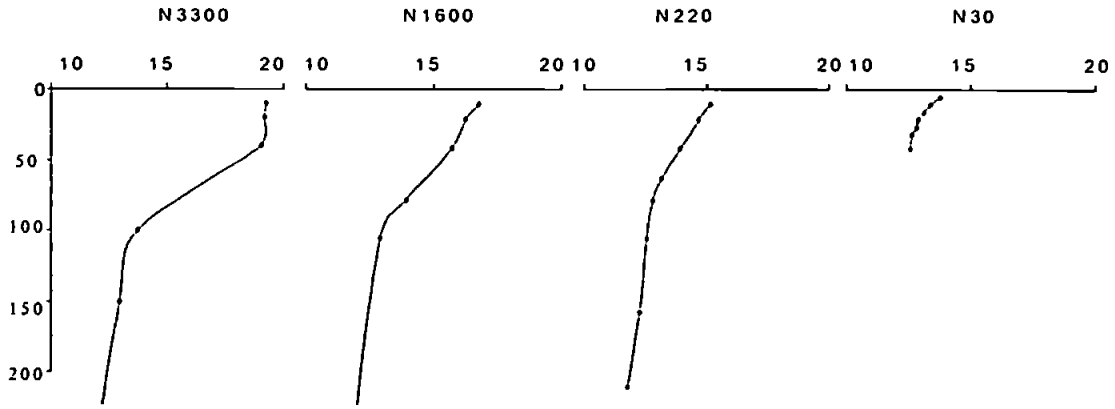

Figure 55. Vertical profiles of temperature (°C) in the upper 200m of OMEX0898 transect N. Note: y-axis is depth (m).

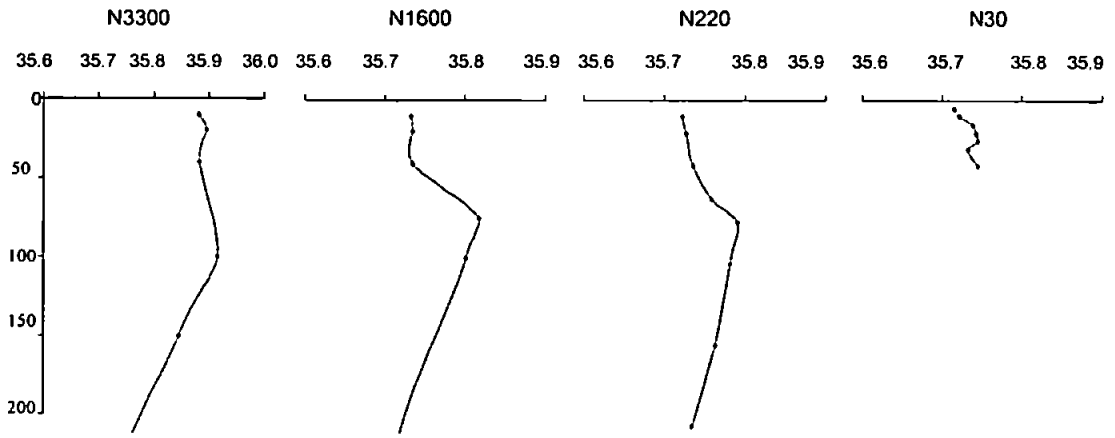

Figure 56. Vertical profiles of salinity in the upper 200m of OMEX0898 transect N. Note: y-axis is depth (m).

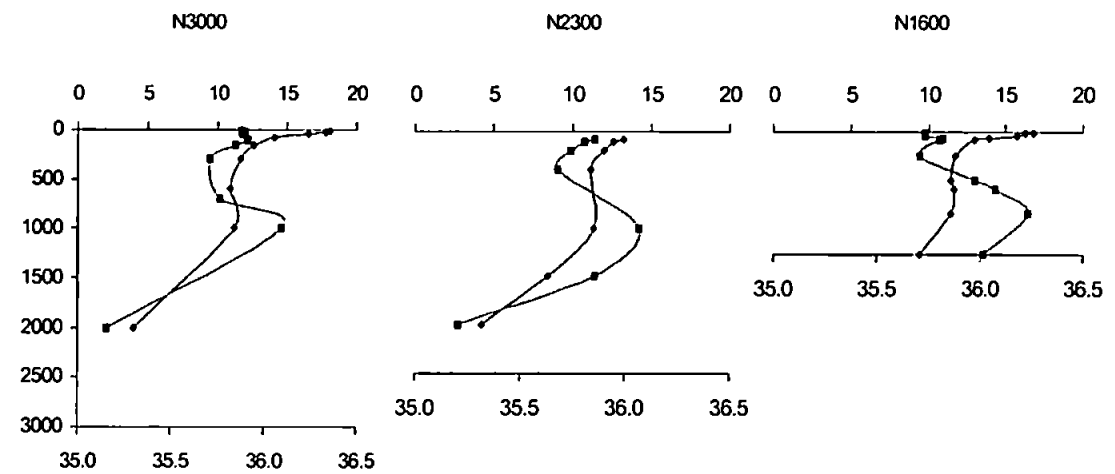

Figure 57. Vertical profiles of salinity and temperature (°C) at offshore stations (OMEX0898 N1600, N2300 and N3000). Note: ♦ - temperature, - salinity; y-axis is depth (m).

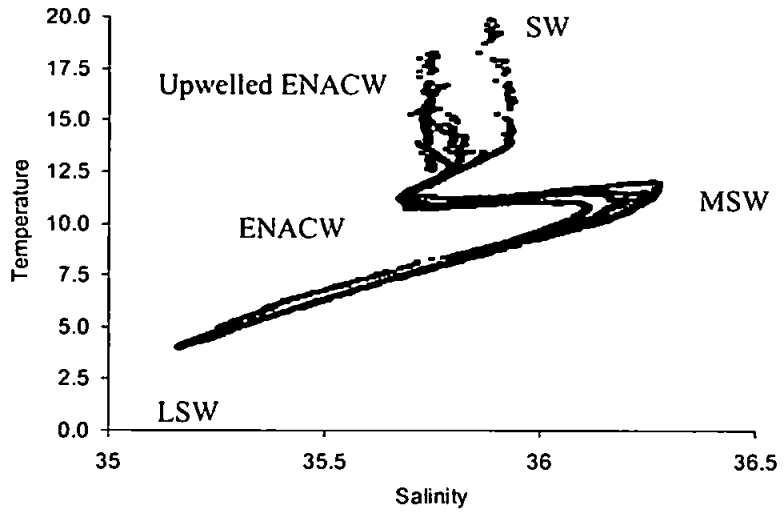

Figure 58. T - S plot of the water column along OMEX0898 transect N. Note: SW – surface water

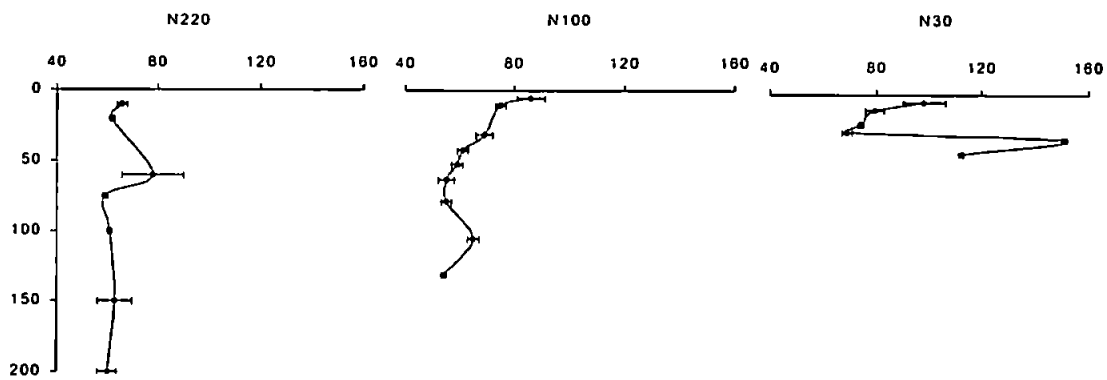

Figure 59. Vertical profiles of DOC concentrations (μM-C) in the upper 200m of OMEX0898 coastal and shelf stations N30, N100 and N220. Note: y-axis is depth (m).

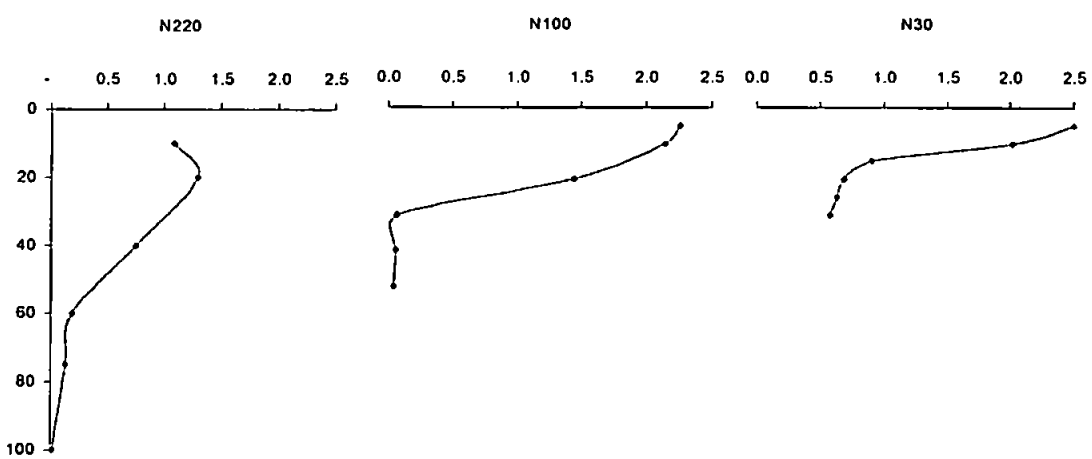

Figure 60. Vertical profiles of chlorophyll-a concentrations (mg m^{-3}) in the upper 100m of the OMEX0898 coastal and shelf stations N30, N100 and N220. Note: y-axis is depth (m).

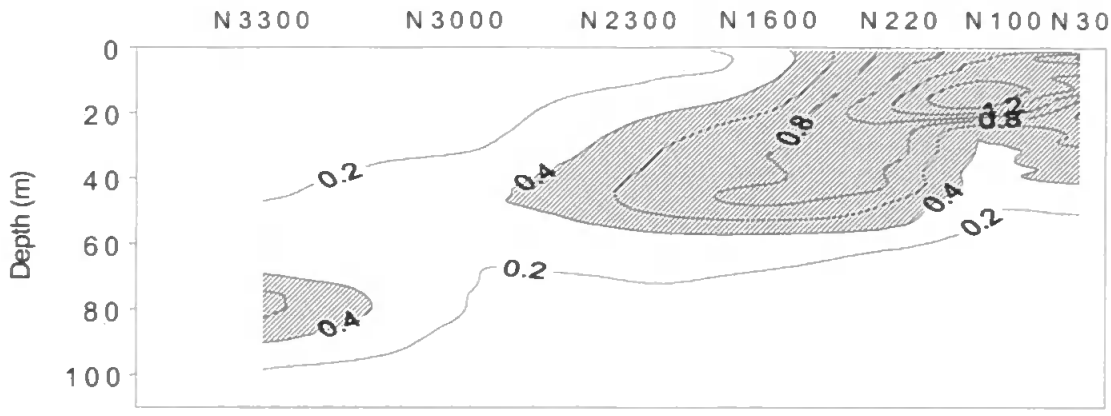

Figure 61. Distribution of in situ fluorescence in the upper 100m of OMEX0898 transect N. Taken from Bode, 1998.

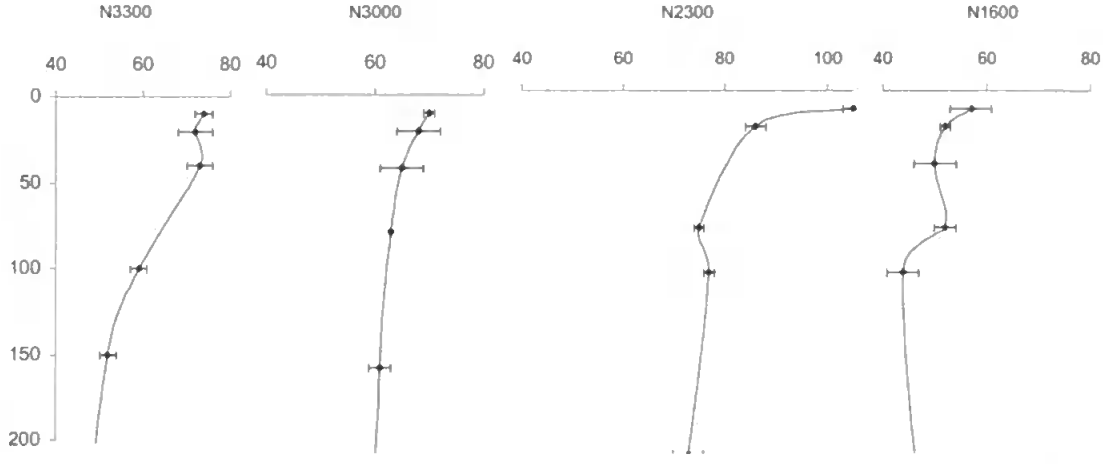

Figure 62. Vertical profiles of DOC concentrations (μM-C) in the upper 200m of OMEX0898 slope and offshore stations N1600, N2300, N3000 and N3300. Note: y-axis is depth (m).

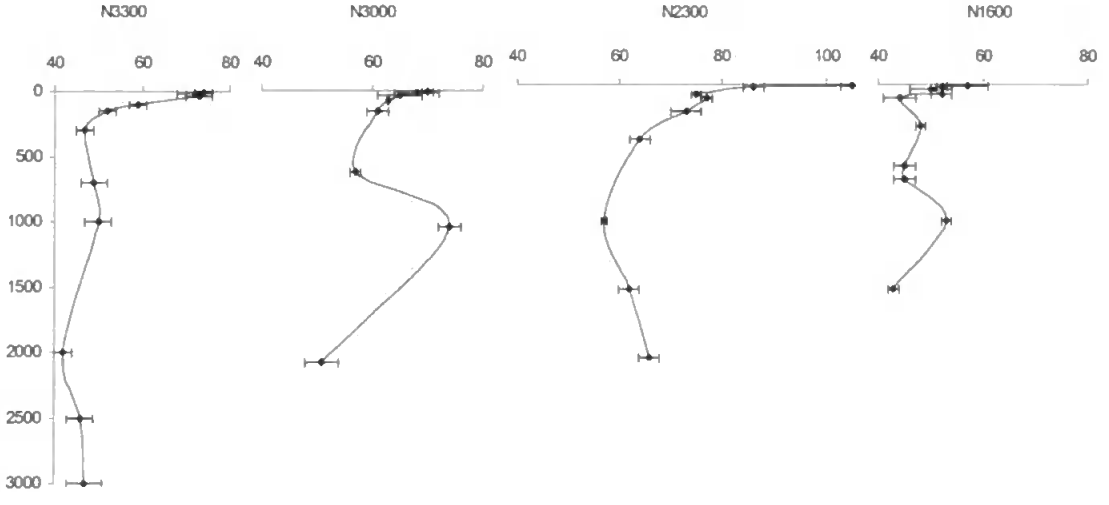

Figure 63. Full vertical profiles of DOC concentrations (μM-C) at OMEX0898 slope and offshore stations N1600, N2300, N3000 and N3300. Note: y-axis is depth (m).

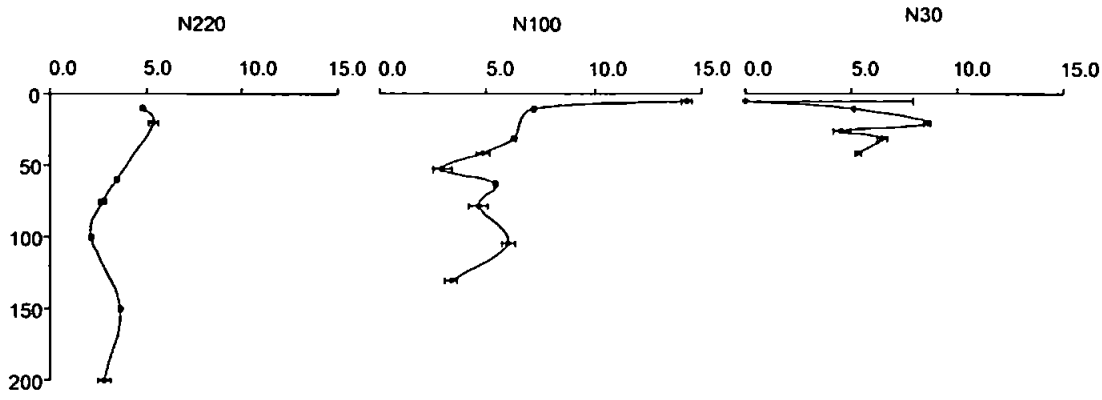

Figure 64. Vertical profiles of DON concentrations (μM-N) in the upper 200m of OMEX0898 coastal and shelf stations N30, N100 and N220. Note: y-axis is depth (m).

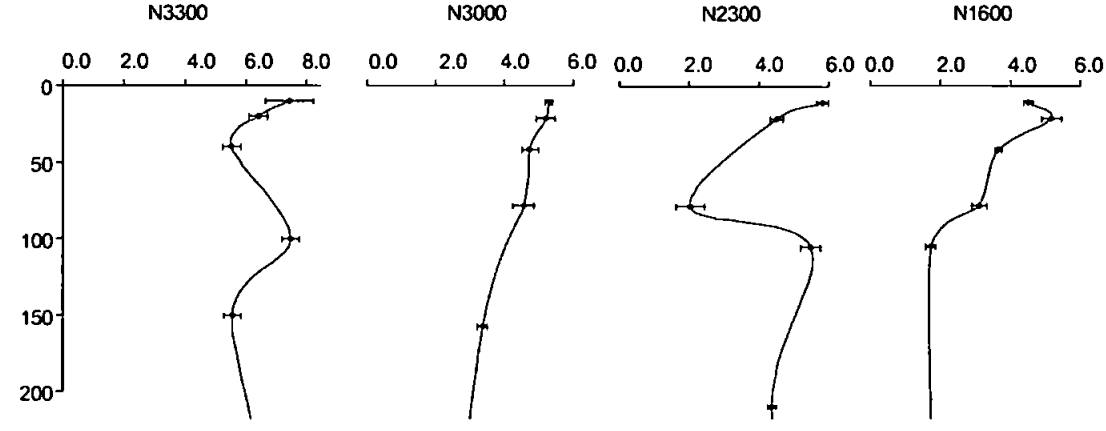

Figure 65. Vertical profiles of DON concentrations (μM-N) in the upper 200m of OMEX0898 slope and offshore stations N1600, N2300, N3000 and N3300. Note: y-axis is depth (m).

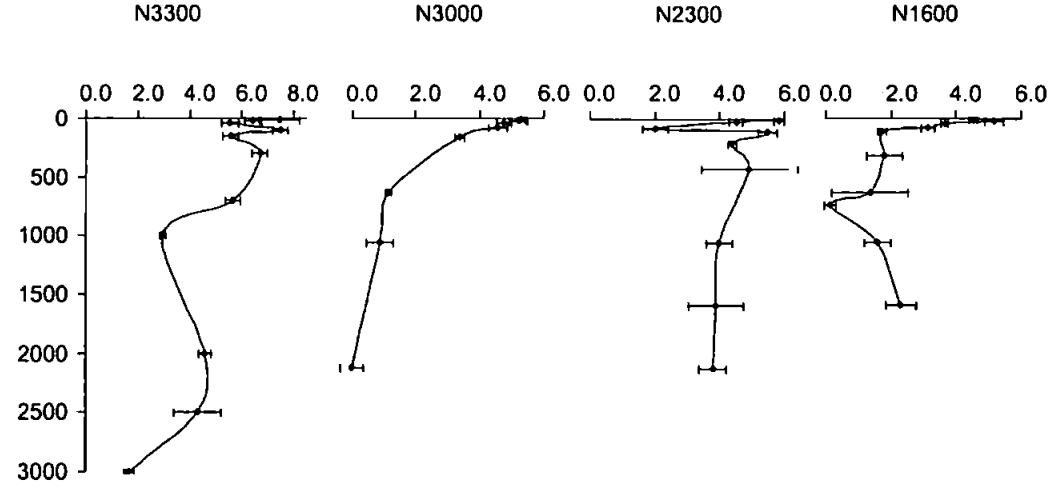

Figure 66. Full vertical profiles of DON concentrations (μM-N) in the OMEX0898 slope and offshore stations N1600, N2300, N3000 and N3300. Note: y-axis is depth (m).

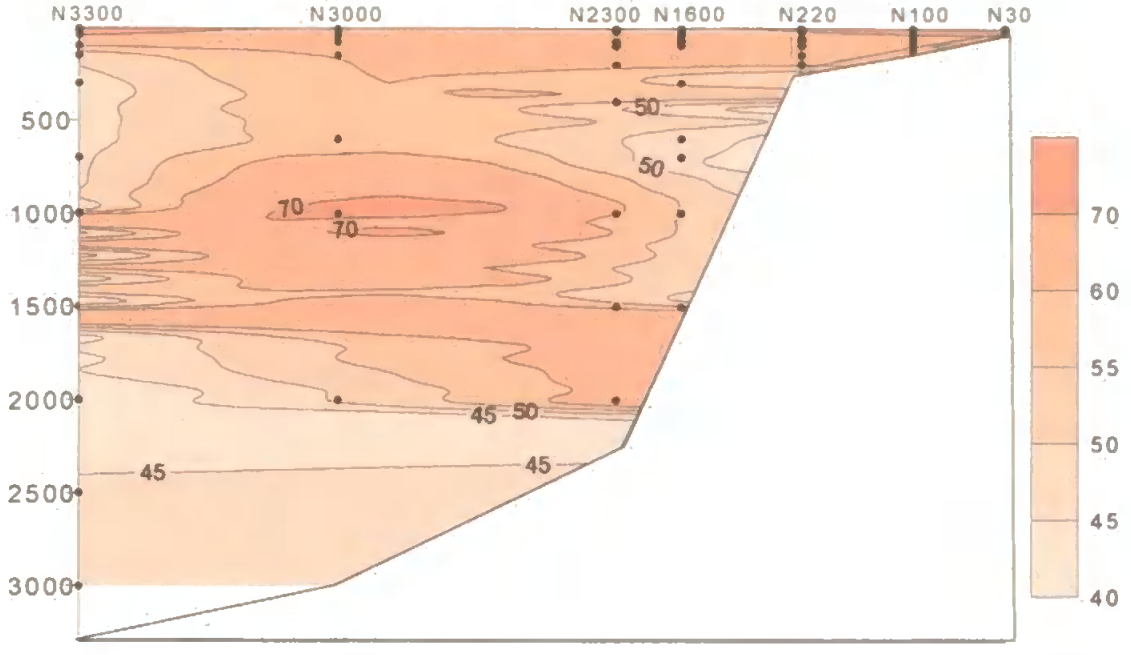

Figure 67. Contour plot of DOC concentrations along OMEX0898 transect N. Note: colour scale is µM-C; y-axis is depth (m).

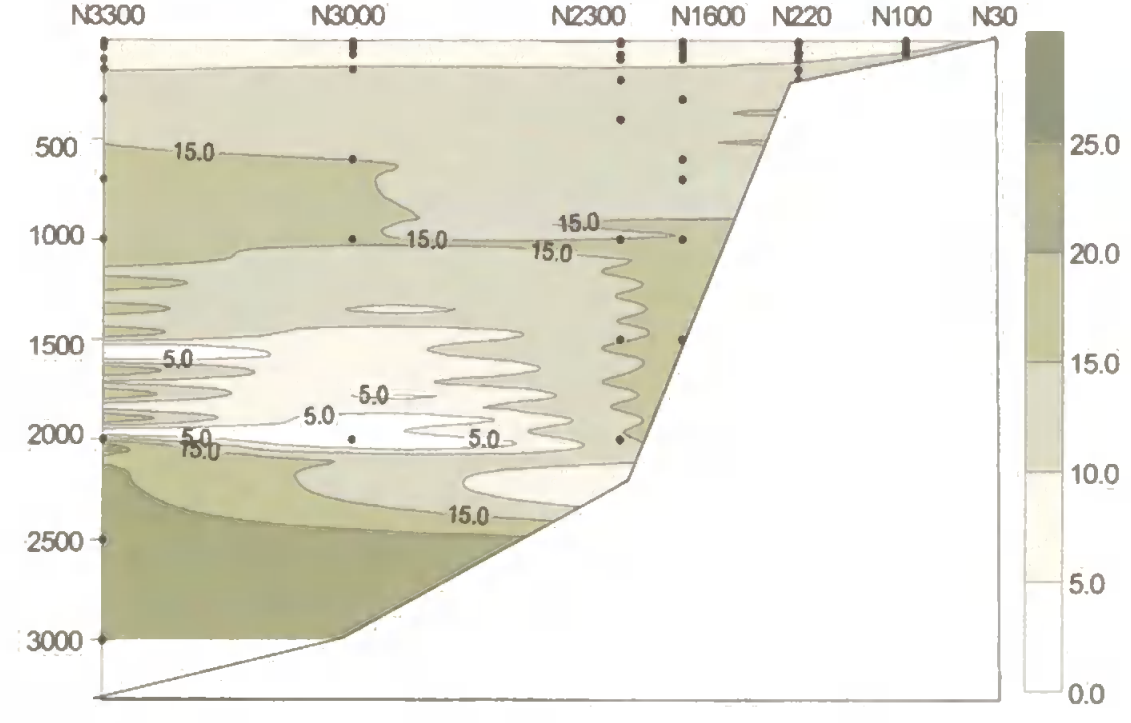

Figure 68. Contour plot of DIN concentrations along OMEX0898 transect N. Note: colour scale is µM-N; y-axis is depth (m).

3.3.5 Transect P (42°40'N) Salinity and Temperature

OMEX0898 transect P is on the same latitude as the northernmost Ria Baixa of the west coast of Galicia. The coastal stations on this transect are subject to the input of waters exported from the Ria by positive estuarine circulation (Fraga, 1981). During the OMEX0898 survey, it was observed from key hydrographic variables (i.e. temperature, salinity) that there was a combined effect of freshwater input from the Ria and upwelled water between 40 - 50m depth at coastal stations. Surface waters at the coast had lower temperatures (<15°C) (Figure 69) and this indicates upwelling of ENACW (signature: ~12°C, ~35.8). Surface temperatures increased towards oceanic waters and stabilised at ~18 - 19°C at station P1000 and further offshore (Figure 70). A sharp decrease in salinity in immediate surface waters of the shelf and shelf-break stations (P100, P200; Figure 71) suggest a freshwater input. Salinity gradually increased further offshore (Figure 72).

A contour plot of salinity in the upper 100m of transect P (Figure 73), shows a nucleus of subsurface water (~40 - 50m) with lower salinity (~35.8) than those at the other stations. The distribution of the isopycnals over the slope, suggests the existence of a zone of active downwelling of subsurface water off the shelf-break, probably as a consequence of upwelling dynamics near the coast (Bode, 1998). It is suggested that this phenomenon was an upwelling counter-current caused by density differences when ENACW upwelled at the coast (Fiuza, 1982). However, Huthnance et al., (to be publ.) determined that this feature is a result of river-runoff causing a sub-surface salinity maximum over the shelf. The primary production associated with the salinity core is likely to be low based on previous measurements (Dr. G.H. Tilstone, pers. com.).

The MSW was located between 700 and 1300m in all slope and offshore stations (P1000, P2250, P2000) as indicated by vertical salinity profiles (Figure 74). LSW was detected in deeper waters by its lower salinity and temperature signature (~4°C, <35.4).

A T - S plot of measurements along transect P showed three main water masses (Figure 75): the LSW (~4°C, ~35.2), the MSW (~11°C, >36.0) and a combined water mass (~10 – 20°C, ~35.6 - 36.0). The large range of the latter is due to a combination of ENACW at depth, surface upwelled water, fresh water from the Ria and surface offshore waters.

3.3.6 Transect P (42°40'N) Dissolved Organic Matter

Five stations were sampled for DOM measurements along 42°40'N during the OMEX0898 summer survey (Table 28): a coastal station (P100), a shelf-break station (P200), a station located on the slope (P1000) and two offshore stations (P2250, P2800).

Table 28. Co-ordinates, maximum depth and number of samples collected from stations on OMEX0898 transect P for DOM measurements.

Station	Cast	Latitude	Longitude	Maximum depth	No. Samples
P100	9	42°40'N	09°13'W	~100m	6
P200	10	42°40'N	09°30'W	~200m	10
P1000	11	42°40'N	09°36'W	~1000m	11
P2000	12	42°40'N	09°51'W	~2000m	10
P2250	14	42°40'N	10°00'W	~2250m	12
P2800	16	42°40'N	10°18'W	~2800m	8

DOC and DON concentrations along transect P ranged from 41 – 90 μM-C and n.d.– 15.8 μM-N, respectively. Concentration ranges at each station are listed in Table 29. C:N ratios of DOM ranged from 5 to infinity with average C:N ratios between 13 and 16. There was no apparent trend across the margin or with depth.

Table 29. DOC and DON concentration ranges at OMEX0898 transect P stations.

Station	Range of DOC, μM-C	Range of DON, μM-N	C:N ratios
P100	45 – 61	N/A	N/A
P200	66 – 90	2.8 – 15.8	(13) 5 – 28
P1000	41 – 57	1.3 – 5.8	(15) 10 – 39
P2000	36 – 60	n.d. – 5.6	11
P2250	48 – 76	n.d. – 4.2	6
P2800	44 – 57	1.7 – 4.6	(15) 12 – 31

Note: values in parentheses = mean; N/A = no data available; n.d. = non-detectable levels.

DOC concentrations along OMEX0898 transect P were significantly (ANOVA; $F_{1,49} = 4.15$, $P = 0.05$) higher in surface (<100m) waters (mean: 59 μM-C) than those in deeper waters (mean: 51 μM-C). Although surface DON concentrations (mean: 5.0 μM-N) were also generally

higher than those in deeper waters, they were not significantly different (ANOVA; $F_{1,44} = 0.94$, $P = 0.34$) to deep concentrations (mean: 3.7 μM-N).

Vertical distributions of DOC in the upper 200m of transect P (Figures 76 and 77) were not homogeneous. There were enhanced concentrations (up to ~25 μM-C excess) measured in the upper 50m of all the water columns and (~10 μM-C excess) between 100 - 200m depth in shelf and offshore stations (P100, P200, P2250, P2800). No cross-slope trend was observed from DOC distributions but it was noted that the shelf-break station had higher DOC concentrations than all other stations at transect P. The DOC vertical profiles of the deep stations (Figure 78) showed a generally homogeneous distribution at depth with an average background concentration of 42 μM-C [16]. Higher DOC concentrations were observed in the offshore stations at approximately 400 – 500m.

DON concentrations in the upper 200m along transect P (Figures 79 and 80) were variable and vertical distributions differed between stations [17]. The shelf-break station exhibited high DON concentrations (over ~15 μM-N) with DON accumulation at several depths in the upper 50m and below 80m depth. Concentrations in the upper 200m of the slope stations and furthest offshore decreased with depth, whereas station P2250 exhibited an increase (~3 μM-N excess) with depth.

DON vertical distributions in deep stations along transect P exhibited variable concentrations with some accumulation of DON at depth (stations P1000 and P2250; Figure 81). Only contour plots of DON concentrations along transect P are presented (Figures 82) to get a general view of the distribution across the continental margin. DOC distributions as depicted by the Surfer diagram were not accurate/representative due to the variable concentrations along the margin and are therefore not presented.

Figure 82 represents the general features observed from vertical profiles of DON concentrations (Figures 79 – 81): DON concentrations in surface waters along transect P were higher than deeper waters, and there was some DON enhancement between 200 – 500m and in deep waters (~1500 – 2000m) at station P2250.

[16] Note: excluded the shelf and shelf-break stations from the calculations.
[17] Note: there was no available data for station P100 due to the TDN analytical system not operating efficiently during the analysis of those samples.

3.3.7 Transect P (42°40'N) Summary

The main features detected in the distribution of DOM along 42°40'N during the OMEX0898 summer survey were:

- Surface waters contained higher DOC concentrations than deeper waters.
- Highest DOC concentrations were observed at the shelf-break station.
- Variation was observed in DOC distributions with depth at transect P with no clear trends.
- DON concentrations in surface waters were not significantly different than those in deeper waters. However, highest DON concentrations were observed in surface waters.
- There was slight accumulation of DON in deep waters of station P2250.
- There were no apparent trends in C:N ratios along transect P or with depth. C:N ratios were highly variable (5 – infinity).

Key hydrographic parameters (i.e. salinity, temperature, NO_2/NO_3, NH_4, and chlorophyll-a) were used with DOC and DON in a multiple stepwise regression analysis (MRA). MRA can be a useful statistical tool for producing multiple regressions using a large database. A dependent variable is chosen (i.e. DOM) and correlated/regressed with several independent variables (e.g. temperature, salinity, DIN) in a step-wise manner. The programme will select all statistically significant correlations and provide detailed information on each (i.e. significance factor, correlation coefficient). However, it will also provide a cumulative correlation coefficient, which can be converted to a percentage, of the combined statistically significant correlations. This is used to explain the variability of the dependent variable in relation to the variability of the significant independent variables. However, MRA was not used for all cruises in this study due to occasional lack of complementary data and its correspondence with DOM samples. Correlation matrices, although more time consuming, can provide equally important information. Primary production (mg-C m^{-3} hr^{-1}) and bacteria biomass (mg m^{-3}) were used in correlation matrices to assess the relationship between biological processes and DOM.

The MRA results (Table 30) showed that 27% of the DOC variation observed along transect P was due to salinity variation (e.g. with decreasing salinity towards the coast, DOC concentrations increased). These results highlight the influence of outwelled Ria waters onto the shelf on DOM concentrations there (Alvarez-Salgado et al., 1999). Approximately 13% of the variation of DOC was due to $NO_2 + NO_3$ distribution, probably indicative of the decrease in DOM with increase in nutrient levels with depth. Approximately 47% of the DON variation at transect P was due to salinity and DOC variations. These results and the large variability in C:N

ratios show that the DOC and DON pools cycle at different rates and are subject to different source and removal mechanisms at a time (Williams, 1995).

Table 30. Summary of results from a multiple regression analysis of measurements taken at OMEX0898 transect P.

DOC		Temp.	Salinity	NO_2+NO_3	NH_4	Chl-*a*	DOC
All transect	β		-0.60	-0.37			
$r^2 = 0.40$	*P*		<0.001	0.018			
DON							
All transect	β		-0.52				0.38
$r^2 = 0.47$	*P*		0.015				0.041

Note: r^2:coefficient of multiple correlation; β: correlation coefficient; *P*: significance index

More importantly, the MRA results indicate that key hydrographic variables did not account for a major (i.e. >50%) percentage of the DOM distributions along transect P. Therefore, it is proposed that biological processes were more quantitatively significant driving mechanisms for the DOM pool throughout the water column. Primary production (mg $m^{-3}.hr^{-1}$) and bacterial biomass data (mg m^{-3}) were used in a correlation matrix to assess the relationship between these and DOM concentrations.

In the upper 40m of the water column near the coast, DOC correlated strongly (0.99; n = 3; P<0.01; Figure 14 in Appendix 2) with bacterial biomass suggesting that where bacterial biomass was elevated, DOC concentrations were high. DOC was not taken up by bacteria and this may have been due to some limitation (i.e. nutrient- or organic-limitation; section 1.7.2). However, since nutrients were supplied *via* the upwelled waters, it is likely that the DOC present was not biologically labile (i.e. organic-limitation; Williams, 2000). Likewise, the supply rate of DOC at the coast (e.g. from terrestrial sources, biomass, and PER) may have exceeded the removal rate, resulting in DOC accumulation. At station P1000, DON correlated well with primary production (0.75; n = 4; P<0.001; Figure 15 in Appendix 2) suggesting that DON was being released as a result of phytoplankton activity. Offshore, DOC and DON concentrations were not correlated with any biological variable used herein. The discontinuity of DOM along transect P reflects the high variation in phytoplankton biomass distribution (Bode, 1998).

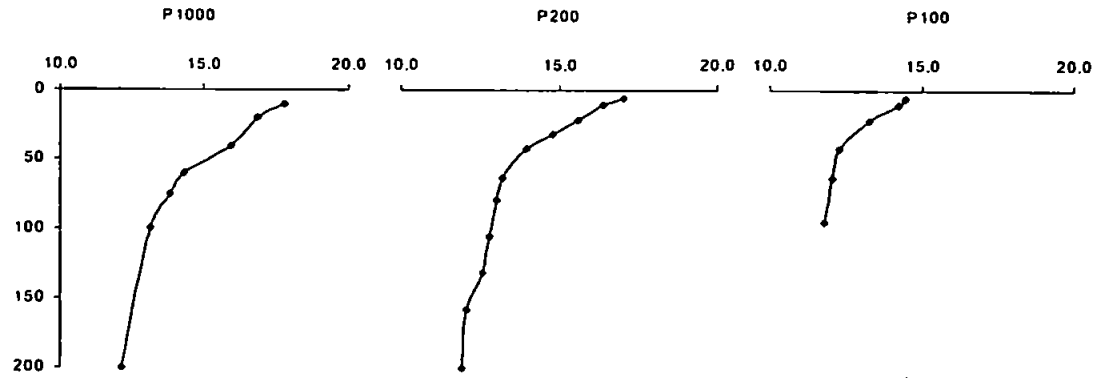

Figure 69. Vertical profiles of temperature (°C) in the upper 200m of OMEX0898 shelf and slope stations P100, P200 and P1000. Note: y-axis is depth (m).

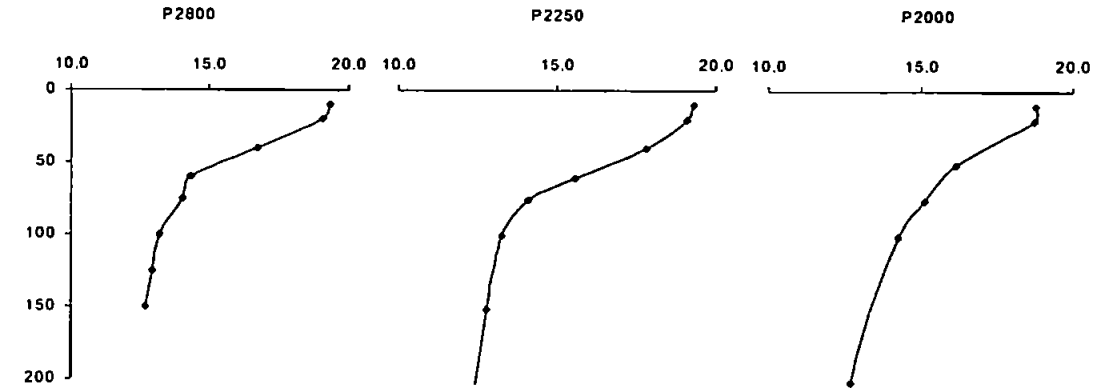

Figure 70. Vertical profiles of temperature (°C) in the upper 200m of OMEX0898 slope and offshore stations P2000, P2250 and P2800. Note: y-axis is depth (m).

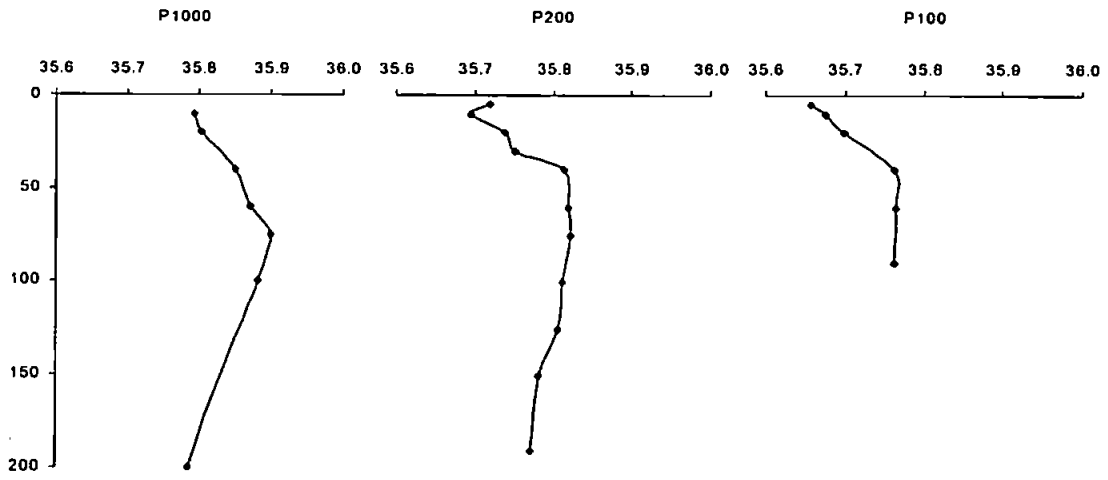

Figure 71. Vertical profiles of salinity in the upper 200m of OMEX0898 shelf and slope stations P100, P200 and P1000. Note: y-axis is depth (m).

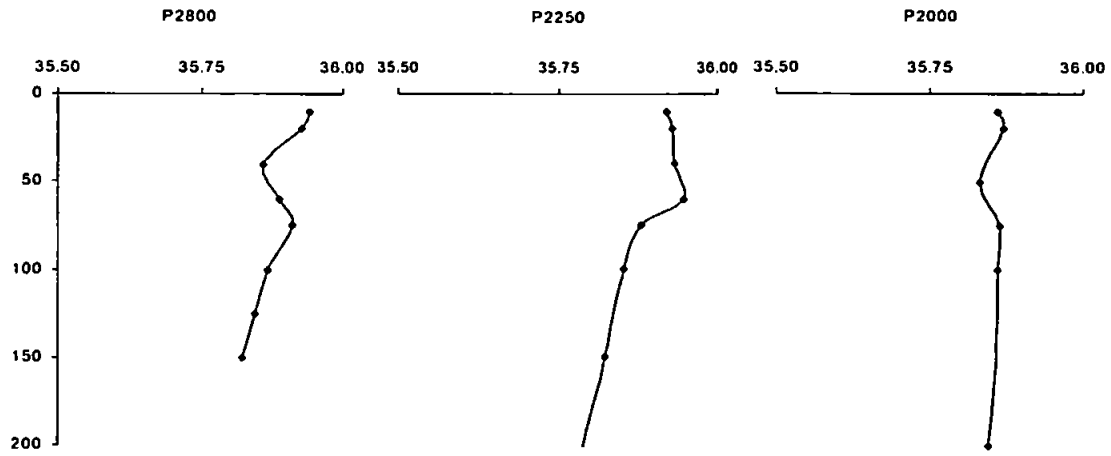

Figure 72. Vertical profiles of salinity in the upper 200m of OMEX0898 slope and offshore stations P2000, P2250 and P2800. Note: y-axis is depth (m).

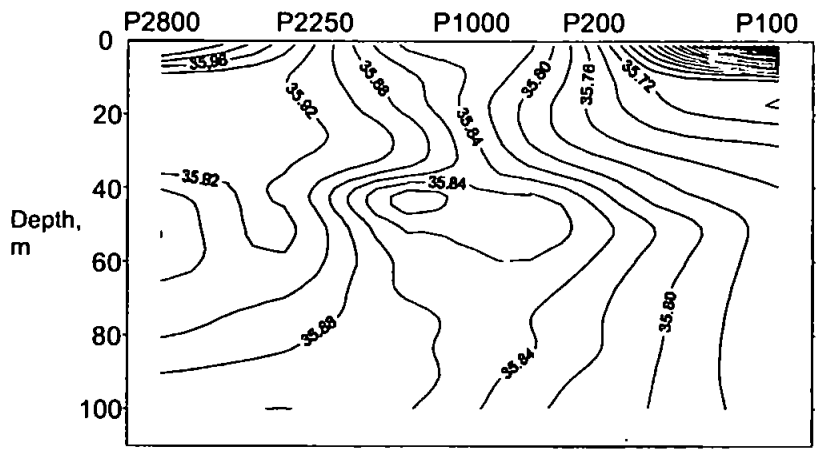

Figure 73. Salinity distribution in the upper 100m of OMEX0898 transect P. Taken from Bode, 1998.

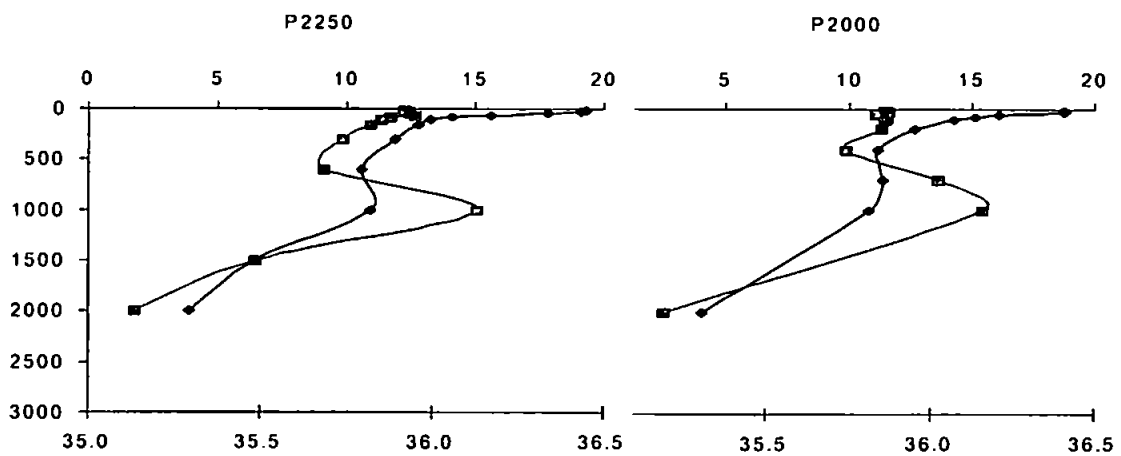

Figure 74. Full vertical profiles of salinity and temperature (°C) at OMEX0898 stations P2000 and P2250. Note: ♦– temperature, – salinity; y-axis is depth (m).

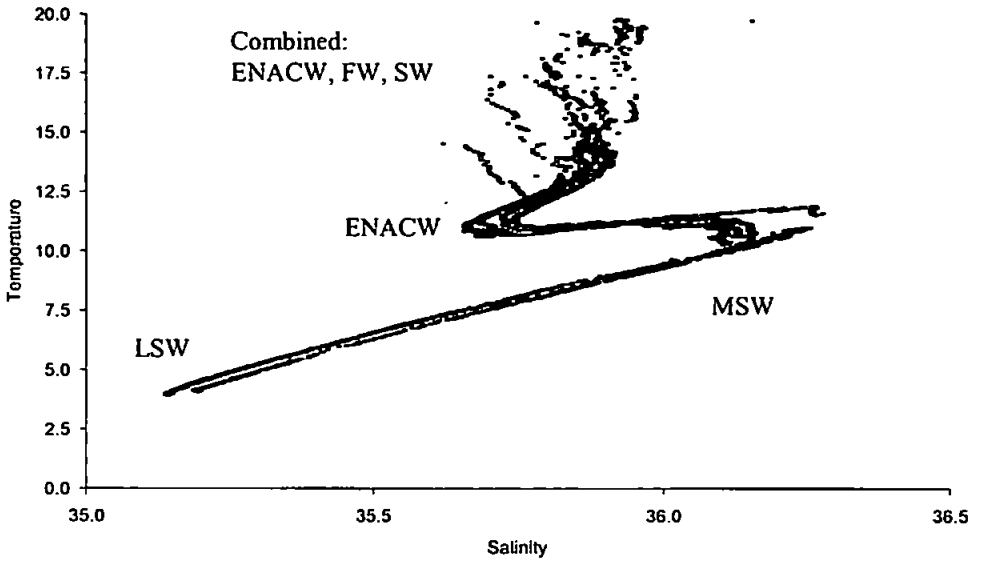

Figure 75. T - S plot of the water column along OMEX0898 transect N.

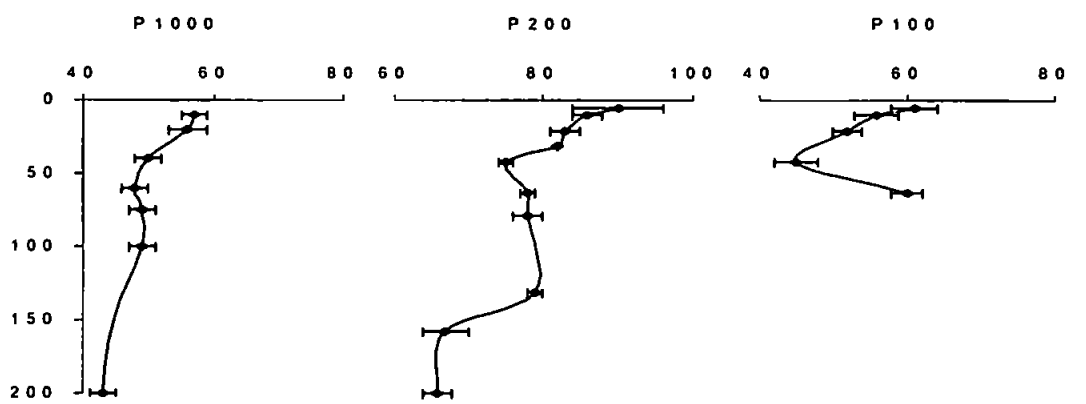

Figure 76. Vertical profiles of DOC concentrations (μM-C) in the upper 200m of OMEX0898 stations P100, P200 and P1000. Note: y-axis is depth (m).

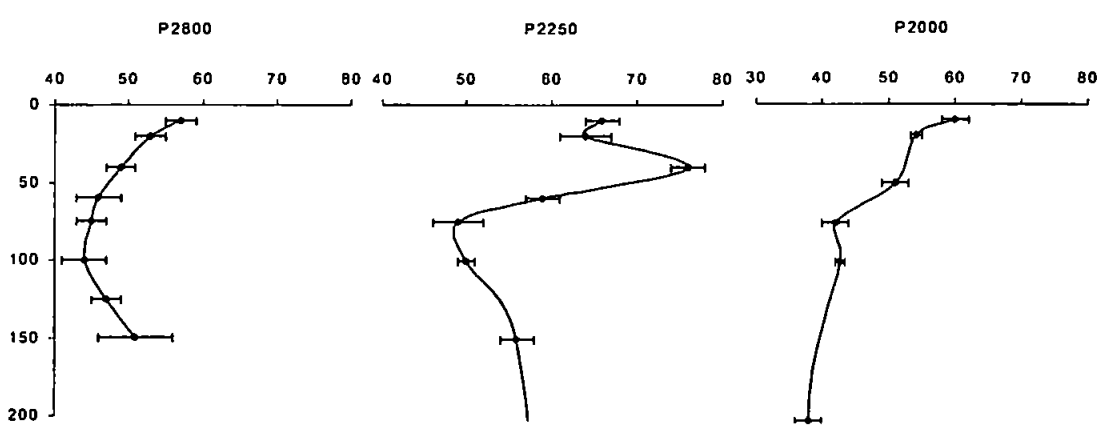

Figure 77. Vertical profiles of DOC concentrations (μM-C) in the upper 200m of OMEX0898 slope and offshore stations P2000, P2250 and P2800. Note: y-axis is depth (m).

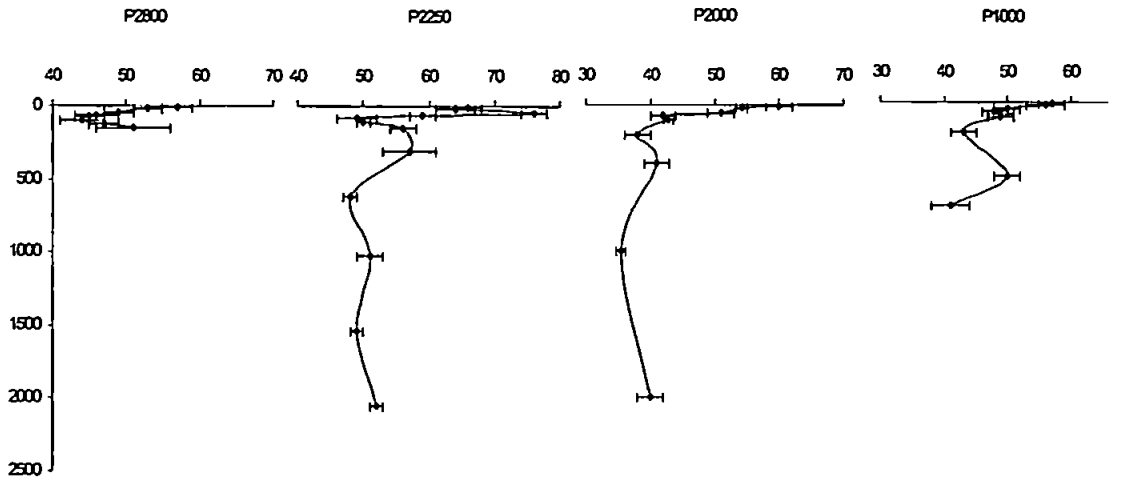

Figure 78. Full vertical profiles of DOC concentrations (μM-C) at the OMEX0898 slope and offshore stations P1000, P2000, P2250 and P2800. Note: y-axis is depth (m).

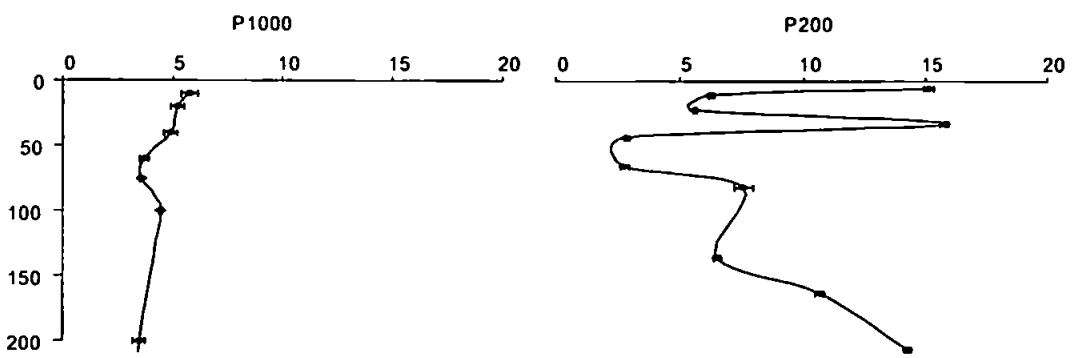

Figure 79. Vertical profiles of DON concentrations (μM-N) in the upper 200m of OMEX0898 stations P200 and P1000. Note: y-axis is depth (m).

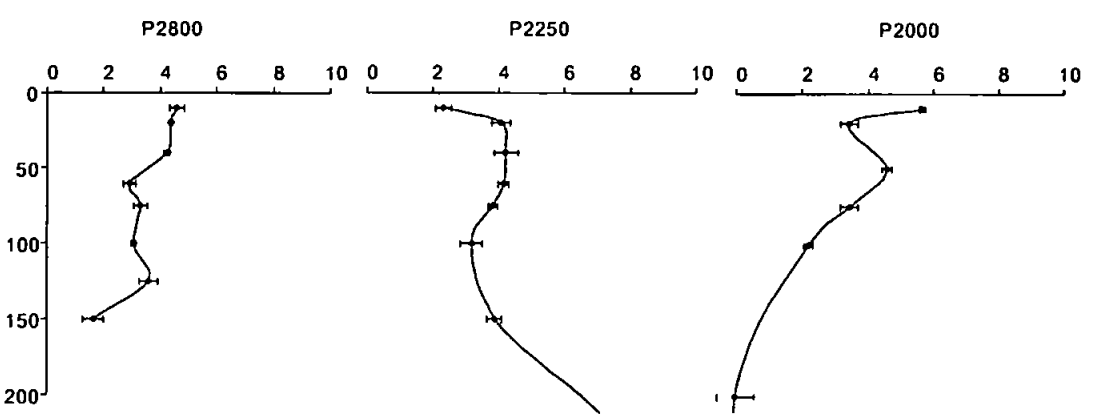

Figure 80. Vertical profiles of DON concentrations (μM-N) in the upper 200m of OMEX0898 offshore stations P2000, P2250 and P2800. Note: y-axis is depth (m).

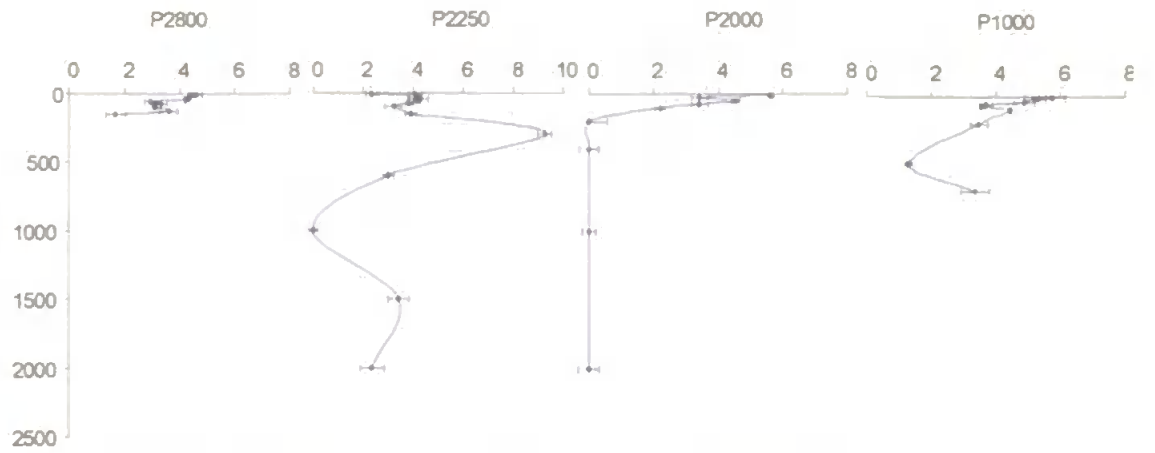

Figure 81. Full vertical profiles of DON concentrations (µM-N) at the OMEX0898 slope and offshore stations P1000, P2000, P2250 and P2800. Note: y-axis is depth (m).

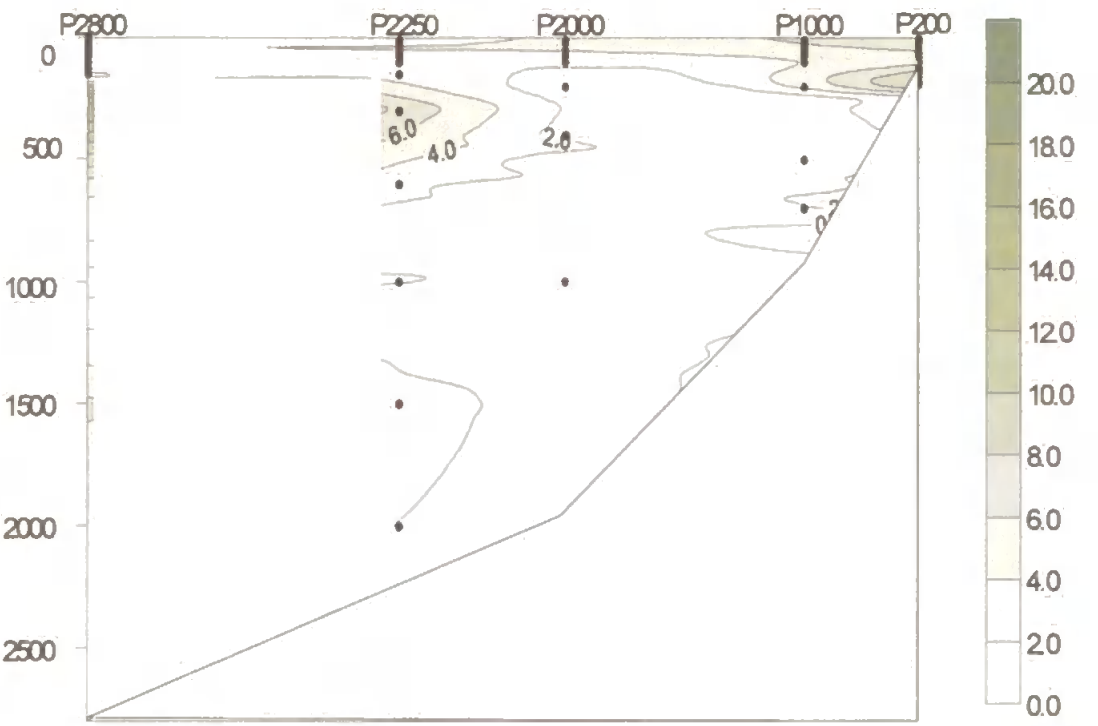

Figure 82. Contour plot of DON concentrations along OMEX0898 transect P. Note: colour scale is µM-N; white area between stations P2250 and P2800 = no data; y-axis is depth (m).

3.3.8 Transect S (42°09'N) Salinity and Temperature

OMEX0898 transect S is located at 42°09'N latitude covering a cross-section from the coast at the mouth of the Ria de Vigo (Figure 17 in section 2.2.2) to offshore oceanic waters away from the continental shelf. The upwelling of ENACW was apparent from comparatively lower salinity and temperature in the upper 200m of the water column at transect S. In the upper 50 - 100m near the coast, temperatures were ~12 – 15°C and progressively increased further offshore to 19°C (S2250) (Figure 83) probably due to solar heating. A contour plot of the temperature distribution in the upper 200m (Figure 84) illustrates the isotherms displaying an upward trend. This clearly depicts the upwelling of colder waters to the surface. Salinity was lower in the upper 50m at transect S. Near the coast values were ~35.75 and remained so until the furthest station offshore (S2250; Figure 85). A subsurface core of more saline water (~36) was present at deep stations (S1000, S2000, S2250) (Figure 86). This may have been a result of upwelling dynamics creating a subsurface counter-current as seen on transect P (Figure 73; Fiuza, 1982, Bode, 1998).

No temperature or salinity data were available below 250 and 500m for stations S1000 and S2250 respectively (Figure 87). The full depth profile of salinity and temperature at station S2000 depicted the MSW between ~700 to 1200m, but a contour diagram (Figure 88) of salinity distributions at transect S (Bode, 1998) shows the MSW nucleus deepening closer to the continental slope. This may be due to an increased influx of LSW (van Aken, 2000a). A T - S plot of high resolution salinity and temperature measurements (Figure 89) along transect S clearly highlights the influence of four main water masses: the ENACW (~35.7, ~11°C), MSW (>36, ~11.5°C) and LSW (~35, ~4°C) and a combined water mass. The upwelled ENACW (~35.7, ~17°C) combined with surface water offshore (SW; ~35.9, ~19°C) and produced branching off from the ENACW at higher temperatures.

3.3.9 Transect S (42°09'N) Dissolved Organic Matter

Six stations were sampled for DOM measurements along 42°09'N during the OMEX0898 summer survey (Table 31): a coastal station positioned at the mouth of Ria de Vigo (S90), a shelf station (S150), a shelf-break station (S300), a station located on the slope (S1000) and two offshore stations (S2000, S2250). Although the coastal area was sampled at a relatively high resolution, most of the stored samples were lost due to an accident[18] on-board the research vessel. Recovered samples were analysed but it was noted that many of them were

contaminated. Contaminated values were excluded from data analysis at the analyst's discretion and depending on oceanographic consistency (see section 2.5.4.1 for "outlier" data).

Table 31. Co-ordinates, maximum depth and number of samples collected at OMEX0898 transect S stations for DOM measurements.

Station	Latitude	Longitude	Maximum depth	No. Samples
S90	42°09'N	08°57'W	~90m	4
S150	42°09'N	09°08'W	~150m	2
S300	42°09'N	09°19'W	~300m	2
S1000	42°09'N	09°28'W	~1000m	6
S2000	42°09'N	09°39'W	~2000m	11
S2250	42°09	10°00	~2550m	8

Due to a low number of samples recovered (n=6) at the coastal and shelf stations, vertical profiles of DOC and DON at these stations were deemed not valuable and are thus not presented. However, the data was included in the construction of the DOC and DON contour diagrams (Figures 94 and 95). Dissolved organic carbon and nitrogen along OMEX0898 transect S ranged from 53 – 135 μM-C and n.d.– 12.6 μM-N, respectively (see Table 32 for individual stations). C:N ratios ranged from 6 – 40. There were no discernible trends in C:N ratio either with depth or along the transect. Although higher DOC concentrations were observed in surface waters of transect S, (i.e. <100m; 80 μM-C) they were not significantly different (ANOVA; $F_{1,28}$ = 3.19, P = 0.09) to those in deeper waters (mean: 66 μM-C). However, DON concentrations were significantly higher in surface (mean: 5.5 μM-N) than those observed in deeper waters (mean: 3.3 μM-N; ANOVA:$F_{1,26}$ = 4.38, P = 0.05).

At the coastal and shelf stations of transect S, DOC concentrations decreased with depth by 9 μM-C at stations S90 and S150 and by 23 μM-C at the shelf-break station (S300). DON concentrations in surface waters (<50m) were also higher (>10 μM-N excess) than subsurface non-detectable levels. Further on the shelf, the DON maximum decreased to ~1.7 μM-N excess over deeper water concentrations (station S150), and at station S300, the vertical DON distribution was homogeneous.

[18] An unidentified person unlocked the sample storage fridge during adverse weather conditions, resulting in the fridge's contents and DOM samples to empty onto the floor and break.

Table 32. DOC and DON concentration ranges at OMEX0898 transect S stations.

Station	Range of DOC, μM-C	Range of DON, μM-N	C:N ratios
S90	63 – 72	n.d. – 12.6	6
S150	54 – 63	1.4 – 3.1	(29) 21 – 38
S300	112 – 135	9.7 – 10.1	(13) 11 – 14
S1000	53 – 107	3.7 – 6.4	(15) 12 – 21
S2000	57 – 106	1.6 – 7.5	(18) 9 – 40
S2250	57 – 70	2.9 – 5.3	(16)13 – 24

Note: values in parentheses = mean; n.d. = non-detectable levels.

In the upper 200m of the slope and offshore stations, DOC concentrations were variable and enhanced at several depths (Figure 90). DOC reached 100 – 105 μM-C at stations S1000 and S2000. Full vertical profiles of DOC concentrations (Figure 91) showed a general decrease with depth and background DOC concentrations were 53 – 57 μM-C. In bottom waters of station S1000 where the MSW was located, there was considerably enhanced DOC (e.g. ~107 μM-C). DON in the upper 200m of the slope and offshore stations at transect S exhibited variable concentrations with localised enhancement at some depths (Figure 92). The full vertical profile at stations S2000 (Figure 93) indicated a DON minimum (1.7 – 3.3 μM-N) between 400 and 700m. DON concentrations increased and stabilised to ~4.1μM-N in deeper waters.

DOC distribution along OMEX0898 transect S (Figure 94) showed surface enhancement off the shelf-break station and subsequent deepening of the DOC-maximum further offshore. Coastal and shelf waters also contained lower DON concentrations than those stations away from the continent (Figure 95). Primary productivity was higher in surface waters (<30m) offshore than on the shelf (Figure 96) thus suggesting that the enhanced DOM there was due to increased production by exudation from phytoplankton. Deeper waters had generally lower DOC and DON concentrations but there was localised enhanced DOC near bottom waters of the slope at approximately 1000m and generally enhanced DON at depths below 1000m. Note that the DON contour plot (Figure 95) depicts an area of low DON concentrations between ~500 – 1000m. This is more likely to be an artefact of the *Surfer®* programme, because there was no DON data below 150m at station S1000. In addition, DON did not correlate well with DIN (i.e. $NO_2 + NO_3$) in waters >100m at transect S.

3.3.10 Transect S (42°09'N) Summary

The main features of the DOM distribution along OMEX0898 transect S were:

- DOM concentrations were generally higher in the upper 100m of the water column compared to those in deeper waters.
- C:N ratios did not follow any apparent trends with depth and across the margin.
- DON concentrations were significantly higher at the surface than in deeper waters.
- Surface DOC concentrations were not statistically significantly different from those in deeper waters. This was probably the result of localised enhancement in concentrations within bottom waters of station S1000.
- Coastal and shelf stations had lower DOM than waters off the continental shelf.
- The DOC maximum in the upper water column deepened with distance from the continental shelf.

The general elevation of DOM concentrations in surface waters is most likely due to the higher rate of input to the surface ocean (i.e. *via* phytoplankton exudation, excretion, grazing, cell lysis). DOC and DON correlated well in the upper 100m of transect S (0.54; n = 18; $P<0.001$; Figure 16 in Appendix 2) suggesting that the source and removal mechanisms may be similar for both pools there. However, DOC:DON ratios were very varied within the water column and across the margin, suggesting that their cycling is essentially independent. DON correlated strongly (0.83; n = 6; P=0.06; Figure 17 in Appendix 2) with bacterial production (i.e. as leucine incorporation, mg-C m^{-3} hr^{-1}) in the upper 100m of the water column and also showed a negative correlation with NO_2+NO_3 (-0.57; n = 18; P=0.07; Figure 18 in Appendix 2). This may be indicative of bacterial attack on phytoplankton biomass in the surface ocean, helping to release DON from phytoplankton *via* cell lysis (Azam, 1998). In addition, as phytoplankton take up inorganic nutrients to photosynthesise, they can release DON *via* direct exudation (Biddanda and Benner, 1997). It is thus possible that the combination of direct exudation and lysis of phytoplankton biomass facilitated by bacterial enzymatic attack was resulting in enhanced DON input to the surface ocean. Additionally, bacteria may be selectively taking up C-rich DOM (Williams, 2000) and inorganic nutrients (Thingstad et al., 1998), allowing N-rich DOM to accumulate in the water column. At depth (>100m) DON correlated negatively with bacterial numbers (-0.46; n = 4; $P<0.01$; Figure 19 in Appendix 2). This suggests that DON was consumed at depth for bacterial growth. Enhanced DOC in bottom waters of station S1000 may have been laterally imported by the MSW or produced from processes associated with the presence of the MSW at the Iberian margin. For example, due to a density difference between the MSW and the overlying ENACW, it is possible that sinking particulate matter will

accumulate at the ENACW-MSW 'front' and result in an accumulation of organic matter (Dr. A. Borges, pers. comm.)

Recently upwelled ENACW is high in nutrients (Alvarez-Salgado et al., 1993) but low in primary productivity due to its deep location. As upwelling events cause ENACW to rise to the surface, older waters are pushed further offshore and the nutrients are utilised as the productivity increases. Coastal and shelf waters may have exhibited lower DOM concentrations than those further off the shelf due to recently upwelled ENACW waters being relatively low in DOM. The average concentration of ENACW waters (~150m) during OMEX0898 cruise was ~75 μM-C and this value was observed in coastal surface waters of transect S.

The DOM-maximum depth in surface waters of the deep stations (S1000, S2000, S2250) increased with distance from the shelf. This correlated well with biomass location as depicted by fluorescence measurements (Figure 98).

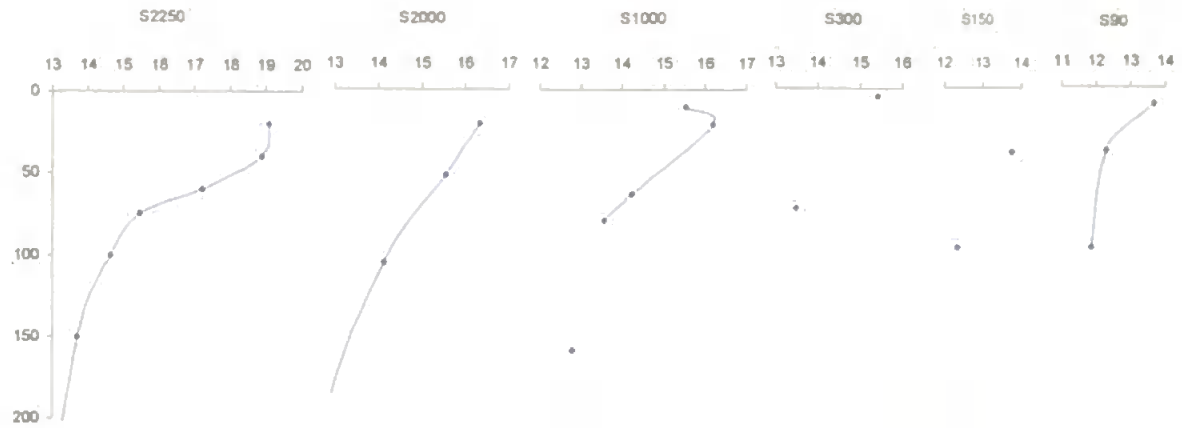

Figure 83. Vertical profiles of temperature (°C) in the upper 200m of OMEX0898 transect S. Note: y-axis is depth (m).

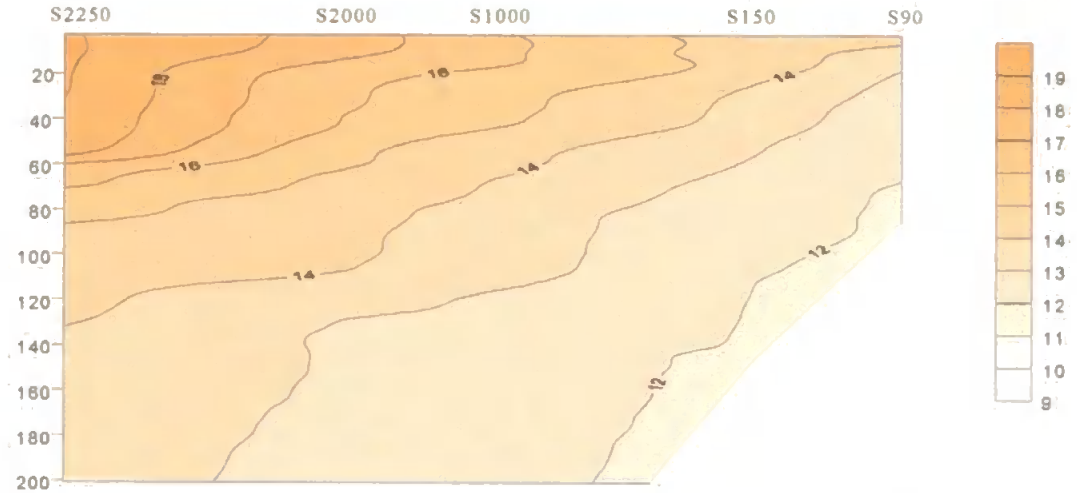

Figure 84. Contour plot of temperature in the upper 200m of OMEX0898 transect S. Note: colour scale is °C; y-axis is depth (m).

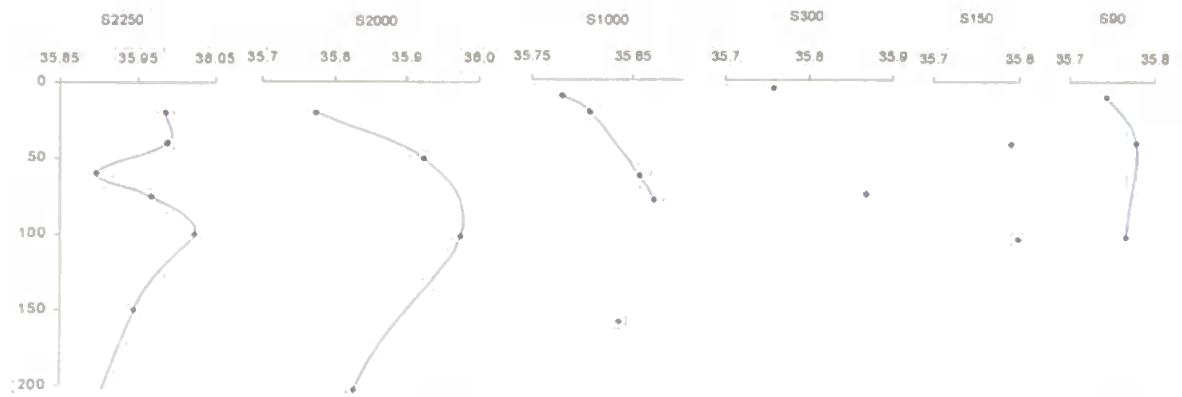

Figure 85. Vertical profiles of salinity in the upper 200m of OMEX0898 transect S. Note: y-axis is depth (m).

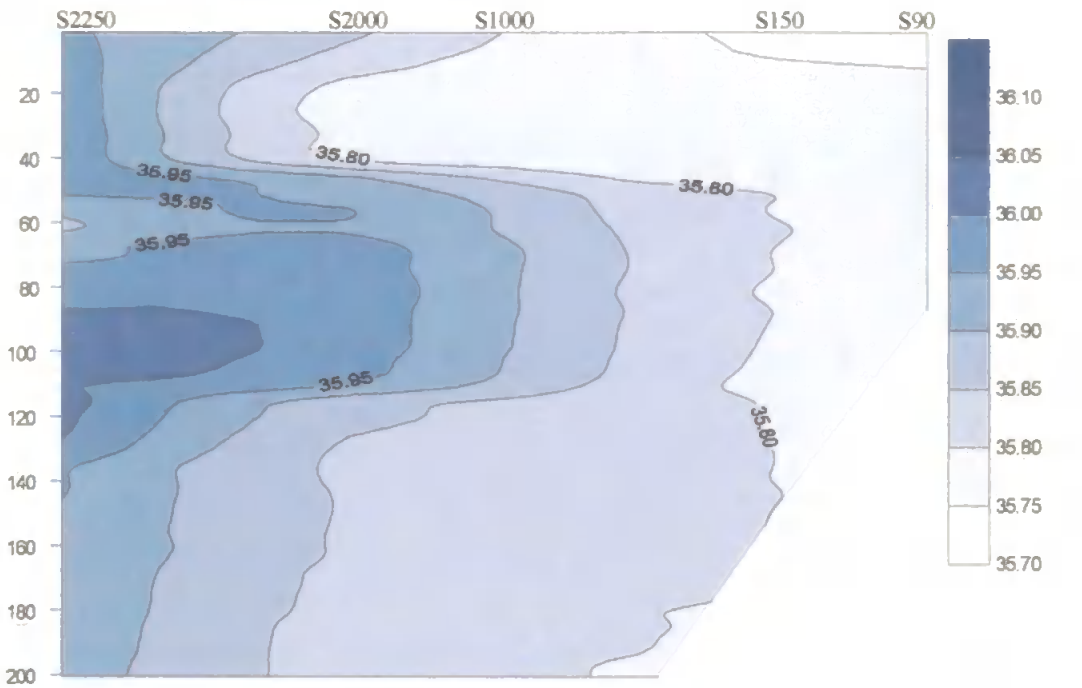

Figure 86. Contour plot of salinity in the upper 200m of OMEX0898 transect S. Note: colour scale units are arbitrary; y-axis is depth (m).

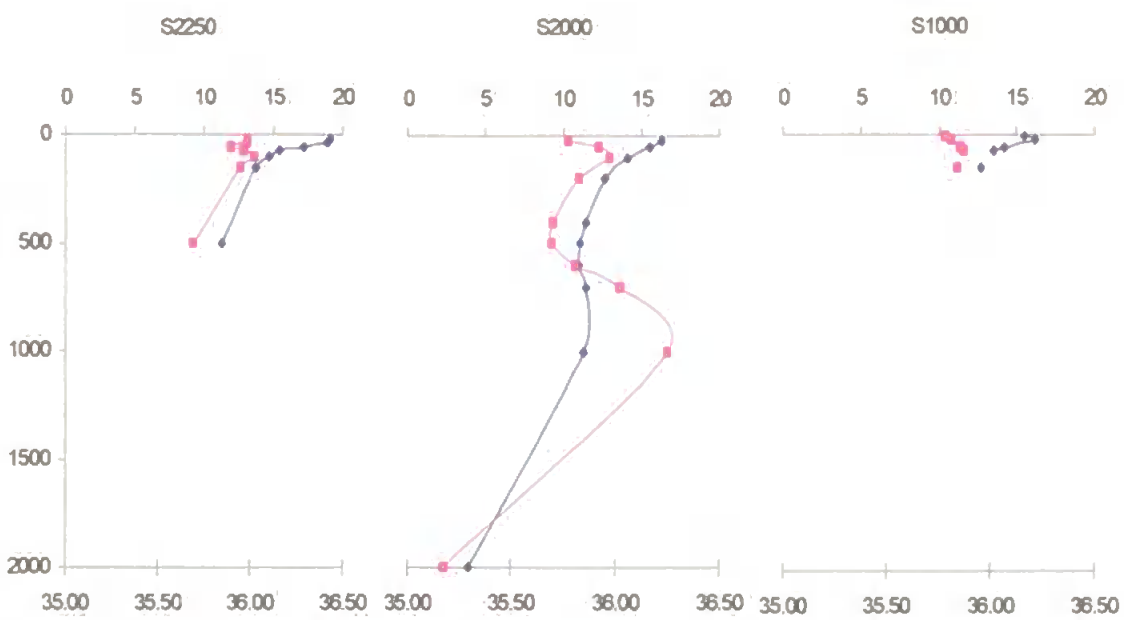

Figure 87. Vertical profiles of salinity and temperature (°C) at OMEX0898 stations S1000, S2000 and S2250. Note: ♦ – temperature, ■ – salinity; y-axis is depth (m).

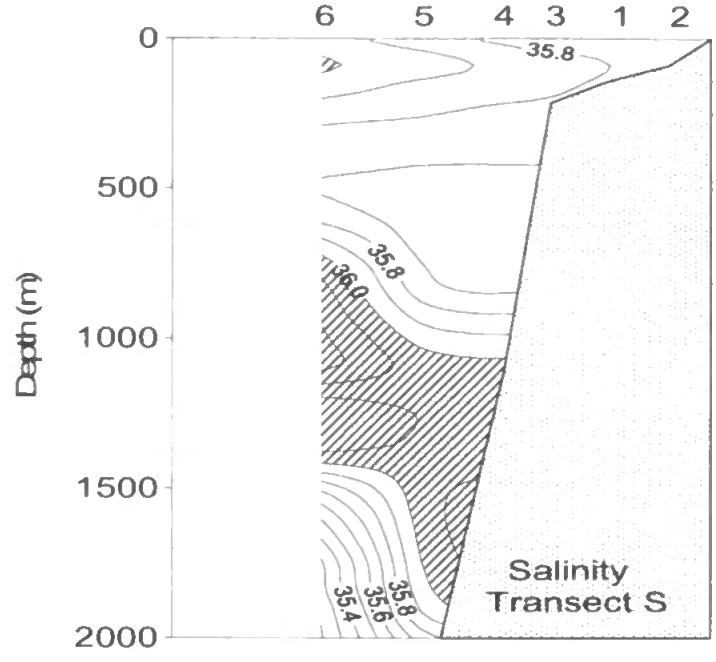

Figure 88. Contour plot of salinity distribution at OMEX0898 transect. Taken from Bode, 1998. Note: station 1 = S150, 2 = S90, 3 = S300, 4 = S1000, 5 = S2000, 6 = S2250.

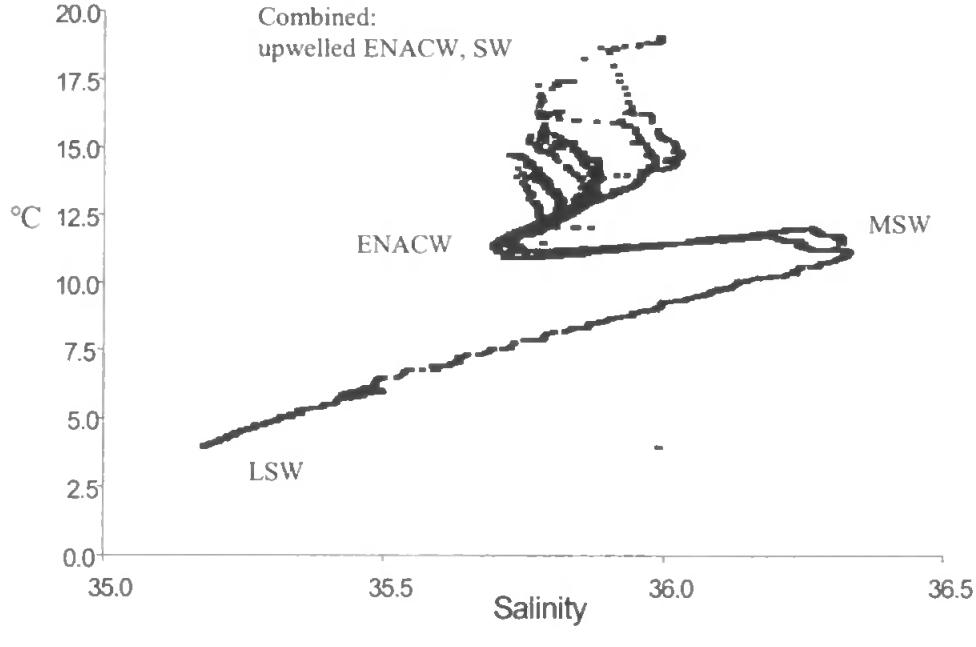

Figure 89. T - S plot of the water column along OMEX0898 transect S.

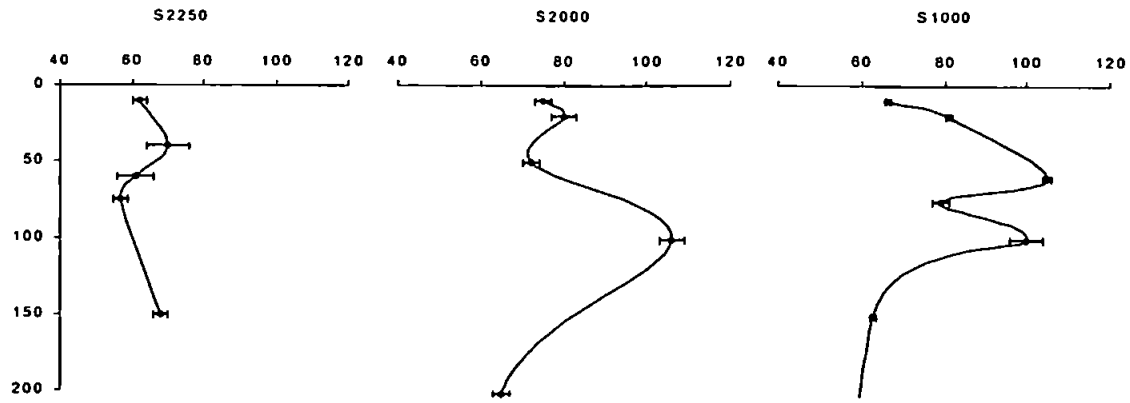

Figure 90. Vertical profiles of DOC concentrations (μM-C) in the upper 200m of OMEX0898 slope and offshore stations S1000, S2000 and S2250. Note: y-axis is depth (m).

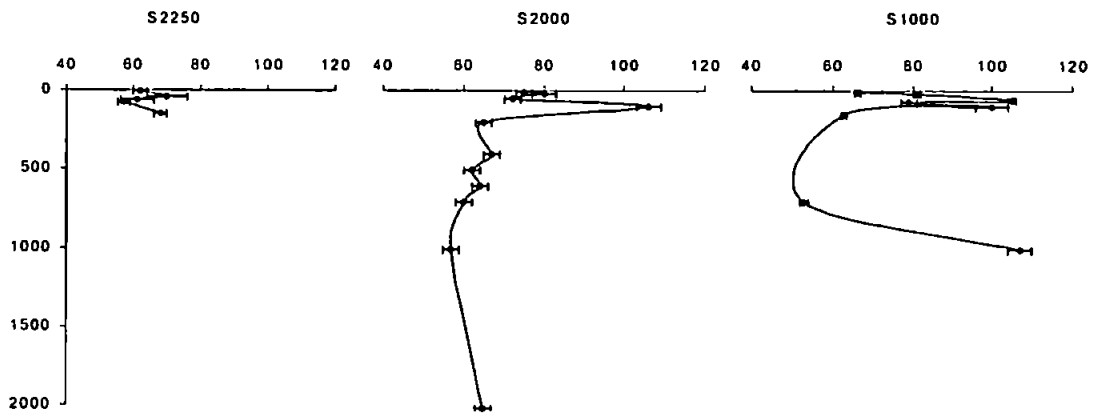

Figure 91. Full vertical profiles of DOC concentrations (μM-C) at the OMEX0898 slope and offshore stations S1000, S2000 and S2250 [19]. Note: y-axis is depth (m).

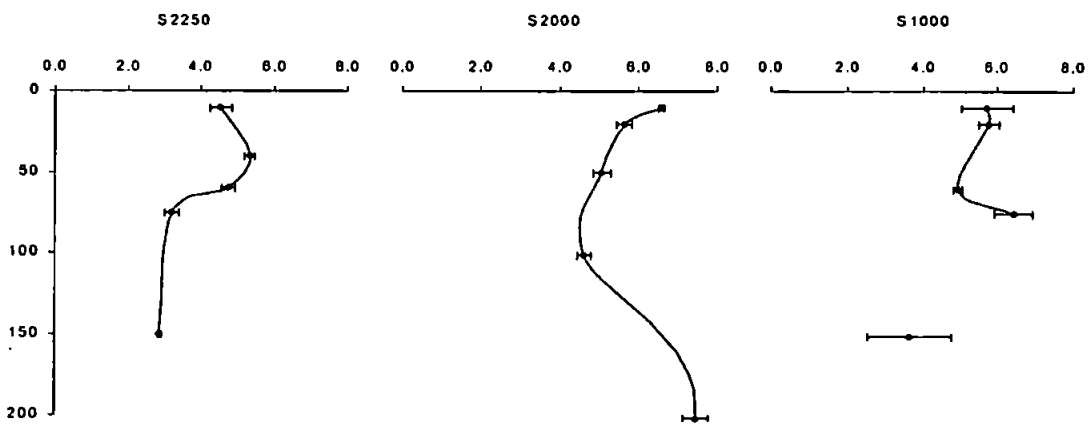

Figure 92. Vertical profiles of DON concentrations (μM-N) in the upper 200m of OMEX0898 offshore stations S1000, S2000 and S2250. Note: y-axis is depth (m).

[19] The chief scientist of the cruise decided that, based on the time schedule, only the surface water column of the deep offshore station would be sampled.

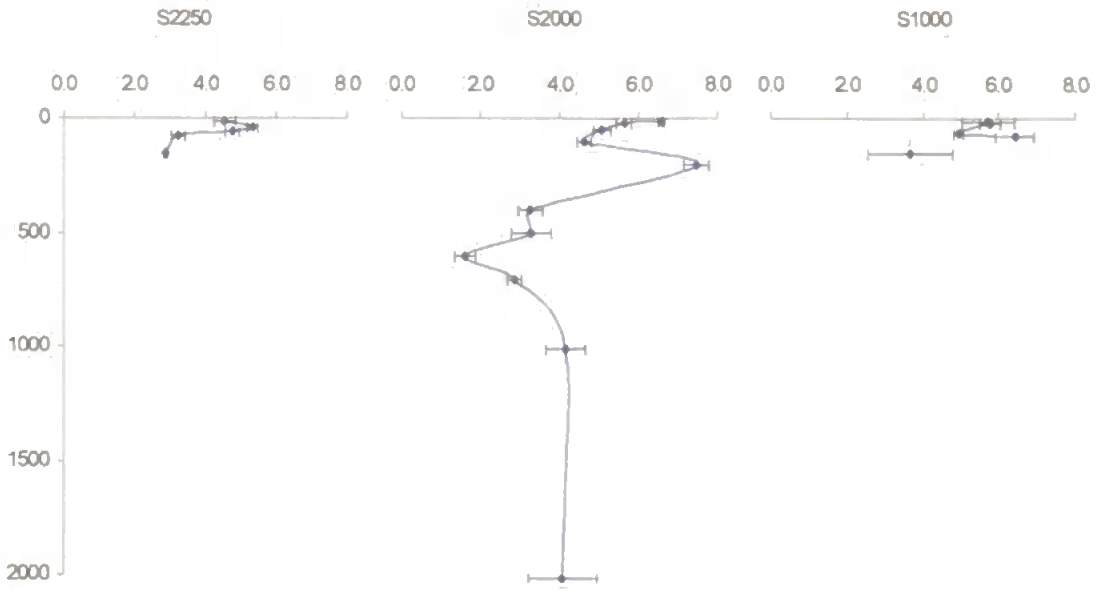

Figure 93. Vertical profiles of DON concentrations (µM-N) at the OMEX0898 slope and offshore stations S1000, S2000 and S2250. Note: y-axis is depth (m).

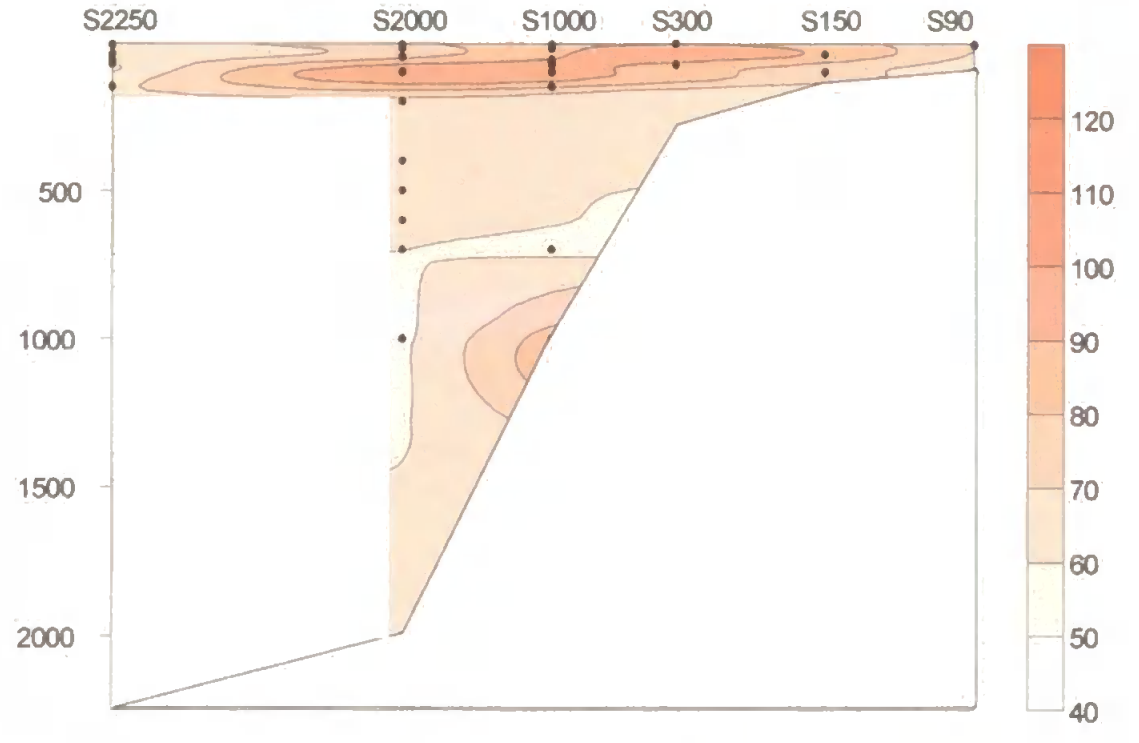

Figure 94. Contour plot of DOC concentrations along OMEX0898 transect N. Note: colour scale is µM-C; white areas = no data; y-axis is depth (m).

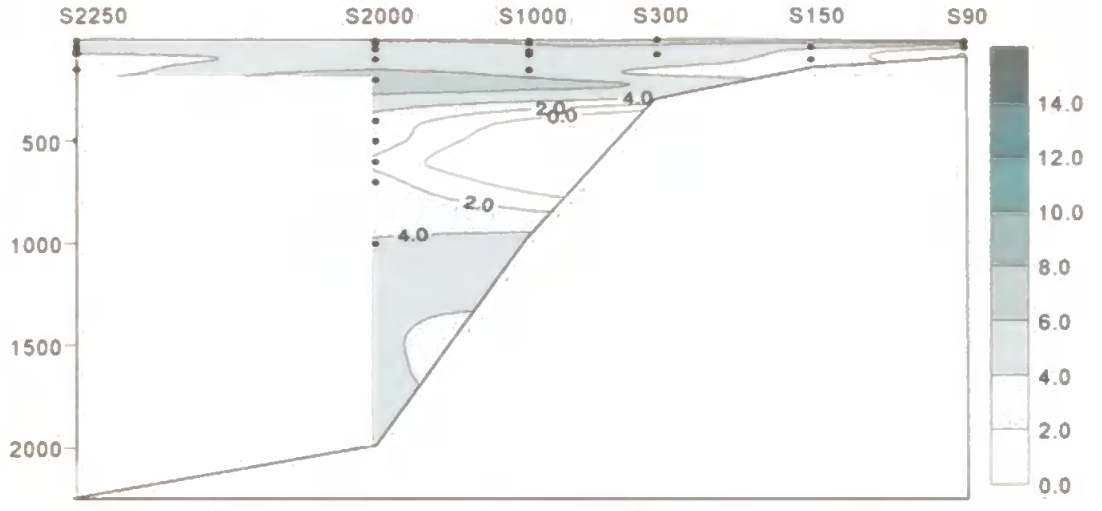

Figure 95. Contour plot of DON concentrations along OMEX0898 transect N. Note: colour scale units are in µM-N; white areas = no data; y-axis is depth (m).

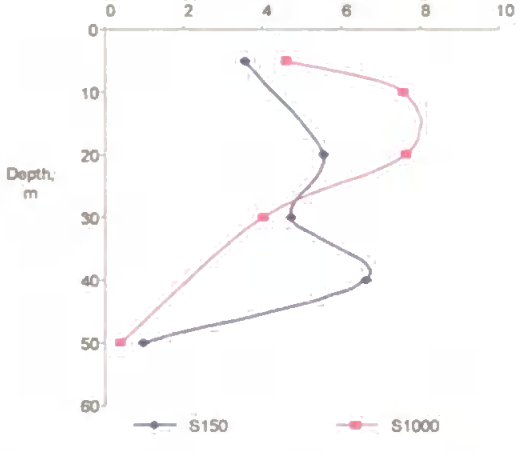

Figure 96. Vertical profile of primary production (mg-C m^{-3} hr^{-1}) measurements at OMEX0898 stations S150 and S1000. Data from Univ. of Vigo, Spain.

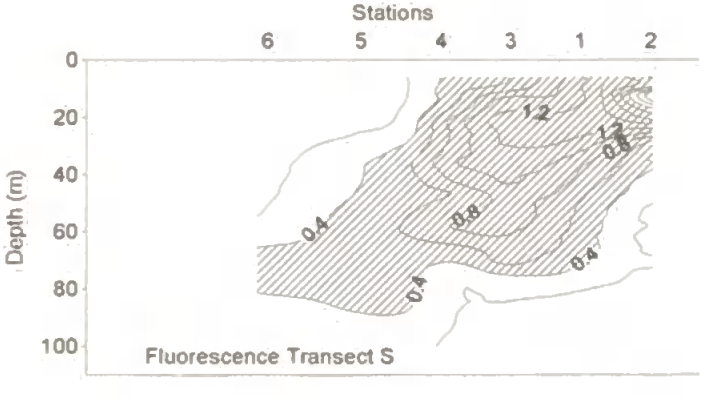

Figure 97. Contour plot of fluorescence distribution along OMEX0898 transect S. Note: taken from Bode, 1998; station 1 – S150, 2 – S90, 3 – S300, 4 – S1000, 5 – S2000, 6 – S2250.

3.4 R/V Meteor Cruise M43/2

Cruise M43/2 of the R/V Meteor took place from 28th December 1998 – 13th January 1999 at the Iberian margin. Due to the adverse climatic conditions, it was only possible to sample along transect S (42°09N). A satellite image of sea surface temperature showed warmer surface waters (>16°C) of the poleward current progressing northwards but its core not having reached the Rias Baixas (Figure 98). Colder waters (<14°C) lined the Iberian coastline resulting in a distinct front between coastal and offshore waters.

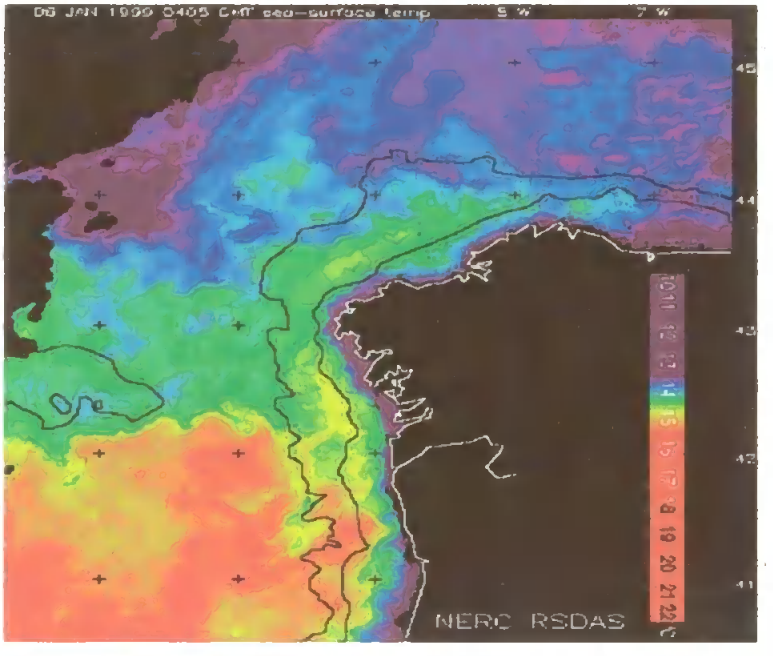

Figure 98. SeaWifs satellite image of the sea-surface temperature (SST) off the north-west coast of the Iberian Peninsula (06-Jan-1999). Courtesy of RSG, PML, U.K. Note: Black colour to the east is cloud coverage.

3.4.1 Transect S (42°09'N) Salinity and Temperature

Temperature and salinity profiles along transect S suggested that a relatively weak upwelling event was taking place. Figures 99 – 104 show the distribution of temperature and salinity in the upper 200m of stations along transect S. Contours in the surface 100m show an upward trend near the coast indicating that upwelling was occurring during January (Figures 101 and 104). Surface waters near the coast (Figure 99) had a temperature of ~14.5°C and remained thus until station S2250 (09°44'W; ~2254m max. depth; Figure 100). The upper 100m of stations along transect S had vertically homogeneous salinity and temperature distributions,

bounded below by a halo- and thermo-cline (Figures 99, 100, 102 and 103). Temperatures around 500m off the shelf (i.e. S600 onwards; Figures 105 and 106) decreased to 11°C. At stations of 1000m depth or more an increase in temperature and salinity was observed due to the presence of the MSW travelling along the continental slope at ~1000m. Cold waters of 3 - 4°C were detected at depths over 2000m, indicating the presence of the LSW. A T - S plot (Figure 107) of measurements taken in the water column along transect S showed the presence of 4 distinct water masses: the surface offshore water, which was of relatively high salinity (~36.0) and temperature (~15°C), the ENACW (~35.6, 11°C), the MSW (>36, 11 - 12°C) and the colder LSW (~35, ~3°C).

3.4.2 Transect S (42°09'N) Dissolved Organic Matter

Eight stations were sampled for DOM measurements along 42°09'N (Table 33): two stations located on the shelf (S200) and shelf-break (S230), on the upper (S600, S1000), and mid-slope (S1500), further offshore at the bottom of the slope (S1950, S2250) and in deep offshore waters (S2700). Although samples were collected at relatively high frequency (>12 depths) at each station, a problem with the sealing methodology resulted in delayed cracking at the mouth of the glass ampoules and subsequent exposure of samples to the atmosphere (i.e. non-airtight seals). Some samples were thus contaminated during storage and exhibited abnormally high concentrations when analysed. About 35% of DOC (total; n=92) and 38% of DON samples (total; n=80) seemed to be contaminated and were thus excluded from the data analysis and interpretation (see section 2.5.4.1 for outlier criteria).

Table 33. Co-ordinates, maximum depth and number of samples collected at M43/2 transect S stations for DOM measurements.

Station	CTD	Latitude, N	Longitude, W	Maximum depth	No. Samples
S200	06	42°09'N	09°18'W	~237m	5
S230	23	42°09'N	09°20'W	~233m	6
S600	21	42°09'N	09°26'W	~602m	9
S1000	09	42°09'N	09°27'W	~1066m	12
S1500	18	42°09'N	09°31'W	~1577m	9
S1950	15, 17	42°09'N	09°35'W	~1943m	10
S2250	13, 14	42°09'N	09°44'W	~2254m	19
S2700	38, 39	42°09'N	10°30'W	~2766m	22

Table 34. DOC and DON concentration ranges at M43/2 transect S stations.

Station	Range of DOC, μM-C	Range of DON, μM-N	C:N ratios
S200	64 – 77	2.4 – 5.9	(19) 13 –27
S230	50 – 86	1.0 – 12.6	(20) 6 – 69
S600	65 – 106	1.7 – 15.2	(20) 7 – 39
S1000	67 – 116	N/A	N/A
S1500	47 – 69	2.1 – 4.5	(19) 13 – 26
S2000	57 – 64	2.5 – 5.8	(16) 12 – 24
S2250	52 – 67	n.d. – 6.9	9
S2700	49 – 63	n.d. – 8.5	6

Note: values in parentheses = mean; N/A = no data available; n.d. = non-detectable levels.

DOC and DON concentrations along M43/2 transect S ranged from 47 – 116 μM-C and n.d. – 15.2 μM-N, respectively (see Table 34 for individual stations). C:N ratios were extremely variable ranging between 6 and 208 but high C:N ratios were probably due to very low DON concentrations at depth. There were no distinct trends in C:N ratios but the range of ratios increased with depth, possibly indicating a range of different source and removal mechanisms to the deep DOM pool. DOC concentrations were significantly higher (ANOVA; $F_{1,58} = 4.86$, $P = 0.03$) in surface waters (i.e. <100m; 72 μM-C) than in deeper waters (mean: 63 μM-C) along transect S. DON concentrations were also significantly higher in surface (mean: 11.4μ M-N) than deeper waters (mean: 6.1 μM-N; ANOVA:$F_{1,42} = 25.8$, $P < 0.001$).

Vertical profiles of DOC and DON concentrations in the upper 200m of the water column along transect S were variable (Figures 108 and 109). The shelf station (S200) had fairly homogeneous DOC concentrations with a mean DOC concentration of ~70 μM-C (Figure 108). This value is slightly lower than that measured for the recently upwelled ENACW (~75μM-C) during the August 1998 cruise (OMEX0898). Similar concentrations were measured for station S230 at the shelf-break. Enhanced values between 75 -120m (75 – 86 μM-C and 8.5 – 12.6 μM-N) were not observed at any other station. There were no clear trends in DOC concentrations across the margin in the upper water column. DON concentrations generally decreased with depth in the upper 200m (Figure 109).

DOM distribution throughout the water column at transect S was relatively patchy. However, higher DOM concentrations were observed at stations nearer to the continental shelf and they generally decreased with depth (Figure 110). The large error bars of certain samples from stations S1000, S2250 and S2700 (Figure 111) represent standard error (i.e. calculated from the

standard deviations of two replicate samples). The mean concentration of two replicates were used in this case because the oceanographic consistency of either sample was uncertain.

Localised enhancement of DON at depth was observed at all stations of transect S (Figures 112 and 113). Contour diagrams of DOC and DON concentrations were produced to highlight any specific trends in the DOM distribution across the margin (Figures 114 and 115). As noted from the vertical profiles, both DOC and DON were enhanced in surface waters but also exhibited localised enhancement with depth. DOC concentrations were elevated on the continental slope above ~1000m and at several other areas off the continental slope and shelf-break. DON concentrations were mainly elevated below ~1500m and at ~500m for the offshore station.

3.4.3 Transect S (42°09'N) Summary

The main features of the DOM distribution along M43/2 transect S were:

- DOM concentrations were significantly higher at the surface (upper 100m) compared to deeper waters.
- DOM distribution was patchy but concentrations generally decreased with distance from the continental shelf and with depth.
- C:N ratios varied greatly and with no clear trends, although the C:N range increased with depth at most stations.
- Localised DOM enhancement was observed in the deep water column.

During this cruise, a weak upwelling event was occurring at the Iberian margin, bringing colder waters to the surface near the coast (see satellite image, Figure 98). This probably disrupted the typical winter characteristics in that region (poleward current), resulting in various meanders at fronts between colder waters that were upwelled and from the north and warmer surface waters of the slope and offshore stations. This may have created a hydrological scenario within which biogeochemical cycling of DOM was complex and resulted in heterogeneous distributions.

The main aims of the winter cruise were to quantify sedimentation, near bottom particle transport, the hydrographical regime and the exchange of biogases during winter (Schmincke and Graf, 2000). Activities were thus mainly focused in deep waters; surface water measurements such as primary productivity and chlorophyll-a were not made. The author collected additional samples for the measurement of inorganic nutrients in order to calculate DON from total dissolved nitrogen (TDN).

DOC and DON were correlated against salinity, temperature and inorganic nutrients (i.e. NO_2 and NO_3) in a correlation matrix. The negative correlation between inorganic nutrients and temperature (-0.81; n = 83) reflected the higher nutrient content of deeper waters. However, the relationship between the two parameters was not linear (Figure 20 in Appendix 3) and thus the correlation coefficient is not significant. DON correlated negatively with inorganic nutrients (-0.56; n = 47; P<0.001; Figure 21 in Appendix 3) suggesting that the remineralisation of DON into inorganic nutrients was taking place with depth. DOC positively correlated with DON (0.60; n = 45; P<0.001; Figure 22 in Appendix 3) suggesting that their cycling was, at least partially, interlinked.

An interesting feature of the distribution of inorganic nutrients (Figure 116) was localised depletion at approximately 1100m on the continental slope. This nutrient minimum does not directly correspond to the DOC or DON accumulations at depth, but is in the same depth range (~1000 – 1500m) and this may suggest some biological activity associated with the proposed biogeochemical character of the MSW (i.e. low DIN and C-rich DOM) or perhaps from re-suspended sediments. It is possible that bacterial activity was higher near the MSW at depth, as has been observed in previous campaigns by Dr. H. Galvao (pers. comm.). Bacterial communities may have been associated with suspended material there, aiding the release of DOM through enzymatic attack within particles (Smith et al., 1992) and assimilation of nutrients during metabolic activity (Pomeroy et al., 1995). Otherwise, the lack of inorganic nutrients may be creating limited conditions that are unfavourable for bacterial uptake of DOM (Thingstad et al., 1998).

Some POC measurements were made by Dr. Lei Chou at the Universite Libre de Bruxelles, Belgium in near-bottom waters of stations S230 to S2700 (Figure 117). There was no clear trend in bottom water POC across the margin (i.e. there were no significant differences between stations) and these measurements did not correlate with DOM concentrations. In addition, attenuation measurements along transect S (Figure 118) showed higher attenuation in surface waters and especially off the shelf indicating that a high concentration of particles (i.e. from biomass or detritus or resuspended sediments) was present there. However, there was no indication of enhanced particle concentrations in deep waters (i.e. ~1000 - 1500m). This suggests that the high DOM and low inorganic nutrients observed were associated with the biogeochemical character of the MSW. Due to a lack of complementary parameters such as primary and bacterial production, it was difficult to assess the biological mechanisms driving the DOM distribution and cycling during January 1999.

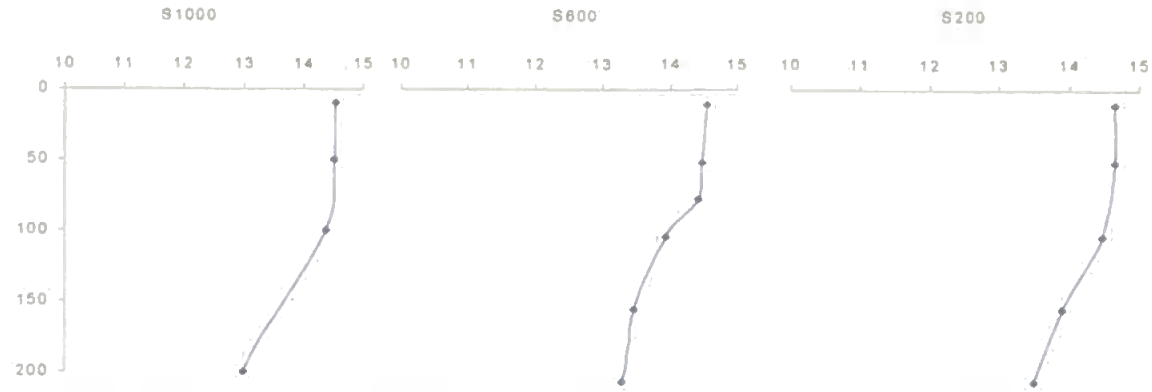

Figure 99. Vertical profiles of temperature (°C) in the upper 200m of M43/2 shelf and slope stations S200, S600 and S1000. Note: y-axis is depth (m).

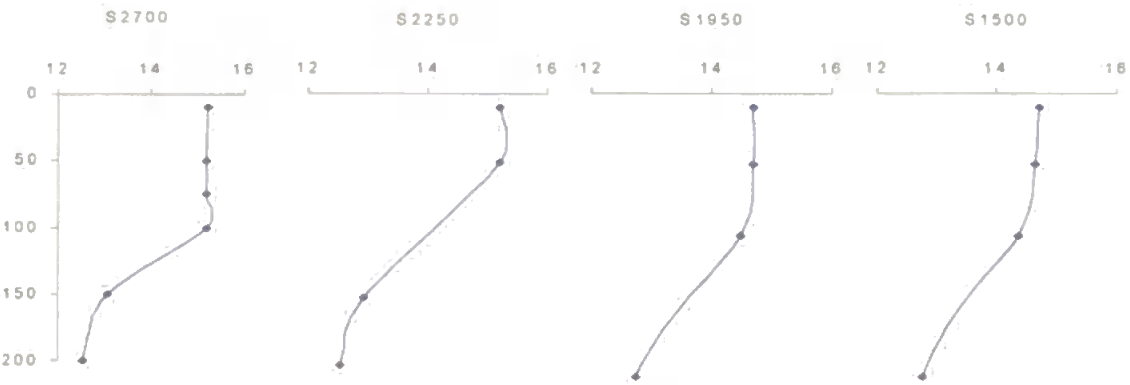

Figure 100. Vertical profiles of temperature (°C) in the upper 200m of M43/2 slope and offshore stations S1500, S1950, S2250 and S2700. Note: y-axis is depth (m).

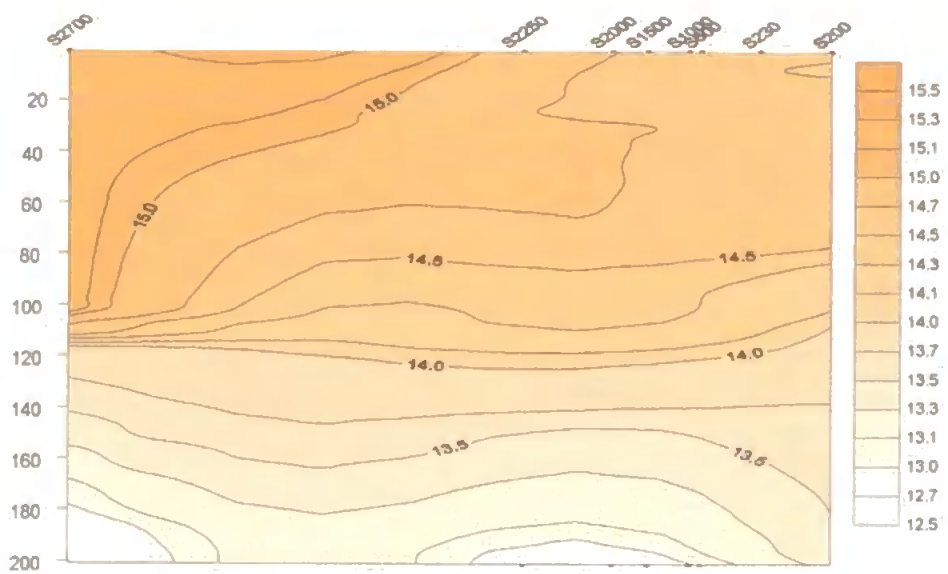

Figure 101. Contour plot of temperature in the upper 200m of M43/2 transect S. Note: colour scale is °C; y-axis is depth (m).

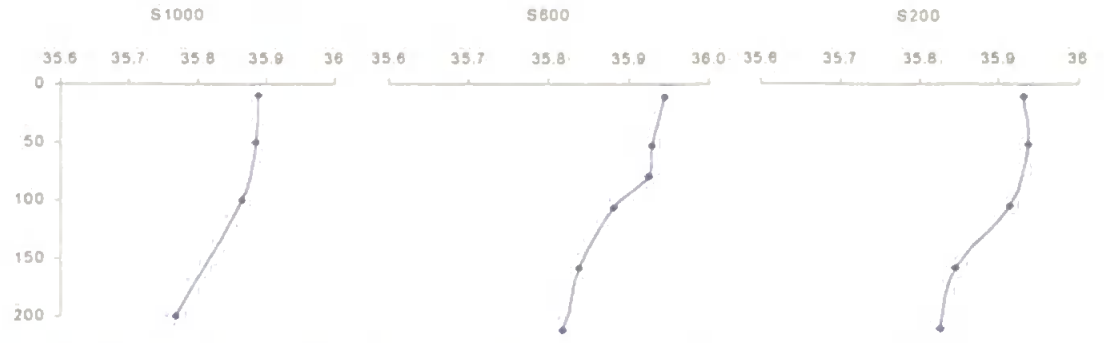

Figure 102. Vertical profiles of salinity in the upper 200m of M43/2 shelf and slope stations S200, S600 and S1000. Note: y-axis is depth (m).

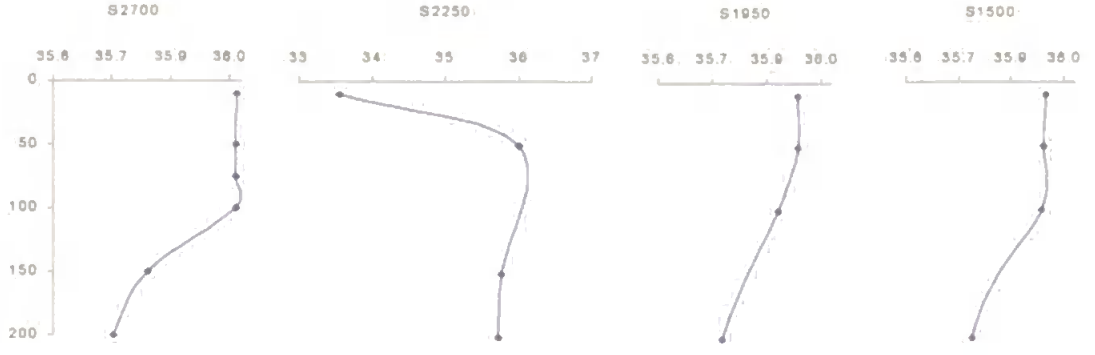

Figure 103. Vertical profiles of salinity in the upper 200m of M43/2 slope and offshore stations S1500, S1950, S2250 and S2700. Note: y-axis is depth (m).

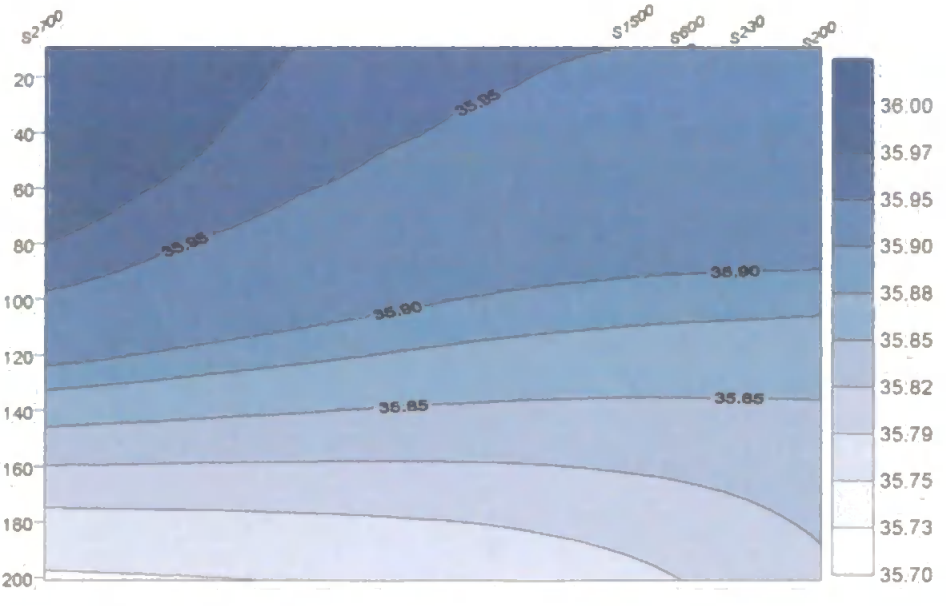

Figure 104. Contour plot of salinity in the upper 200m of M43/2 transect S. Note: colour scale units are arbitrary; y-axis is depth (m).

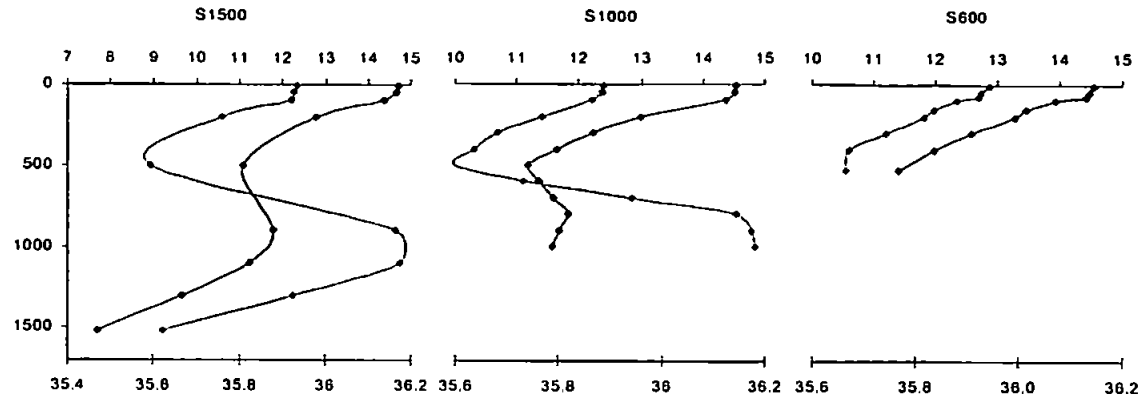

Figure 105. Vertical profiles of salinity and temperature (°C) in M43/2 stations S600, S1000 and S1500. Note: ♦– temperature, – salinity; y-axis is depth (m).

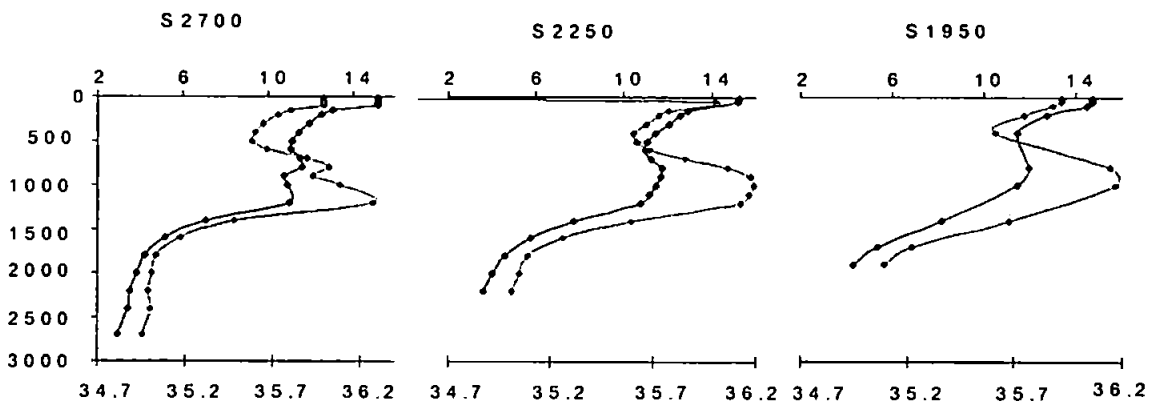

Figure 106. Vertical profiles of salinity and temperature (°C) in M43/2 stations S1950, S2250 and S2700. Note: ♦– temperature, – salinity; y-axis is depth (m).

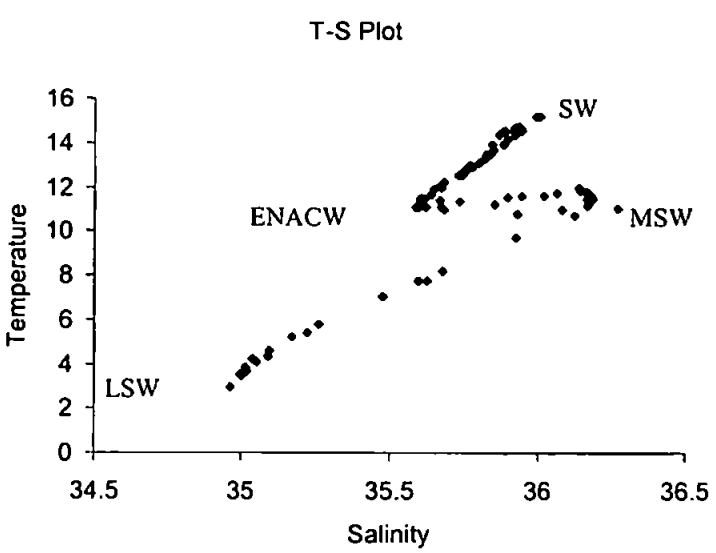

Figure 107. T - S plot of the water column along M43/2 transect S.

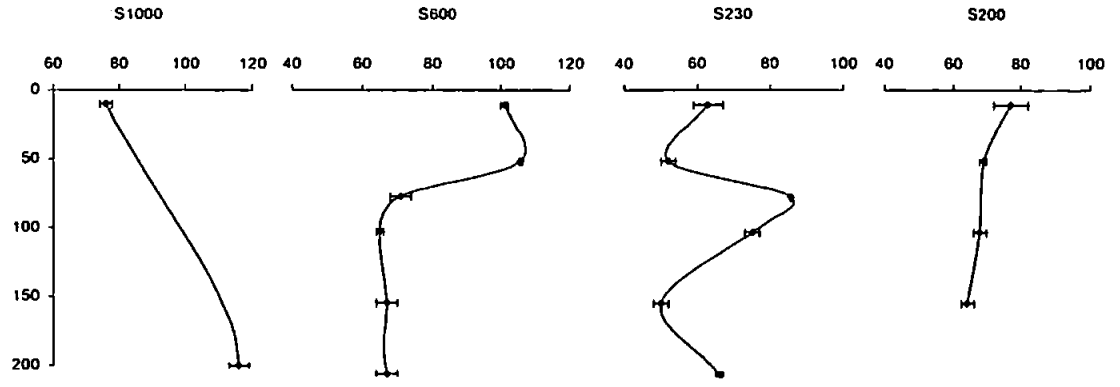

Figure 108. Vertical profiles of DOC concentrations (μM-C) in the upper 200m of M43/2 stations S200, S230, S600 and S1000. Note: y-axis is depth (m).

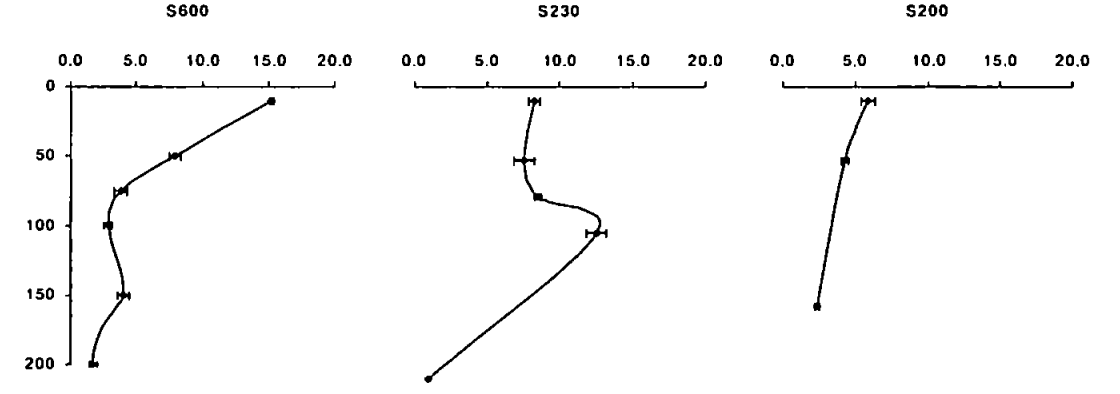

Figure 109. Vertical profiles of DON concentrations (μM-N) in the upper 200m of M43/2 stations S200, S230 and S600. Note: y-axis is depth (m).

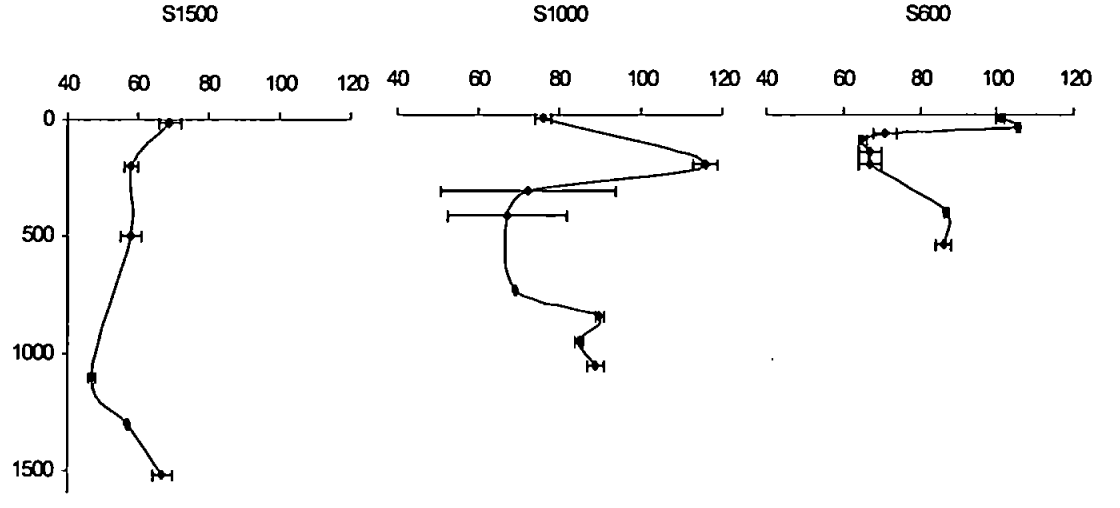

Figure 110. Full vertical profiles of DOC concentrations (μM-C) at the M43/2 shelf and slope stations S600, S1000 and S1500. Note: y-axis is depth (m).

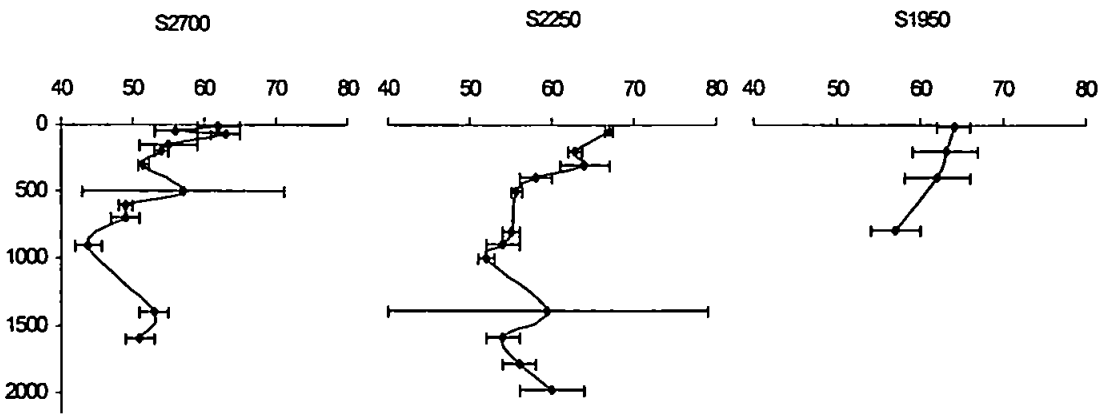

Figure 111. Full vertical profiles of DOC concentrations (μM-C) at the M43/2 slope and offshore stations S1950, S2250 and S2700. Note: y-axis is depth (m).

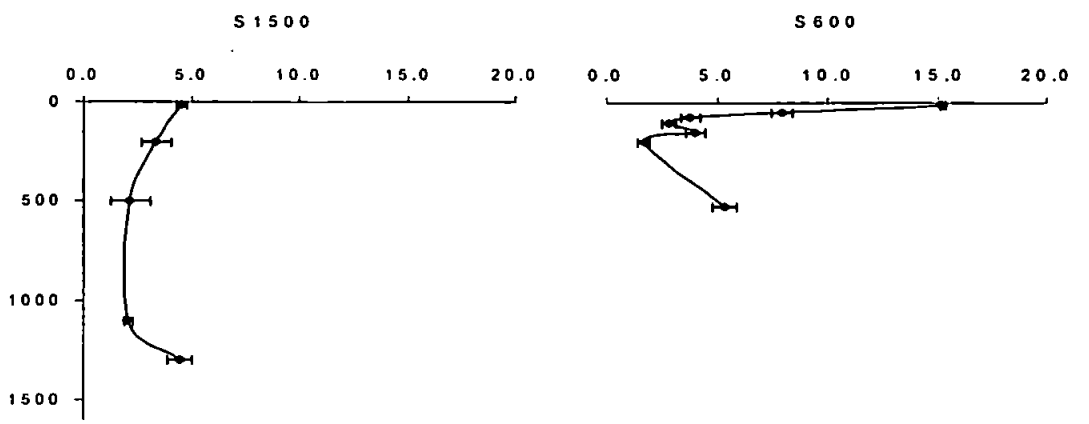

Figure 112. Full vertical profiles of DON concentrations (μM-N) at the M43/2 shelf and slope stations S600 and S1500. Note: y-axis is depth (m).

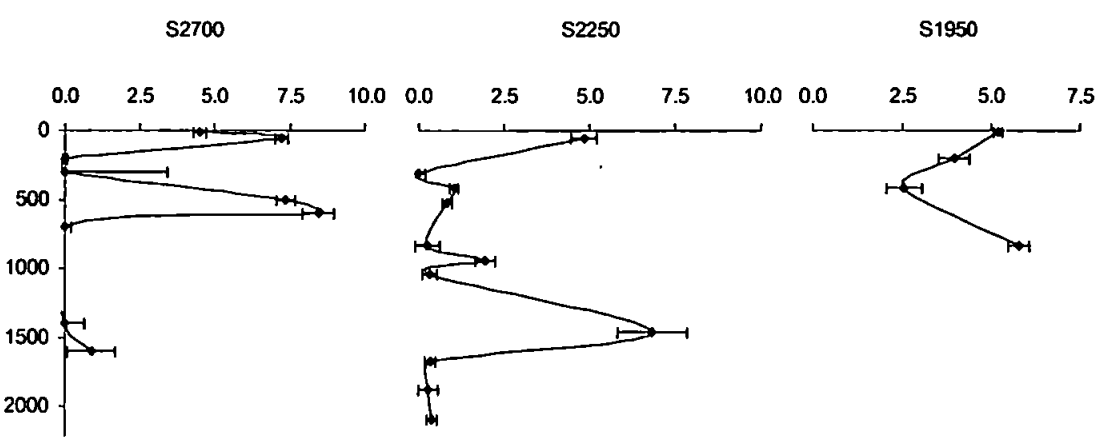

Figure 113. Vertical profiles of DON concentrations (μM-N) at the M43/2 slope and offshore stations S1950, S2250 and S2700. Note: y-axis is depth (m).

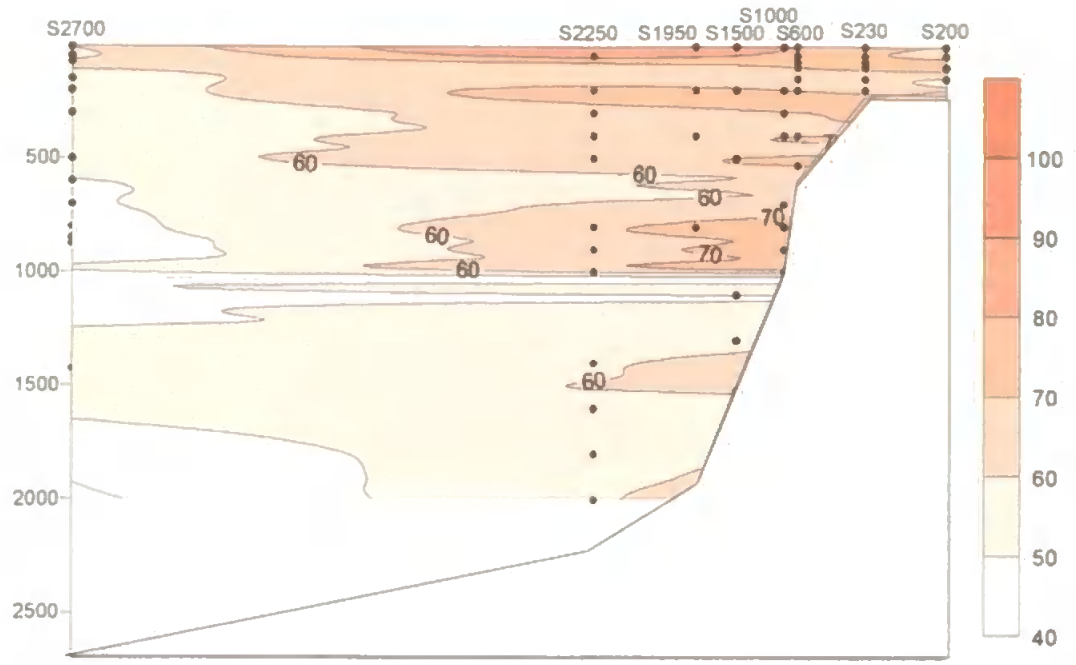

Figure 114. Contour plot of DOC concentrations along M43/2 transect S. Note: colour scale is µM-C; blank areas = no data; y-axis is depth (m).

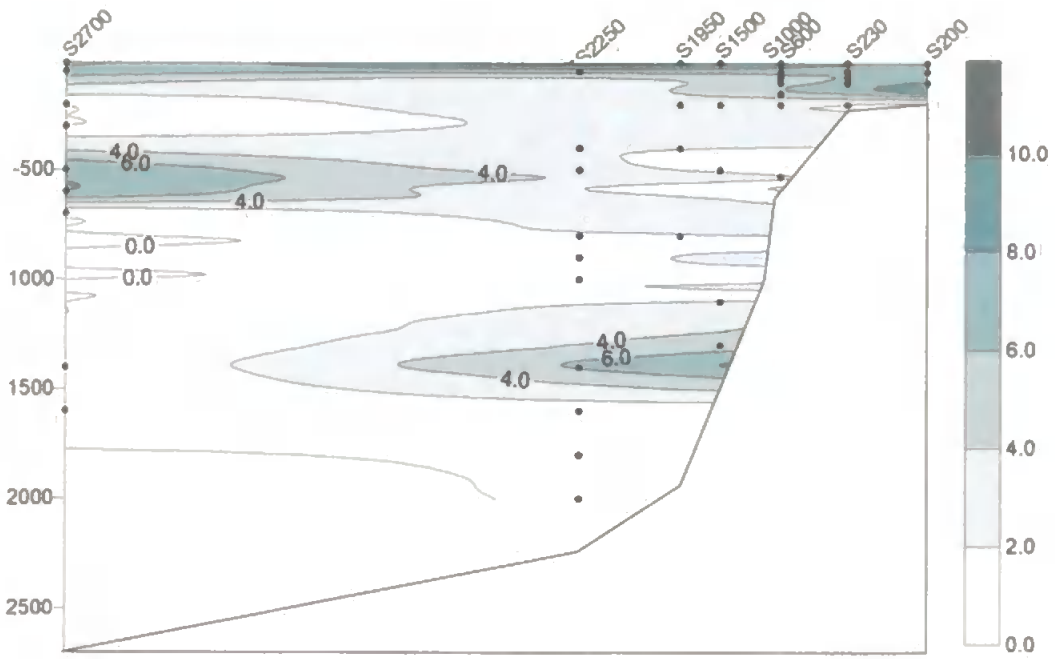

Figure 115. Contour plot of DON concentrations along M43/2 transect S. Note: colour scale is µM-N; blank areas = no data; y-axis is depth (m).

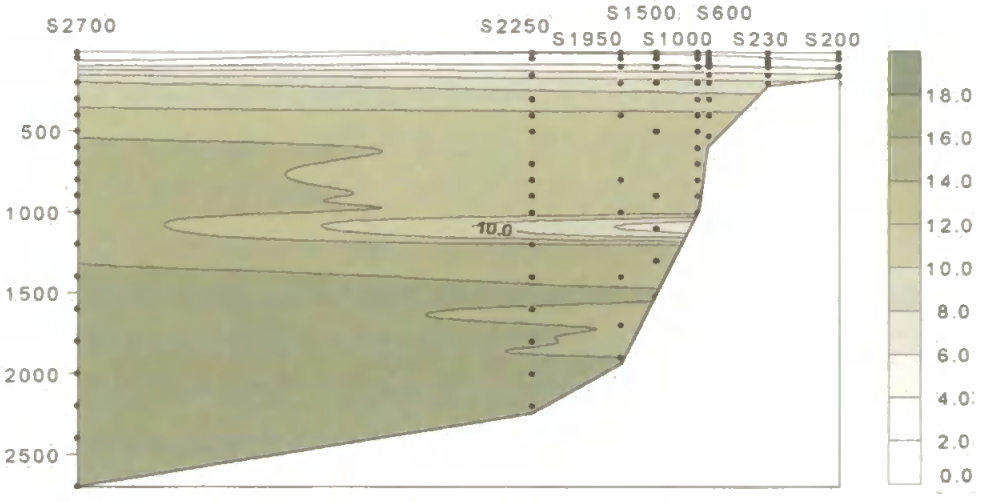

Figure 116. Contour plot of dissolved inorganic nitrogen (DIN) concentrations along M43/2 transect S. Note: colour scale is µM-N; y-axis is depth (m).

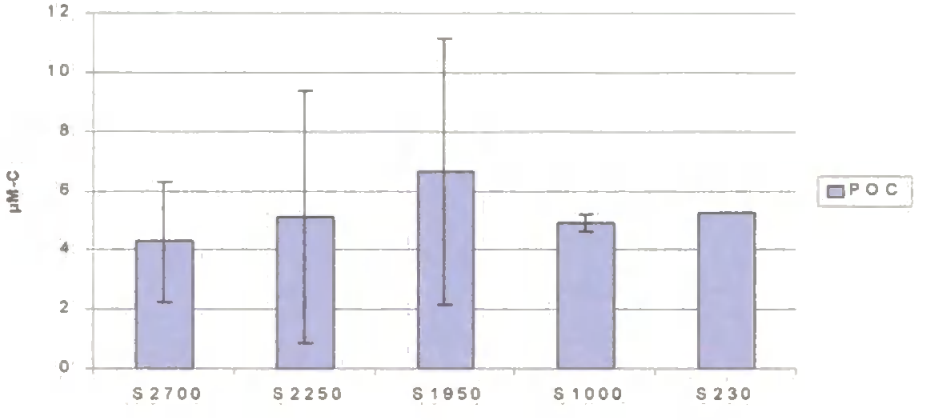

Figure 117. POC (µM-C) concentrations in near-bottom waters of M43/2 stations S230, S1000, S1950, S2250 and S2700. Data from Université Libre de Bruxelles, Belgium.

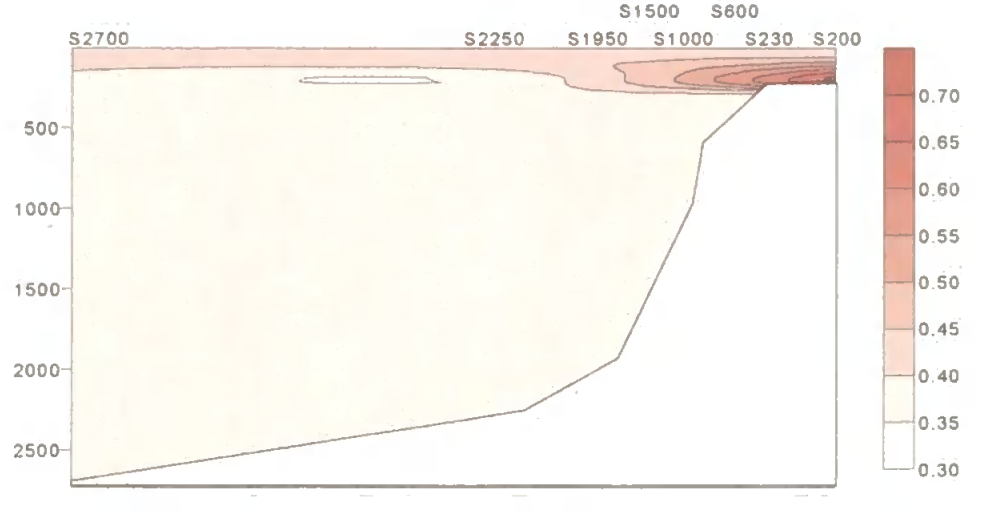

Figure 118. Contour plot of light attenuation along M43/2 transect S. Note: y-axis is depth (m).

3.5 R/V Belgica Cruise BG9919

Cruise BG9919 on the R/V Belgica took place from the 4th to the 17th September 1999 and aimed to map water properties along the main OMEX cross-shelf transects (N, P & S; see Figure in Methodology) during upwelling conditions. The weather during BG9919 was generally favourable allowing extensive sampling of transects (Table 8 in section 2.2.2) and short time-series sampling at a coastal station off Cape Finisterre.

3.5.1 General Hydrography

Cruise BG9919 took place during the summer period, when upwelling conditions are characteristic. SST Satellite images (Figure 119) and *in situ* temperature measurements showed that surface waters of the shelf were colder than surface waters offshore. Upwelling intensity in the first week (5 - 11th September) was highest off Cape Finisterre in the north as indicated by the comparatively lower temperatures there.

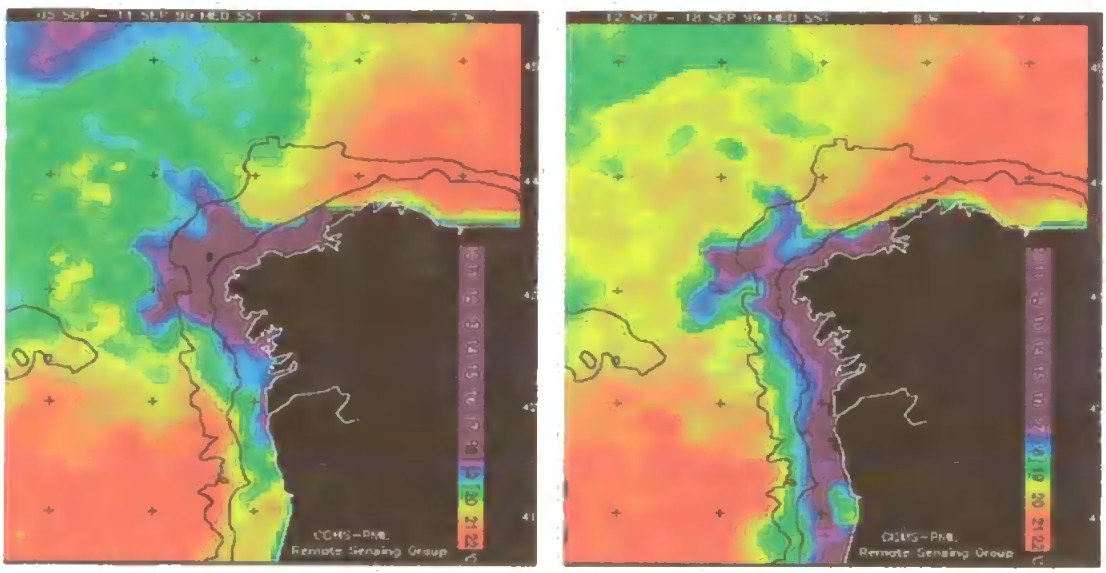

Figure 119. SeaWifs satellite image [20] of the sea-surface temperature (SST) off the north-west coast of the Iberian Peninsula from 5 - 11th September 1999 (left) and 12 - 18th September 1999 (right). Note: colour scale is °C; black colour to the east is cloud coverage.

However the upwelling front was not maintained with time and small meanders from the upwelled waters formed into filaments during the second week of the research cruise (12 - 17th

[20] SSTs are composite satellite images, courtesy of RSG, Plymouth, U.K.

September). During the second week, the upwelling intensity increased along the Rias Baixas and no distinct offshore filaments had formed.

3.5.2 Transect N (43°00'N) Salinity and Temperature

Temperature and salinity profiles of the upper 200m of transect N clearly indicated upwelling along the coast. Temperatures in surface waters (<30m) ranged from 13.2 to 18.8°C, generally increasing offshore (Figure 120). A sharp decrease was observed at all stations down to approximately 30 - 50m below which temperatures were more homogeneous (~12°C). Salinity profiles in the upper 200m of the shelf stations showed that subsurface waters (20 –75m) were more saline than surface waters (Figure 122). This subsurface salinity core was deeper (~100 - 150m) in offshore stations. Surface waters of the coastal station (N80) had relatively low salinity (i.e. up to 0.03 lower) and this may suggest a weak terrestrial water influence. The shelf and shelf-break stations had the highest salinity and with the observed lower temperatures this indicates that upwelling activity was more intense or more recent in these stations. The contour lines of the temperature and salinity contour plots slope upward particularly at the shelf and shelf-break compared to the coastal station (Figures 121 and 123). This confirms that either upwelling intensity was higher on the shelf or that surface waters at the coast were mixed with warmer, less saline waters from the coastal embayments. At deeper stations offshore (Figure 124), the MSW was clearly present with its core between 1000 – 1200m, below which temperature and salinity both decreased.

A T - S plot of measurements along transect N (Figure 125) shows the presence of four water masses with characteristic signatures: the LSW with low temperature and salinity (~5°C and 35), the saline MSW (11°C, ~36), the ENACW (~11 - 12°C, 35.6), and surface water (SW) that is a combination of upwelled ENACW and surface offshore water with slightly higher salinity (35.7) and significantly higher temperatures (up to 18.8°C) due to solar heating at the surface.

3.5.3 Transect N (43°00'N) Dissolved Organic Matter

Five stations were sampled along transect N during cruise BG9919 for DOC and DON measurements (Table 35): three coastal and shelf stations (N80, N136, N220) and two offshore stations (N2000, N3100). The coastal station N80 was sampled three times over 10 days (i.e. N80A – 05/09; N80B – 11/09; N80C – 14/09) to serve as a small-scale time-series study on DOM cycling influenced by upwelling dynamics.

DOC concentrations ranged from 48 – 180 μM-C and were significantly higher (ANOVA; $F_{1,54}$ = 5.59, P = 0.02) in surface waters (mean: 78 μM-C) than in deeper waters (>200m; mean: 65 μM-C). DON was not measured due to technical problems with the TDN analyser that resulted in a decrease in sensitivity of the chemiluminescence detector. Replicate samples have been stored at 4°C in the dark awaiting analysis.

Table 35. Co-ordinates, maximum depth, number of samples and range of DOM concentrations at BG9919 transect N stations.

Station	CTD	Latitude, N	Longitude, W	Max depth	No. Samples	Range of DOC (μM-C)
N80A	44A	43°00'N	09°18'W	~80m	5	68 – 87
N80B	44B	43°00'N	09°18'W	~80m	4	74 – 84
N80C	44C	43°00'N	09°18'W	~80m	4	76 – 180
N136	45	43°00'N	09°28W	~136m	9	77 – 130
N220	46	43°00'N	09°31W	220m	11	59 – 75
N2000	48	43°00'N	09°48'W	~2000m	14	48 – 84
N3100	49	43°00'N	10°01'W	~3100m	11	57 - 75

DOC concentrations at the coastal and shelf stations ranged between 74 and 180 μM-C (Figures 126 - 127). Lower DOC concentrations were observed further offshore but there was no apparent trend across the margin. A contour plot of the DOC distribution in the upper 200m of the water column (Figure 128) shows enhancement of DOC in the upper 100m of transect N and deepening of this to 150m at station N2000. Subsurface DOC maxima are shown at several depths but the extent of these maxima across the margin are more likely to be interpolations of the *Surfer* programme. Each vertical profile on a contour plot represents a sampling point with a specified concentration. The further away from these sampling points in the diagram, the higher the uncertainty in the diagram depicting accurate DOM concentrations. Despite these drawbacks, contour plots can be helpful for plotting a large data set and for detecting any discernible cross-margin features in DOM distribution.

On the first sampling date at station N80 (i.e. N80A) DOC concentration ranged from 68 – 85 μM-C (Figure 129). Six days later (N80B), the DOC vertical profile did not differ significantly but chlorophyll-a had increased by an average of 0.4 mg m^{-3} (Figure 130). Three days later (i.e. N80C), DOC concentrations increased in the top 30m by up to an excess of 96 μM-C, almost twice that of N80B concentrations. Likewise, chlorophyll-a concentrations (mg m^{-3}) had increased in the upper 30m on the last sampling day by approximately five times that measured

previously at station N80. It would thus seem that the increase in phytoplankton biomass, as indicated by increased chlorophyll-a, resulted in higher production of DOM by photosynthetic extra-cellular release (PER). However, the two parameters did not correlate strongly and so it is most likely that the accumulated DOC on the last sampling date may have been a result of various source mechanisms (e.g. PER combined with lysis, grazing, sloppy feeding and/or particle dissolution).

Bacteria numbers[21] in surface waters at N80B (i.e. 5m) were higher than N80C (Figure 131) suggesting that the removal rate of DOM (e.g. bacterial uptake) on the third day of sampling was lower than the input rate thus allowing DOC to accumulate. In addition, POC measurements[22] at station N80 (Figure 132) show that POC concentrations in surface waters significantly increased on the second day probably as a result of continued utilisation of upwelled nutrients and increased production by the microbial community. However, on the last sampling day, although chlorophyll-a increased, bacterial numbers and POC decreased suggesting that not only was DOC input high due to increased PER but that POC was being remineralised *via* the DOC pool (Azam et al., 1983).

Further offshore, DOC concentrations exhibited a decreasing trend with depth (Figure 133) although deep waters (>200m) contained DOC concentrations above those of typical deep oceanic waters[23]. The contour plot of DOC distribution along transect N (Figure 134) showed higher DOC concentrations in surface waters and decreasing with depth and distance from the continental shelf. The higher concentrations of DOC observed in surface waters was most likely due to higher input rates of DOC by increased primary production (e.g. PER) and biomass (e.g. lysis) as indicated by higher chlorophyll-a concentrations there (Figure 135). Relatively high chlorophyll-a concentrations (0.8 mg m^{-3}) were also observed in offshore stations.

3.5.4 Transect N (43°00'N) Summary

High DOC concentrations were observed near the coast decreasing with depth further offshore. At the coast and on the shelf section of transect N, DOC correlated well with biological parameters such as bacterial numbers (e.g. station N80C; 0.83; n = 4; $P<0.001$; Figure 23 in Appendix 4) and chlorophyll-a (e.g. station N136; -0.60; n = 4; $P<0.001$; Figure 24 in Appendix 4). Further offshore, DOC was strongly correlated to hydrological parameters such as

[21] Bacterial data obtained from Dr. H. Galvao and co-workers at the University of Algarve, Faro, Portugal.
[22] POC data obtained from Dr. L. Chou at the Universite Libre de Bruxelles, Belgium.
[23] NW Mediterranean: 50 – 58 µM-C (Copin-Montegut and Avril, 1993); NW Atlantic: 50 – 55 µM-C (Chen et al., 1996c); Equatorial Atlantic: 46±6 µM-C (Thomas et al., 1995).

temperature. For example, at shelf stations DOC and temperature were not strongly correlated (range: -0.41; n = 9; P<0.001; Figure 25 in Appendix 4 to 0.47; n = 10; P<0.001; Figure 26 in Appendix 4) whereas in offshore stations they were (range: 0.64; n = 13; P<0.001; Figure 27 in Appendix 4 to 0.91; n = 11; P<0.001; Figure 28 in Appendix 4). This may suggest that as biological activity was lower in deep offshore waters, DOC removal and input rates followed hydrological time-scales (i.e. water circulation rates).

The observed accumulation of DOC in surface waters of transect N compared to deeper waters was most likely due to higher chlorophyll-a and hence higher phytoplankton biomass that was producing DOM *in situ*. Bacterial numbers were also higher in surface waters helping the release of DOM from phytoplankton by facilitating cell lysis. In addition, the higher bacterial biomass observed in surface waters may have contributed a fraction of its biomass to the HMW DOM pool (Ogawa et al., 2001) *via* cell breakage from bacteriophages and protozoan grazing (Nagata, 2000).

The time-series study at station N80 showed that DOC can significantly accumulate within three days highlighting the dynamic nature of its cycling. Complementary data indicated that the DOC accumulation at N80C was due to PER and particle dissolution.

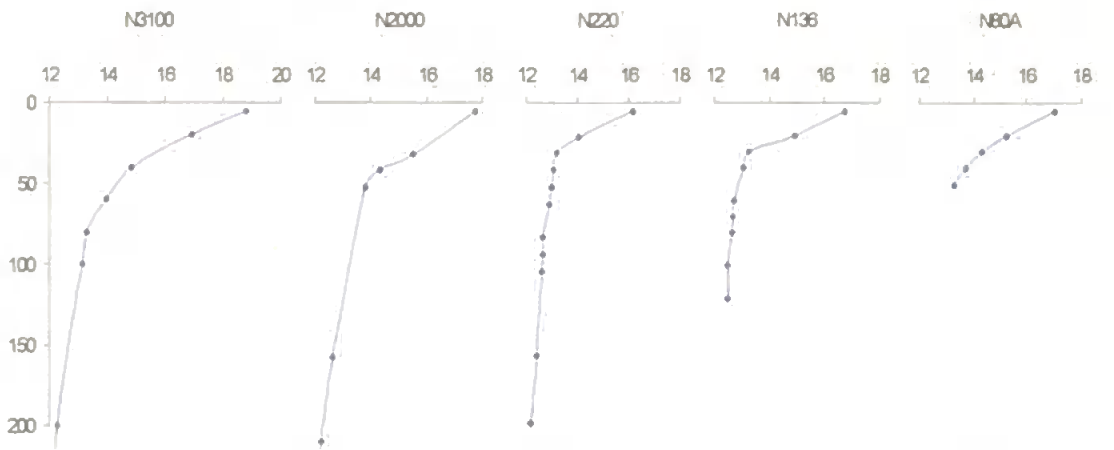

Figure 120. Vertical profiles of temperature (°C) in the upper 200m of BG9919 transect N. Note: y-axis is depth (m).

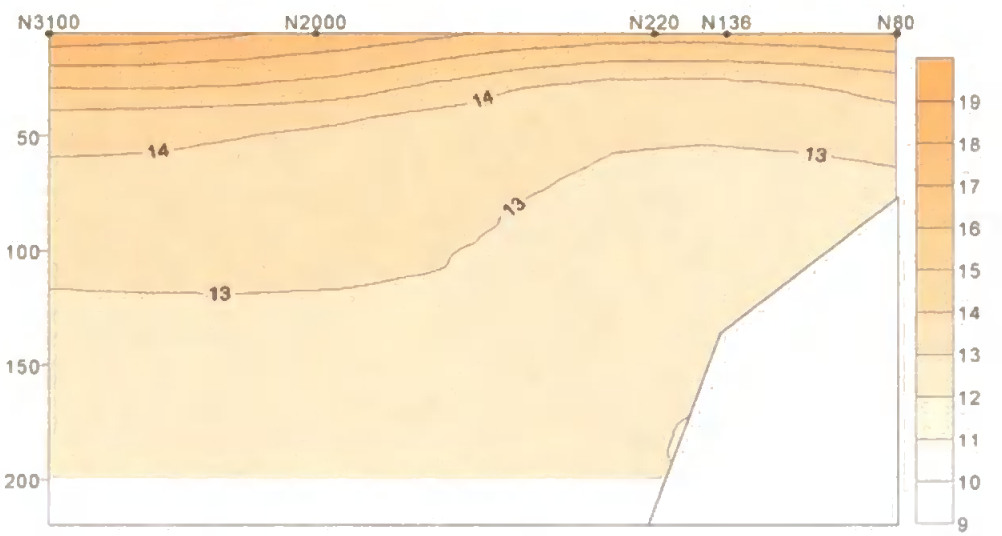

Figure 121. Contour plot of temperature in the upper 200m of BG9919 transect N. Note: colour scale is °C; y-axis is depth (m).

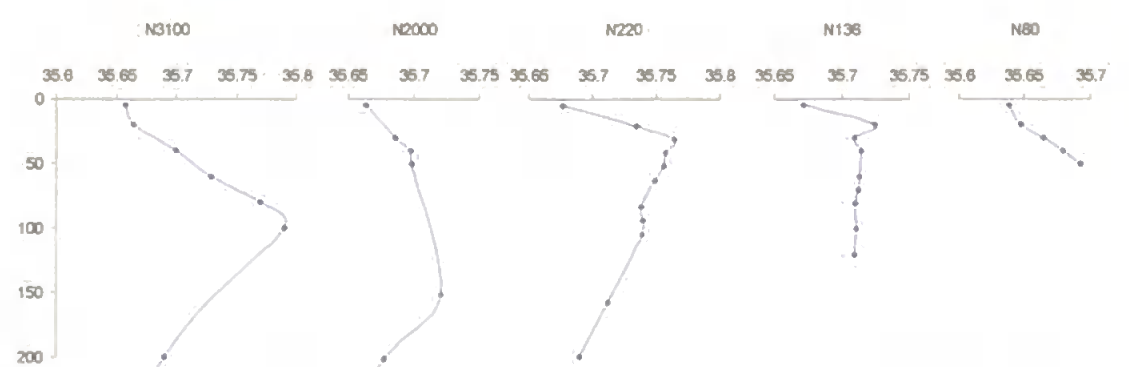

Figure 122. Vertical profiles of salinity in the upper 200m of BG9919 coastal and shelf stations N80A, N136 and N220. Note: y-axis is depth (m).

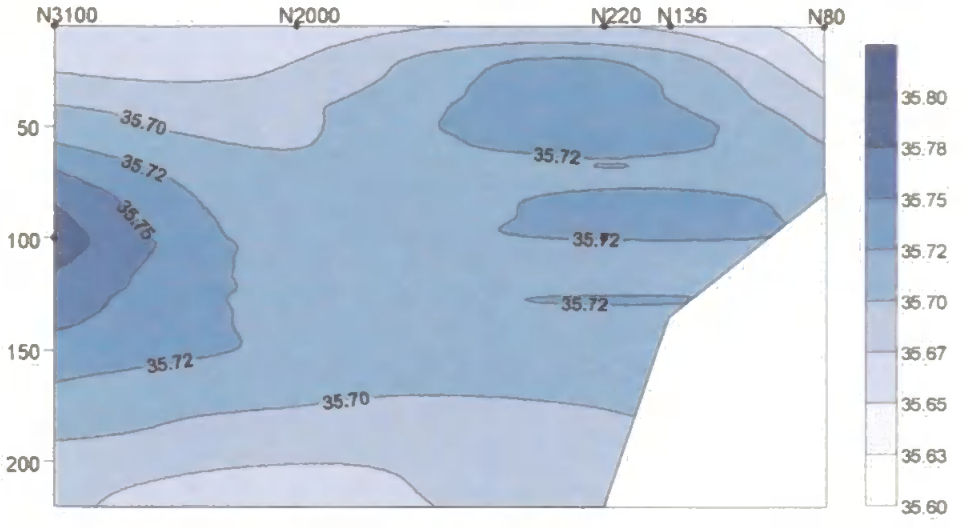

Figure 123. Contour plot of salinity in the upper 200m of BG9919 transect N. Note: colour scale is in arbitrary units; y-axis is depth (m).

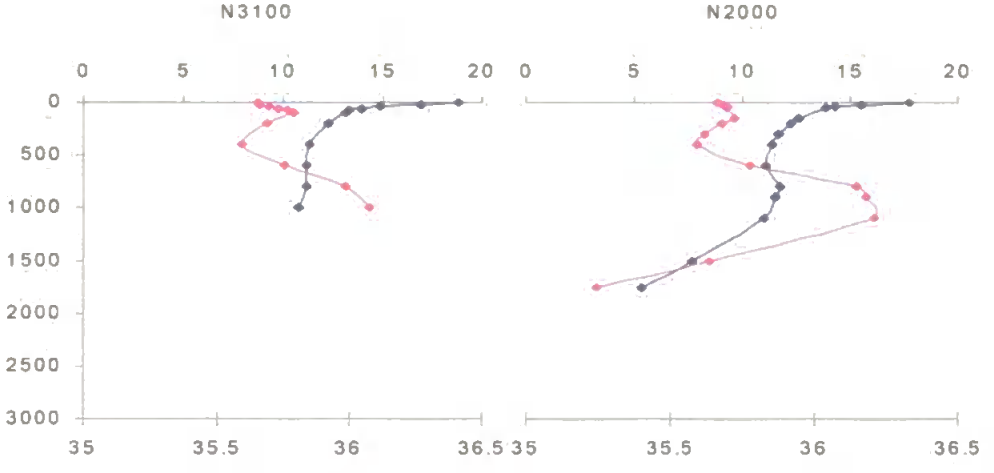

Figure 124. Full vertical profiles of salinity and temperature (°C) in BG9919 stations N2000 and N3100. Note: ♦ – temperature, ■ – salinity; y-axis is depth (m).

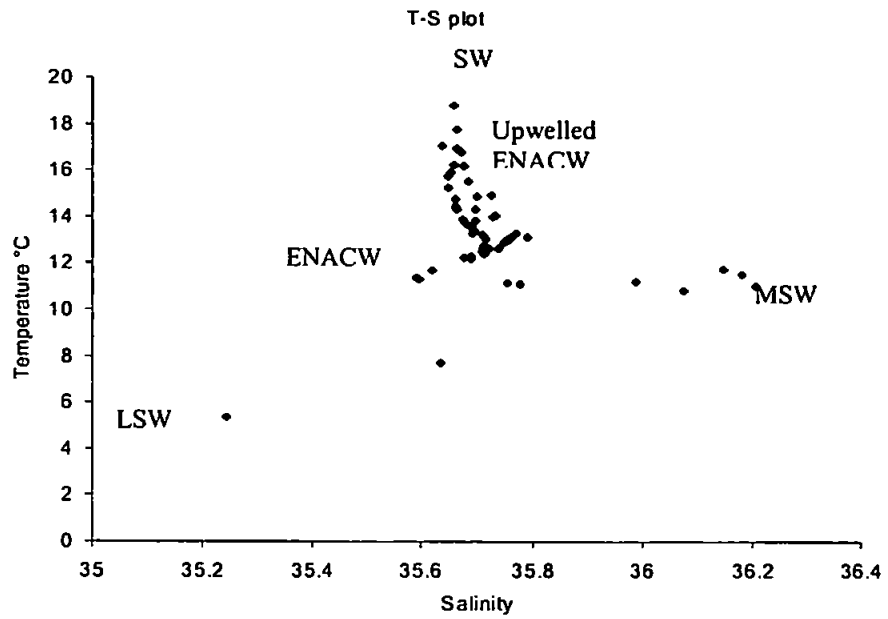

Figure 125. T - S plot of the water column along BG9919 transect N.

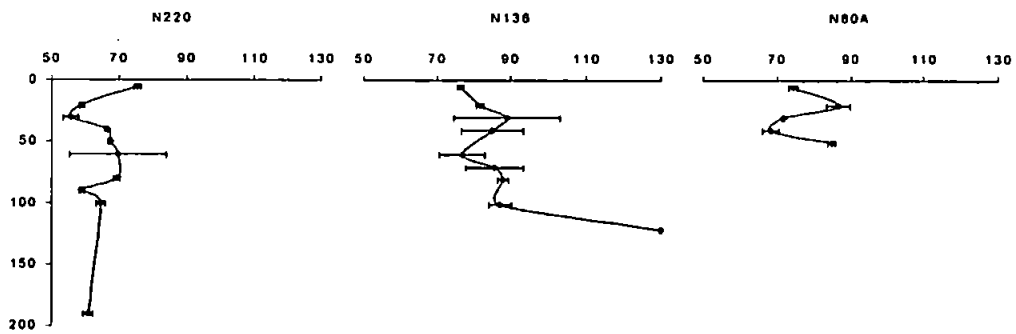

Figure 126. Vertical profiles of DOC concentrations (μM-C) at BG9919 stations N80A, N136 and N220. Note: y-axis is depth (m).

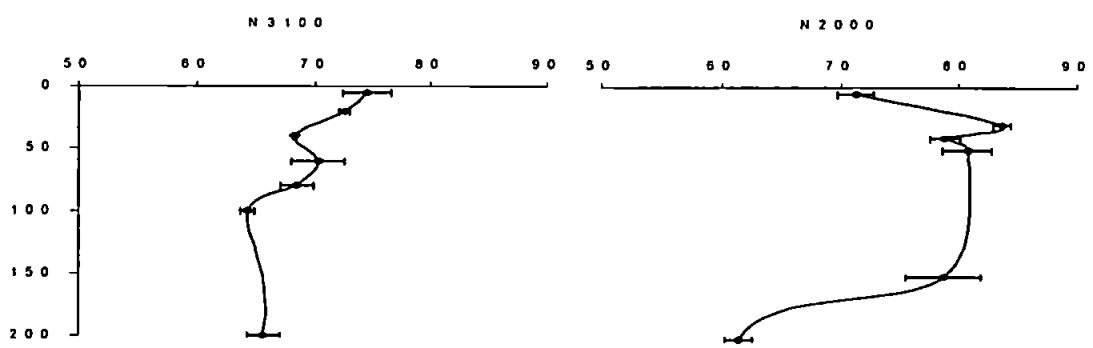

Figure 127. Vertical profiles of DOC concentrations (μM-C) in the upper 200m of BG9919 offshore stations N2000 and N3100. Note: y-axis is depth (m).

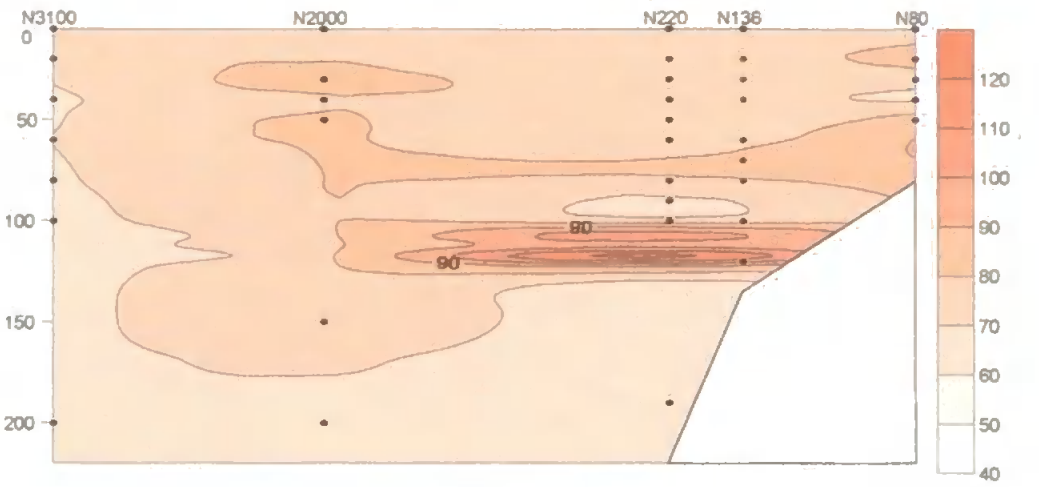

Figure 128. Contour plot of DOC concentrations in the upper 200m of BG9919 transect N. Note: colour scale is µM-C; y-axis is depth (m).

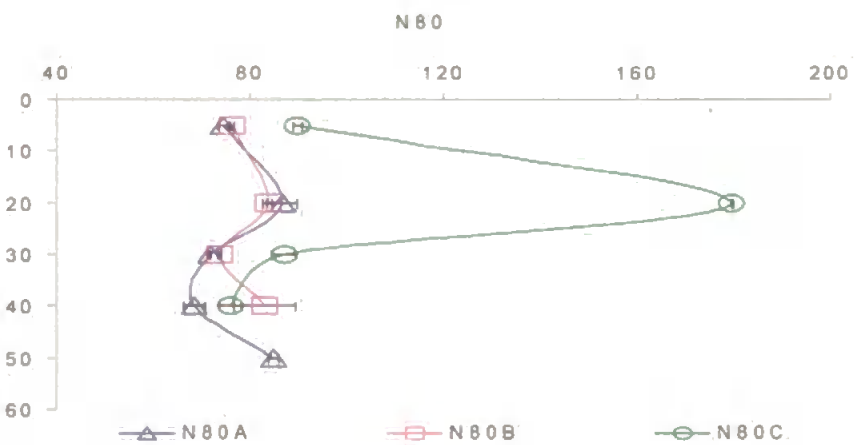

Figure 129. Vertical profiles of DOC concentrations (µM-C) at BG9919 station N80. Note: N80A – 05/09/99 ; N80B – 11/09/99 ; N80C – 14/09/99; y-axis is depth (m).

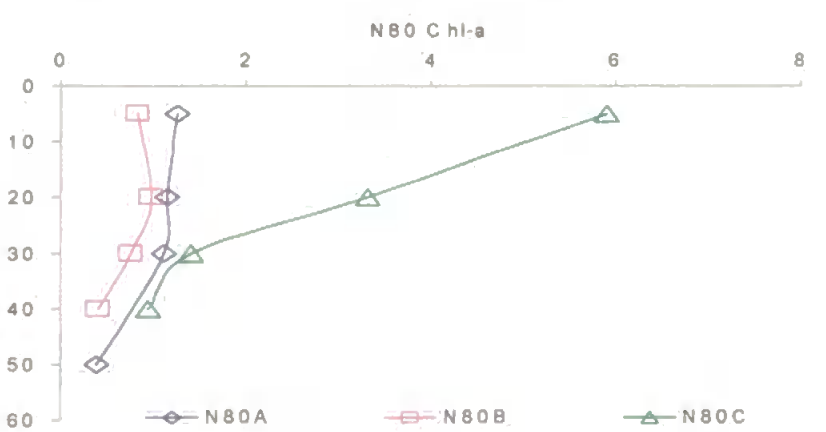

Figure 130. Vertical profiles of chlorophyll-a (mg m^{-3}) at BG9919 station N80. Note: N80A – 05/09/99 ; N80B – 11/09/99 ; N80C – 14/09/99; y-axis is depth (m).

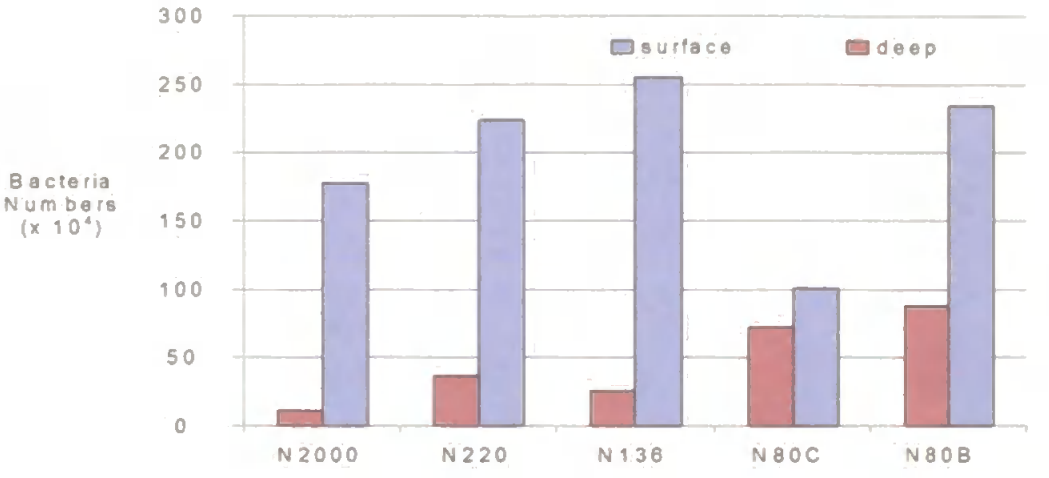

Figure 131. Bacteria numbers (per ml.) in surface and deep waters along BG9919 transect N. Note - surface: 5m, deep: ~ maximum depth of station.

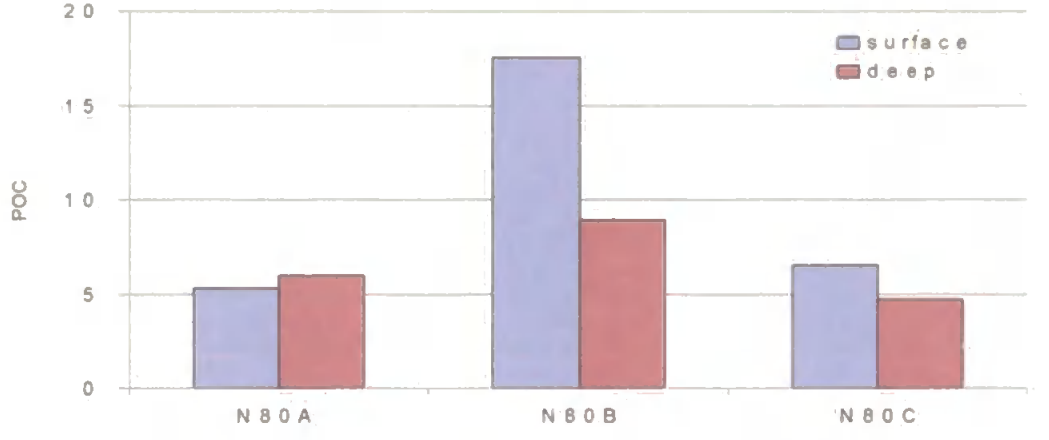

Figure 132. POC concentrations (μM-C) in surface and deep waters of BG9919 station N80. Note: N80A – 05/09/99 ; N80B – 11/09/99 ; N80C – 14/09/99; surface: 5m; deep: ~40m.

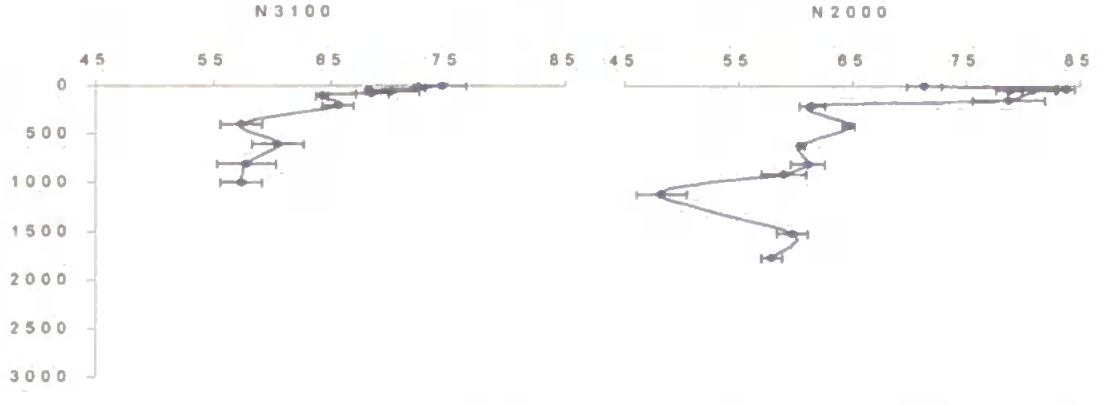

Figure 133. Full vertical profiles of DOC concentrations (μM-C) in BG9919 offshore stations N2000 and N3100. Note: y-axis is depth (m).

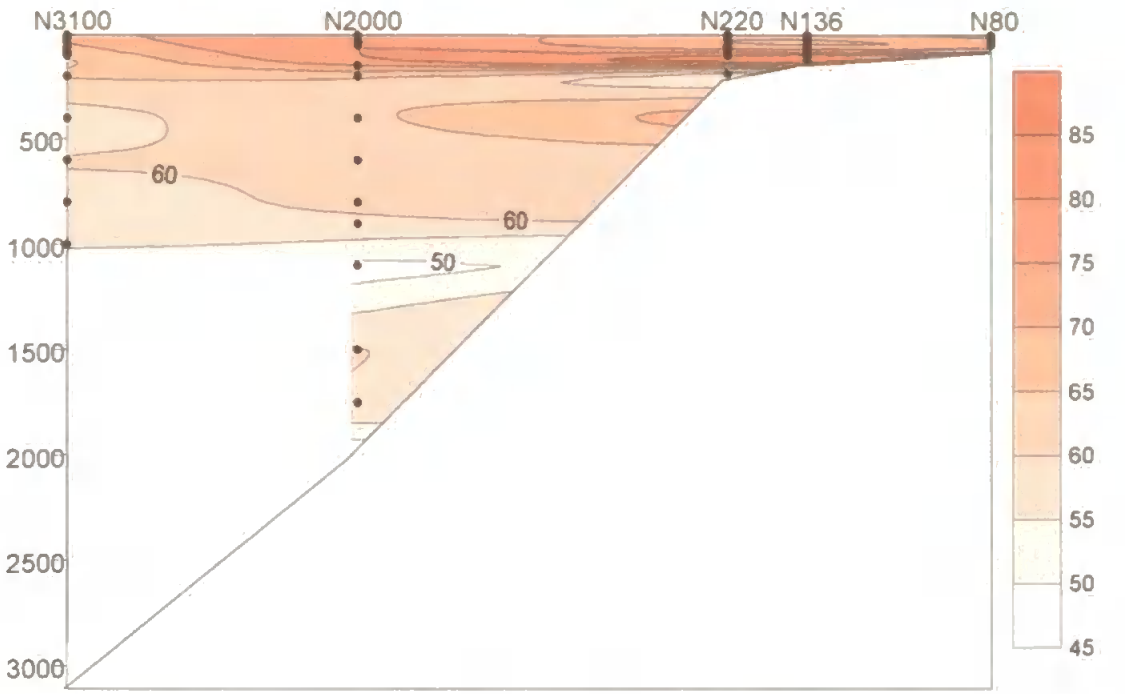

Figure 134. Contour plot of DOC concentrations along BG9919 transect N. Note: colour scale is μM-C; blank areas = no data; y-axis is depth (m).

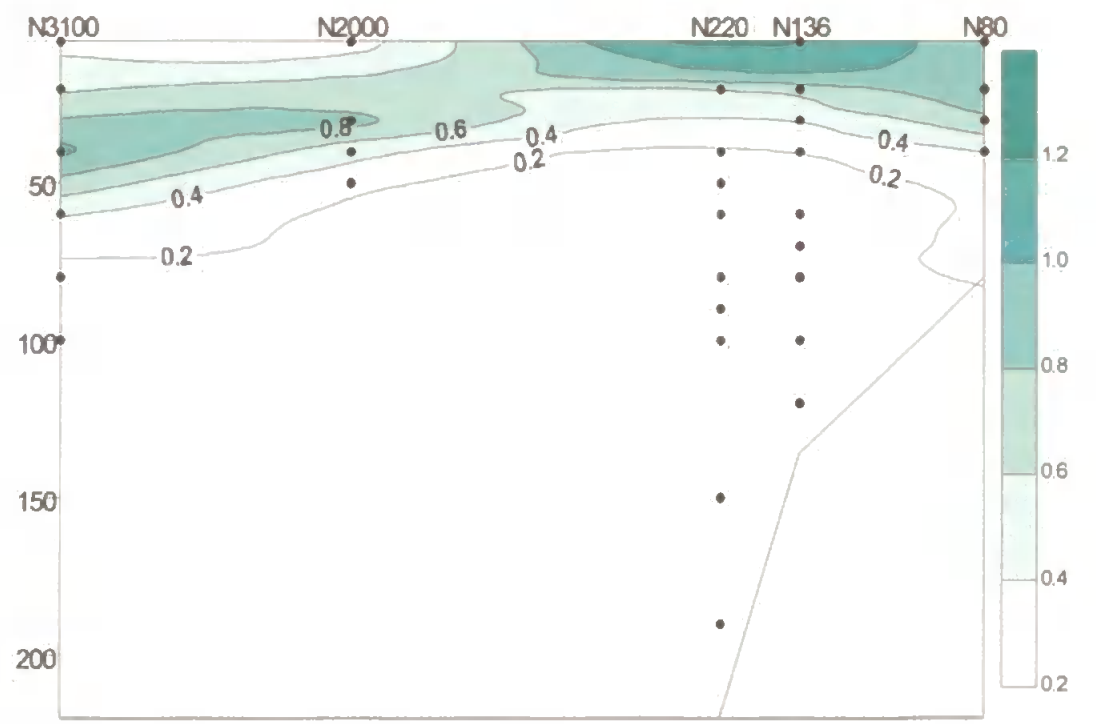

Figure 135. Contour plot of chlorophyll-a concentrations in the upper 200m of BG9919 transect N. Note: colour scale is mg m^{-3}; y-axis is depth (m).

3.5.5 Transect P (42°40'N) Salinity and Temperature

Upwelling of deeper waters (~100m) to the surface was observed during sampling along transect P (42°40'N) at the Iberian margin. Temperature profiles exhibited colder waters (~18°C) near the coast and on the shelf (Figure 136) with warmer waters (~19°C) over the slope and further offshore (~18.4°C) (Figure 137). A thermocline was present below surface waters with temperatures decreasing to approximately 12.2°C down to 200m. The contour plot of temperature distribution in the upper 200m of transect P (Figure 138) clearly shows the upwelling of sub-surface waters to the top of the water column and temperatures decreasing with depth. Further offshore, there is a deepening of warmer waters, probably a product of the upwelling phenomena (i.e. colder upwelled waters at the coast pushing warmer surface waters offshore).

Salinity profiles in the upper 200m of the water column indicated a heterogeneous vertical distribution of water whereby less saline waters (~35.68l) were located at the top of the water column and more saline waters (~35.77) were found at ~50 - 100m (Figures 139 - 140). A contour plot of salinity distribution in the upper 200m of the water column (Figure 141) indicated that there was a subsurface salinity maximum over the slope at approximately 75m and saline patches of water below this core at approximately 150m.

Full vertical profiles of temperature and salinity at slope and offshore stations (>1000m depth; Figures 142 - 143) showed that the MSW core was present at ~1000m with the LSW below (>1500m). The contour plot of salinity distribution across the margin (Figure 144) suggests that the MSW signature prevails even offshore at station P2800 (10°18'W). A T - S plot of measurements across the margin along transect P (Figure 145) depicted five main water masses with characteristic T - S signatures: the LSW (~35, 4.5°C), the MSW (~36.2, 11.4°C), the ENACW (~35.6, 11.2°C) and its slightly more saline and warmer upwelled waters (~35.8, 13.4°C), and surface waters with a salinity and temperature range of 35.6 - 35.7 and 15 - 20°C, respectively.

3.5.6 Transect P (42°40'N) Dissolved Organic Matter

Eight stations were sampled along transect P during cruise BG9919 for DOM measurements (Table 36): three coastal and shelf stations (P80, P130, P200), two slope stations (P1000, P1485) and three stations sampled further offshore (P2000, P2250, P2800).

Table 36. Co-ordinates, maximum depth, number of samples and DOM concentrations at BG9919 transect P stations.

Station	CTD	Latitude	Longitude	Max depth	No. Samples	Range of DOC (μM-C)
P80	29	42°40'N	09°09'W	~80m	8	68 – 100
P130	31	42°40'N	09°22'W	~130m	10	57 – 94
P200	32	42°40'N	09°30'W	~200m	10	63 – 93
P1000	33	42°40'N	09°36'W	~1000m	11	54 – 130
P1485	34	42°40'N	09°43'W	~1485m	20	71 – 136
P2000	35	42°40'N	09°50'W	~2000m	10	49 – 69
P2250	36	42°40'N	10°00'W	~2250m	9	62 – 72
P2800	37	42°40'N	10°18'W	~2800m	12	47 – 67

DOC concentrations along transect P ranged from 47 – 136 μM-C. The upper 200m of the water column had significantly higher (ANOVA; $F_{1,81} = 8.45$, $P = 0.005$) DOC concentrations (mean: 77 μM-C) compared to deeper waters (mean: 66 μM-C). In the upper 200m DOC concentrations ranged from 54 – 136 μM-C. No trends were detected in surface waters across the margin but maximum concentrations were generally observed in surface coastal, shelf and slope waters with lower concentrations measured offshore (Figures 146 - 147). A contour plot of DOC distribution in the upper 200m of transect P (Figure 148) shows patchy DOC enhancement near the coast and over the shelf and decreasing DOC concentrations with distance from the shelf. DOC concentrations generally decreased with depth at slope and offshore stations with deeper waters exhibiting a fairly homogeneous distribution (Figures 149 - 150). A contour plot was produced to detect any DOC trends with depth across the margin (Figure 151). It shows higher DOC concentrations in surface waters near the coast decreasing with distance from the shelf. Higher concentrations were also detected in deeper waters of the slope stations at ~1000m where the MSW core was present; DOC concentrations gradually decreased away from the continental slope.

At the location of the MSW (~1000m), low oxygen concentrations were measured (Figure 152). This is generally characteristic of the MSW (van Aken, 2000b) due to decreasing solubility and higher biological activity near the continental shelf (Hinrichsen et al., 1993). Localised DOC accumulation in that area, may result partly due to remineralisation of organic matter *via* the dissolved phase; this is supported by the higher apparent oxygen utilisation (AOU) found in the MSW compared to adjacent waters (83.5μmol kg^{-1}; van Aken, 2000b)

3.5.7 Transect P (42°40'N) Summary

The following main trends were observed along transect P during the BG9919 research cruise:

- DOC concentrations were higher in surface waters on the shelf and near the coast and decreased offshore
- DOC concentrations generally decreased with depth and away from the continental slope but localised DOC accumulation was observed in bottom waters of the slope stations (P1000 and P1485).

The higher DOC concentrations observed nearer the coast were most likely due to increased sources of DOC there, such as the production of DOC from phytoplankton biomass (e.g. PER and lysis). Chlorophyll-a concentrations (Figure 153) were higher in the top 100m of the water column along transect P and significantly higher at the coastal station where DOC concentrations were also high.

In the coastal and shelf stations, DOC correlated well with chlorophyll-a measurements (0.73 – 0.99)[24] whereas further offshore a strong correlation was observed between heterotrophic parameters (i.e. bacterial biomass or bacterial numbers) and DOC (e.g. 0.81 at station P2800; n = 4; P = 0.06; Figure 32 in Appendix 4). This would suggest that near the recently upwelled waters phytoplankton biomass might be the primary source of DOC (e.g. direct exudation or PER) whereas heterotrophic processes may be facilitating DOC production further offshore (e.g. bacterial transformation of POC to DOC).

DOC concentrations decreased with depth and away from the continental slope due to increasing distance from DOM sources and subsequent removal mechanisms (e.g. bacterial uptake). However, at depth, the MSW may provide a lateral source of C-rich DOM to the Iberian margin.

[24] Station P80: 0.73; n = 5; P<0.001; Figure 29 in Appendix 4. Station P130: 0.95; n = 6; P<0.001; Figure 30 in Appendix 4. Station P200: 0.99; n = 4; P<0.001; Figure 31 in Appendix 4

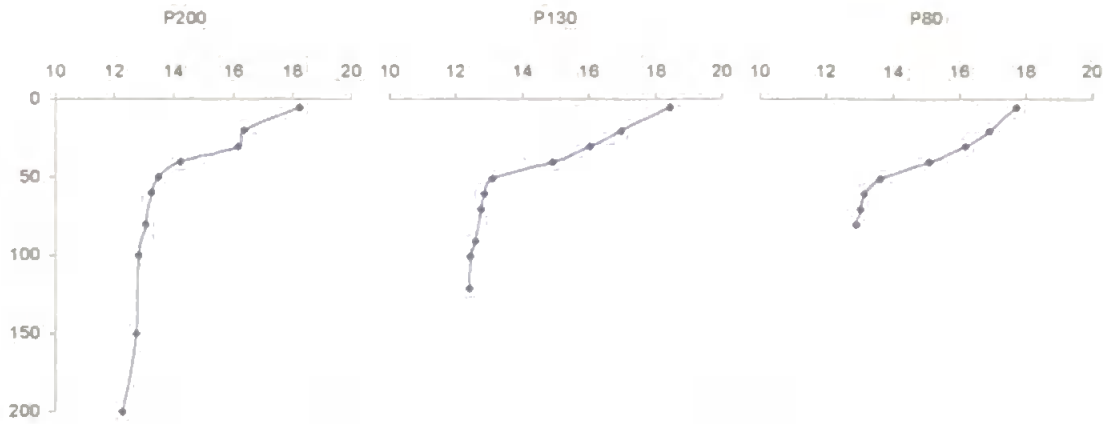

Figure 136. Vertical profiles of temperature (°C) in the upper 200m of BG9919 coastal and shelf stations P80, P130 and P200. Note: y-axis is depth (m).

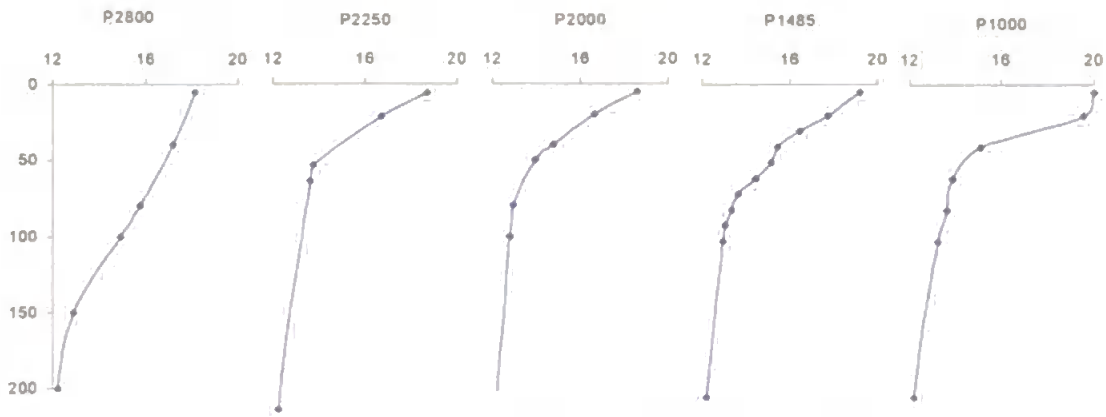

Figure 137. Vertical profiles of temperature (°C) in the upper 200m of BG9919 slope and offshore stations P1000, P1485, P2000, P2250 and P2800. Note: y-axis is depth (m).

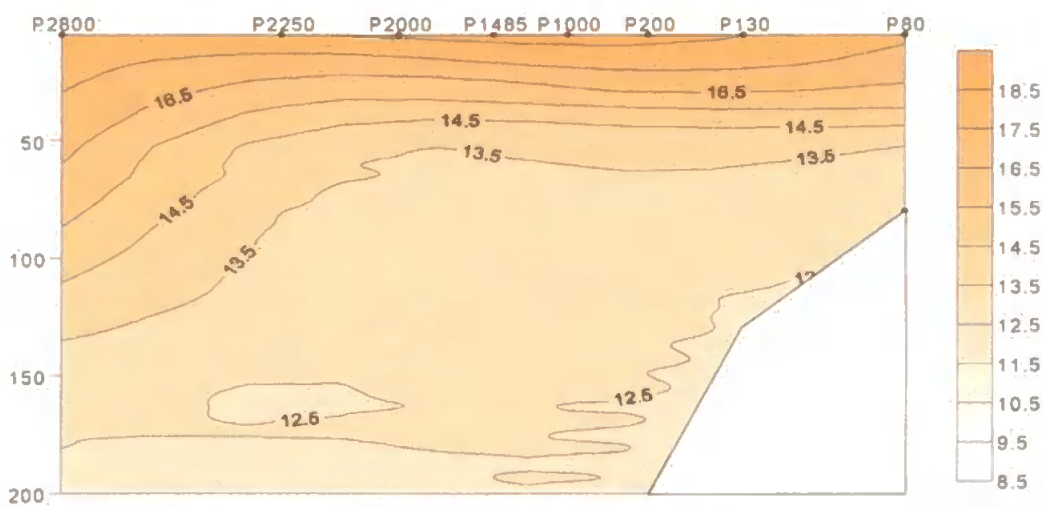

Figure 138. Contour plot of temperature in the upper 200m of BG9919 transect N. Note: colour scale is °C; y-axis is depth (m).

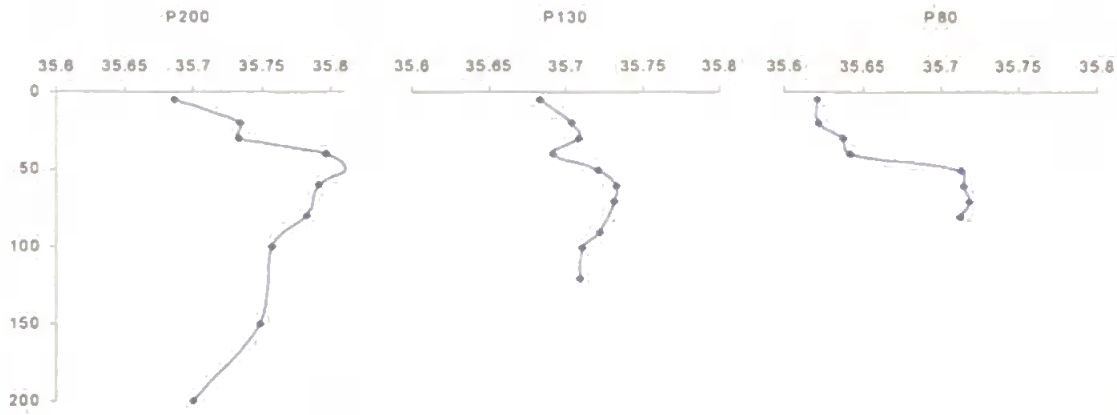

Figure 139. Vertical profiles of salinity in the upper 200m of BG9919 coastal and shelf stations P80, P130 and P200. Note: y-axis is depth (m).

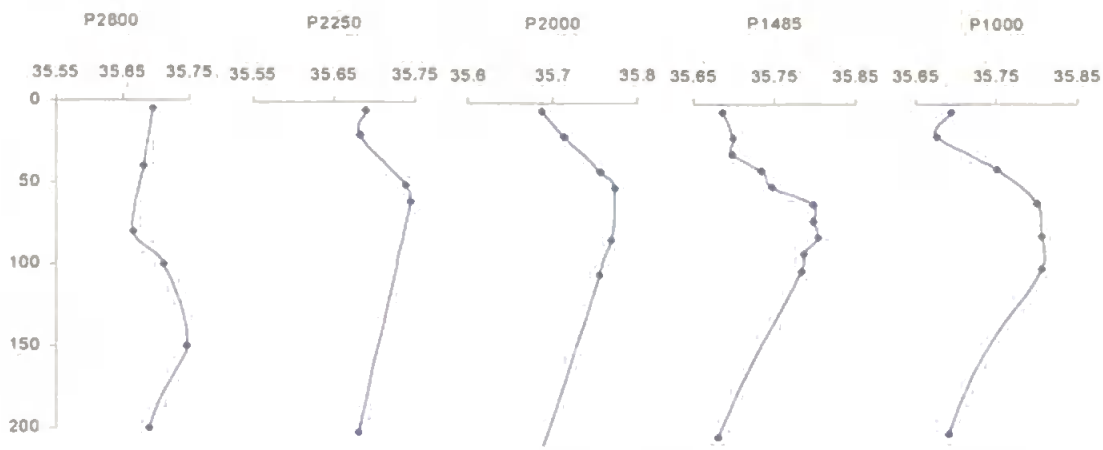

Figure 140. Vertical profiles of salinity in the upper 200m of BG9919 slope stations P1000, P1485, P2000, P2250 and P2800. Note: y-axis is depth (m).

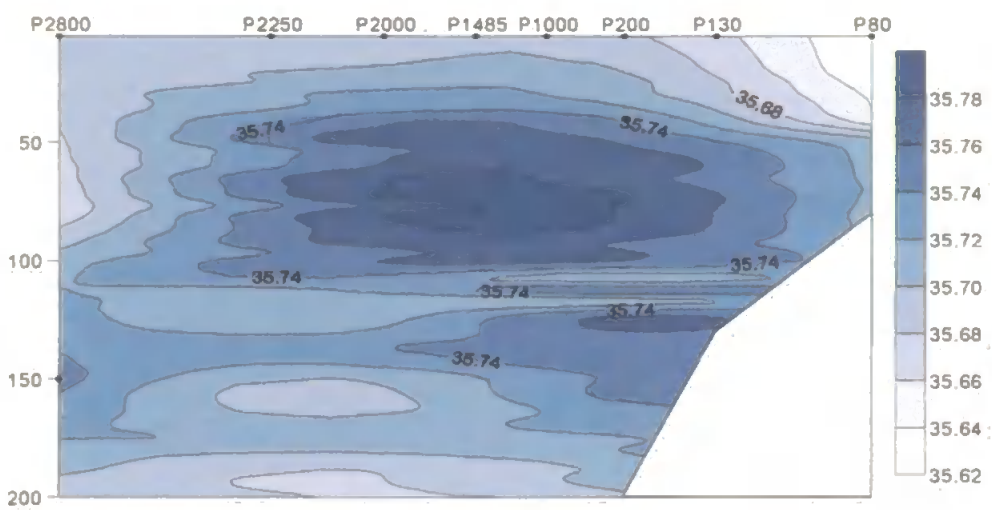

Figure 141. Contour plot of salinity in the upper 200m of BG9919 transect P. Note: colour scale is in arbitrary units; y-axis is depth (m).

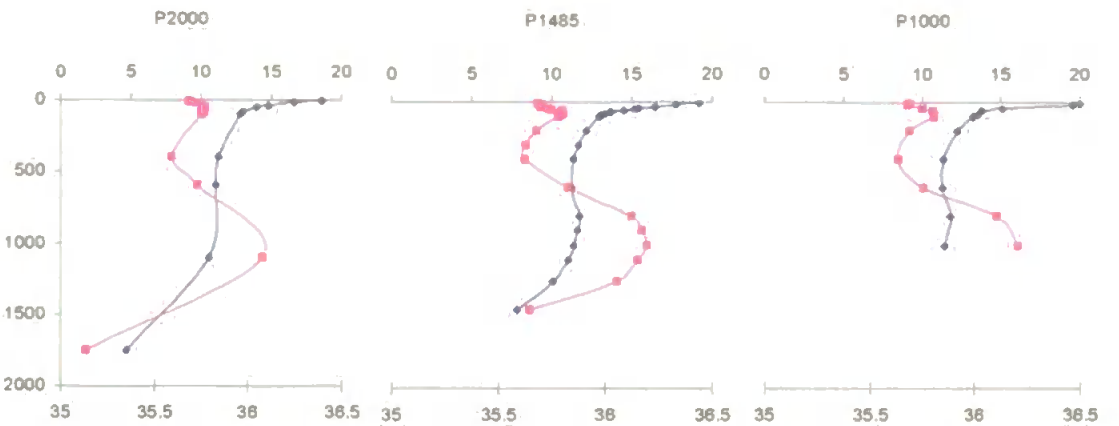

Figure 142. Full vertical profiles of salinity and temperature (°C) in BG9919 stations P1000, P1485 and P2000. Note: ♦– temperature, ■ – salinity; y-axis is depth (m).

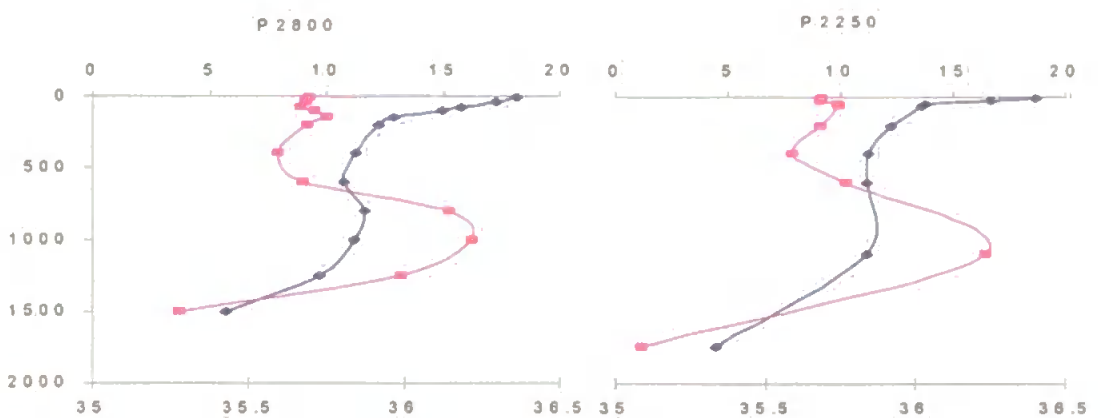

Figure 143. Full vertical profiles of salinity and temperature (°C) in BG9919 stations P2250 and P2800. Note: ♦– temperature, ■ – salinity; y-axis is depth (m).

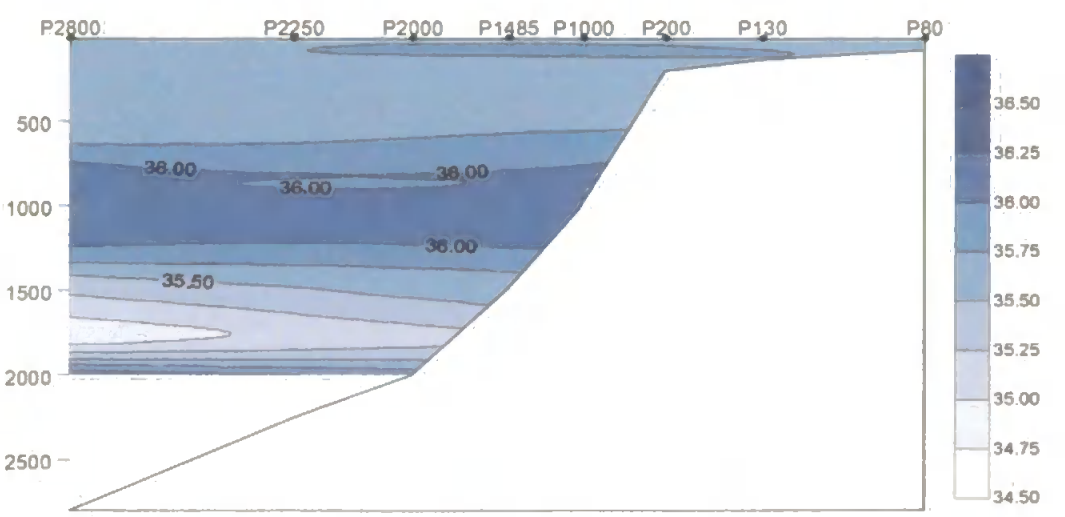

Figure 144. Contour plot of salinity along BG9919 transect P. Note: colour scale is in arbitrary units; white areas = no data; y-axis is depth (m).

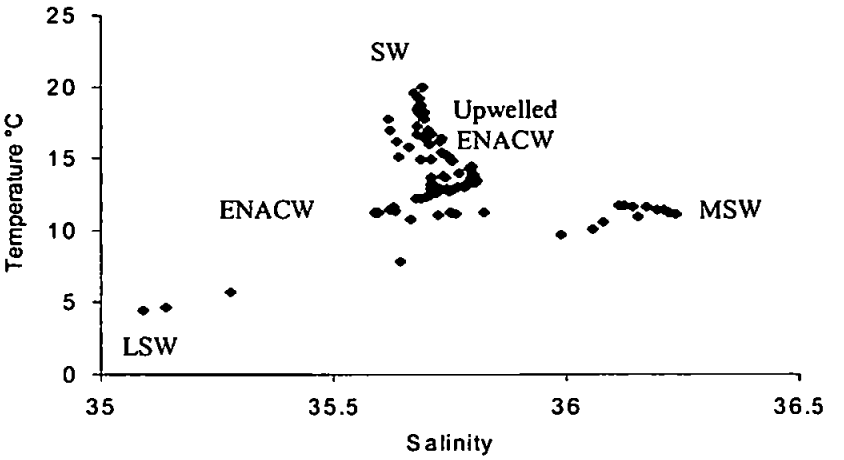

Figure 145. T - S plot of the water column along BG9919 transect P.

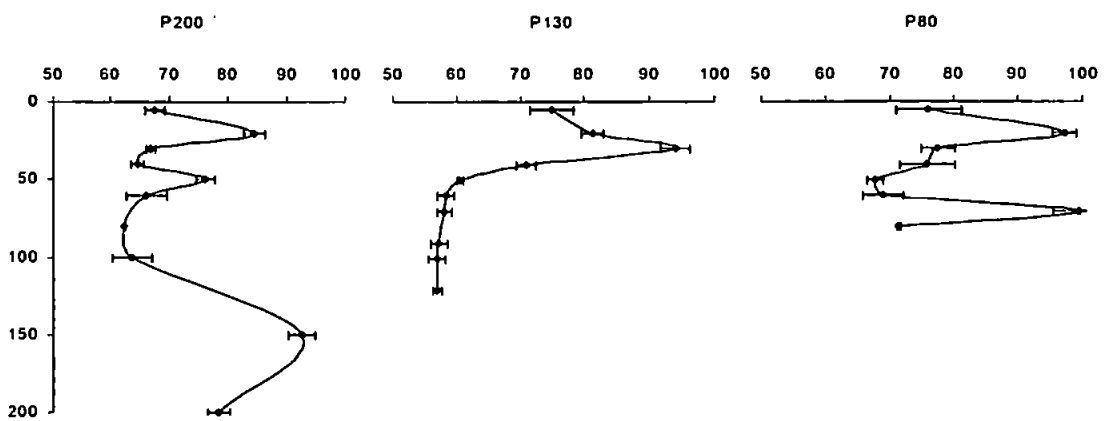

Figure 146. Vertical profiles of DOC concentrations (μM-C) at BG9919 stations P80, P130 and P200. Note: y-axis is depth (m).

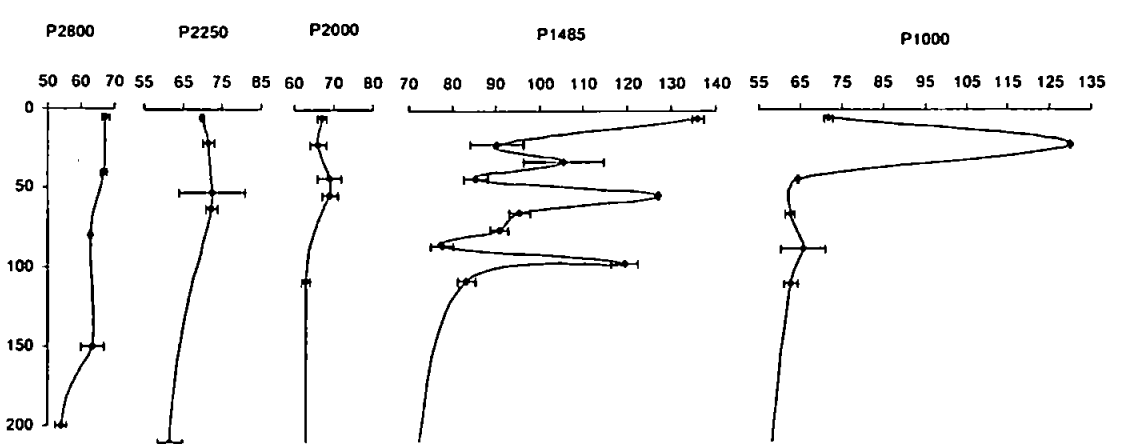

Figure 147. Vertical profiles of DOC concentrations (μM-C) in the upper 200m of BG9919 slope stations P1000, P1485 and P2000. Note: y-axis is depth (m).

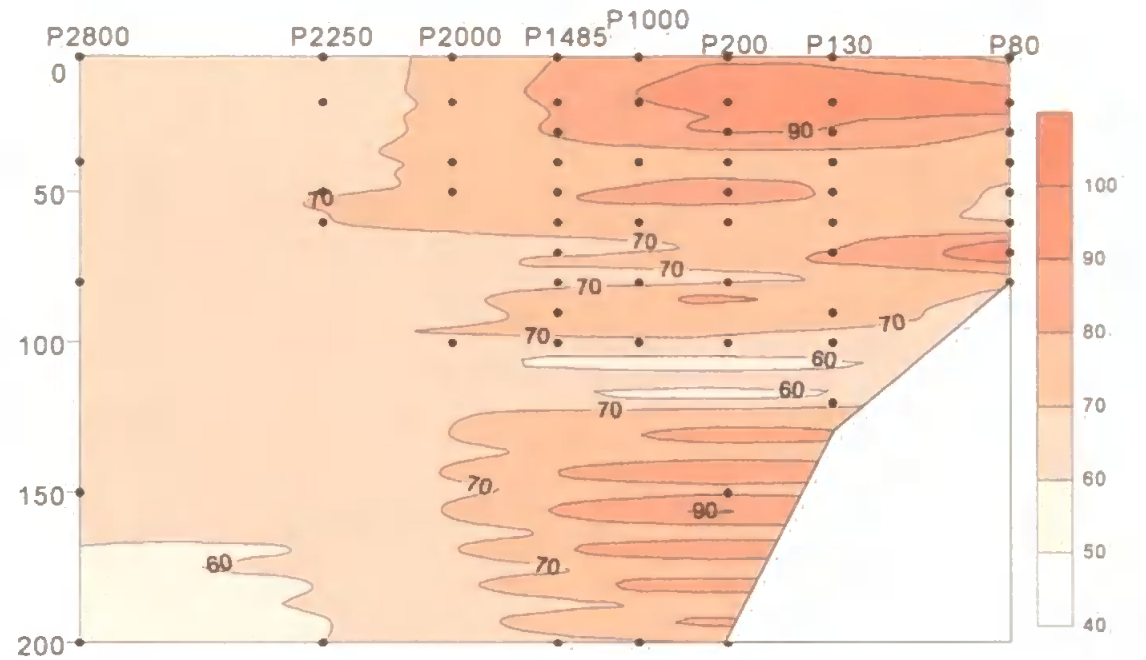

Figure 148. Contour plot of DOC concentrations in the upper 200m of BG9919 transect P. Note: colour scale is µM-C; y-axis is depth (m).

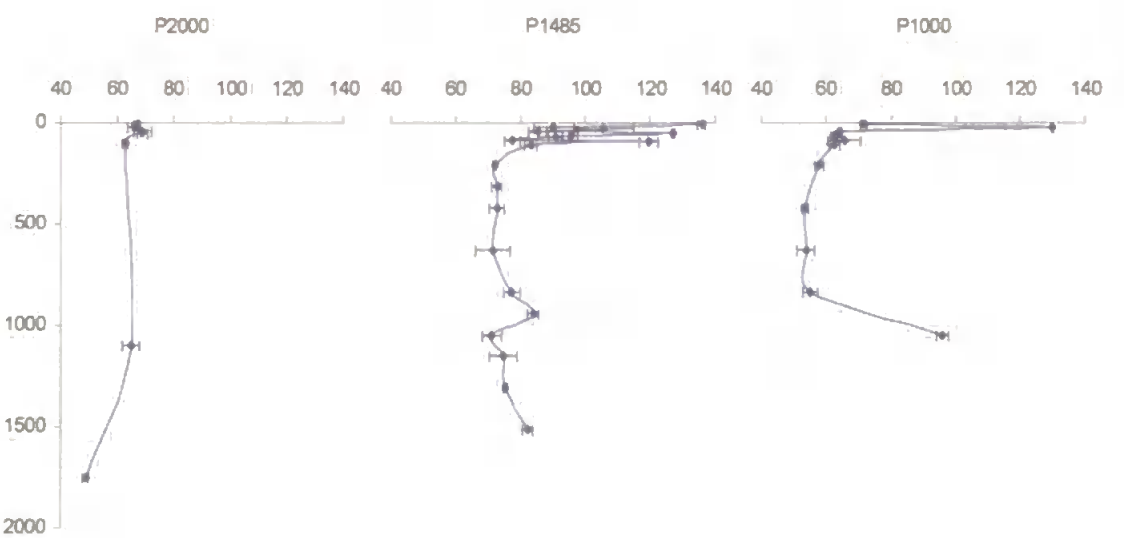

Figure 149. Full vertical profiles of DOC concentrations (µM-C) at BG9919 slope stations P1000, P1485 and P2000. Note: y-axis is depth (m).

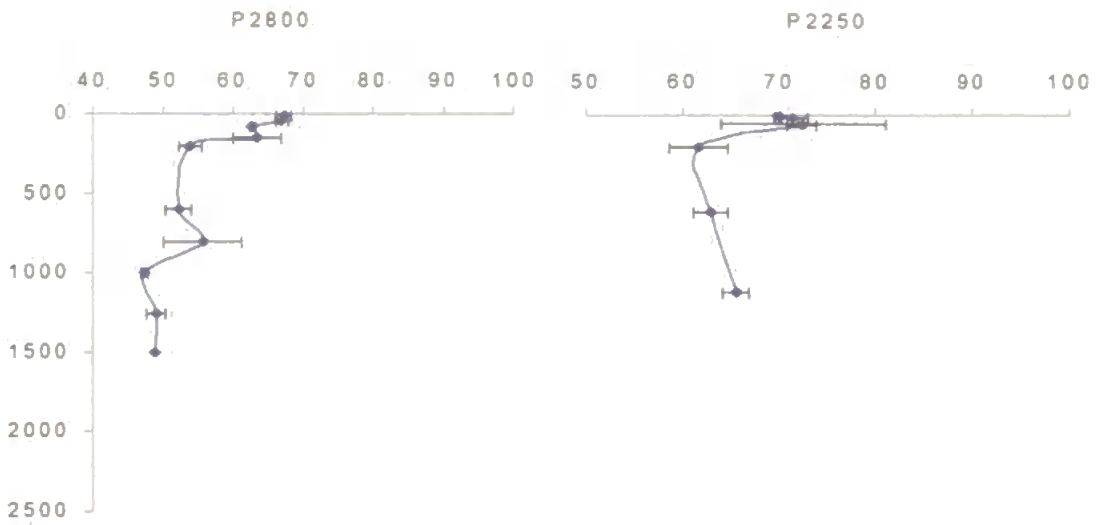

Figure 150. Full vertical profiles of DOC concentrations (µM-C) at BG9919 offshore stations P2250 and P2800. Note: y-axis is depth (m).

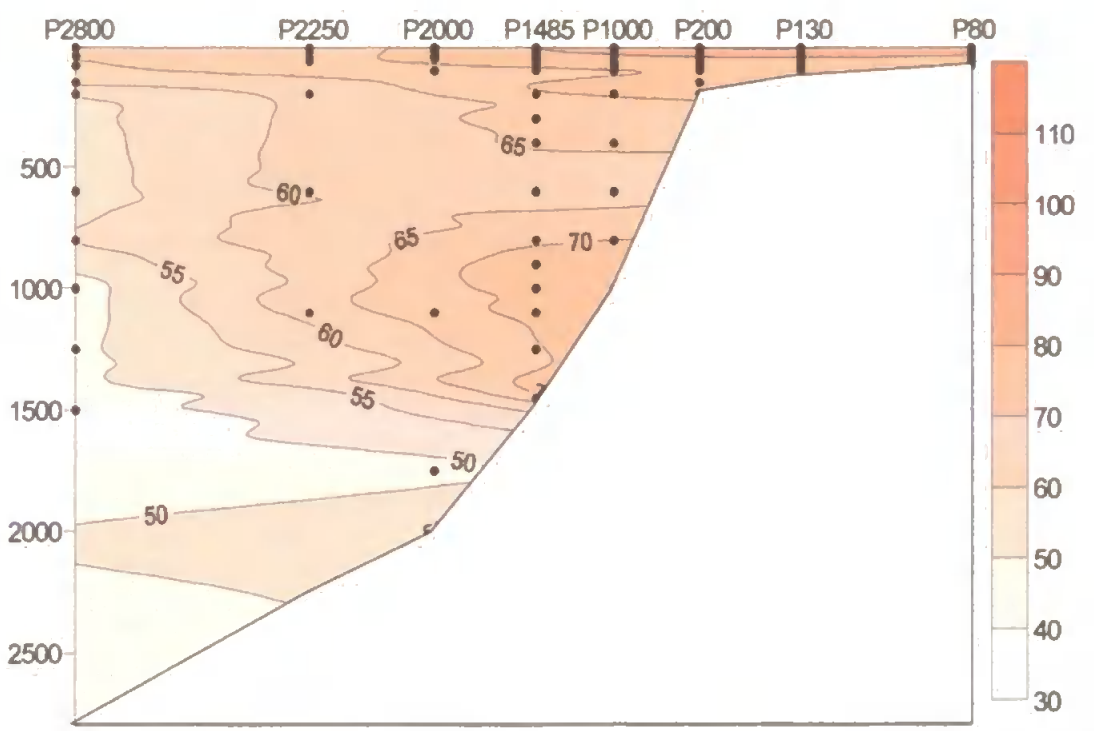

Figure 151. Contour plot of DOC concentrations along BG9919 transect P. Note: colour scale is µM-C; y-axis is depth (m).

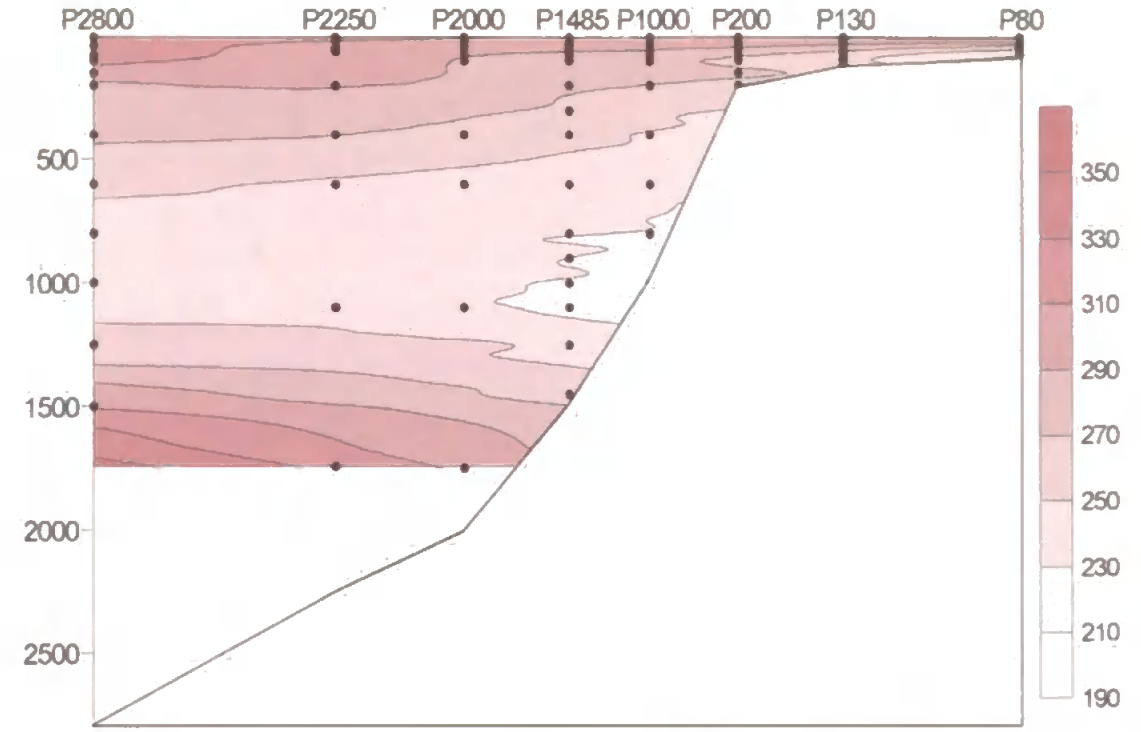

Figure 152. Contour plot of oxygen concentrations along BG9919 transect P. Note: colour scale is µmol kg^{-1}; white areas = no data; y-axis is depth (m).

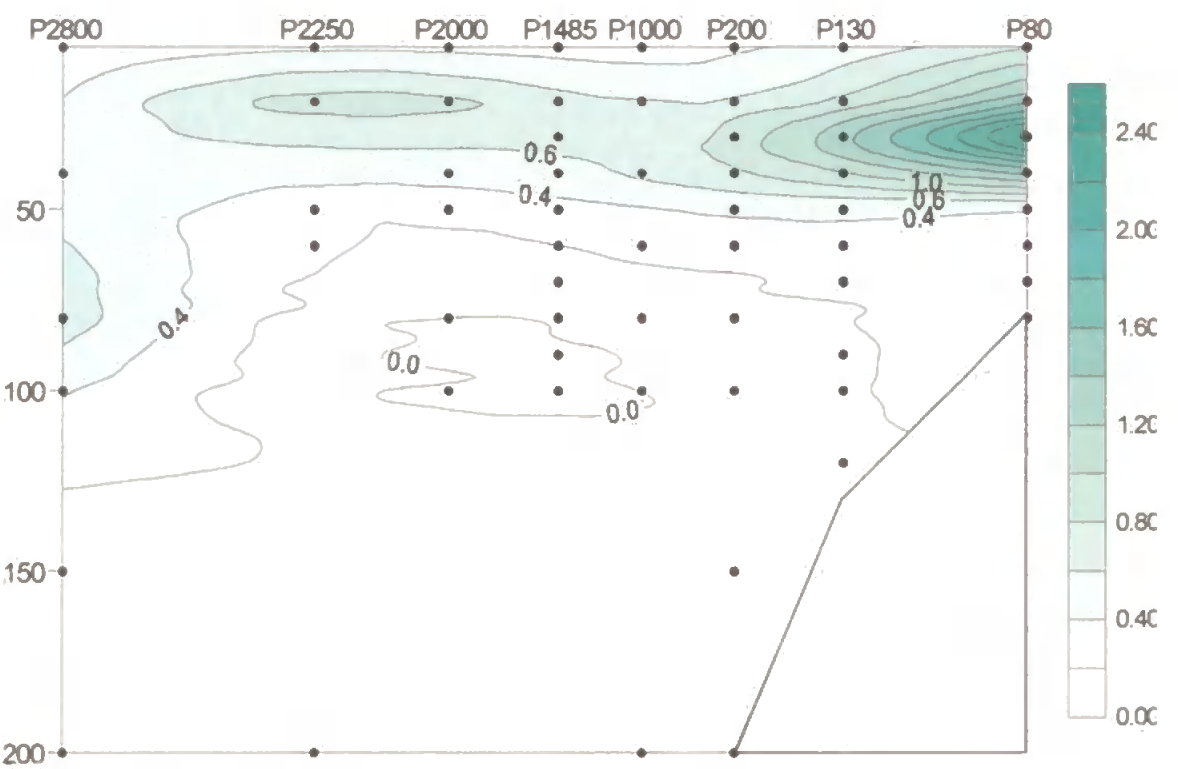

Figure 153. Contour plot of chlorophyll-a concentrations in the upper 200m of BG9919 transect P. Note: colour scale is mg m^{-3}; y-axis is depth (m).

3.5.8 Transect S (42°09'N) Salinity and Temperature

Transect S is located at 42°00'N from the mouth of the Ria de Vigo and offshore. Temperature and salinity measurements along transect S indicate upwelling of colder, more saline waters to the surface near the coast and on the shelf. Temperatures in the upper 200m of transect S ranged from 12 – 20.6°C with warmer waters detected in the top 50m (Figures 154 - 155). Contour lines of the temperature distribution plot (Figure 156) slope upwards on the shelf clearly depicting an upwelling event.

Salinity measurements at the coastal station (S90; Figure 157) show a sharp decrease (i.e. by 0.7) in the top 30m and this indicates that less saline waters were outwelling from the coastal embayment (i.e. Ria de Vigo). Salinity ranged from 35.6 –35.8 in the upper 200m of stations on the shelf and further offshore. A subsurface maximum (~50 - 100m) was observed in stations off the shelf (Figures 157 - 158); this feature and the input of less-saline waters at the coast are clearly depicted in the contour plot of the salinity distribution of transect S (Figure 159).

Full vertical profiles of salinity and temperature at slope and offshore stations (Figure 160) show the characteristic salinity maximum of the MSW at approximately 1000m depth and a decrease of both salinity and temperature in deeper waters. A contour plot of salinity distribution along transect S (Figure 161) shows the subsurface maximum extending to station S2250 and a deeper increase from ~800 – 1200m, with highest salinity on the continental slope.

There were six water masses present at the Iberian margin (transect S) with distinct temperature and salinity characteristics (T - S plot, Figure 162): the LSW (~5°C, ~35), the MSW (~11°C, ~36), the ENACW (~11°C, 35.6), upwelled waters (13 - 15°C, ~35.8), outwelled waters (~18.7°C, ~35), and surface waters offshore (16 - 20°C, ~35.7).

3.5.9 Transect S (42°09'N) Dissolved Organic Matter

Six stations were sampled for DOC measurements along BG9919 transect S (Table 37): a coastal (S90), shelf (S150) and shelf-break (S300) station and three stations further offshore (S1500, S2250 and S2550).

Table 37. Co-ordinates, maximum depth, number of samples and DOC concentrations at BG9919 transect S stations.

Station	CTD	Latitude, N	Longitude, W	Max depth	No. Samples	Range of DOC (μM-C)
S90	11	42°09'N	08°58'W	~90m	8	63 – 147
S150	12	42°09'N	09°08'W	~150m	9	56 – 72
S300	13	42°09'N	09°19'W	~300m	9	63 – 88
S1500	14	42°09'N	09°30'W	~1500m	15	47 – 172
S2250	15	42°09'N	09°44'W	~2250m	11	59 – 95
S2550	16	42°09'N	10°00'W	~2550m	11	54 – 92

DOC concentrations ranged from 47 – 172 μM-C along transect S and surface water concentrations (<100m; mean: 81 μM-C) were significantly higher (ANOVA; $F_{1,57} = 16.615$, $P < 0.001$) than those in deeper waters (mean: 57 μM-C). Coastal and shelf waters generally had a decreasing trend in DOC concentrations with the exception of sub-surface coastal waters (>50m) which exhibited enhanced DOC (i.e. up to 84 μM-C excess; Figure 163). A sub-surface DOC maximum between 50 – 100m was also observed in stations further offshore (i.e. up to 115 μM-C excess; Figure 164). Background DOC in the upper 200m of transect S averaged to approximately 60 μM-C. Deep-water concentrations ranged from 47 – 75 μM-C and exhibited a homogeneous distribution (Figure 165). The contour plot of DOC distribution across the margin at transect S shows surface enhancement of DOC and a deepening of this with distance from the shelf break towards offshore waters (Figure 166). Extensive deep-water accumulation of DOC in the contour plot is most likely an artefact of the *Surfer®* programme since the vertical profiles did not exhibit DOC enhancement to such a spatial extent. However, there was evidence of DOC increase in deeper waters at stations S1500, S2250, S2550 (Figure 165).

3.5.10 Transect S (42°09'N) Summary

- DOC concentrations were enhanced in surface waters along transect S of the BG9919 sampling campaign with a subsurface maximum extending from the shelf break to offshore waters.
- Deeper waters had lower DOC concentrations and exhibited a homogeneous DOC distribution with the exception of a single sampling point at station S2250 (1700m depth) which had a higher DOC concentration.

Chlorophyll-a measurements along transect S (Figure 167) suggest enhanced phytoplankton biomass near the coast and a deepening of this biomass further offshore. This reflects the DOM subsurface distribution across the margin. Overall, in surface waters along transect S (<100m), DOC correlated strongly with POC and particulate nitrogen (PN) concentrations (0.80; n = 6; P<0.001; Figure 33 in Appendix 4 and 0.86; n = 6; P<0.001; Figure 34 in Appendix 4, respectively) whereas in deeper waters, DOC correlated well with inorganic nutrients (-0.83; n = 9; P<0.001; Figure 35 in Appendix 4). This might suggest that in surface waters where biomass was higher there was enhanced DOC production from source mechanisms such as PER, cell lysis, "sloppy-feeding" and POM to DOM transformation. The negative correlation between DOC and inorganic nutrients in deeper waters was probably due to organic matter being consumed by bacteria and remineralised to inorganic nutrients.

The enhanced DOC observed in bottom waters at station S2250 cannot be explained with certainty. It may reflect the presence of a nepheloid layer within which DOM may be enhanced. However, there is no POC data to actually confirm this. Random contamination is another possibility, but there are not enough data points in that region to confirm oceanographic consistency.

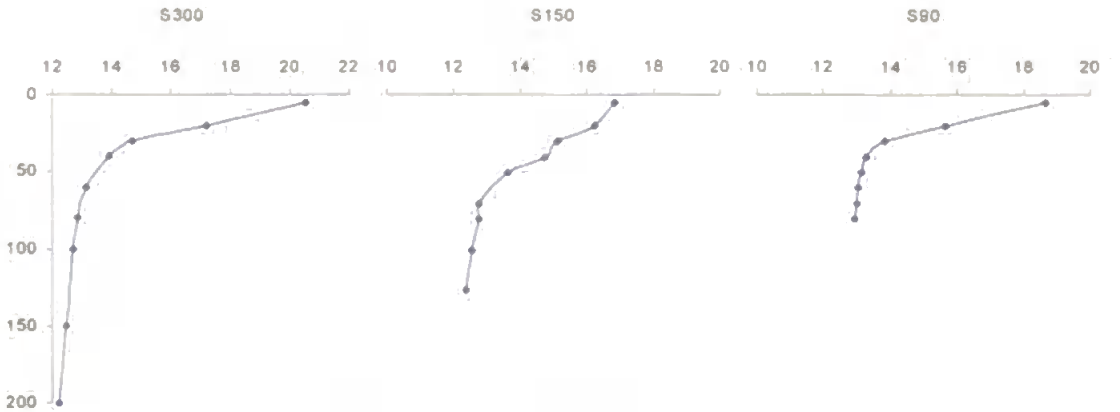

Figure 154. Vertical profiles of temperature (°C) at BG9919 coastal, shelf and shelf-break stations S90, S150 and S300. Note: y-axis is depth (m).

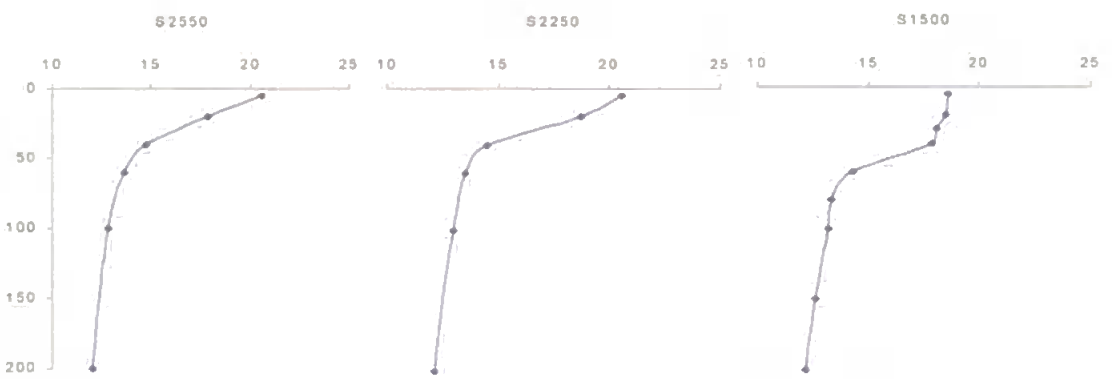

Figure 155. Vertical profiles of temperature (°C) in the upper 200m of BG9919 slope and offshore stations S1500, S2250 and S2550. Note: y-axis is depth (m).

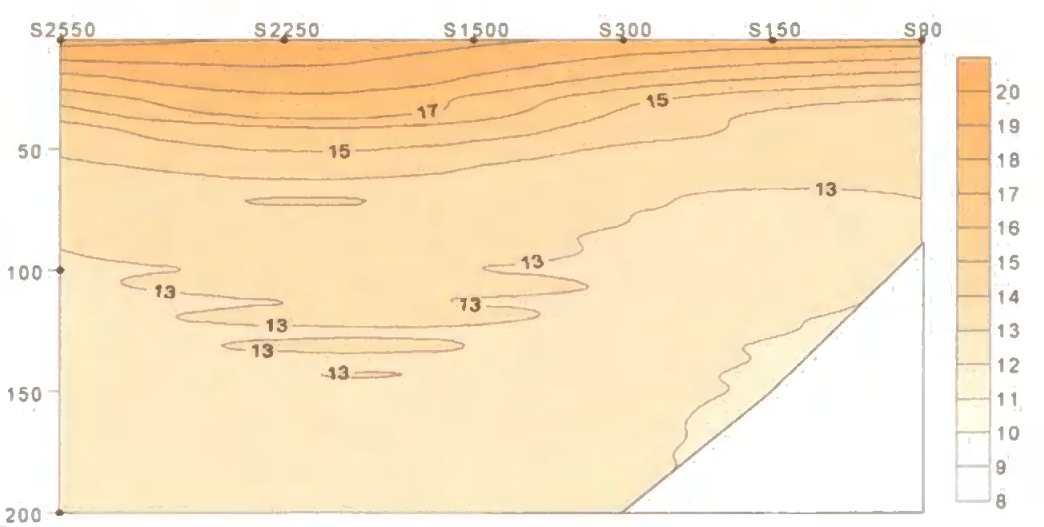

Figure 156. Contour plot of temperature in the upper 200m of BG9919 transect S. Note: colour scale is °C; y-axis is depth (m).

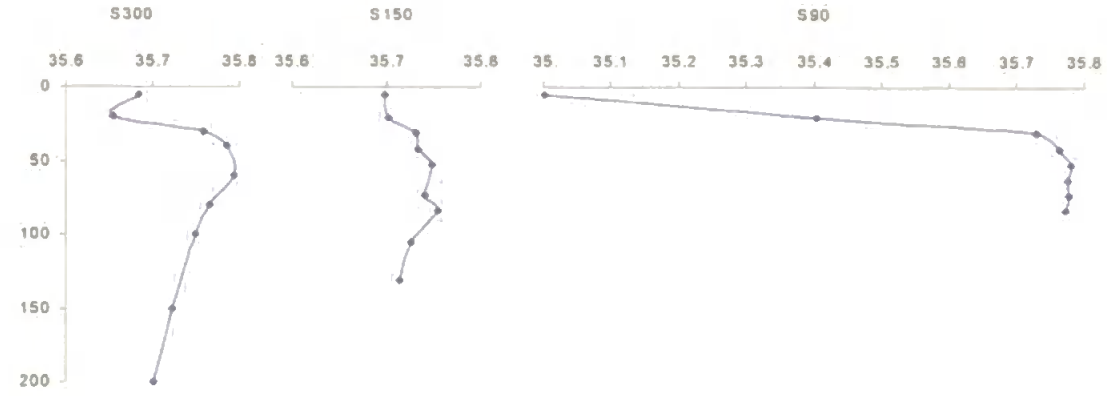

Figure 157. Vertical profiles of salinity at BG9919 coastal, shelf and shelf-break stations S90, S150 and S300. Note: y-axis is depth (m).

Figure 158. Vertical profiles of salinity in the upper 200m of BG9919 slope and offshore stations S1500, S2250 and S2550. Note: y-axis is depth (m).

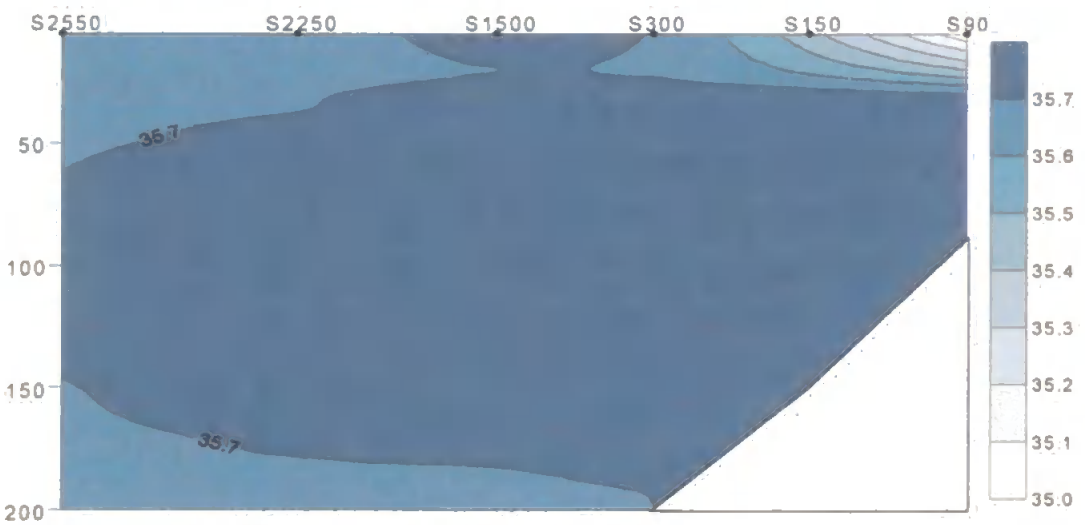

Figure 159. Contour plot of salinity in the upper 200m of BG9919 transect S. Note: colour scale is in arbitrary units; y-axis is depth (m).

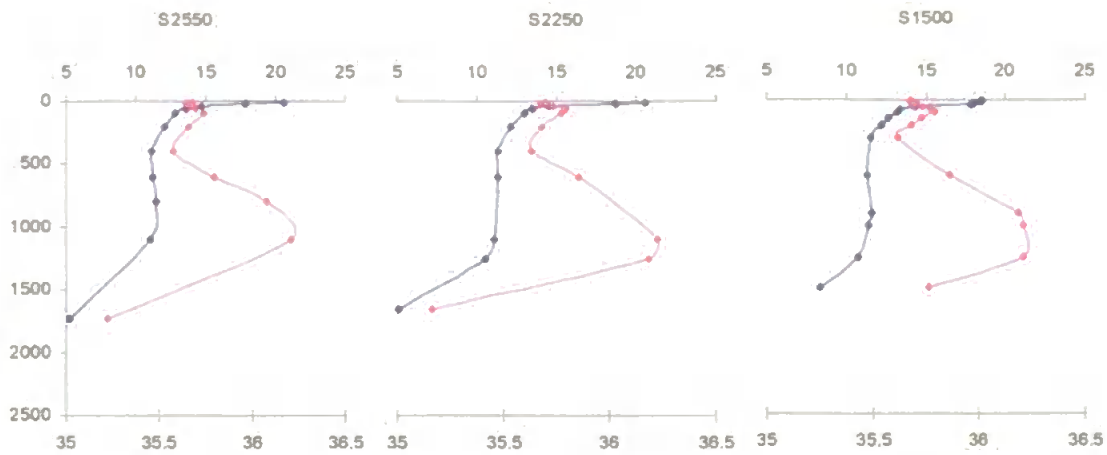

Figure 160. Vertical profiles of salinity and temperature (°C) in BG9919 stations S1500, S2250 and S2550. Note: ♦ – temperature, ■ – salinity; y-axis is depth (m).

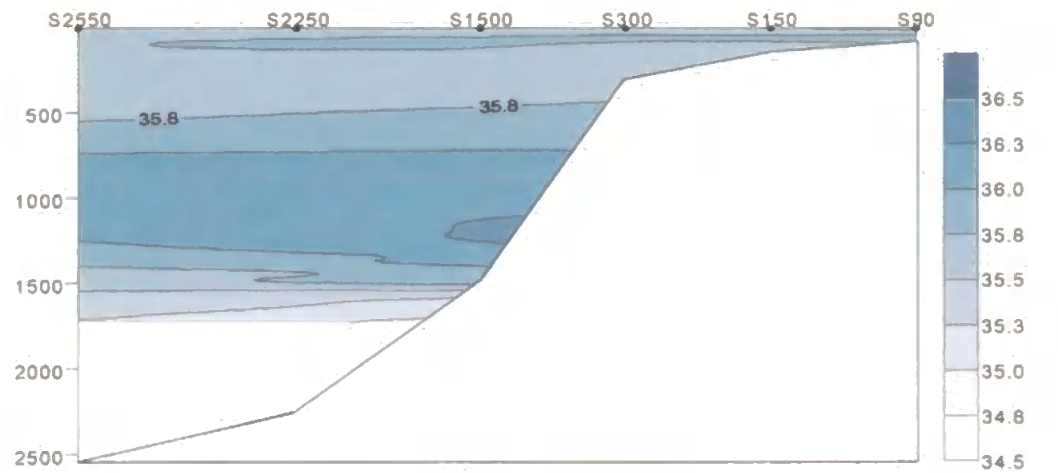

Figure 161. Contour plot of salinity along BG9919 transect S. Note: white areas = no data; y-axis is depth (m).

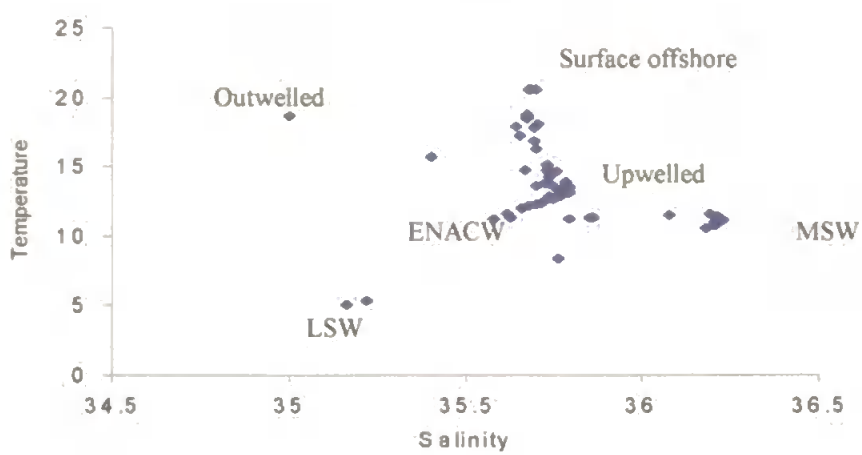

Figure 162. T - S plot of the water column along BG9919 transect S.

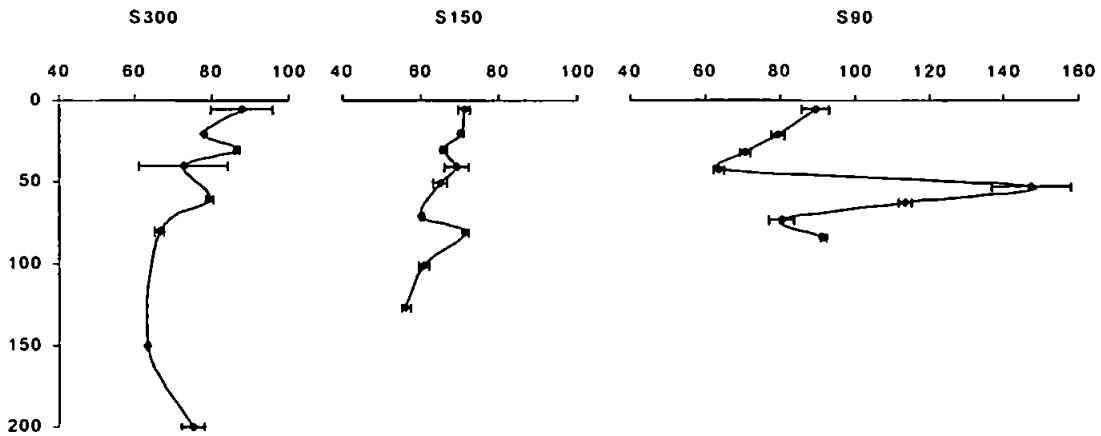

Figure 163. Vertical profiles of DOC concentrations (μM-C) at BG9919 stations S90, S150 and S300. Note: y-axis is depth (m).

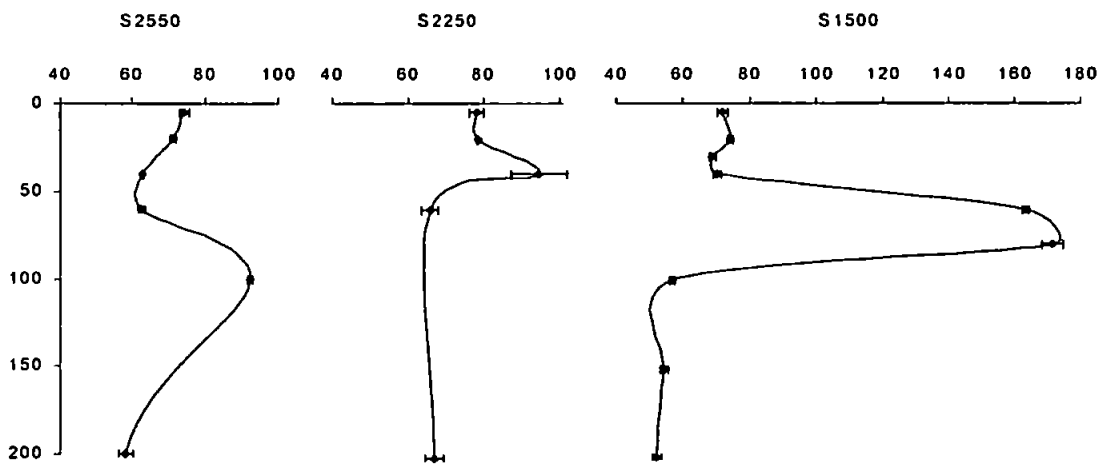

Figure 164. Vertical profiles of DOC concentrations (μM-C) in the upper 200m of BG9919 slope and offshore stations S1500, S2250 and S2550. Note: y-axis is depth (m).

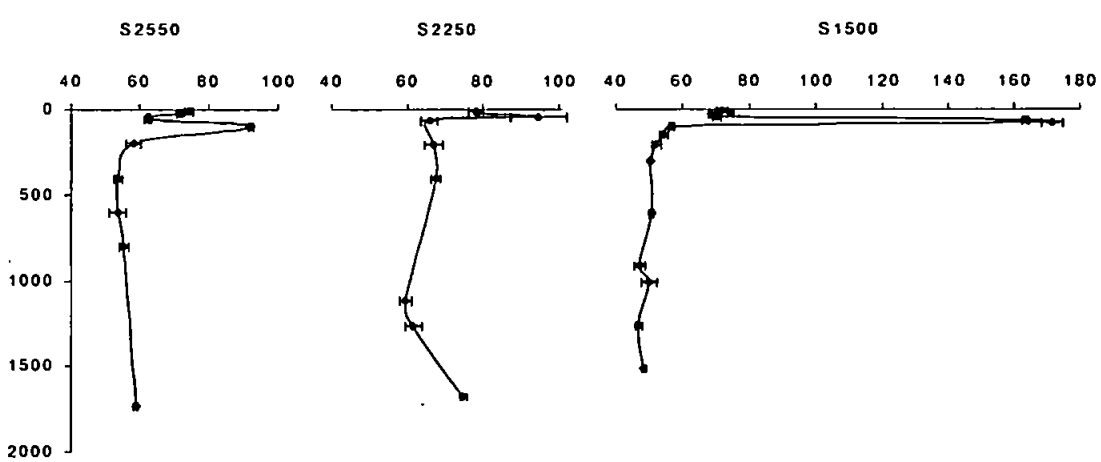

Figure 165. Full vertical profiles of DOC concentrations (μM-C) at BG9919 slope and offshore stations S1500, S2250 and S2550. Note: y-axis is depth (m).

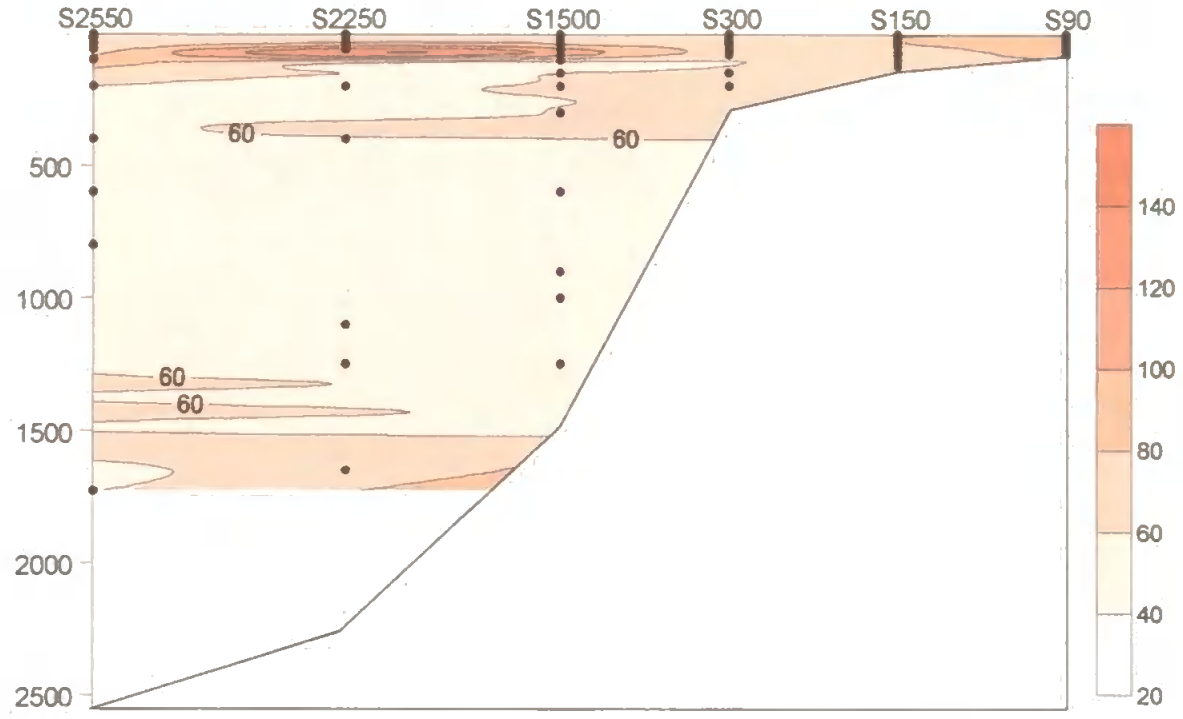

Figure 166. Contour plot of DOC concentrations along BG9919 transect S. Note: colour scale is µM-C; blank areas = no data; y-axis is depth (m).

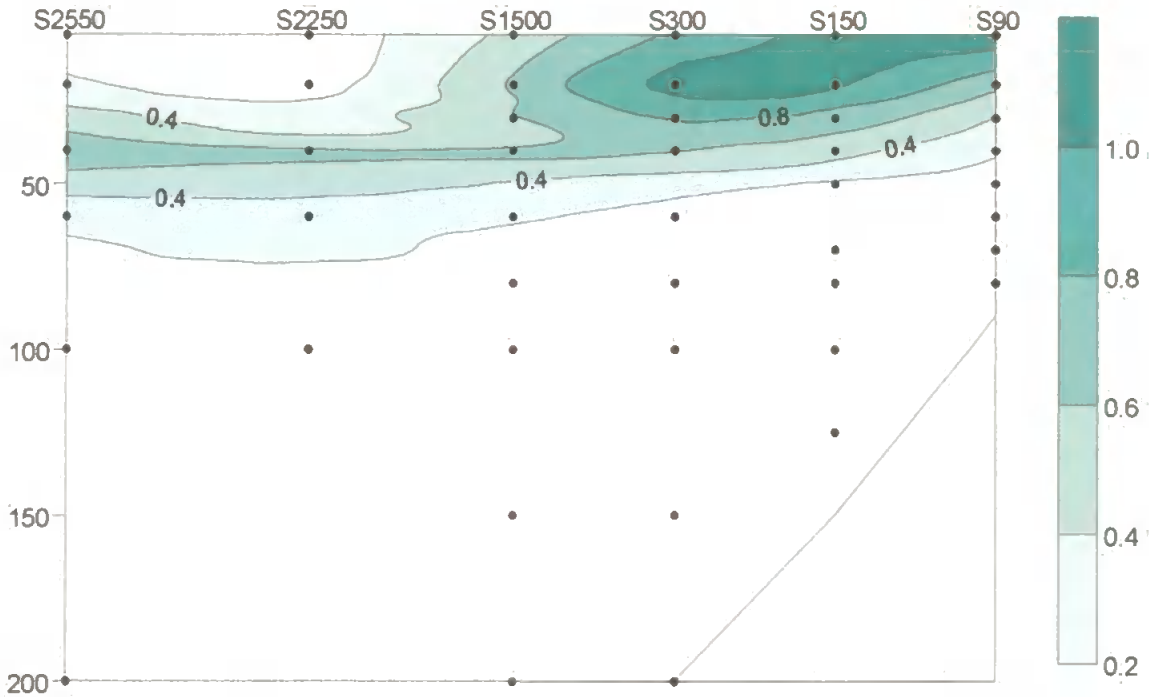

Figure 167. Contour plot of chlorophyll-a concentrations in the upper 200m of BG9919 transect S. Note: colour scale is mg m^{-3}; y-axis is depth (m).

3.6 Cross-slope trends

The following section describes the upper ocean integrated and mean DOC concentrations across the Iberian margin. To determine whether there were any systematic trends between shelf, slope and offshore stations during each sampling cruise line-column graphs were plotted and statistically significant differences on a spatial and seasonal scale were determined using ANOVA tests. Integrated DOC in the upper 100m were used as normalised DOC standing stocks in the surface water column and to compare with literature (Table 7 in section 1.9).

3.6.1 Surface-water integrated DOC

There were no discernible trends in the upper 100m of CD110B transect P across the Iberian margin (Figure 168) and no statistically significant difference between shelf stations (P100 and P200) and slope and offshore stations (P1000 and P2800). This may be indicative of similar net production and removal rates along transect P during the winter season.

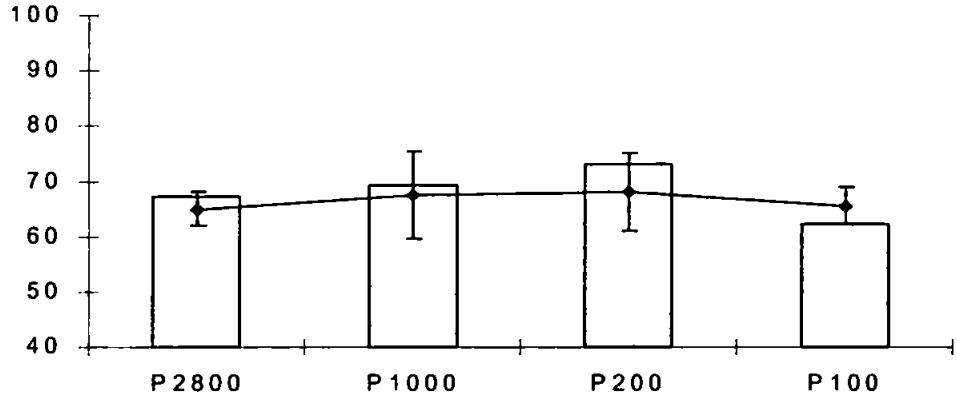

Figure 168. Integrated ($x10^{-1}$ mol-C m^{-2}) and mean DOC (μM-C) in the upper100m of CD110B transect P. Note: solid bars – integrated DOC; line – mean DOC.

Relatively large differences in surface integrated DOC were detected across the margin during cruise OMEX0898 (Figure 169). Coastal and shelf stations along transects N and S had generally lower integrated DOC than those offshore, although there were no statistically significant differences between shelf (i.e. maximum depth up to ~200m), slope (i.e. ~200 - 1900m) and offshore stations (i.e. maximum depth over ~2000m). The lower DOM concentrations observed near the coast/shelf region may reflect concentrations in the recently upwelled ENACW.

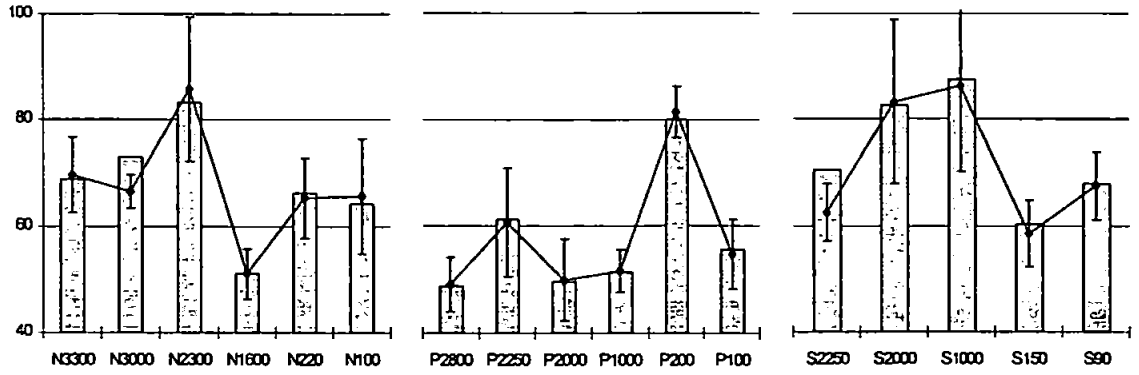

Figure 169. Integrated ($x10^{-1}$ mol-C m^{-2}) and mean DOC (μM-C) in the upper 100m of OMEX0898 transects N, P and S. Note: solid bars – integrated DOC; line – mean DOC.

Current velocity and direction measurements during the summer season show a net onshore trend in surface waters of the Iberian margin (42-43°N; Huthnance et al., in press.). Thus, it is not possible to ascertain whether DOC was being exported offshore with the upwelled waters; DOC sampling was not performed in an upwelling filament. However, cross-slope concentrations and complementary data suggest that DOC was being recycled relatively rapidly in coastal and shelf waters and being incorporated into biomass that was transported offshore with the progressive displacement from upwelled waters. DOM was probably being released in offshore waters possibly *via* bacterial enzymatic attack and dissolution of biomass, but this dissolved material was not subsequently remineralised. It is suggested that bacteria residing on aggregates solubilise particulate material faster than they take up the dissolved material (Vetter et al., 1998; Kiorboe and Jackson, 2001).

During cruise M43/2 (winter 1999), slope stations of transect S had statistically significant higher integrated DOC than coastal/shelf (ANOVA; $F_{1,5} = 10.7$, $P = 0.05$) and offshore stations (ANOVA; $F_{1,6} = 19.3$, $P = 0.01$). There were no significant differences between coastal/shelf and offshore stations (Figure 170). This suggests that the poleward current may have been a lateral source of DOC to the Iberian margin; with an estimated current velocity of ~0.15 m s^{-1} it would take approximately 12 minutes for the poleward current to travel 1° northwards along the Iberian margin. This is a dynamic lateral input to the Iberian margin and its rate may equal the rate of biological activity there.

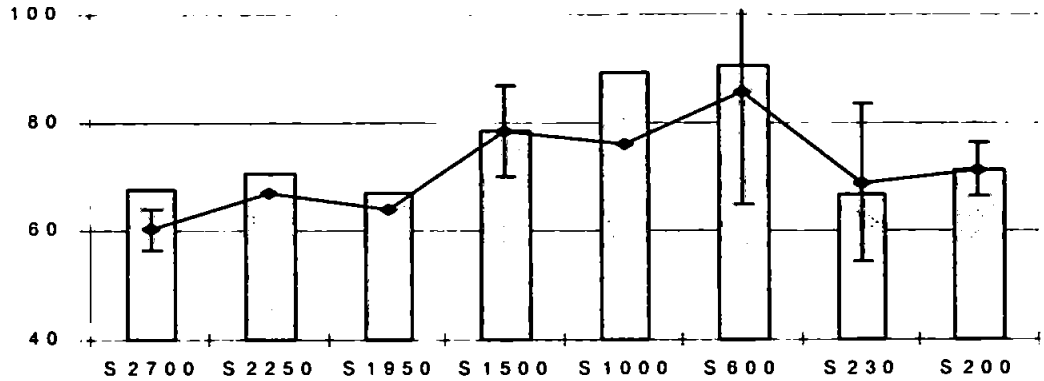

Figure 170. Integrated ($x10^{-1}$ mol-C m^{-2}) and mean DOC (μM-C) in the upper 100m of M43/2 transect S. Note: solid bars – integrated DOC; line – mean DOC.

No statistically significant differences were found between integrated DOC concentrations at shelf, slope and offshore stations of transects sampled during cruise BG9919. However, slope stations at transects P and S exhibited higher integrated DOC (Figure 171). The results from cruise BG9919 typically showed lower integrated DOC at coastal and shelf stations compared to slope and offshore stations. These findings were similar to those observed during summer cruise OMEX0898. During the summer season when characteristic upwelling occurs, ENACW from ~150m can upwell (current velocity: ~0.1 m s^{-1}; Huthnance et al., in press) to the surface along the Iberian coast within ~50 minutes. Continuous upwelling ensures that integrated DOC values at the coastal and shelf area do not typically exceed ~7 mol-C m^{-2}. Further offshore, biological activity seems to favour the net accumulation of DOC (e.g. production rates of DOC exceed removal rates).

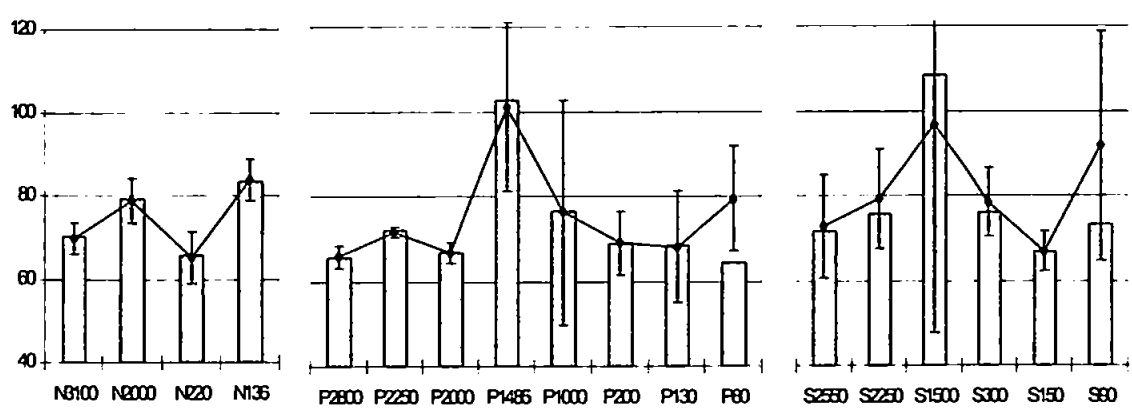

Figure 171. Integrated DOC ($x10^{-1}$ mol-C m^{-2}) in the upper 100m of BG9919 transects N, P and S. Note: solid bars – integrated DOC; line – mean DOC.

The range of mean DOC concentrations in surface waters across the Iberian margin (i.e. ~50 – 100μM-C) agrees well with other reported values in ocean margin areas (Table 7 section 1.9). In particular, previous measurements of DOC in the NW Atlantic ranged between 48 - >100μM-C (Doval et al., 1997 and 1998; Dafner et al., 1999). In addition, total DOC standing stocks ranged from 5 - 10 mol-C m^{-2}. These values compare well to those of Carlson et al. (1994) in their study of DOC in the north-western Sargasso Sea (~6 – 7 mol-C m^{-2}).

3.6.2 Seasonal and Spatial Comparisons of Integrated DOC

ANOVA tests were performed on integrated DOC results from each transect to compare overall concentrations between different seasons (Table 38). There were no statistically significant differences between seasons with the exception of transect P during the summer cruises. Integrated DOC in surface-waters of OMEX0898 (August 1998) transect P was significantly lower ($F_{2,6} = 5.08$; $P = 0.05$) than that measured during cruise BG9919 (September 1999).

Table 38. Results from seasonal comparisons (ANOVA) of integrated DOC.

Transect	Depth	Seasons*	n	P	F-crit	F	Result
N	0 – 100m	Summer98 vs. Summer99	4	0.65	5.99	0.23	NSD
P	0 – 100m	Winter98 vs. Summer98	4	0.28	5.99	1.42	NSD
P	0 – 100m	Winter98 vs. Summer99	4	0.84	5.99	0.04	NSD
P	0 – 100m	Summer98 vs. Summer99	6	0.05	4.96	5.08	SD
S	0 – 100m	Winter98 vs. Summer98	4	0.95	5.99	0.004	NSD
S	0 – 100m	Winter98 vs. Summer99	5	0.29	5.32	1.3	NSD
S	0 – 100m	Summer98 vs. Summer99	5	0.57	5.32	0.36	NSD

*Note: winter98 – CD110B; summer98 – OMEX0898; winter99 – M43/2; summer – BG9919; NSD – no significant difference, SD – significant difference.

Spatial comparisons (ANOVA) were performed to determine any north to south difference or trend during each cruise. Transects N, P and S were all sampled only during the summer surveys (i.e. OMEX0898 and BG9919). No significant differences were observed between

transects during either cruise with the exception of OMEX0898 transects S and P. Integrated DOC of surface waters along transect S were statistically significantly higher than those along transect P ($F_{1,6}$ = 42.4, P = 0.001). Table 39 shows a summary of the ANOVA results although individual transects were compared within each cruise.

Table 39. Results from spatial comparisons (ANOVA) of integrated DOC

Seasons	Depths	Transects	Mean Integrated DOC ($x10^{-1}$ mol-C m^{-2})	n	P	Result
Summer98	<100m	N - P - S	68 - 58 - 75	6	0.09	NSD
Summer99	<100m	N - P - S	75 - 73 - 80	8	0.67	NSD

The above comparisons show that transect P during the OMEX0898 had comparatively lower DOC concentrations. Primary productivity and chlorophyll-a at OMEX0898 transect P decreased with distance offshore at a relatively faster rate than at other transects. The coastal/shelf station of OMEX0898 transect P exhibited higher levels of chlorophyll-a (up to ~5 mg m^{-3}) compared to those at OMEX0898 transect S and BG9919 transect P (e.g. ~3 mg m^{-3} at station BG9919 P80). However, at slope and offshore stations OMEX0898 transect P had lower chlorophyll-a concentrations (<0.6 mg m^{-3}) compared to other transects (typically < 1 mg m^{-3}). This suggests that primary producers at OMEX0898 transect P did not extend across the margin into surface oceanic waters, thus possibly reducing the production of DOC offshore.

3.7 A DOC budget for the Iberian ocean margin

DOC concentrations were higher in the photic zone compared to offshore deep waters. They generally decreased with increasing depth and distance from the continental shelf due to an increasing distance from areas of higher biological activity (Joint et al., 2001). DON distributions followed a similar pattern of surface enhancement and depletion at depth (Figure 172). Station N1600 sampled during OMEX0898 depicts a typical vertical profile of the dissolved nitrogen and DOC pools at the Iberian margin. In the more biologically productive surface waters (i.e. <100m), the larger proportion of TDN was organic; this decreased with increasing depth. However, there were localised areas of enhanced DOM production and accumulation in surface shelf-edge/slope and in deep waters. Such areas may have resulted due to several factors (e.g. particle dissolution, pore-water diffusion); these were discussed within the context of the results (see sections 3.1 – 3.5).

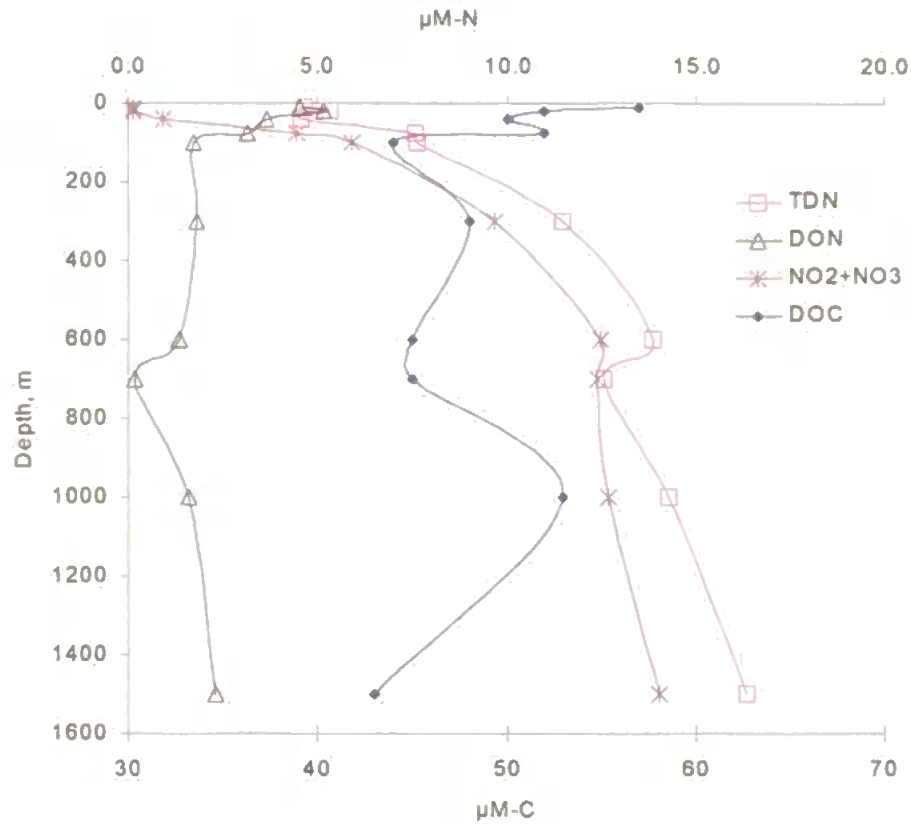

Figure 172. Vertical profiles of dissolved organic carbon and dissolved nitrogen species (µM) at OMEX0898 station N1600. Note: TDN – total dissolved nitrogen, DON – dissolved organic nitrogen, NO_2+NO_3 –nitrite and nitrate, DOC – dissolved organic carbon.

A general DOC budget was constructed for three main areas across the slope (Figure 173) by calculating the excess mean DOC above that found in deep waters (i.e. ~51µM-C); deep water concentrations presumably represent the refractory pool of DOC (Sharp, 1997). A cross-slope section of the Iberian margin was divided into three key areas: the upper 200m across the continental margin, deeper waters over 200m depth and the MSOW region on the continental slope between 650 – 1450m depth. The compartments were chosen to partition the more biologically active surface region (<200m) of the water column and the MSOW from deeper offshore and slope waters. The compartments should be sufficiently large to give confidence in the calculations of the means (Huthnance et al., in press). The amount of excess DOC in the upper 200m of the Iberian margin (~14 – 25µM-C) compared to that measured in deep waters represented the semi-labile and labile fractions of the DOC pool (i.e. ~22 – 33%) that had accumulated due to the production/input of DOC exceeding removal rates. The MSOW contained higher average DOC concentrations than deep offshore waters with an excess of up to ~20µM-C. This is a significant amount of DOC accumulated in deep waters and its transport

may potentially fuel bacterial production elsewhere. During 1999, mean excess DOC concentrations were higher than those in 1998 suggesting that lateral inputs of DOC to the NW Iberian margin had increased. Alternatively, the DOC produced during winter 1999 (i.e. combined upwelling and poleward current events) had not been remineralised during the spring season.

DOC was not measured in an upwelling filament so it was not possible to calculate any associated DOC export. However, a Lagrangian experiment tracking a filament was performed by other OMEX II – II partners and their results were recently published in a special issue of Progress in Oceanography (2001) vol. 51. DOC measurements in this study agree well with those of Alvarez-Salgado et al. (2001) made in coastal/shelf and filament waters at the Iberian margin during August 1998 (i.e. refractory DOC estimated as 57μM-C with 20μM-C excess representing semi-labile and labile DOC).

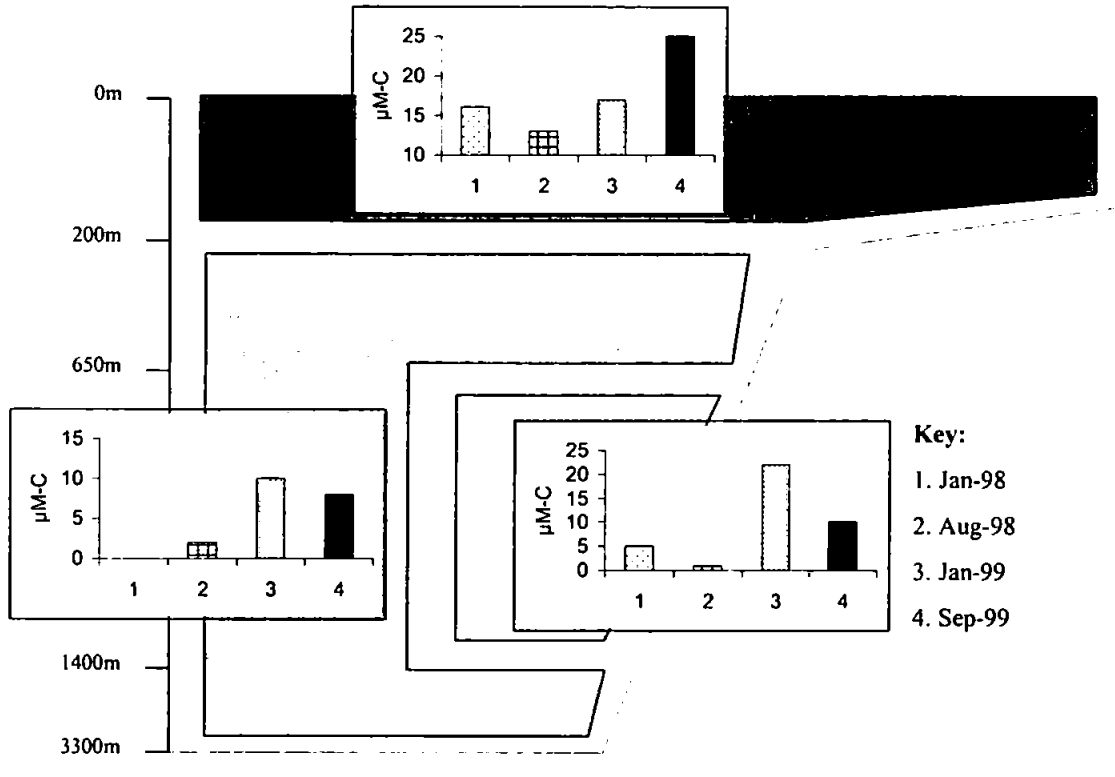

Figure 173. Schematic of the Iberian margin cross-section with seasonal average excess DOC concentrations.

If concentrations in each defined region are described in relation to seasonal hydrography [25] (Figure 174), one could suggest that during the winter, the poleward current and its biogeochemistry bring in approximately 15μM-C of excess DOC (i.e. over deep offshore concentrations). At the coast where there is increased input of terrestrial waters, an excess 11μM-C is produced and accumulated; this is a similar amount to that found in surface offshore waters throughout the year. During the summer, a mean excess of 16μM-C is produced and accumulated on the shelf. In deep waters, the presence of the MSOW may result in a small mean excess of DOC on the continental slope (i.e. ~2μM-C).

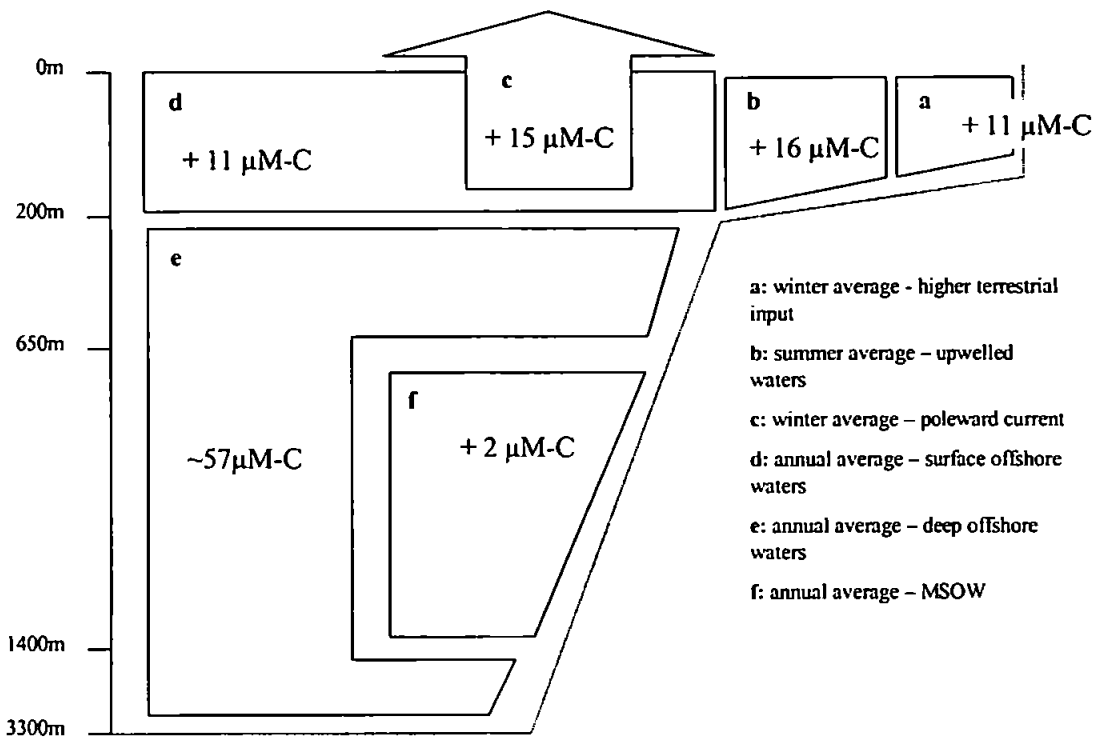

Figure 174. Schematic of the Iberian cross-margin with average excess DOC concentrations (+μM-C) in key regions/water masses.

[25] The upper 200m box was further partitioned to reflect mean concentrations in shelf (winter and summer values), slope (winter values) and offshore areas (annual values).

Chapter 4

4. CONCLUSIONS AND FUTURE STUDIES

Precise and accurate measurements of DOM at the upwelling region of the Iberian ocean margin (NE Atlantic Ocean) have been presented. Extensive spatial and seasonal coverage of the Iberian ocean margin ensured the characterisation of the distribution of DOM during contrasting hydrographic and seasonal regimes. Key biogeochemical processes driving the cycling of DOM were identified and, where possible, quantified to assess the contribution of DOM to organic carbon export to offshore deep oceanic waters.

4.1 Assessment of the analytical methodology

The measurement of dissolved organic carbon and dissolved organic nitrogen in aquatic environments is now performed with increased precision and accuracy as a result of the critical evaluation of analytical problems encountered and resolved within the last decade. It has been proposed that the analytical precision necessary to identify small-scale changes in the DOM pool should be <2% (Carlson et al., 1994). This goal was achieved in this study with the use of a hybrid HTC system developed by Alvarez-Salgado and Miller (1998). The handling and sampling methodologies were adopted following recommendations in peer-reviewed papers by the international analytical community and critically evaluated by undertaking several investigations on the performance of the technique at different stages (Chapter 2).

4.1.1 Conclusions

Investigations to evaluate the analytical performance of the methodologies and HTC techniques employed in this study have resulted in several conclusions:

- Rigorous washing and rinsing of sampling apparatus is essential for the clean and representative collection of seawater samples. The procedures adopted in this study were evaluated and found to be satisfactory.
- The use of the positive-pressure all-glass filtration system resulted in the efficient filtration of samples. The closed-system filtration unit ensured that there was no contamination from atmospheric sources on-board ship.
- Glass fibre filters were used throughout this study and it is calculated that the bacterial fraction that may have passed through the filter matrix was "lost" in the standard error of the analyses (i.e. <1 μM-C). Alternatively, Anopore filters may be suitable for filtration of

oceanic waters but are not suitable for highly turbid waters as they are rapidly saturated with the particles.

- High purity acid was used to convert the inorganic carbon content of the sample to purgeable CO_2 and to arrest any biological activity during storage of samples. The amount of acid used did not result in contamination and the decarbonation procedure (i.e. approximately 20 minutes purging with high-purity oxygen gas) effectively removed all inorganic carbon from the sample.
- A major challenge in the analytical determination of DOC using an Al/Pt catalyst column is the accurate determination of the system blank. In the current study, two methods of accurately determining the system blank were identified and were compared giving similar results.
- The use of 'mock' certified reference materials provided by an international CRM programme aided the monitoring of the analytical system's daily performance and provided an external inter-calibration between laboratories. In this study, CRM data agreed well with the certified concentrations indicating that the analytical system employed consistently produced data of a high quality.
- Intercomparison exercises performed between the analytical system adopted in the current study and of other laboratories produced similar results for DOC and TDN measurements.

4.1.2 Future studies

When adopting a new technique, it is essential that the analyst follows recommendations from previously published studies and performs a critical evaluation of the different stages of the analytical methodology to identify and remove artefacts. With increasing experience and a systematic approach to evaluation criteria for the methodology employed, the analyst may then develop and improve the technique used.

In any future studies, several precautionary measures must be taken to ensure a consistently high performance. These include:

- Performing tests on the cleaning procedures of the apparatus used to reduce contamination artefacts. Replicate sampling is a precautionary measure against loss of samples due to damage and/or contamination, and can be used to check the reproducibility of sampling.
- Running daily performance checks and ensuring that the analytical system is maintained in pristine condition. This will ensure that the system is used properly and that any problems are identified in time.
- Running percentage recovery tests on KHP and glycine standards and using CRMs to determine the oxidation efficiency of the catalyst used. A suite of compounds with varying

refractivity would allow a more rigorous evaluation of the analytical system's accuracy in this study. A "Recommended Protocol for the Measurement of DOC" is being developed and will be accessible *via* the HTCO website (www.pml.ac.uk/gs/htco.asp).

4.2 The biogeochemical cycling of DOC at the Iberian margin

This study was part of the EU MAST OMEX II - II programme investigating the marine carbon cycle in the upwelling system of the Iberian ocean margin. Work reported here benefited greatly from the use of supplementary hydrological and biological data from other project partners. The spatial and temporal coverage of the OMEX II - II area was extensive and covered approximately 150km across the continental shelf/slope between 41 – 42°N. This area is unique for its steep bathymetry and is characteristic of dynamic seasonal hydrographic phenomena. During the summer when northerly winds predominate, upwelling of deeper water occurs along the north-west coastline of the Iberian peninsula; this is associated with offshore-travelling filaments and eddies. In contrast, during the winter, southerly winds force surface waters into the embayments lining the coast called the Rias Baixas. Any off-shelf transport is restricted due to a poleward surface current of subtropical origin travelling over the continental slope. In deeper waters, the most prominent feature was the presence of the more saline Mediterranean Sea Outflow Water (MSOW) between ~650 – 1450m (Huthance et al., in press) travelling northwards on the slope.

The above features form the underpinning hydrography for the cycling of organic material at the Iberian ocean margin. The upwelling of deeper waters to the photic zone ensures a supply of new nutrients for primary production and hence biomass. This biomass is associated with high bacterial production (Barbosa et al., 2001) and other heterotrophic organisms (Joint et al., 2001) continuously grazing and consuming organic matter. As surface waters are pushed further off the shelf with increasing duration of upwelling events, organic material is also transported offshore. To assess the export potential of DOM at the Iberian margin, the following question must be asked: How much excess DOC is produced in the photic zone as a result of upwelling events and what is its fate? The approach taken in this study was to establish the distribution of DOC at the Iberian margin on a spatial and seasonal scale and to identify the main processes (hydrographic and/or biological) influencing these distributions.

Previous studies of DOM distribution in marine environments have established that i) DOC concentrations in coastal waters are typically higher than those measured in offshore and oligotrophic waters; ii) DOC vertical profiles in the open ocean exhibit a concentration gradient in surface waters and a typically homogeneous distribution of minimum concentrations in

deeper waters; and iii) DOC concentrations during the more productive summer season are significantly higher than winter values (Miller, 1996 and references therein).

4.2.1 Conclusions

The upwelling region of the Iberian margin although highly productive, is considered to be a relatively small exporter of particulate material to offshore waters (Slagstad and Wassmann, 2001). This may be due to an observed net onshore velocity component during both winter and summer seasons (Huthnance et al., in press). Therefore, although upwelling filaments can create conditions by which organic material, both particulate and dissolved, may be exported to offshore waters (Alvarez-Salgado et al., 2001), extensive transport of DOC across the margin is not expected. In addition, intra-seasonal and inter-annual variability in the cycling of water masses was observed between 1998 and 1999, and this likely resulted in different trophic webs in the Iberian margin affecting the quality and quantity of organic matter produced (Joint and Wassmann, 2001).

Although DOC distributions generally followed the expected pattern of decreasing concentration with increasing distance from the coast and with depth, there were localised areas of enhanced concentrations in slope waters and in deeper waters. Furthermore, there was no marked difference in DOC concentrations between the summer and winter periods. The main findings in relation to the biogeochemical cycling of DOC at the Iberian margin are thus defined in terms of key regions of the Iberian margin and hydrographic phenomena observed during the sampling campaigns:

Terrestrial run-off:

The influx of waters from the Rias to the shelf had a relatively small effect on DOC concentrations. The labile fraction of the DOM pool in Ria waters was recycled at the coast where bacterial activity was higher (Barbosa et al., 2001), before it could be exported to the shelf. Some C-rich DOM from the Rias reached the shelf and accumulated there. During the winter, the poleward current precluded any shelf-edge exchange of DOM.

Poleward current:

The winter poleward surface current travelling over the slope of the Iberian margin is a relatively large lateral input of DOC to the NE Atlantic Ocean. It carries semi-labile and labile DOC that has accumulated in this low inorganic-nutrient water mass probably due to nutrient-limitation (Thingstad et al., 1998).

Upwelled waters:

When ENACW is recently upwelled at the Iberian coastline, DOC concentrations reflect the content of the original water mass because biological activity is still relatively low. DOC concentrations increase with higher biological activity in upwelled waters that have resided in the photic zone long enough for uptake of nutrients to take place. Overall, DOC production and accumulation is primarily a result of bacterial enzymatic attack of phytoplankton biomass and detritus, whereas higher DON concentrations, which were closely related to the chlorophyll maximum, were a result of direct exudation or PER. Grazing processes may have played an important role in DOM production (Teira et al., 2001) but it is impossible to distinguish sources due to a lack of heterotrophic grazing and other 'direct-process' data.

Offshore deep waters:

Further offshore, DOC concentrations are lower than those in upwelled or winter slope waters and decrease with depth as a result of increasing distance from DOM sources associated with the continental slope (i.e. suspended sediments, higher biological activity) and continuing remineralisation. Any seasonal and inter-annual differences observed are likely to be due to variable lateral input from deep water mass circulation (i.e. MSOW, LSW, ENADW; van Aken, 2000b) and/or organic matter contribution from intermediate and nepheloid layers.

Mediterranean Sea Outflow Water:

The denser MSOW results in along-slope transport with its core at approximately 1000m depth. This density difference with the water mass above (ENACW) may arrest the vertical transport of sinking POC and result in its accumulation there. This can facilitate the formation of intermediate nepheloid layers containing high levels of suspended material within which DOC concentrations are higher. MSOW at its origin (i.e. the Strait of Gibraltar) generally contains background concentrations (Dafner et al., 2001), reflecting deep water DOC concentrations and is therefore not a lateral mechanism for significant DOC import to the Iberian margin. However, its friction along the continental slope creates resuspension of sediments resulting in diffusion of pore-water DOC into overlying waters and occasionally, uncoupled release of DOC from suspended particles *via* bacterial enzymatic hydrolysis.

Varying extents of DOM accumulation are caused by enhanced biological activity related to seasonal hydrodynamic phenomena characteristic to the Iberian ocean margin. Due to a lack of direct-process and rate studies, supplementary data was used to help provide an 'educated guess' as to the biological processes influencing the DOM distribution and the extent to which these affect the spatial distribution of DOM on a temporal basis at the Iberian ocean margin. The area studied is an open system subject to variable lateral and horizontal inputs both in

surface and in deep waters. DOC production exceeds removal rates in areas such as upwelled surface waters during the summer, the surface poleward current during the winter and in bottom waters with high levels of suspended particulates. Photosynthetic extra-cellular release in this region seems to favour DON production whereas DOC release is mainly facilitated by dissolution of biomass *via* bacterial enzymatic hydrolysis and heterotrophic grazing. Although DOC accumulates in surface and slope waters, the cycling and position of water masses does not allow extensive shelf-edge exchange and/or offshore transport. However, accumulated DOC may be used by the microbial community when conditions allow (e.g. nutrient availability; abiotic transformation of refractory DOM to labile DOM) and/or may be transported along-slope to fuel bacterial production elsewhere.

4.2.2 Future Studies

This project primarily characterised the seasonal and spatial distribution of DOM across and along the Iberian ocean margin and estimated production and accumulation of semi-labile and labile dissolved material in relation to primary and bacterial production as well as hydrographic events. Further investigations of total dissolved nitrogen and inorganic nutrients following from this study would allow elucidation of the biogeochemical cycling of the dissolved nitrogen pool at the Iberian upwelling system and may give further information on the biological processes occurring there.

This study highlighted the extent of accumulation of DOC in surface and deep waters but it lacks direct-process measurements to ascertain the mechanisms of its production and the reasons for its preservation. Several studies are proposed to determine why bacteria were unable to consume the accumulated DOC. However, bacteria-organic matter interactions are complex and poorly understood (Williams, 2000 and references therein) and so this would not be a trivial task. It is proposed to:

- Investigate the geochemical character of the accumulated DOC by performing molecular size studies and organic compound class analyses using ultrafiltration and chromatographic techniques, respectively, to determine inherent chemical properties of refractory material. Mesocosm nutrient-dosing experiments would determine whether accumulation is caused as a result of nutrient limitation. Photochemical experiments would determine the proportion of surface water DOC that is subject to transformation by photodegradation processes.

- Investigate POM-DOM dissolution processes in suspended particulate matter of intermediate and benthic nepheloid layers to ascertain the dominant dissolution mechanisms (i.e. bacterial or abiotic hydrolysis). Determining the geochemical composition of the hydrolysed DOM would give valuable information on inherent chemical properties that make it refractory.

- Estimate the pore-water flux of DOM at regions of contrasting activity (e.g. bioturbidity and water mass friction); this would help establish whether DOM accumulates along the northerly path of the MSOW as a result of enhanced pore-water diffusion and/or due to POM dissolution.

- DOC production as a result of biological activity is not well established. Several studies have examined PER but the marine community is lacking estimates of DOC release from zooplankton grazing (i.e. "sloppy feeding") and bacterial activity. During OMEX II-II, bacterial production correlated well with DOC (Barbosa et al., 2001) suggesting that bacteria may be sources of non bio-available DOM. To investigate bacterial-DOM dynamics, a whole suite of investigations can be proposed. Following this study and in light of recent findings (Nagata, 2000 and references therein; Ogawa et al., 2001), it would be of interest to evaluate the contribution of bacterial biomass to the DOM pool using bacterial biomarker/tracer studies and incubation experiments, and determining the geochemical composition and the mechanisms by which this material is produced.

APPENDIX 1 – CORRELATION MATRIX REGRESSIONS FOR CRUISE CD110B – TRANSECT P

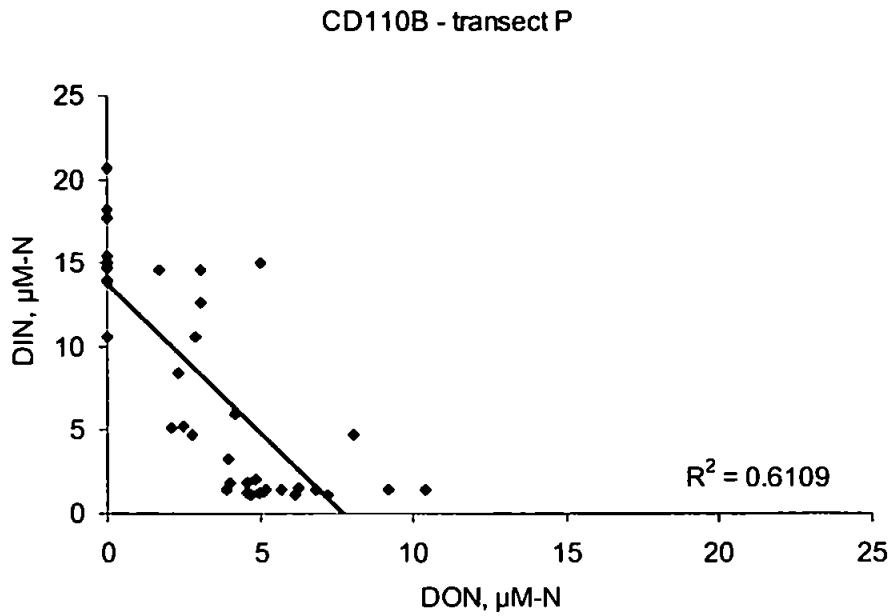

Figure 1. Regression of DON and NO_2 + NO_3 (DIN) data (µM-N) at CD110B transect P. Note: R^2 is the square of the correlation coefficient and represents the percentage of change in one variable due to the other variable.

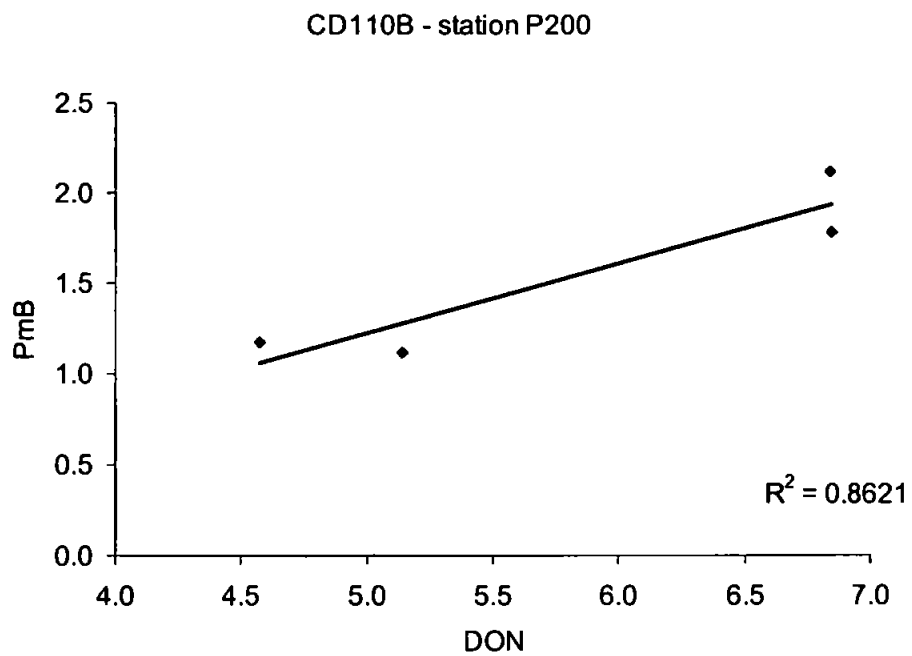

Figure 2. Regression of DON (µM-N) and PmB data (arbitrary units) at CD110B station P200.

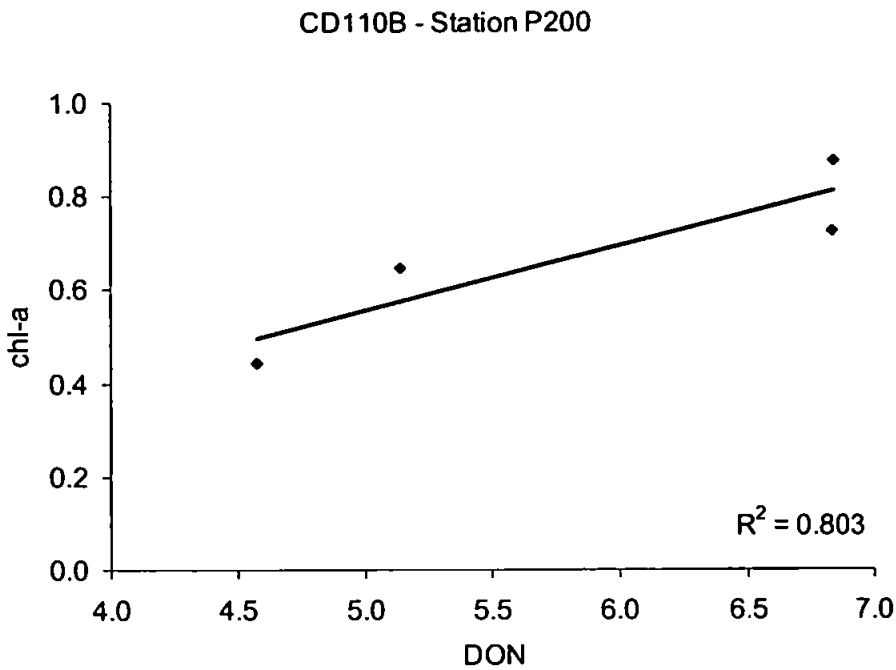

Figure 3. Regression of DON (μM-N) and chl-a data (mg m^{-3}) at CD110B station P200.

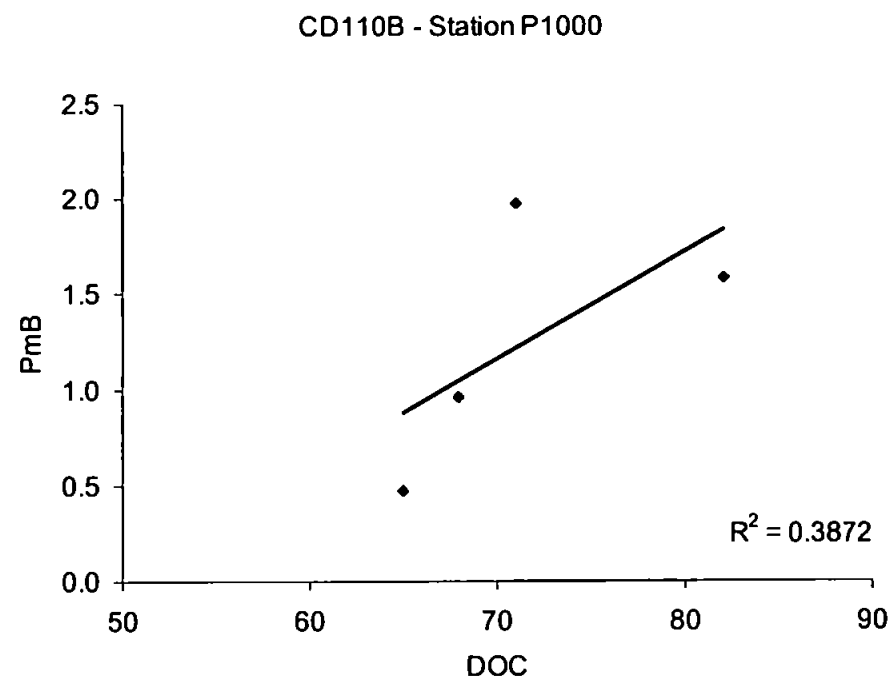

Figure 4. Regression of DOC (μM-C) and PmB data (arbitrary units) at CD110B station P1000.

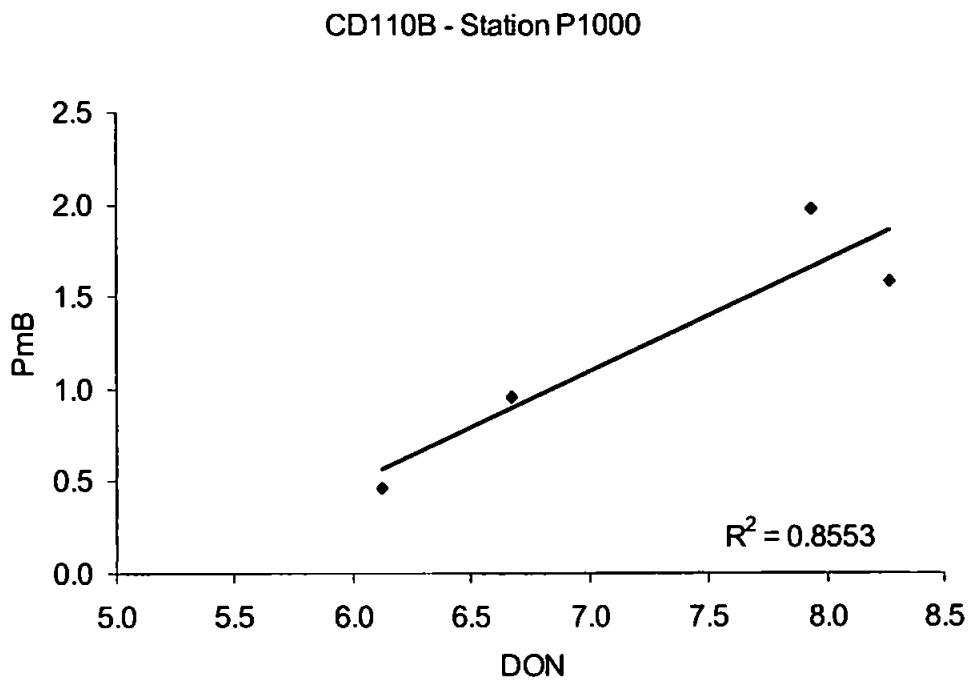

Figure 5. Regression of DON (μM-N) and PmB data (arbitrary units) at CD110B station P1000.

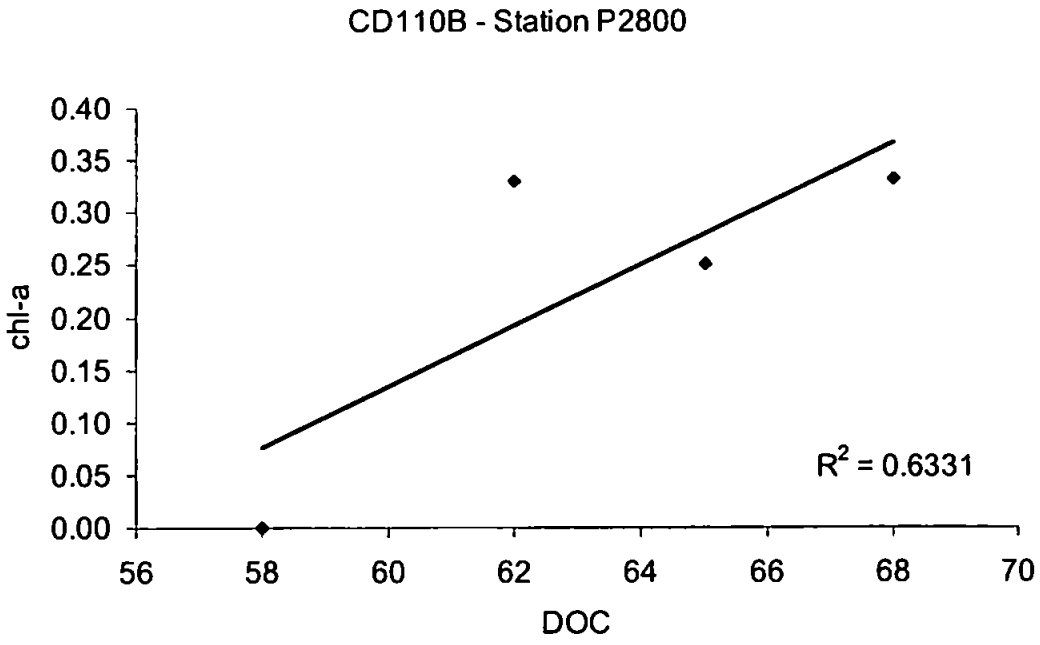

Figure 6. Regression of DOC (μM-C) and chl-a data (mg m^{-3}) at CD110B station P2800.

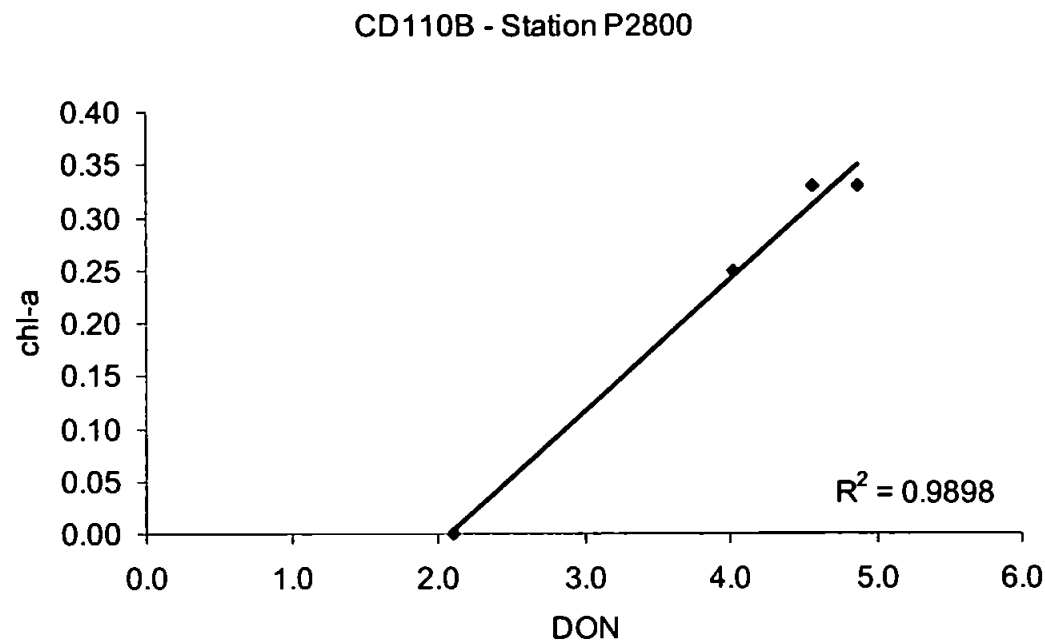

Figure 7. Regression of DON (μM-N) and chl-a data (mg m^{-3}) at CD110B station P2800.

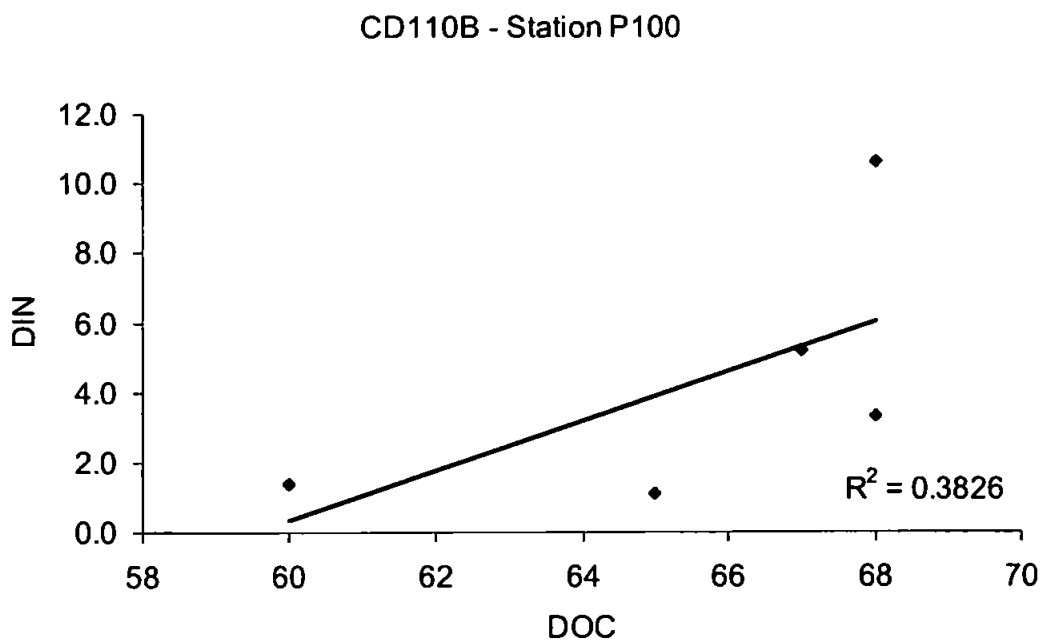

Figure 8. Regression of DOC (μM-C) and NO_2 + NO_3 (DIN) data (μM-N) at CD110B station P100.

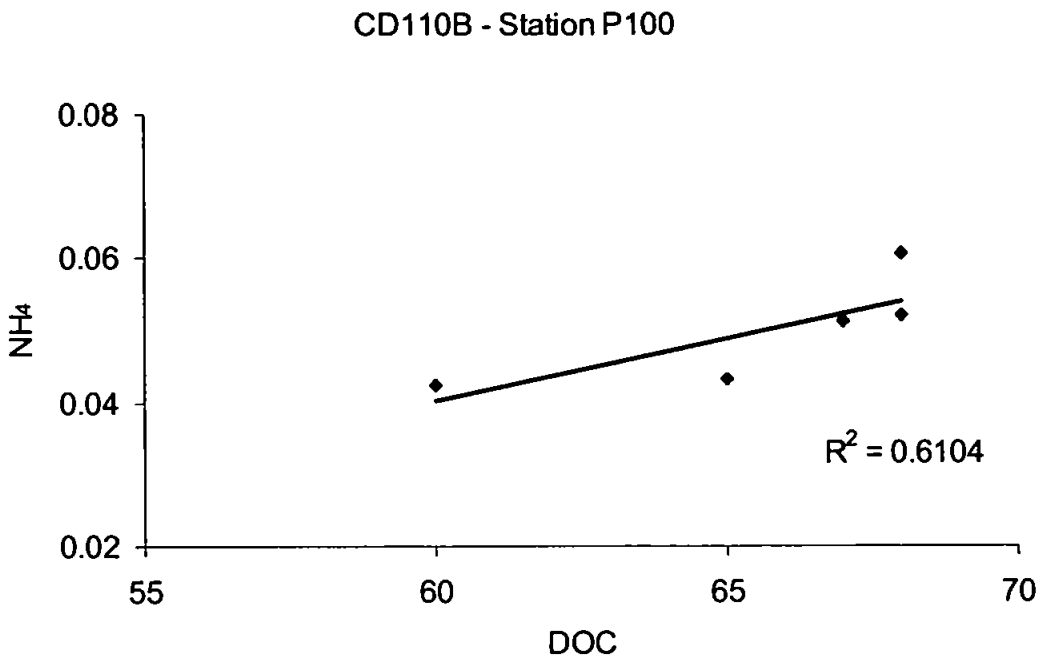

Figure 9. Regression of DOC (μM-C) and NH_4 data (μM-N) at CD110B station P100.

APPENDIX 2 – CORRELATION MATRIX REGRESSIONS FOR CRUISE OMEX0898

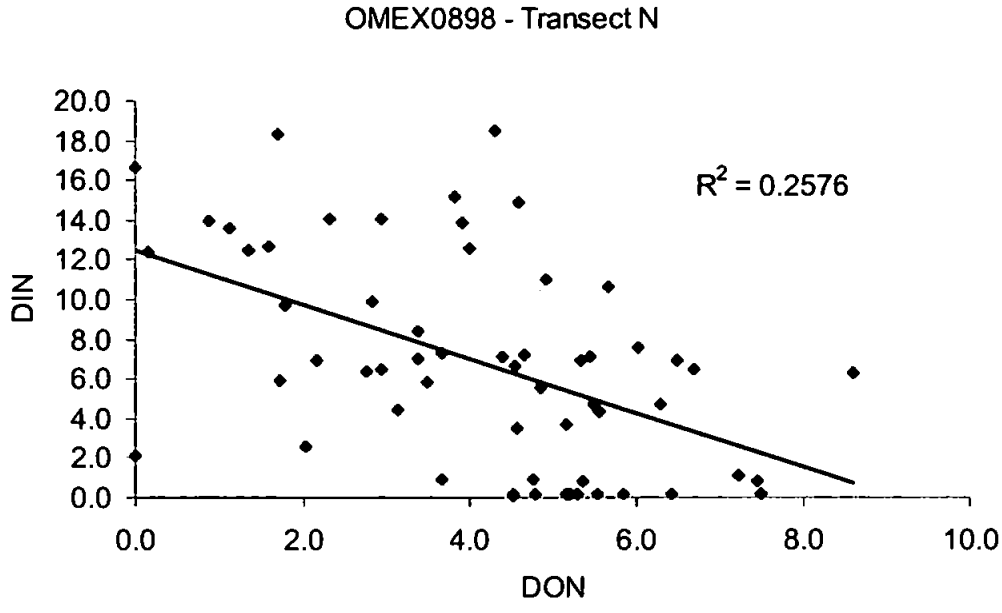

Figure 10. Regression of DON and NO_2 + NO_3 (DIN) data (μM-N) at OMEX0898 stations.

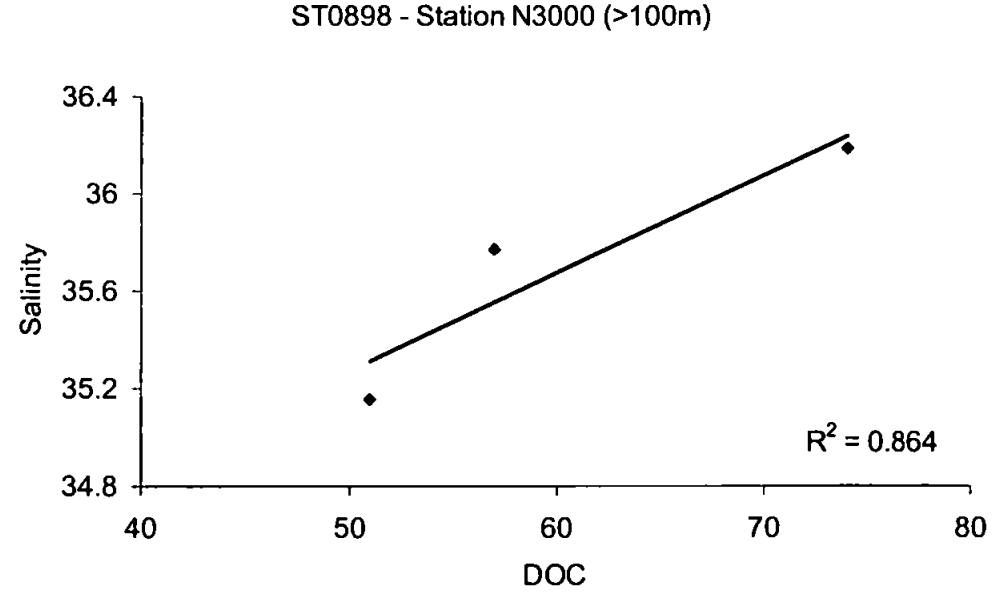

Figure 11. Regression of DOC (μM-C) and salinity data in deep (>100m) waters of OMEX0898 station N3000.

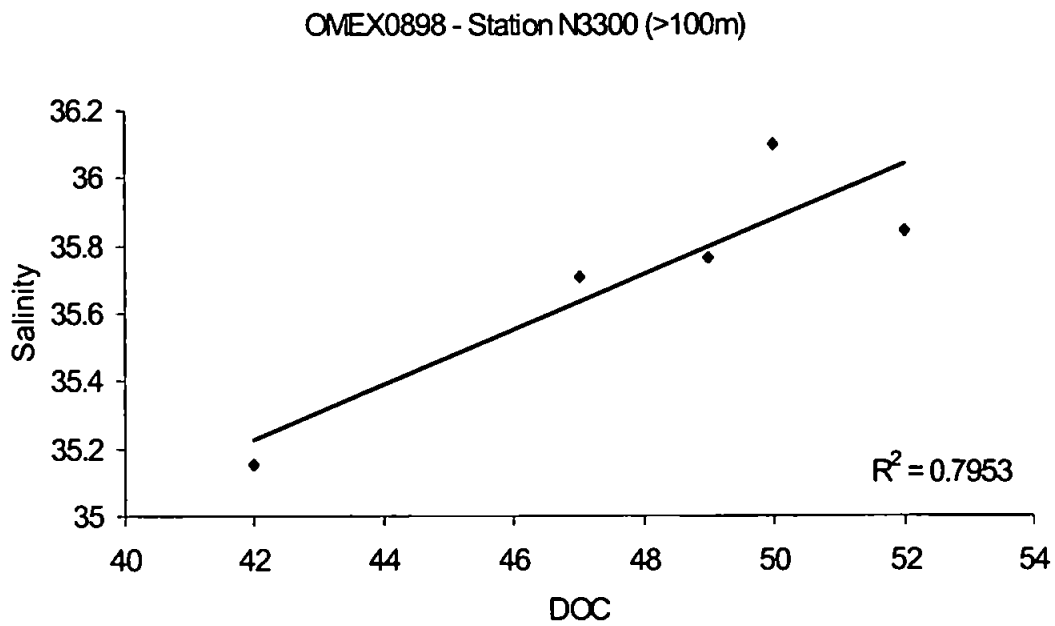

Figure 12. Regression of DOC (μM-C) and salinity data in deep (>100m) waters of OMEX0898 station N3300.

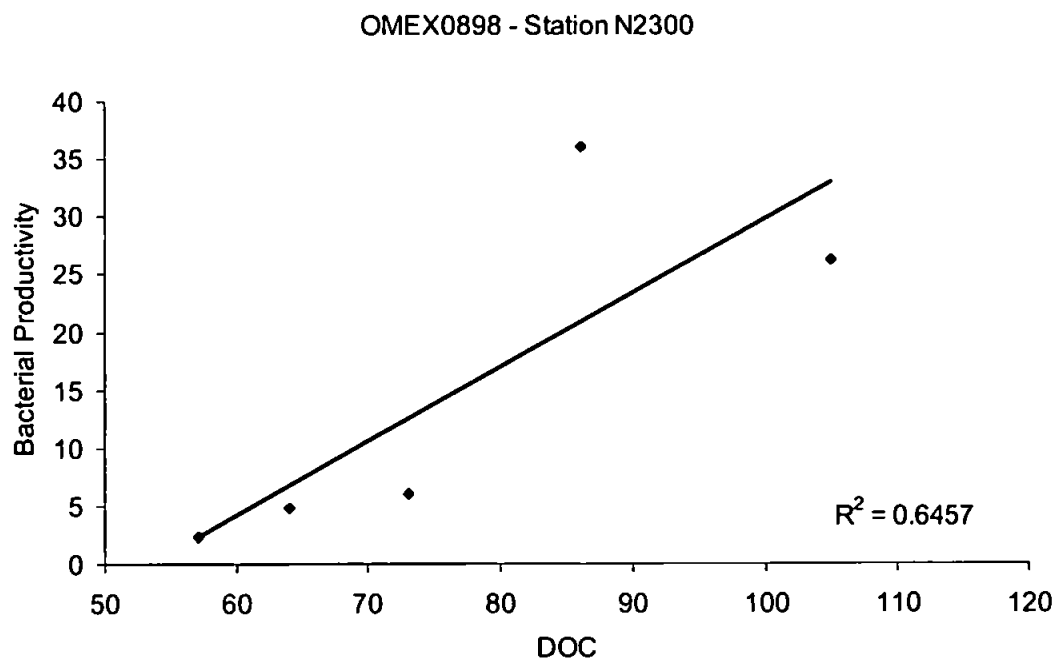

Figure 13. Regression of DOC (μM-C) and bacterial productivity (leucine uptake rate, pmol L^{-1} hr^{-1}) data at OMEX0898 station N2300.

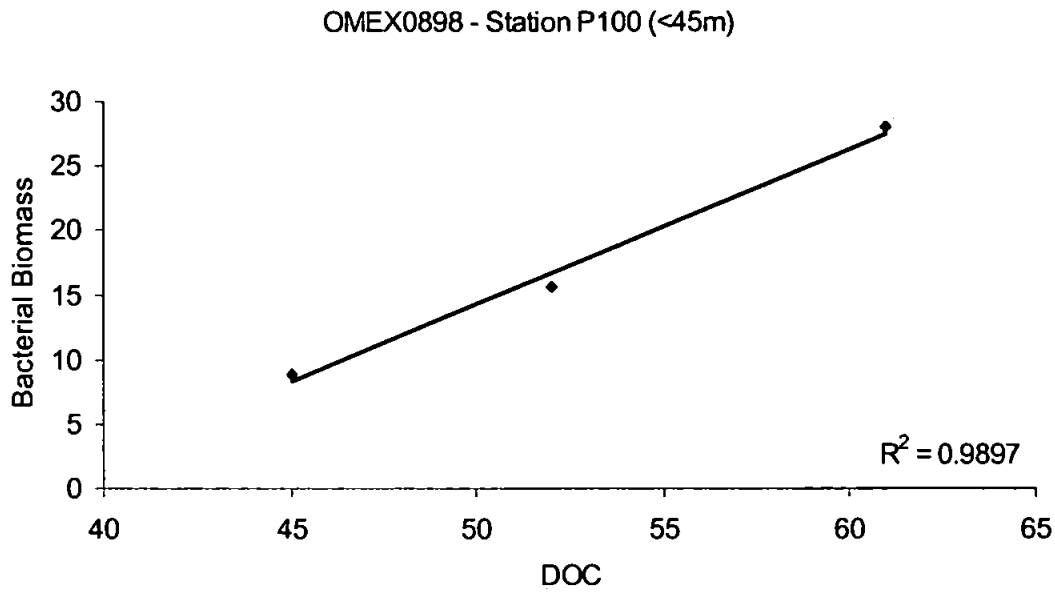

Figure 14. Regression of DOC (μM-C) and bacterial biomass (mg m^{-3}) data in the upper 40m of OMEX0898 station P100.

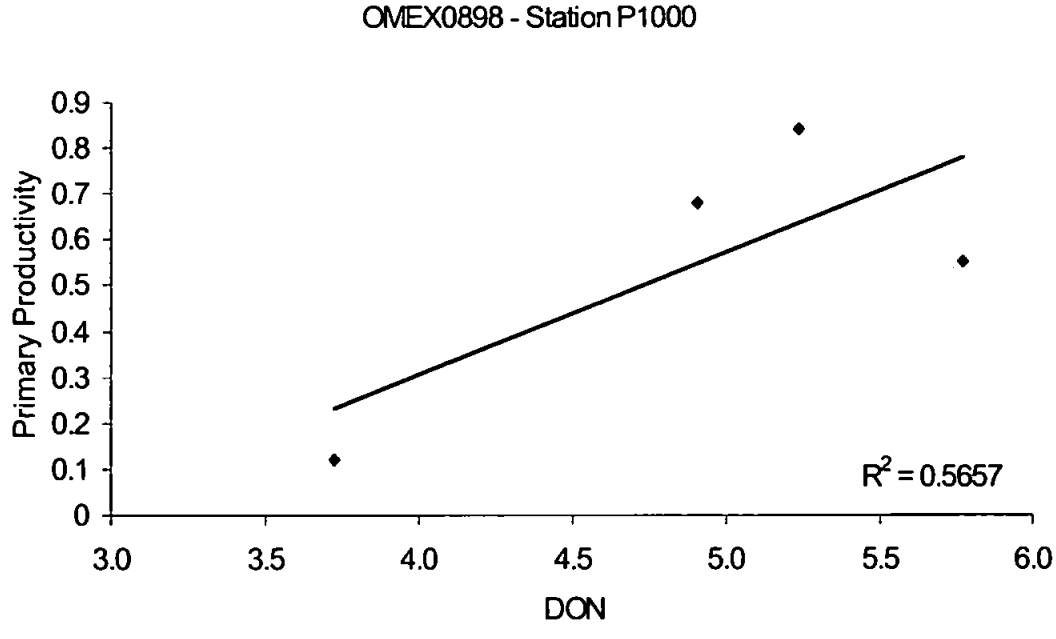

Figure 15. Regression of DON (μM-N) and primary productivity (mg m^{-3} hr^{-1}) data at OMEX0898 station P1000.

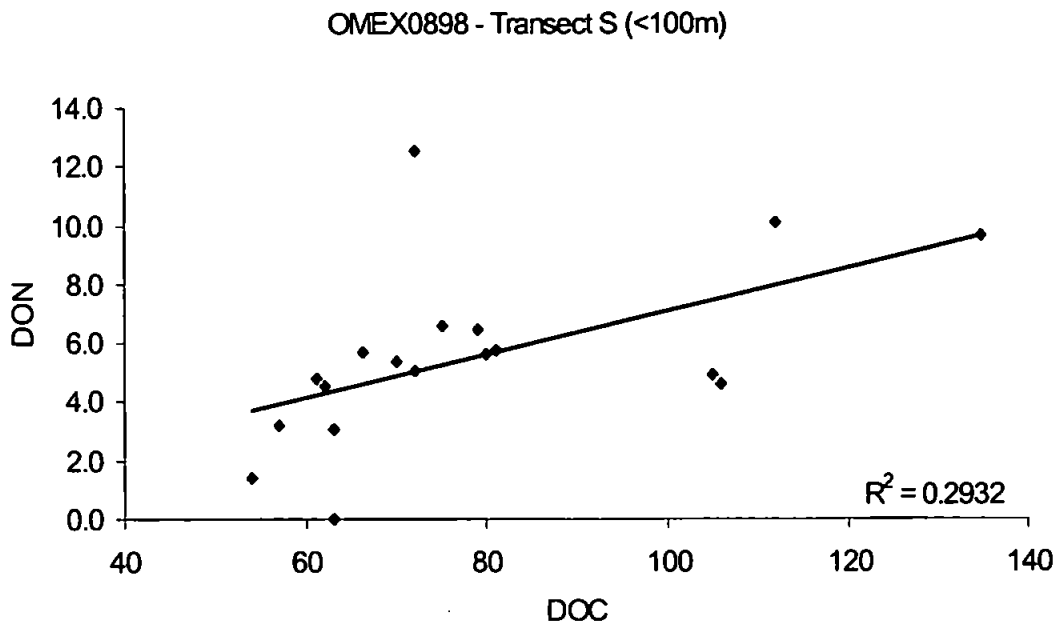

Figure 16. Regression of DOC (μM-C) and DON (μM-N) data in the upper 100m of OMEX0898 transect S.

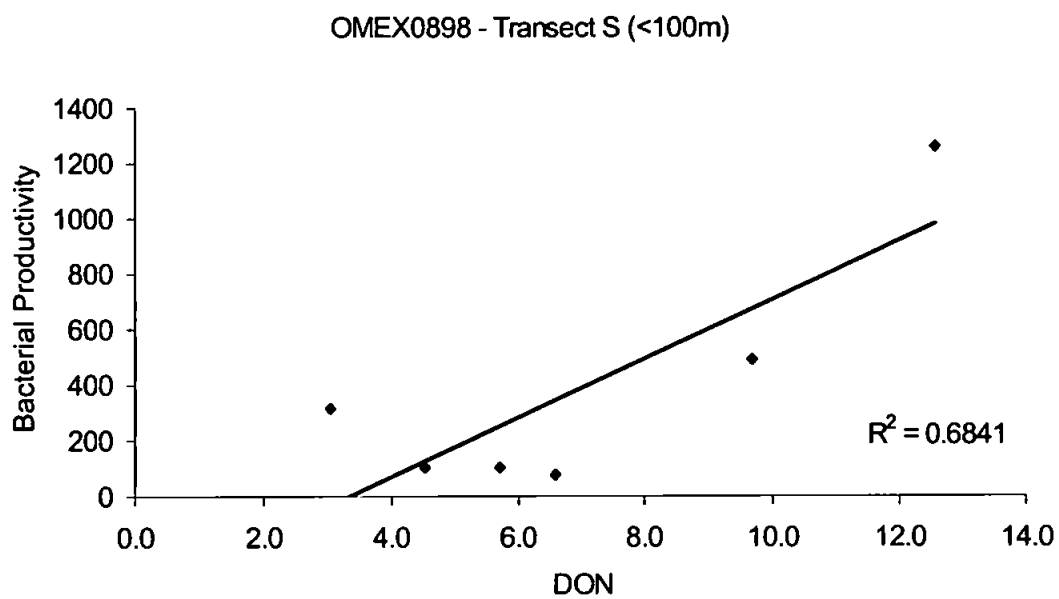

Figure 17. Regression of DON (μM-N) and bacterial production (leucine uptake rate, mg-C m^{-3} hr^{-1}) data in the upper 100m of OMEX0898 transect S.

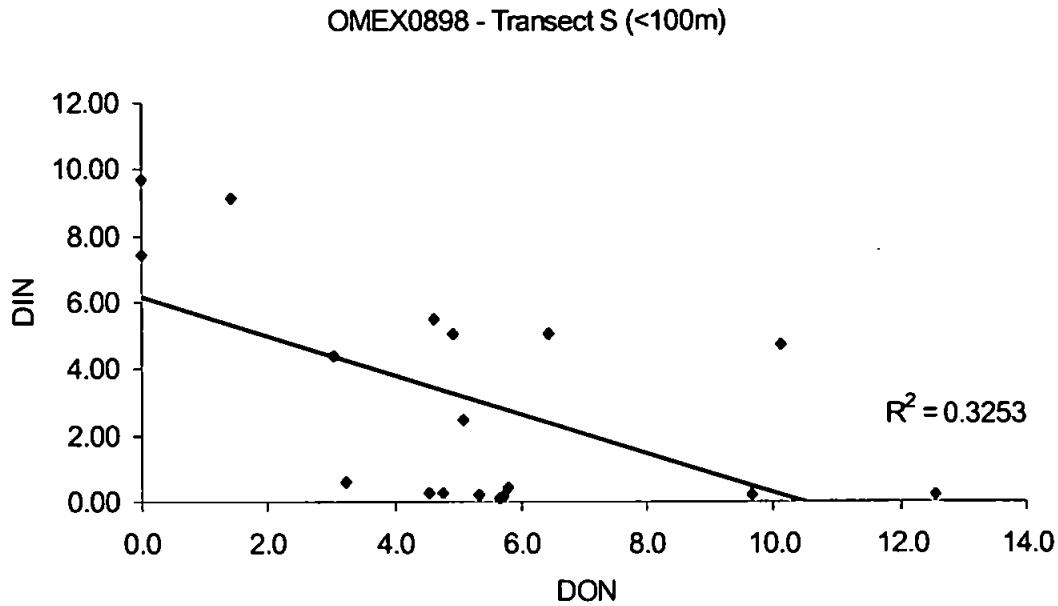

Figure 18. Regression of DON and NO_2 + NO_3 (DIN) data (μM-N) in the upper 100m of OMEX0898 transect S.

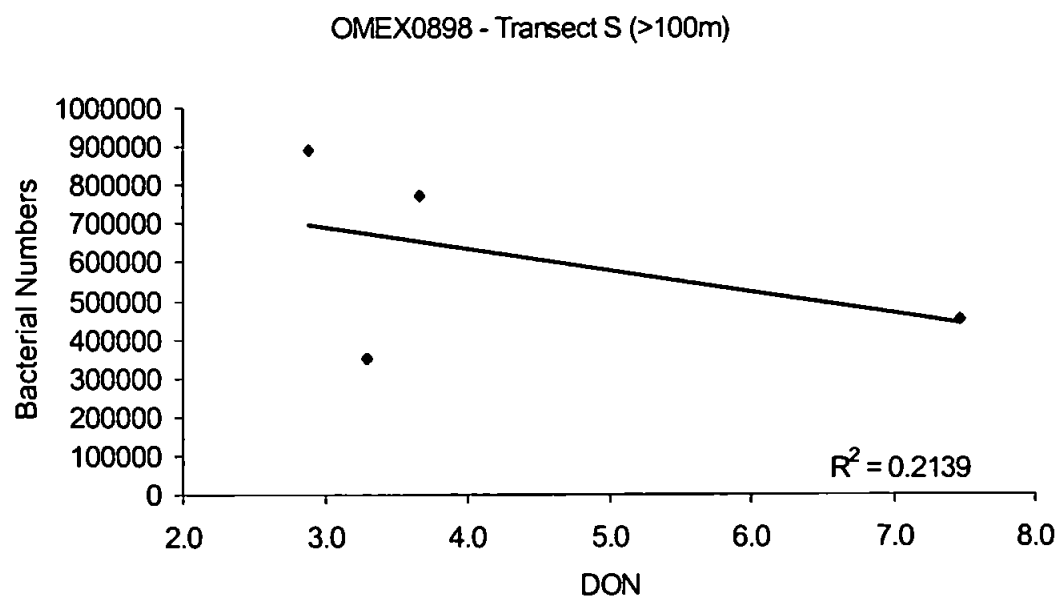

Figure 19. Regression of DON (μM-N) and bacterial number data (ml^{-1}) in deep waters (>100m) of OMEX0898 transect S.

APPENDIX 3 – CORRELATION MATRIX REGRESSIONS FOR CRUISE M43/2

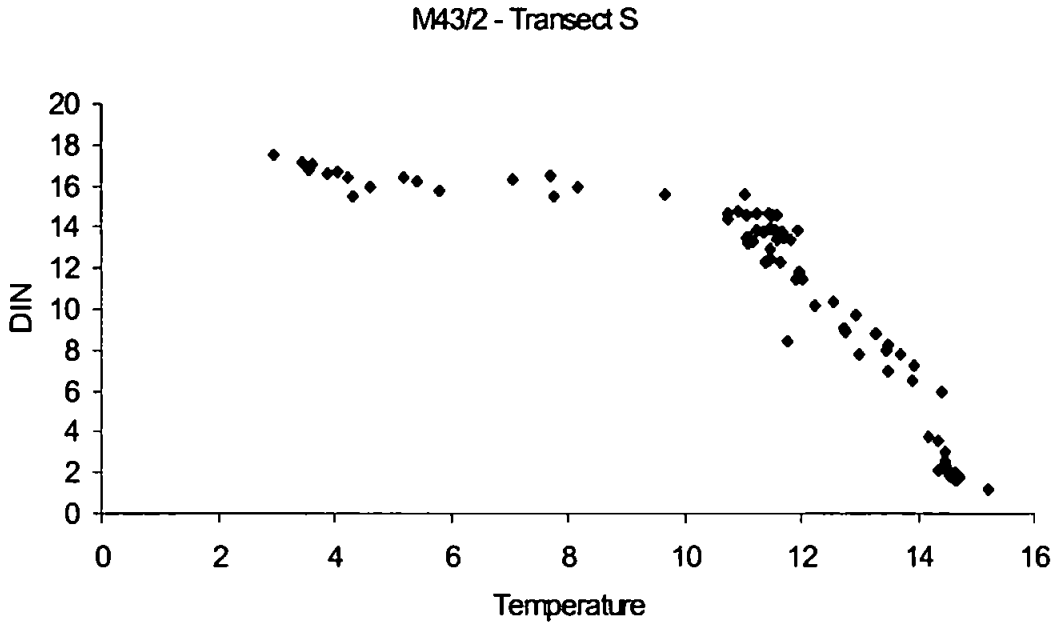

Figure 20. Regression of temperature (°C) and NO_2 + NO_3 (DIN) data (µM-N) at M43/2 transect S.

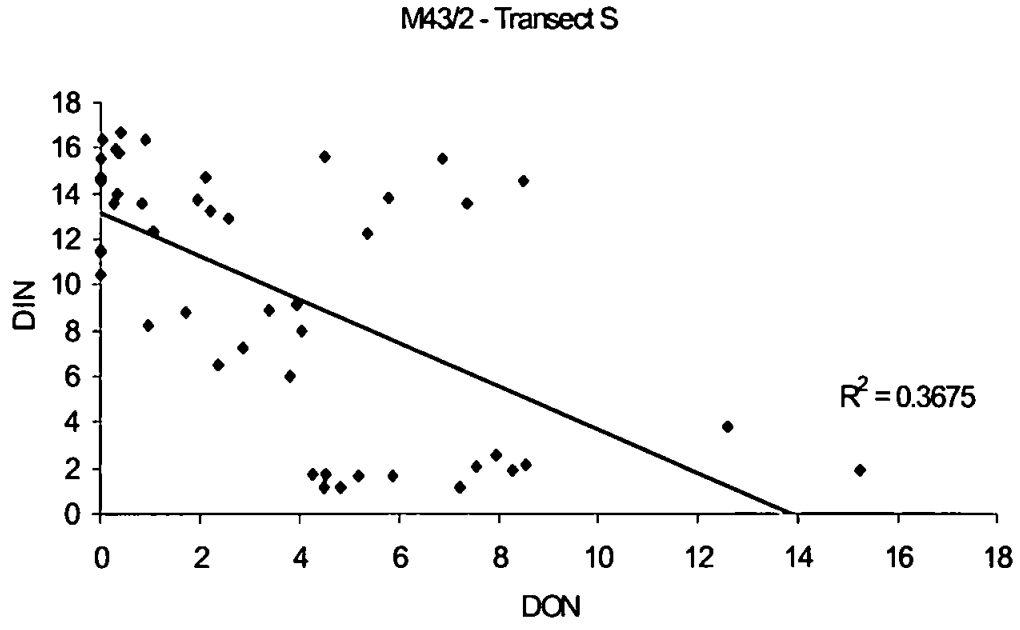

Figure 21. Regression of DON and NO_2 + NO_3 (DIN) data (µM-N) at M43/2 transect S.

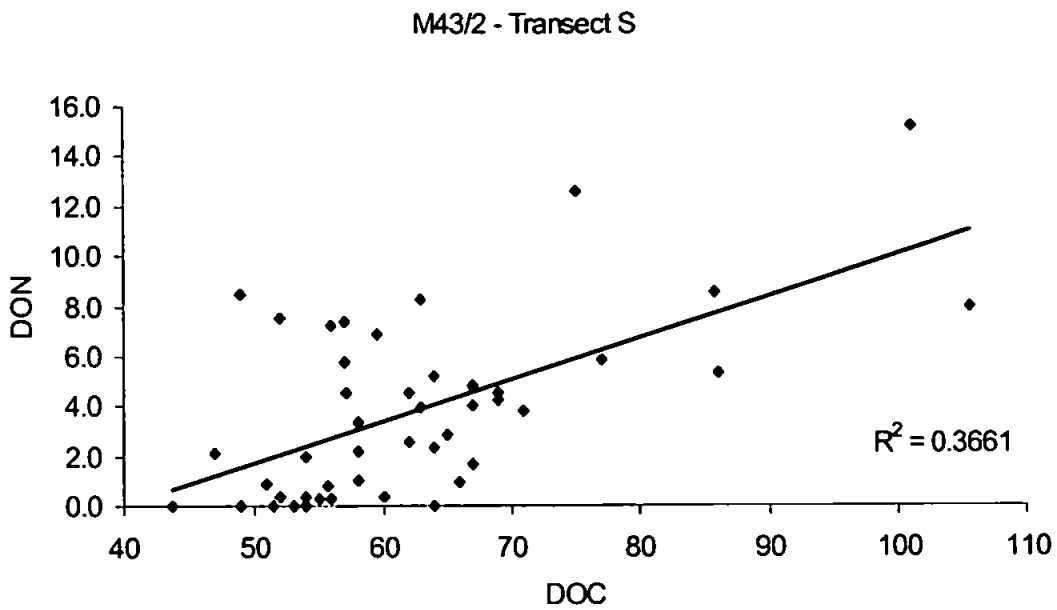

Figure 22. Regression of DOC and DON data (μM) at M43/2 transect S.

APPENDIX 4 – CORRELATION MATRIX REGRESSIONS FOR CRUISE BG9919

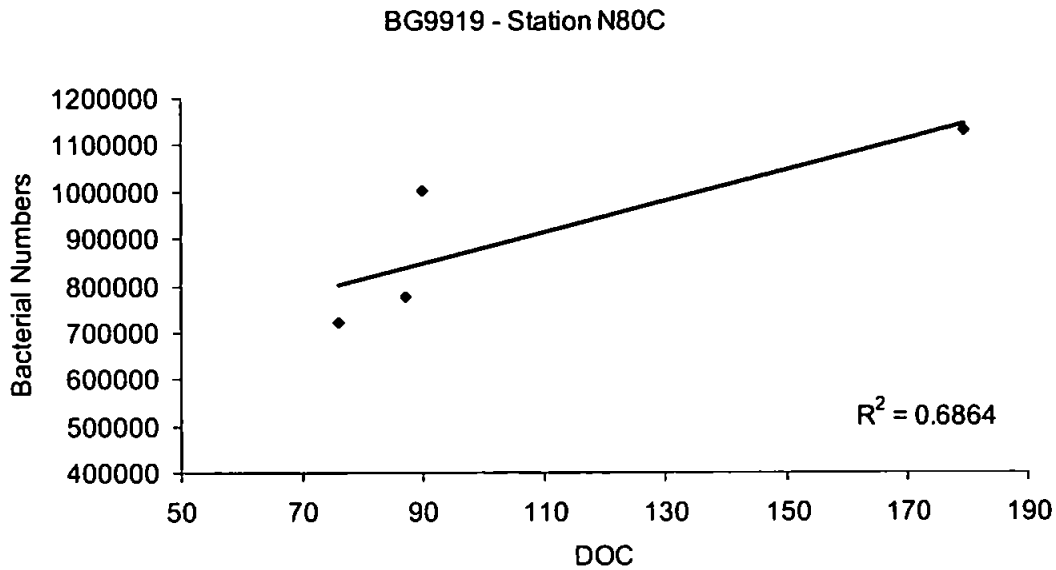

Figure 23. Regression of DOC (μM-C) and bacterial number (ml^{-1}) data at BG9919 station N80C.

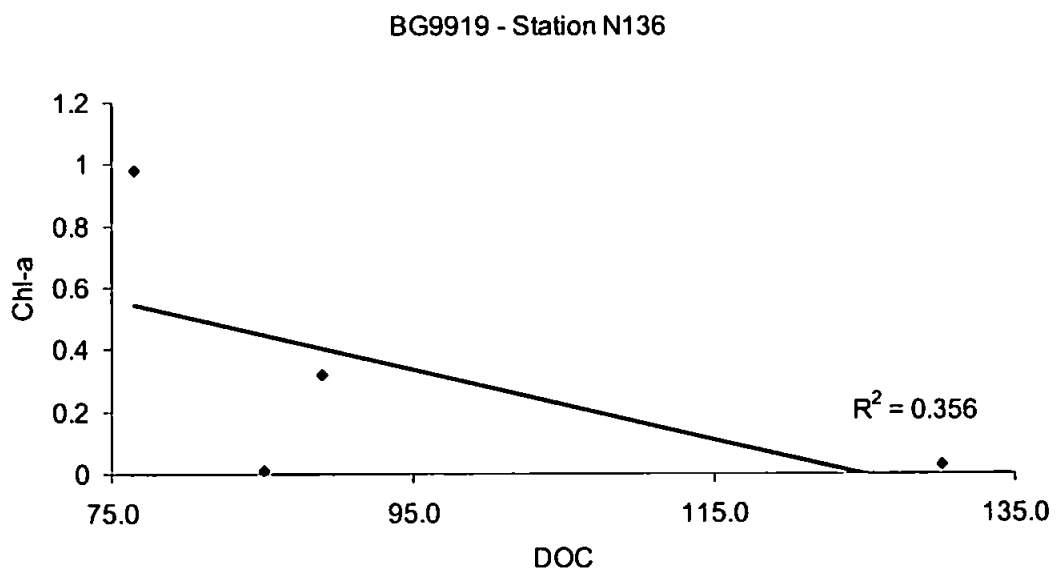

Figure 24. Regression of DOC (μM-C) and chl-a ($mg\ m^{-3}$) data at BG9919 station N136.

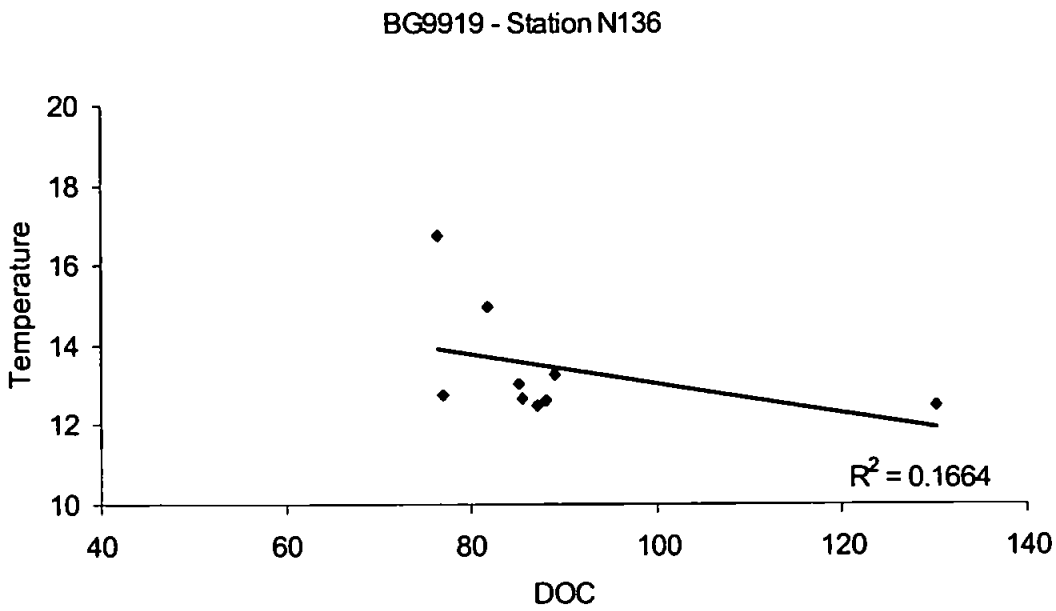

Figure 25. Regression of DOC (μM-C) and temperature (°C) data at BG9919 station N136.

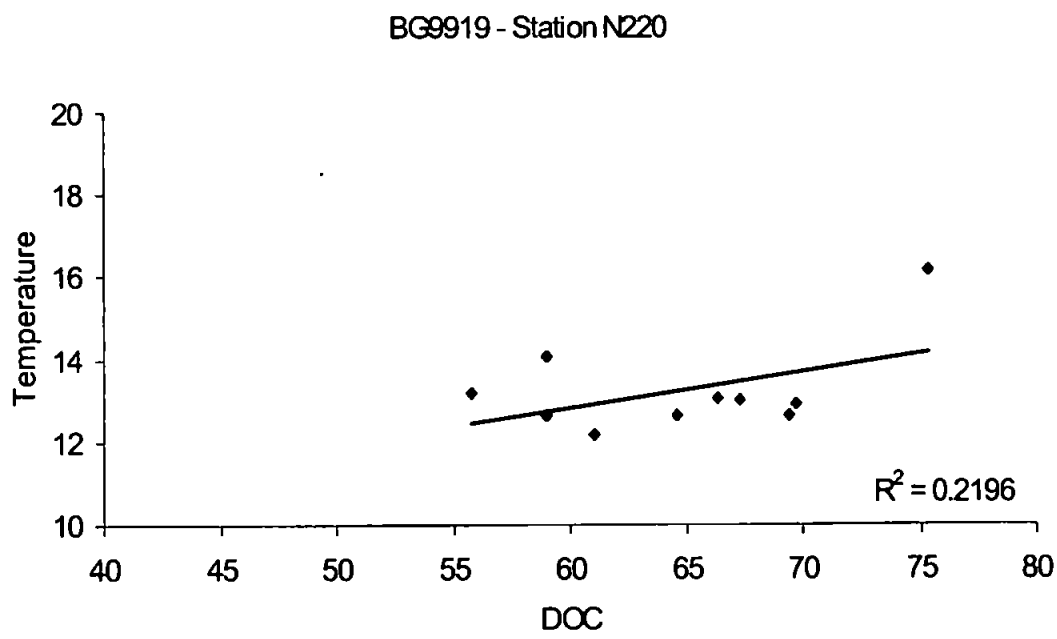

Figure 26. Regression of DOC (μM-C) and temperature (°C) data at BG9919 station N220.

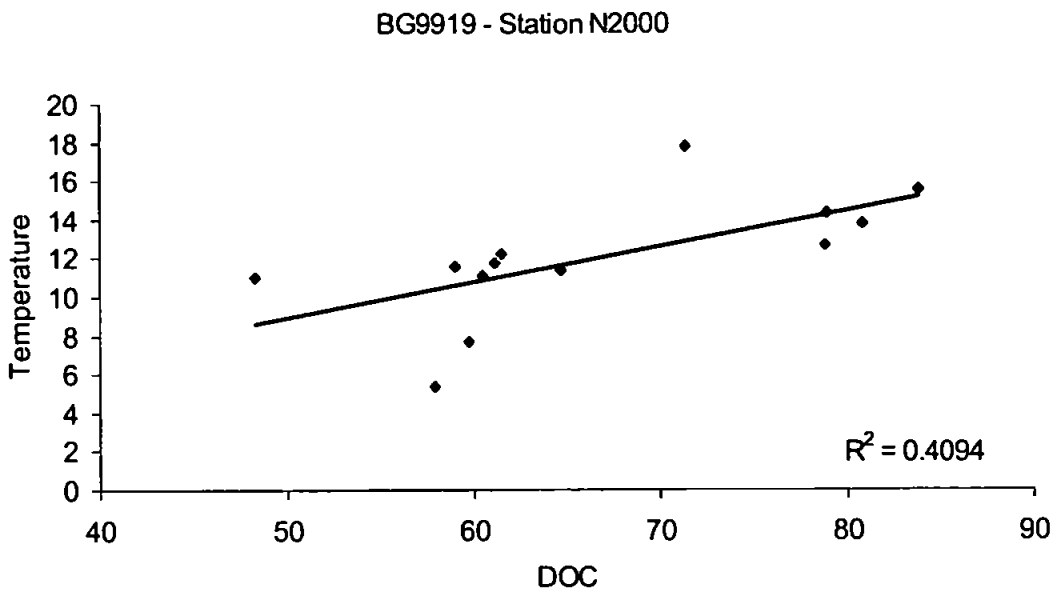

Figure 27. Regression of DOC (μM-C) and temperature (°C) data at BG9919 station N2000.

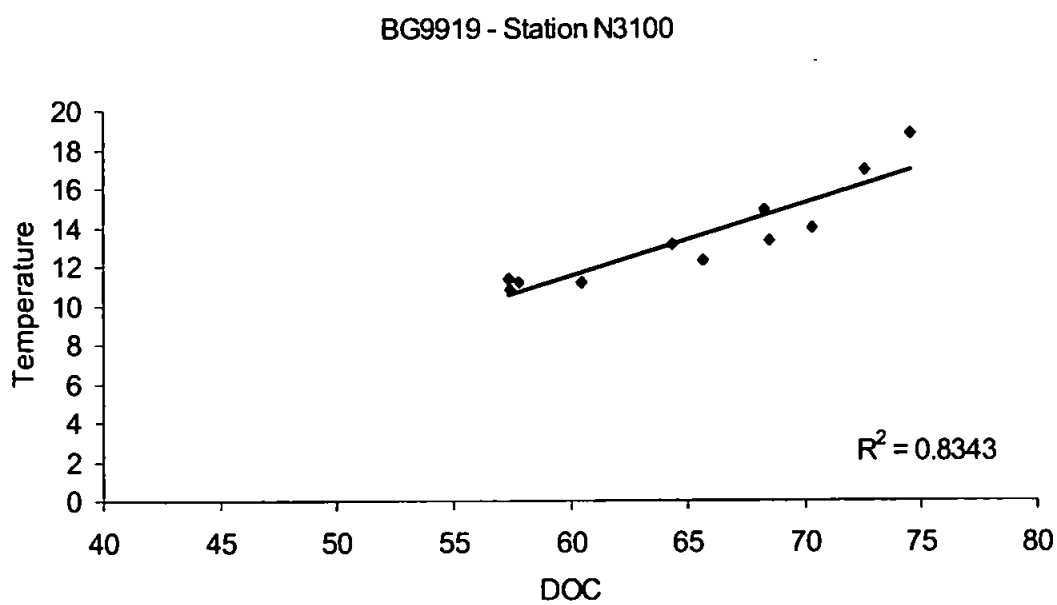

Figure 28. Regression of DOC (μM-C) and temperature (°C) data at BG9919 station N3100.

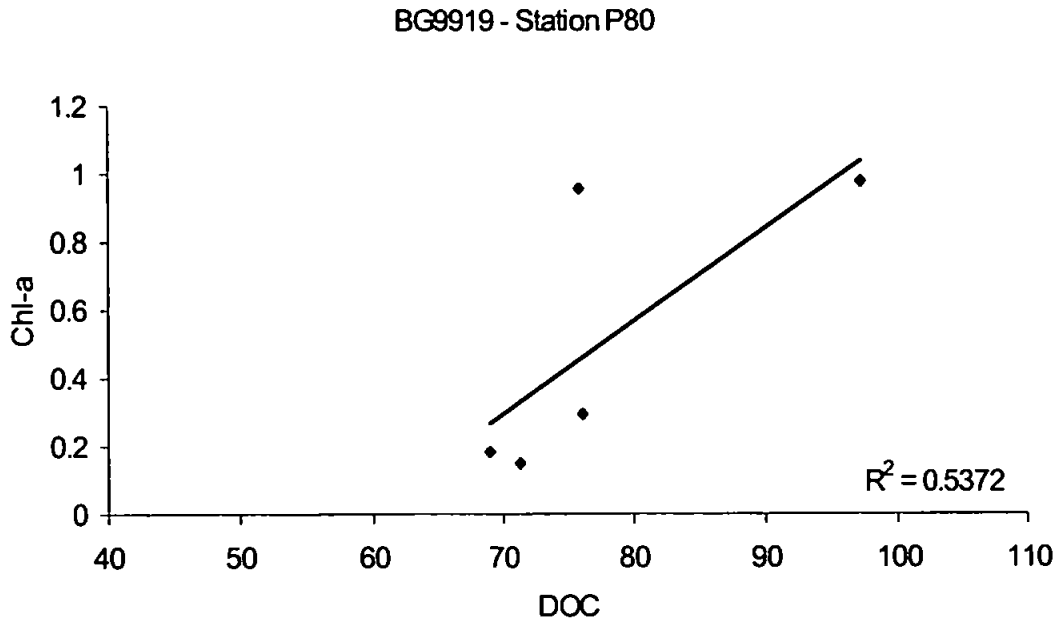

Figure 29. Regression of DOC (μM-C) and chl-a (mg m^{-3}) data at BG9919 station P80.

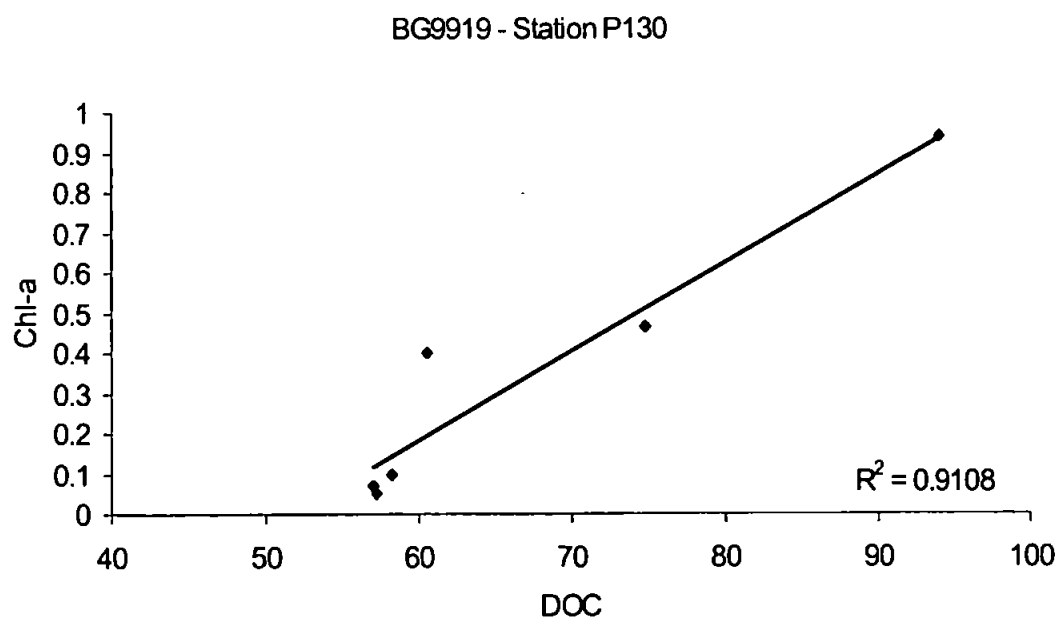

Figure 30. Regression of DOC (μM-C) and chl-a (mg m^{-3}) data at BG9919 station P130.

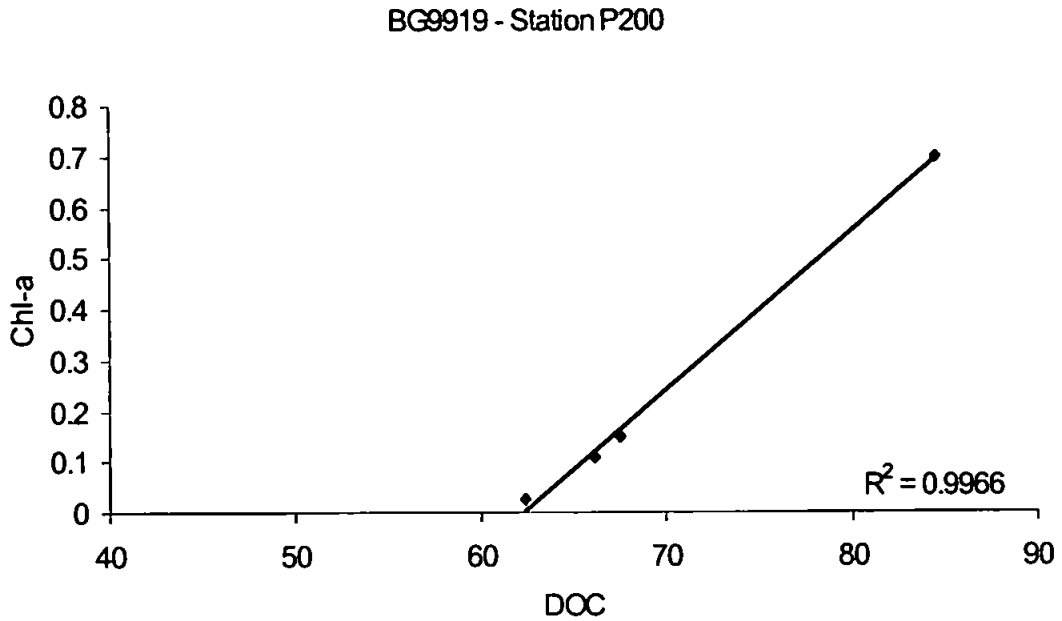

Figure 31. Regression of DOC (μM-C) and chl-a (mg m^{-3}) data at BG9919 station P200.

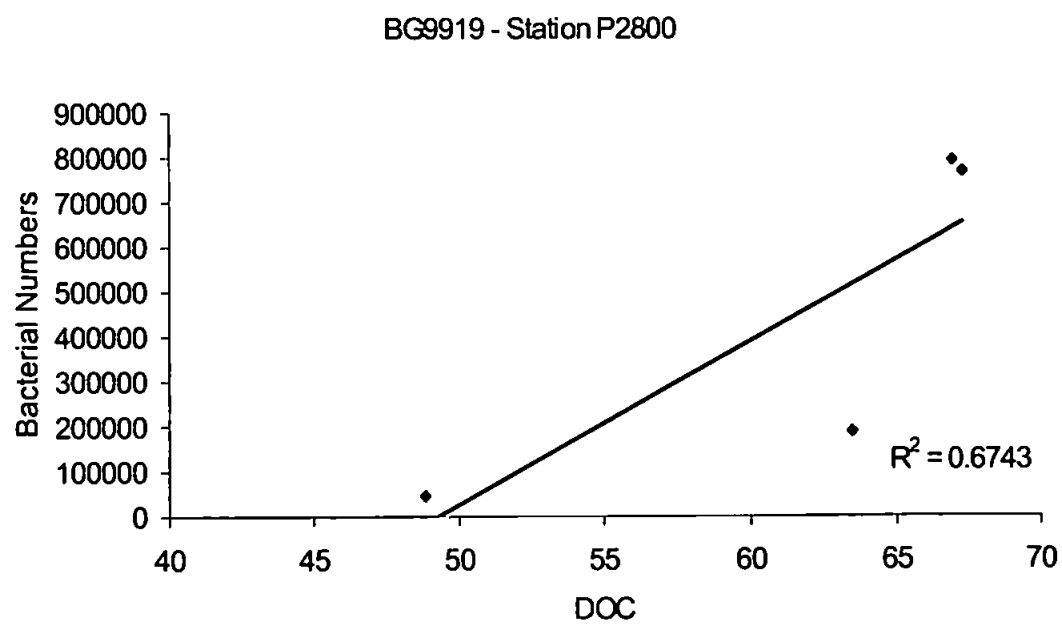

Figure 32. Regression of DOC (μM-C) and bacterial number (ml^{-1}) data at BG9919 station P2800.

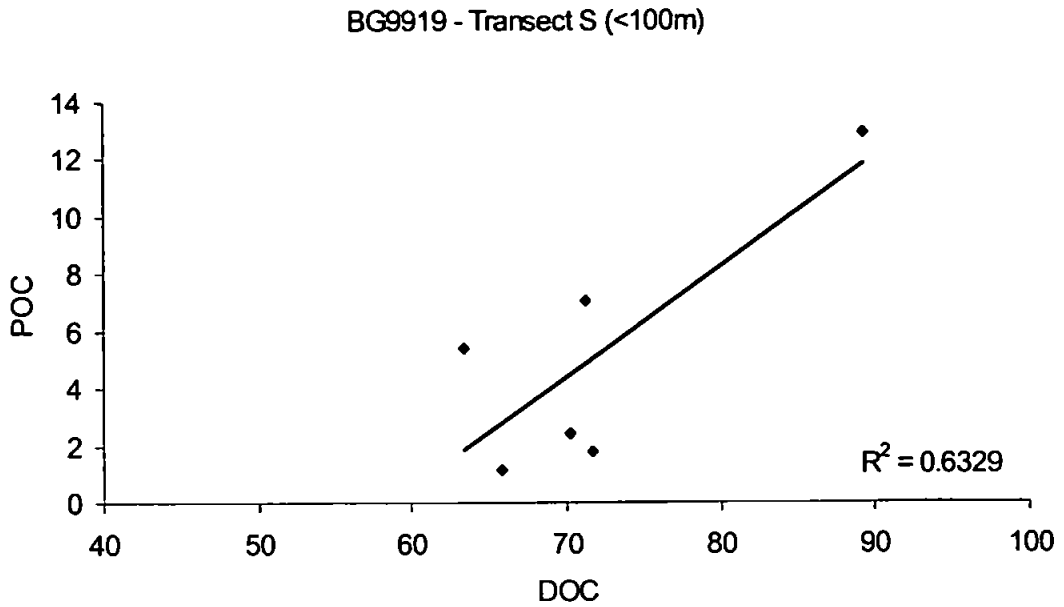

Figure 33. Regression of DOC (μM-C) and POC data (μM-C) in the upper 100m of BG9919 transect S.

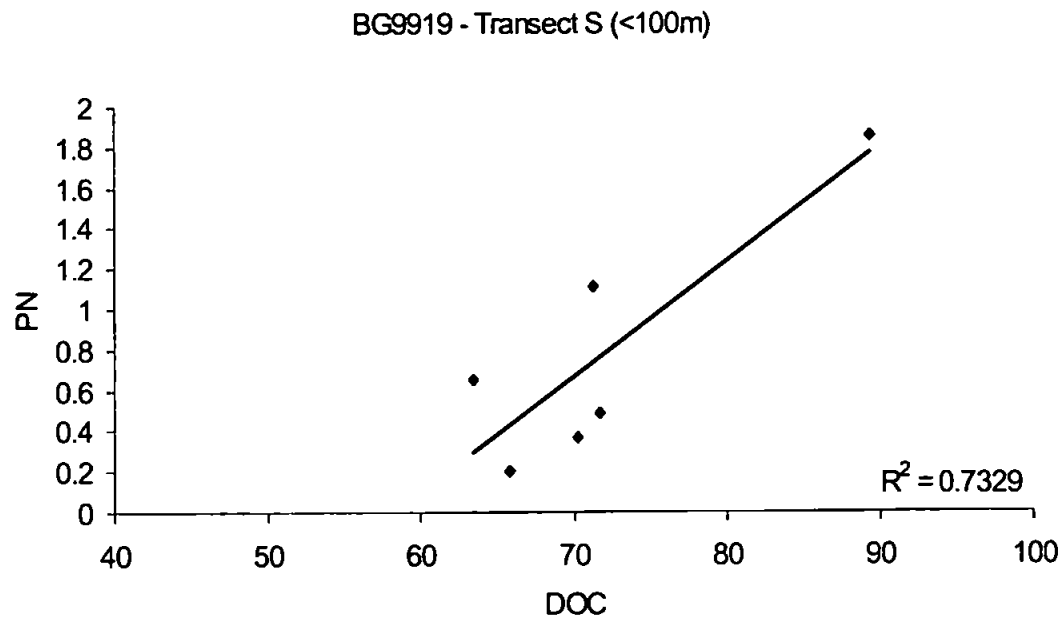

Figure 34. Regression of DOC (μM-C) and PN (μM-N) data in the upper 100m of BG9919 transect S.

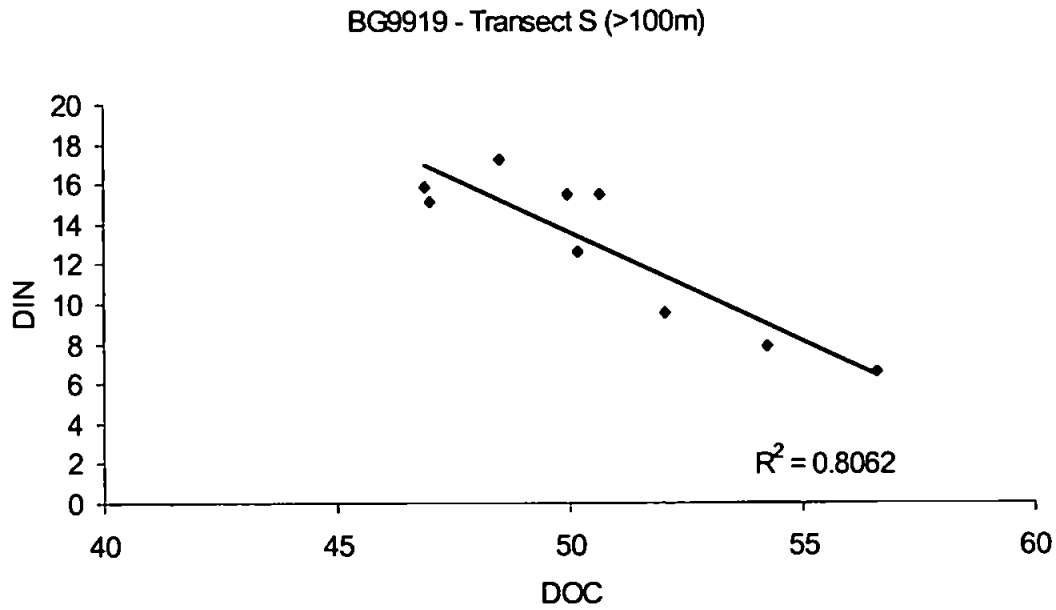

Figure 35. Regression of DOC (μM-C) and NO_2 + NO_3 (DIN) (μM-N) data in deep waters (>100m) of BG9919 transect S.

References

Aiken G., D. McKnight, R. Harnish and R. Wershaw (1996) Geochemistry of aquatic humic substances in the Lake Fryxell Basin, Antarctica. Biogeochemistry. 34:157-188

Alldredge A.L. (2000) Insterstitial DOC concentrations within sinking marine aggregates and their potential contribution to carbon flux. Limnology and Oceanography. 45(6)1245-1253

Alperin M.J. and Martens C.S. (1993) Dissolved organic carbon in marine pore waters: a comparison of three oxidation methods. Marine Chemistry 41:135-143

Aluwihare L.I., D.J. Repeta, and R.F Chen (1997) A major polymeric component to DOC is surface sea water. Nature. 387(6629)166-169

Alvarez-Salgado X.A., G. Roson, F.F. Perez, and Y. Pasos (1993) Hydrographic Variability off the Rias Baixas (NW Spain) During the Upwelling Season. Journal of Geophysical Research. 98(C8):14447-14455

Alvarez-Salgado X.A. and A.E.J. Miller (1998) Simultaneous determination of dissolved organic carbon and total dissolved nitrogen in seawater by high temperature catalytic oxidation: conditions for precise shipboard measurements. Marine Chemistry 62:325-333

Alvarez-Salgado X.A., M.D. Doval and F.F. Perez (1999) Dissolved organic matter in shelf waters off the Ria de Vigo (NW Iberian upwelling system). Journal of Marine Systems. 18:383-394

Alvarez-Salgado X.A., M.D. Doval, A.V. Borges, I. Joint, M. Frankignoulle, E.M.S. Woodward and F.G. Figueiras (2001) Off-shelf fluxes of labile materials by an upwelling filament of the NW Iberian upwelling system. Progress in Oceanography. 51:321-337

Amon R.M.W. and R. Benner (1994) Rapid cycling of HMW DOM in the ocean. Nature. 369(6481)549-552

Amon R.M.W. and R. Benner (1996) Bacterial utilisation of different size classes of DOM. Limnology and Oceanography. 41(1):41-51

Anderson, R.F., G.T. Rowe, P.F. Kemp, S. Trumbore and P.E. Biscaye (1994) Carbon budget for the mid-slope depocenter of the Middle Atlantic Bight. Deep Sea Research II – Topical Studies in Oceanography 41(2/3): 669-703

Andrews S.S., S. Caron and O.C. Zafiriou (2000) Photochemical oxygen consumption in marine waters: A major sink for colored DOM? Limnology and Oceanography. 45(2): 267-277

Azam F., T. Fenchel, J.G. Field, J.S. Gray, L.A. Meyer-Reil and F. Thingstad (1983). The ecological role of water-column microbes in the sea. Marine Ecology Progress Series.10:257-263

Azam, F. (1998) Microbial control of oceanic carbon flux: the plot thickens. Science. 280 (5364) 694-696

Baines S.B. and M.L.Pace (1991) The production of DOM by phytoplankton and its importance to bacteria:patterns across marine and freshwater systems. Limnology and Oceanography. 36(6):1078-1090

Barbosa A.B., H.M. Galvao, P.A. Mendes, X.A. Alvarez-Salgado, F.G. Figueiras and I. Joint (2001) Short-term variability of heterotrophic bacterioplankton during upwelling off the NW Iberian margin. Progress in Oceanography. 51:339-359

Bartz R., J.R.V. Zaneveld, and H. Pak. (1978). A transmissometer for profiling and moored observations in water. Proceedings of the Society of Photo-optical Instrumentation Engineers. 160:102-108

Bauer J.E., P.M. Williams and E.R.M. Druffel (1992) ^{14}C activity of DOC fractions in the north-central Pacific and Sargasso Sea. Nature. 357:667-670

Bauer J.E., M.L. Occelli, P.M. Williams and P.C. McCaslin (1993) Heterogeneous catalyst structure and function: review and implications for the analysis of dissolved organic carbon and nitrogen in natural waters. Marine Chemistry. 41:75-89

Bauer, J.E. and E.R.M. Druffel (1998) Ocean margins as a significant source of organic matter to the deep ocean. Nature 392(6675) 482-485

Benner R., J.D. Pakulski, M. McCarthy, J.I. Hedges, P.G. Hatcher (1992) Bulk chemical characteristics of DOM in the ocean. Science. 255:1561-1564.

Benner R. and M. Strom (1993) A critical evaluation of the analytical blank associated with DOC measurements by HTCO. Marine Chemistry. 41(1-3):153-160

Benner R., B. Biddanda, B. Black, M. McCarthy (1997) Abundance, size distribution, and stable carbon and nitrogen isotopic compositions of marine organic matter isolated by tangential-flow ultrafiltration. Marine Chemistry 57 (3-4): 243-263

Bianchi T.S., C. Lambert, P.H. Santschi, M. Baskaran and L.D. Guo (1995) Plant pigments as biomarkers of HMW DOC. Limnology and Oceanography 40(2):422-428

Biddanda B. and R. Benner (1997) Carbon, nitrogen, and carbohydrate fluxes during the production of particulate and DOM by marine phytoplankton. Limnology and Oceanography. 42(3): 506-518

Blank M., M. Leinen and J.M. Prospero (1985) Major Asian aeolian inputs indicated by the mineralogy of aerosols and sediments in the western North Pacific. Nature. 314:84-86

Bode A. (1998) OMEX II-II Cruise Report: R/V Professor Shtokman Cruise OMEX-0898 1st - 11th August, 1998. IEO Publications. 31pp.

Bronk D.A. and P.M. Glibert (1991) A ^{15}N tracer method for the measurement of DON release by phytoplankton. Marine Ecology Progress Series. 7(2-3):171-182

Buesseler K.O., J.E. Bauer, R.F. Chen, T.I. Eglinton, O. Gustafsson, W. Landing , K. Mopper, S.B. Moran, P.H. Santschi, R. VernonClark and M.L. Wells (1996) An intercomparison of cross-flow filtration techniques used for sampling marine colloids: overview and organic carbon results. Marine Chemistry. 55(1-2):1-31

Buesseler K.O. (1998)a The decoupling of production and particulate export in the surface ocean. Global Biogeochemical Cycles. 12(2)297-310.

Buesseler K, L. Ball, J. Andrews, C. Benitez-Nelson, R. Belastock, F. Chai and Y. Chao (1998)b Upper ocean export of POC in the Arabian Sea derived from Th-234. Deep-Sea Research II – Topical Studies in Oceanography. 45(10-11):2461-2487

Burdige, D.J., M.J. Alpering, J. Homstead and C.S. Martens (1992) The role of benthic fluxes of DOC in oceanic and sedimentary carbon cycling. Geophysical Research Letters. 19(18):1851-1854

Burdige, D.J. and J. Homstead (1994) Fluxes of DOC from Chesapeake Bay sediments. Geochimica et Cosmochimica Acta. 58(16)3407-3424

Burdige, D.J. and K.G. Gardner (1998) Molecular weight distribution of DOC in marine sediment pore waters. Marine Chemistry. 62:45-64

Bushaw, K.L., R.G. Zepp, M.A.Tarr, D.Schulz-Jander, R.A. Bourbonniere, R.E. Hodson, W.L.Miller, D.A. Bronk, M.A. Moran (1996) Photochemical release of biologically available nitrogen from aquatic DOM. Nature 381:404-407

Carlson C.A., M.L. Brann, T.H. Mague and L.M. Mayer (1985) Molecular weight distribution of DOM in seawater determined by ultrafiltration: A reexamination. Marine Chemistry. 16:155-171

Carlson, C.A., H.W. Ducklow, and A.F. Michaels (1994) Annual flux of DOC from the euphotic zone in the northwestern Sargasso Sea. Nature. 371(6496)405-408

Carlson C.A. and H.W. Ducklow (1995) DOC in the upper ocean of the central equatorial Pacific Ocean. Deep Sea Research II – Topical Studies in Oceanography. 42:639-656

Carlson C.A. and H.W. Ducklow (1996) Growth of bacterioplankton and consumption of dissolved organic carbon in the Sargasso Sea. Aquatic Microbial Ecology. 10(1):69-85

Caron D.A., E.L. Lim, R.W. Sanders, M.R. Dennett and U.G. Berninger (2000) Responses of bacterioplankton and phytoplankton to organic carbon and inorganic nutrient additions in contrasting oceanic ecosystems. Aquatic Microbial Ecology. 22(2):175-184

Castro, C.G., F.F. Perez, X.A. Alvarez-Salgado, G. Roson and A. F. Rios (1994) Hydrographic conditions associated with the relaxation of an upwelling event off the Galician coast (NW Spain). Journal of Geophysical Research. 99(C3):5135-5147

Castro C.G, X.A. Alvarez-Salgado, F.G. Figueiras, F.F. Perez and F. Fraga (1997) Transient hydrographic and chemical conditions affecting microplankton populations in the coastal

transition zone of the Iberian upwelling system (NW Spain) in September 1986. Journal of Marine Research. 55(2):321-352

Cauwet, G. (1994) HTCO method for dissolved organic carbon analysis in seawater: influence of catalyst on blank estimation. Marine Chemistry. 47: 55-64

Cauwet, G. (1999) Determination of dissolved organic carbon and nitrogen by high temperature combustion. In: *Methods of Seawater Analysis.3rd ed.* Grasshoff K., Kremling, K., Ehrhardt, M., (eds) Wiley-VCH pp.407-420

Chavez F.P. and J.R. Toggweiler (1995) Physical estimates of global new production: the upwelling contribution. In: Upwelling in the Ocean: Modern Processes and ancient records. Summerhayes C.P., K.-C. Emeis, M.V. Angel, R.L. Smith and B. Zeitzschel, eds. Wiley, Chichester, pp.313-320.

Chen, W. and P.J. Wangersky (1996a) Production of DOC in phytoplankton cultures as measured by HTCO and UV photo-oxidation methods. Journal of Plankton Research. 18(7)1201-1211

Chen, W. and P.J. Wangersky (1996b) Rates of microbial degradation of DOC from phytoplankton cultures. Journal of Plankton Research.18(9)1521-1533

Chen R.F., B. Fry, C.S. Hopkinson, D.J. Repeta, E.T. Peltzer (1996c) DOC on Georges Bank. Continental Shelf Research. 16: 409-420

Chen R.F. (1999) In situ fluorescence measurements in coastal waters. Organic Geochemistry 30(6):397-409

Cherrier J., J. Bauer and E.R.M. Druffel (1996) The utilization and turnover of labile DOM by bacterial heterotrophs in eastern North Pacific waters. Marine Ecology Progress Series. 139:267-279

Chester, R. (1990) *Marine Geochemistry.* Chapman & Hall. London. 698pp.

Chin, W.C., M.V. Orellana and P. Verdugo (1998) Spontaneous assembly of marine DOM into polymer gels. Nature. 391(6667):568-572

Clark, L.L., E.D. Ingall and R. Benner (1998) Marine phosphorus is selectively remineralized. Nature. 393(6684):426

Copin-Montegut G. and B. Avril (1993) Vertical distribution and temporal variation of dissolved organic carbon in the North-Western Mediterranean Sea. Deep-Sea Research I. 40(10):1963-1972

Cottrell M.T. and D.L. Kirchman (2000) Natural assemblages of marine proteobacteria and members of the Cytophaga-Flavobacter cluster consuming low- and high-molecular-weight DOM. Applied and Environmental Microbiology. 66(4):1692-1697

Dai, M.H., K.O. Buesseler, P. Ripple, J. Andrews, R.A. Belastock, O. Gustaffson, and S.B. Moran. (1998) Evaluation of two CF ultrafiltration membranes for isolating marine organic colloids. Marine Chemistry. 62:117-136

Dafner E.V., R. Sempere, N. Gonzalez, F. Gomez and M. Goutx (1999) Cross-slope variations of dissolved organic carbon in the Gulf of Cadiz, NE Atlantic Ocean (February 1998) Marine Ecology Progress Series. 189:301-306

Dafner E.V., R. Sempere and H.L. Bryden (2001) TOC distribution and budget through the Strait of Gibraltar in April 1998. Marine Chemistry. 73:233-252

de Haas H., W. Boer, T.C.E. van Weering (1997) Recent sedimentation and organic carbon burial in a shelf sea: the North Sea. Marine Geology. 144(1-3):131-146

Dehairs F, N. Fagel, A.N. Antia, R. Peinert, M. Elskens and L. Goeyens (2000) Export production in the Bay of Biscay as estimated form barium-barite in settling material: a comparison with new production. Deep-Sea Research I – Oceanographic Research Papers. 47(4):583-601

Doetsch R.N. and T.M. Cook (1973). *Introduction to Bacteria and Their Ecobiology*. University Park Press. pp 371

Doval, M.D., X.A. Alvarez-Salgado, and F.F. Perez (1997) Dissolved organic matter in a temperate embayment affected by coastal upwelling. Marine Ecology Progress Series. 157: 21-37

Doval, M. D., et al., (1998) Spatio-temporal variability of the thermohaline and biogeochemical properties and DOC in a coastal embayment affected by upwelling: the Ria de Vigo (NW Spain). Journal of Marine Systems. 14: 135-150

Doval M.D., F.F. Perez and E. Berdalet (1999) Dissolved and particulate organic carbon and nitrogen in the Northwestern Mediterranean. Deep Sea Res. Part I – Oceanographic Research Papers 46(3):511-527

Duce, R.A. and E.K. Duursma (1977) Inputs of organic matter to the ocean Marine Chemistry. 5: 319-339

Erhardt, M. (1977) Organic substances in seawater. Marine Chemistry. 5: 307-316

Ertel J.R., J.I. Hedges, A.H. Devol, J.E. Richey and M. Ribeiro (1986) Dissolved humic substances of the Amazon River system. Limnology and Oceanography 31: 739-754.

Fernandez E., E. Maranon, J. Cabal, F. Alvarez and R. Anadon (1995) Vertical particle-flux in outer shelf waters of the southern Bay of Biscay in summer 1993. Oceanologica Acta 18(3)379-384.

Fitzwater, S.F. and J.H. Martin (1993) Notes on the JGOFS North Atlantic Bloom Experiment-dissolved organic carbon intercomparison. Marine Chemistry. 41 : 179-185

Forsgren G., M. Jansson and P. Nilsson (1996) Aggregation and sedimentation of iron, phosphorus and organic carbon in experimental mixtures of freshwater and estuarine water. Estuarine Coastal & Shelf Science. 43(2):259-268

Frouin, R., A.F.G. Fiuza, I. Ambar and T. J. Boyd (1990) Observations of a Poleward Surface Current off the Coasts of Portugal and Spain During Winter. Journal of Geophysical Research. 95 (C1):679-691

Fry, B., S. Saupe, M. Hullar, and B.J. Peterson (1993). Platinum-catalyzed combustion of DOC in sealed tubes for stable isotopic analysis. Marine Chemistry. 41:187-193

Fry, B. et al., (1996) Analysis of marine DOC using a dry combustion method Marine Chemistry. 54(3-4):191-201

Fuhrman J. (1999) Marine viruses and their biogeochemical and ecological effects. Nature. 399:541-548

Fuhrman J. (2000) Impact of viruses on bacterial processes. In: *Microbial Ecology of the Oceans* Ed. D.L. Kirchman. Wiley-Liss, Inc. pg.327

Guo, L.D., P.H. Santschi and K.W. Warnken (1995) Dynamics of DOC in oceanic environments. Limnology and Oceanography. 40(8): 1392-1403

Guo L.D. and P.H. Santschi (1997) Composition and cycling of colloids in marine environments. Reviews of Geophysics. 35(1):17-40

Hagstrom A., F. Azam, A. Andersson, J. Wikner, F. Rassoulzadegan (1988) Microbial loop in an oligotrophic pelagic marine ecosystem: possible roles of cyanobacteria and nanoflagellates in the organic fluxes. Marine Ecology Progress Series.49:171-178

Hall I.R., S. Schmidt, I.N. McCave and J.L. Reyss (2000) Particulate matter distribution and Th-234/U-238 dis-equilibrium along the Northern Iberian Margin: implications for POC export. Deep-Sea Research I – Oceanographic Research Papers 47(4):557-582

Hansell D.A. (1993) Results and observations from the measurement of DOC and DON in seawater using a HTCO technique. Marine Chemistry. 41:195-202

Hansell, D.A., N.R. Bates, and K. Gundersen (1995) Mineralization of dissolved organic carbon in the Sargasso Sea. Marine Chemistry. 51:201-212

Haynes R and E.D. Barton (1990) A poleward flow along the Atlantic coast of the Iberian peninsula. Journal of Geophysical Research – Oceans. 96(C7):11425-11441

Haynes, R., E.D. Barton, and I. Pilling. (1993). Development, Persistence, and Variability of Upwelling Filaments off the Atlantic Coast of the Iberian Peninsula. Journal of Geophysical Research. 98(C12):22681-22692.

Hedges, J.I. (1987) Organic matter in seawater. Nature. 330:205-206

Hedges, J.I. (1992). Global biogeochemical cycles: progress and problems. Marine Chemistry. 39:67-93

Hedges, J.I., B.A. Bergamaschi, and R. Benner (1993) Comparative analyses of DOC and DON in natural waters. Marine Chemistry. 41:1-3(121-134)

Hedges, J.I. and Farrington. (1993) Measurement of dissolved organic carbon and nitrogen in natural waters. Marine Chemistry.41:5-10

Hedges J.I., J.A. Baldock, Y. Gellnas, C. Lee, M. Peterson and S.G. Wakeham (2001) Evidence for non-selective preservation of organic matter in sinking marine particles. Nature. 409(6822):801-804

Hinrichsen, H, M. Rhein, R.H. Kase and W. Zenk (1993) The Mediterranean Water Tongue and Its Chlorofluoromethane Signal in the Iberian Basin in Early Summer 1989 Journal of Geophysical Research. 98(C5): 8405-8412

Hobbie J.E. and P.J. leB. Williams eds. (1984) *Heterotrophic activity in the Sea.* NATO Conference Series IV, Marine Sciences; v.15 Plenum Press, NY.

Holcombe B.L., R.G. Keil and A.H. Devol (2001) Determination of pore-water DOC fluxes from Mexican margin sediments. Limnology and Oceanography 46(2):298-308

Hopkinson C.S. and L. Cifuentes (1993) DON subgroup report. Marine Chemistry 41:23-36

Hopkinson, C.S., B. Fry and A.L. Nolin (1997) Stoichiometry of DOM dynamics on the continental shelf of the northeastern U.S.A. Continental Shelf Research. 17(5): 473-489

Hulth S., A. Tengberg, A. Laden and P.O.J. Hall (1997) Mineralization and burial of organic carbon in sediments of the southern Weddell Sea (Antarctica). Deep Sea Research I – Oceanographic Research Papers. 44(6):955-981

Huthnance J.M., H.M. van Aken, M. White, E.D. Barton, B. LeCann, E.F. Coelho, E.A. Fanjul, P. Miller and J. Vitorino (in press) Ocean Margin Exchange – Water Flux Estimates. Journal of Marine Systems.

Jeandel C., K. Tachikawa, A. Bory and F. Dehairs (2000) Biogenic barium in suspended and trapped material as a tracer of export production in the tropical NE Atlantic (EUMELI sites). Marine Chemistry. 71(1-2)125-142

Johnson M.D. and A.K. Ward (1997) Influence of phagotrophic protistan bacterivory in determining the fate of DOM in a wetland microbial food web. Microbial Ecology. 33(2):149-162

Joint Global Ocean Flux Study (JGOFS) (1994) Protocols manual. 210pp.

Joint I., M. Inall, R. Torres, F.G. Figueiras, X.A. Alvarez-Salgado, A.P. Rees and E.M.S. Woodward (2001) Two Lagrangian experiments in the Iberian upwelling system: tracking an upwelling event and an offshore filament. Progress in Oceanography. 51:221-248

Joint I. and P. Wassman (2001) Lagrangian studies of the Iberian uwelling system - an introduction. A study of the temporal evolution of surface production and fate of organic matter during upwelling on and off the NW Spanish continental margin. Progress in Oceanography. 51: 217-220

Kahler P. and W. Koeve (2001) Marine DOM: can its C:N ratio explain carbon over-consumption? Deep-Sea Research I – Oceanographic Research Papers. 48(1):49-62

Keil R.G. and D.L. Kirchman (1994) Abiotic transformation of labile protein to refractory protein in sea-water. Marine Chemistry. 45(3)187-196

Kepkay, P.E. and B.D. Johnson (1989) Coagulation on bubbles allows microbial respiration of oceanic DOC . Nature. 338(6210)63-65

Kepkay, P.E. and M.L. Wells, (1992) DOC in North Atlantic surface waters. Marine Ecological Progress Series. 80: 275-283

Kepkay, P.E., S.E.H. Niven and J.F. Jellett (1997) Colloidal organic carbon and phytoplankton speciation during a coastal bloom. Journal of Plankton Research. 19(3)369-389

Kieber, R.J., L.H. Hydro, and P.J. Seaton (1997) Photo-oxidation of triglycerides and fatty acids in seawater: implication toward the formation of marine humic substances. Limnology and Oceanography. 42(6) 1454-1462

Kiorboe T. and G.A. Jackson (2001) Marine snow, organic solute plumes and optimal chemo-sensory behavior of bacteria. Limnology and Oceanography. 46(6):1309-1318.

Kirchman, D.L., Y. Suzuki, C. Garside and H.W. Ducklow (1991) High turnover rates of DOC during a spring phytoplankton bloom. Nature. 352: 612-614

Kirchman D.L. and J. H. Rich (1997) Regulation of bacterial growth rates by DOC and temperature in the Equatorial Pacific Ocean. Microbial Ecology. 33:11-20

Kirchman D.L. and P.J. leB. Williams (2000) Introduction. In: *Microbial Ecology of the Oceans* Ed. D.L. Kirchman. Wiley-Liss, Inc. pg.8

Koike I.S., S. Hara, K. Terauchi and K. Kogue (1990) Role of sub-micron particles in the ocean. Nature. 345:242-244.

Kortzinger A, W. Koeve, P. Kahler and L. Mintrop (2001) C:N ratios in the mixed layer during the productive season in the NE Atlantic Ocean. Deep-Sea Research I – Oceanographic Research Papers. 48(3):661-688

Kuznetsova M. and C. Lee (2001) Enhanced extra-cellular enzymatic peptide hydrolysis in the sea-surface micro-layer. Marine Chemistry. 73:319-332

Lalli C.M. and T. R. Parsons (1993). Biological Oceanography: An Introduction. Butterworth-Heinemann Ltd., Oxford. 301pp.

Lara, R.J. and D.N. Thomas (1995) Formation of recalcitrant OM: Humification dynamics of algal derived DOC and its hydrophobic fractions. Marine Chemistry.51(3)193-199

Lebaron P., P. Servais, M. Troussellier, C. Courties, G. Muyzer, L. Bernard, H. Schafer, R. Pukall, E. Stackebrandt, T. Guindulain, and J. Vives-Rego (2001) Microbial community dynamics in Mediterranean nutrient-enriched seawater mesocosms: changes in abundances, activity and composition. FEMS Microbiology Ecology. 34(3):255-266

Lee, C. and Wakeham, S.G. (1992) Organic matter in the water column: future research challenges Marine Chemistry. 39:95-118

Lee, C. and S.M. Henrichs (1993) How the nature of DOM might affect the analysis of DOC. Marine Chemistry. 41:105-120

Libes, S.M. (1992) An Introduction to Marine Biogeochemistry. John Wiley & Sons, Inc.

Liss P.S., G. Billen, R.A. Duce, V.V. Gordeev, J.-M. Martin, I.N. McCave, J. Meincke, J.D. Milliman, M.-A. Sicre, A. Spitzy and H.L. Windom. (1991) Group Report: What Regulates Boundary Fluxes at Ocean Margins? In: Ocean margin processes in global change: report of the Dahlem Workshop on Ocean Margin Processes in Global Change, Berlin, 1990. R.F.C. Mantoura, J.-M. Martin and R. Wollast eds. John Wiley & Sons Ltd. pg. 111

Liss P.S., R.A. Duce (1997) Eds. *The Sea Surface and Global Change*. Cambridge Univ. Press., Oxford. 362pp.

Longhurst A., S. Sathyendranath, T. Platt and C. Caverhill (1995) An estimate of global primary production in the ocean from satellite radiometer data. Journal of Plankton Research. 17(6):1245-1271

Malinsky-Rushansky N.Z. and C. Legrand (1996) Excretion of DOC by phytoplankton of different sizes and subsequent bacterial uptake. Marine Ecology Progress Series. 132(1-3):249-255

Mantoura R.F.C., J.-M. Martin and R. Wollast (1991) Introduction In: *Ocean margin processes in global change: report of the Dahlem Workshop on Ocean Margin Processes in Global Change*, Berlin, 1990. R.F.C. Mantoura, J.-M. Martin and R. Wollast eds. John Wiley & Sons Ltd. pg.1

Mari X. and A. Burd (1998) Seasonal size spectra of transparent exopolymeric particles (TEP) in a coastal sea and comparison with those predicted using coagulation theory. Marine Ecology Progress Series. 163:63-76

Martin, J.H. and S.E. Fitzwater (1992) DOC in the Atlantic Southern and Pacific Oceans. Nature. 356:699-700

McCarthy, M., J.I. Hedges, and R. Benner (1996) Major biochemical composition of dissolved high molecular weight organic matter in seawater. Marine Chemistry. 55: 281-297

McCarthy, M., T. Pratum, J. Hedges, and R. Benner. (1997). Chemical composition of dissolved organic nitrogen in the ocean. Nature. 390:150-154

McCave I. N., I. R. Hall, A. N. Antia, L. Chou, F. Dehairs, R. S. Lampitt, L. Thomsen, T. C. E. van Weering and R. Wollast (2001) Distribution, composition and flux of particulate material over the European margin at 47°-50° Deep Sea Research II – Topical Studies in Oceanography. 48(14-15):3107-3139

Meybeck M. (1982) Carbon, nitrogen and phosphorus transport by world rivers. American Journal of Science 282:401-450.

Meyers-Schulte K.J. and J.I. Hedges (1986) Molecular evidence for a terrestrial component of organic matter dissolved in ocean water. Nature. 321:61-63

Miller, A.E.J. (1996) A reassessment of the determination of dissolved organic carbon in natural waters using HTCO. Thesis, University of Liverpool.

Miller, A.E.J., Alvarez-Salgado, X.A. and Mantoura, R.F.C. (1997) EU MAST OMEX grant no. MAS3-CT-96-0056 - Final Report: Determinations of dissolved organic carbon and nitrogen fluxes across the Goban Spur using a novel high temperature catalytic oxidation technique, July, 1997, 13 pp.

Miller, A.E.J. (1998) OMEX II-II Cruise Report: R.R.S. Charles Darwin Cruise CD110B - Iberian Shelf Seas 5th - 19th January, 1998. PML Publications. 61pp.

Miller J.C., and J.N. Miller. (1993) *Statistics for Analytical Chemistry*. 2nd ed. Ellis Horwood Limited., 227 pp.

Miller, W.L. and M.A. Moran (1997) Interaction of photochemical and microbial processes in the degradation of refractory DOM from a coastal marine environment. Limnology and Oceanography. 42(6)1317-1324

Mitra S., T.S. Bianchi, L.D. Guo and P.H. Santschi (2000) Terrestrially derived dissolved organic matter in the Chesapeake Bay and the Middle Atlantic Blight. Geochimica et Cosmochimica Acta. 64(20): 3547-3557

Moller E.F. and T.G. Nielsen (2000) Plankton community structure and carbon cycling off the western coast of Greenland with emphasis on sources of DOM for the bacterial community. Aquatic Microbial Ecology 22(1):13-25

Mopper K., X. Zhou, R.J. Kieber, D.J. Kieber, R.J. Sikorski and R.D. Jones (1991) Photochemical degradation of DOC and its impact on the oceanic carbon cycle. Nature. 353:60-62

Mopper K. and C.A. Schultz (1993) Fluorescence as a possible tool for studying the nature and water column distribution of DOC components Marine Chemistry 41 (1-3): 229-238

Mopper K., Z. Feng, S.B. Bentjen and R.F. Chen (1996) Effects of cross-flow filtration on the absorption and fluorescence properties of seawater. Marine Chemistry 55:53-74

Mopper K. and J. Qian (1998). Organic carbon, Analysis methods for aqueous samples. *In:* Encyclopedia of Environmental Analysis and Remediation. R.A. Meyers (Ed.) John Wiley and Sons, Inc.

Moran S.B., K.M. Ellis and J.N. Smith (1997) Th-234/U-238 dis-equilibrium in the central Arctic Ocean: implications for POC export. Deep-Sea Res. II – Topical Studies in Oceanography. 44(8)1593-1606

Moran, M.A. and Zepp, R.G. (1997) Role of photo-reactions in the formation of biologically labile compounds from dissolved organic matter. Limnology and Oceanography. 42(6)1307-1316

Moran, S.B., M.A. Charette, S.M. Pike and C.A. Wicklund (1999) Differences in seawater particulate organic carbon concentration in samples collected using small- and large-volume methods: the importance of DOC adsorption to the filter blank. Marine Chemistry 67:33-42

Moran S.B. and R.G. Zepp (2000) UV radiation effects on microbes and microbial processes. In: *Microbial Ecology of the Oceans* Ed. D.L. Kirchman. Wiley-Liss, Inc. pg.201

Nagata T. and D.L. Kirchman (1996) Bacterial degradation of protein adsorbed to model submicron particles in seawater. Marine Ecology Progress Series. 132:241-248

Nagata T. (2000) Production mechanisms of DOM. In: *Microbial Ecology of the Oceans* Ed. D.L. Kirchman. Wiley-Liss, Inc. pg.121

Noji T.T., K.Y. Borsheim, F. Rey and R. Nortvedt (1999) DOC associated with sinking particles can be crucial for estimates of vertical carbon flux. SARSIA 84(2): 129-135.

Norrman, B (1993) Filtration of water samples for DOC studies. Marine Chemistry. 41 239-242

Norrman B., U.L. Zweifel, C.S. Hopkinson and B. Fry (1995) Production and utilisation of DOC during an experimental diatom bloom. Limnology and Oceanography. 40(5):898-907

Obernosterer I. and G. Herndl (1995). Phytoplankton extra-cellular release and bacterial-growth-dependence on the inorganic N-P ratio. Marine Ecology Progress Series. 116(1-3):247-257

Ogawa, H. and Ogura, N. (1992) Comparison of two methods for measuring DOC in seawater. NATURE 356:696-698

Ogawa H., R. Fukuda and I. Koike (1999) Vertical distributions of DOC and nitrogen in the Southern Ocean. Deep Sea Res. Part I – Oceanographic Res. Papers. 46(10):1809-1826

Ogawa H, Amagai Y, Koike I, Kaiser K, Benner R (2001) Production of refractory dissolved organic matter by bacteria. Science. 292 (5518): 917-920

Ogura, N (1977) High molecular weight organic matter in seawater Marine Chemistry. 5:535-549

Otsuki A., J.C. Park, T. Fukushima, M. Aizaki and D.S. Kong (2000) Effect of omnivorous fish on the production of labile and refractory DOC by zooplankton excretion in a simulated eutrophic lake. Water Research 34(1): 230-238

Passow U., A.L. Alldredge and B.E. Logan (1994) The role of particulate carbohydrate exudates in the flocculation of diatom blooms. Deep Sea-Res. I – Oceanographic Papers. 41(2):335-357

Peltzer, E.T. and Brewer (1993) Some practical aspects of measuring DOC-sampling artifacts and analytical problems with marine samples. Marine Chemistry. 41:243-252

Piskaln C.H., J.B. Paduan, F.P. Chavez, R.Y. Anderson and W.M. Berelson (1996) Carbon export and regeneration in the coastal upwelling system of Monterey Bay, central California. Journal of Marine Research. 54(6)1149-1178

Pomeroy L.R., J.E. Sheldon, W.M.J. Sheldon and F. Peters (1995) Limits to growth and respiration of bacterioplankton in the Gulf of Mexico. Marine Ecology Progress Series.117:259-268

Qian J. and K. Mopper (1996) Automated high-performance HTC TOC Analyzer. Analytical Chemistry 68(18)3090-3097

Redfield A.C., B.H. Ketchum, and F.A. Richards (1963) The influence of organisms on the composition of seawater. In: The Sea vol.2, M.N. Hill (ed). Interscience Publishers, New York, 26-77pp.

Richards F.A. (1984) Nutrient interactions and Microbes *In*: Heterotrophic activity in the Sea. Hobbie J.E. and P.J. leB. Williams eds. NATO Conference Series IV, Marine Sciences; v.15 Plenum Press, NY p.292.

Richardson P.L. and K. Mooney (1975) The Mediterranean outflow – A simple advection – diffusion model. Journal of Physical Oceanography. 5: 476-482

Ridal, J.J. and R.M. Moore (1993) Resistance to UV and persulphate oxidation of DOC produced by selected marine phytoplankton. Marine Chemistry 42(3-4)167-188

Robards K., I.D. McKelvie, R.L. Benson, P.J. Worsfold, N.J. Blundell, and H. Casey (1994) Determination of carbon, phosphorus, nitrogen, and silicon species in waters. Analytica Chimica Acta. 287 (3): 147-190

Roson, G., F.F. Perez, X.A. Alvarez-Salgado and F.G. Figueiras (1995) Variation of Both Thermohaline and Chemical Properties in an Estuarine Upwelling Ecosystem: Ria de Arousa I. Time evolution. Estuarine, Coastal and Shelf Science (41) 195-213

Roson G., X.A. Alvarez-Salgado and F.F. Perez (1997) A non-stationary box model to determine residual fluxes in a partially mixed estuary, based on both thermohaline properties: Application to the Ria de Arousa (NW Spain). Estuarine, Coastal and Shelf Science. 44(3):249-262

Schluter M., E.J. Sauter, A. Schafer and W. Ritzrau (2000) Spatial budget of organic carbon flux to the seafloor of the northern North Atlantic (60°N – 80°N). Global Biogeochemical Cycles 14 (1):329-340.

Schminke H. -U. and G. Graf (2000) DECOS/OMEX II, Cruise No. 43, 25 November 1998-14 January 1999. METEOR-Berichte, Universitat Hamburg, 00-2, 99p.

Scott F.J., A.T. Davidson, and H.J. Marchant (2000) Seasonal variation in plankton, submicrometre particles and size-fractionated dissolved organic carbon in Antarctic coastal waters. Polar Biology. 23 (9): 635-643

Shaffer G. (1996) Biogeochemical cycling in the global ocean 2. New production, Redfield ratios, and remineralization in the organic pump. Journal of Geophysical Research. 101(C2)3723-3745

Sharp, J. H. (1991) Review of Carbon, Nitrogen and Phosphorus Biogeochemistry. Review of Geophysics (Supplement): 648- 657

Sharp, J.H., (1993) Procedures subgroup report. Marine Chemistry. 41:37-49

Sharp, J.H., R. Benner, L. Bennett, C.A. Carlson, S.E. Fitzwater, E.T. Peltzer, and L.M. Tupas (1995) Analyses of dissolved organic carbon in seawater: the JGOFS EqPac methods comparison. Marine Chemistry. 48: 91-108.

Sharp, J.H., R. Benner, L. Bennett, C.A. Carlson, R. Dow, and S.E. Fitzwater (1993) Re-evaluation of HT combustion and chemical oxidation measurements of DOC in seawater. Limnology and Oceanography. 38:1774-1782

Sharp, J.H. (1997) Marine dissolved organic carbon: Are the older values correct? Marine Chemistry. 56: 265-277

Sharp J.H., C.A. Carlson, E.T. Peltzer, D.M. Castle-Ward, K.B. Kavidge, K.R. Rinker (in prep.) Final DOC broad community intercalibration and preliminary use of DOC reference materials.

Sharp J.H., K.R. Rinker, K.B. Savidge, J. Abell, J.Y. Benaim, D. Bronk, D.J. Burdige, G. Cauwet, W. Chen, M.D. Doval, D. Hansell, C. Hopkinson, G. Kattner, N. Kaumeyer, K.J. McGlathery, J. Merriam, N. Morley, K. Nagel, H. Ogawa, C. Pollard, P. Raimbault, R. Sambrotto, S. Seitzinger, G. Spyres, F. Tirendi, T.W. Walsh, C.S. Wong (to be publ.). A preliminary methods comparison for measurement of DON in seawater. Marine Chemistry.

Sherr E. and B. Sherr (2000) Marine Microbes: An Overview. In: *Microbial Ecology of the Oceans*. Ed. D.L. Kirchman. Willey-Liss, Inc. pg.13

Siegenthaler U. and J.L. Sarmiento (1993). Atmospheric carbon dioxide and the ocean. Nature. 365:119-125

Skoog A., D. Thomas, R. Lara, K. Richter (1997) Methodological investigations on DOC determinations by the HTCO method. Marine Chemistry. 56: 39-44

Skoog A., B. Biddanda and R. Benner (1999) Bacterial utilization of dissolved glucose in the upper water of the Gulf of Mexico. Limnology and Oceanography. 44(7):1625-1633

Slagstad D. and P. Wassman (2001) Modelling the 3-D carbon flux across the Iberian margin during the upwelling season in 1998. Progress in Oceanography. 51:467-497

Slawyk G., P. Raimbault and N. Garcia (1998) Measuring gross uptake of N15 labeled nitrogen by marine phytoplankton without particulate matter collection: Evidence of low N15 losses to the DON pool. Limnology and Oceanography. 43(7): 1734-1739

Smith D.C., M. Simon, A.L. Alldredge and F. Azam (1992) Intense hydrolytic enzyme activity on marine aggregates and implications for rapid particle dissolution Nature. 359(6391):139-142.

Smith D.C., G.F. Steward, R.A. Long and F. Azam (1995) Bacterial mediation of carbon fluxes during a diatom bloom in a mesocosm. Deep Sea Research II, 42(1):75-97

Sondergaard M. and M. Middelboe (1995) A cross-system analysis of labile DOC. Marine Ecology Programme Series. 118(1-3):283-294

Sondergaard M., P.J.L. Williams, G. Cauwet, B. Riemann, C. Robinson, S. Terzic, E.M.S. Woodward and J. Worm (2000) Net accumulation and flux of DOC and DON in marine plankton communities. Limnology and Oceanography. 45(5)1097-1111

Spyres G., M. Nimmo, P.J. Worsfold, E.P. Achterberg and A.E.J. Miller (2000) Determination of DOC in seawater using HTCO techniques. trends in analytical chemistry vol.19, no.8. pp.498-506

Steinberg, D.K., C.H. Piskaln, and M.W. Silver (1998) Contribution of zooplankton associated with detritus to sediment trap "swimmer" carbon in Monterey Bay, California USA. Marine Ecology Progress Series. 164:157-166

Steinberg, D.K., C.A. Carlson, N.R. Bates, S.A. Goldthwait, L.P. Madin and A.F. Michaels (2000) Zooplankton vertical migration and the active transport of dissolved organic and inorganic carbon in the Sargasso Sea Deep Sea Research Part I – Oceanographic Research Papers. 47(1):137-158

Stoderegger K.E. and G.J. Herndl (1998) Production and release of bacterial capsular material and its subsequent utilization by marine bacterioplankton. Limnology and Oceanography. 43(5):877-884

Stoderegger K.E. and G.J. Herndl (1999) Production of exopolymer particles by marine bacterioplankton under contrasting turbulence conditions. Marine Ecology Progress Series. 189:9-16

Strom S.L., R. Benner, S. Ziegler and M.J. Dagg (1997) Planktonic grazers are a potentially important source of marine dissolved organic carbon. Limnology and Oceanography. 42(6):1364-1374

Sugimura, Y. and Suzuki, Y. (1988) A HTCO method for the determination of non-volatile DOC in seawater by direct-injection of a liquid sample. Marine Chemistry 24:105-131

Suzuki, Y. and E. Tanoue. (1991) Dissolved Organic Carbon Enigma: Implications for Ocean Margins. In Ocean Margin Processes in Global Change. R.F.C. Mantoura, J.M. Martin and R. Wollast. (eds.) John Wiley and Sons Ltd. 197-209pp.

Suzuki Y, Y. Sugimura and T. Itoh (1985) A catalytic oxidation method for the determination of total nitrogen dissolved in seawater. Marine Chemistry. 16:83-97

Suzuki, Y. (1993) On the measurement of DOC and DON in seawater Marine Chemistry 41:287-288

Tanoue, E. (1992) Vertical distribution of DOC in the North Pacific as determined by the HTCO method. Earth and Planetary Science Letters. 111: 201-216

Tanoue E. (1993) Three vertical profiles of DOC in the North Pacific. Marine Chemistry. 41: 261-264

Teira E., Serret P. and E. Fernandez (2001) Phytoplankton size-structure, particulate and dissolved organic carbon production and oxygen fluxes through microbial communities in the NW Iberian coastal transition zone. Marine Ecology Progress Series. 219: 65-83

Thimsen C.A. and R.G. Keil (1998) Potential interactions between sedimentary DOM and mineral surfaces. Marine Chemistry 62:65-76

Thingstad T.F., A. Hagstrom, and F. Rassoulzadegan (1997) Accumulation of degradable DOC in surface waters: Is it caused by a malfunctioning microbial loop? Limnology and Oceanography. 42(2)398-404

Thingstad T.F., U.L. Zweifel and F. Rassoulzadegan (1998) P-limitation of both phytoplankton and heterotrophic bacteria in NW Mediterranean summer surface waters. Limnology and Oceanography. 43:88-94

Thingstad T.F., H. Havskum, H. Kaas, D. Lefevre, T.G. Nielsen, B. Reimann and P.J.leB. Williams (1999) Bacteria-protist interactions and organic matter degradation under P-limited conditions: Analysis of an enclosure experiment using a simple model. Limnology and Oceanography. 44:62-79

Thingstad T.F., N. Kress, B. Herut, T. Zohary, P. Pitta, S. Psarra, T. Polychronaki, G. Spyres, F. Mantoura, T. Tanaka, F. Rassoulzadegan, and M. Krom (2001) Mixed indications of mineral nutrient limitation in a microcosm experiment using eastern Mediterranean surface water. CIESM 2001 proceedings.

Thomas, C., G. Cauwet and J. Minster (1995) Dissolved organic carbon in the equatorial Atlantic Ocean. Marine Chemistry. 49: 155-169

Thunell R.C., R. Varela, M. Llano, J. Collister, F. Muller-Karger and R. Bohrer (2000) Organic carbon fluxes, degradation, and accumulation in an anoxic basin: Sediment trap results from the Cariaco Basin. Limnology and Oceanography. 45(2): 300-308

Toggweiler, J.R. (1990) Diving into the organic soup. Nature. 345:203-204

Tupas, L.M., B.N. Popp and D.M. Karl (1994) Dissolved organic carbon in oligotrophic waters: experiments on sample preservation, storage and analysis. Marine Chemistry. 45:207-216

Van Aken, H.M. (2000a) The hydrography of the mid-latitude Northeast Atlantic Ocean I. The deep water masses. Deep Sea Research I. 47:757-788

Van Aken, H.M. (2000b) The hydrography of the mid-latitude Northeast Atlantic Ocean II. The intermediate water masses. Deep Sea Research I. 47:789-825

Verardo D.J., P.N. Froelich and A. McIntyre (1990) Determination of organic carbon and nitrogen in marine sediments using the Carlo Erba NA-1500 Analyzer Deep Sea Res. 37:157-165

Verity P.G, T.A. Villareal and T.J. Smayda (1988) Ecological investigations of blooms of colonial Phaeocystis pouchetti – I. Abundance, biochemical composition, and metabolic rates. Journal of Plankton Research. Vol.10 no.2 pp.219-248.

Vetter Y.A., J.W. Deming, P.A. Jumars, and B.B. Krieger-Brockett (1998) A predictive model of bacterial foraging by means of freely released extra-cellular enzymes. Microbial Ecology. 36:75-92

Vodacek A., N.V. Blough, M.D. DeGrandpre, E.T. Peltzer, R.K. Nelson (1997). Seasonal variation of CDOM and DOC in the Middle Atlantic Bight: Terrestrial inputs and photo-oxidation. Limnology and Oceanography. 42(4), 674-686

Wangersky, P.J. (1993) DOC methods: A critical review. Marine Chemistry. 41:61-74

Weinbauer M.G. and M.G. Hofle (1998) Significance of viral lysis and flagellate grazing as factors controlling bacterioplankton production in a eutrophic lake. Applied and Environmental Microbiology. 64(2):431-438

Wells M.L. and E.D. Goldberg (1991) Occurrence of small colloids in seawater Nature. 353(6342):342-344

Wells M.L. (1998) Marine colloids – A neglected dimension. Nature. 391(6667):530-531

Wheeler, P.A., J.M. Watkins, R.L. Hansing (1997) Nutrients, organic carbon and organic nitrogen in the upper water column of Arctic ocean: implications for the sources of DOC. Deep-Sea Research II. 44(8)1571-1592

Whitehead R.F., S. de Mora, S. Demers, M. Gosselin, P. Monfort and B. Mostajir (2000) Interactions of ultraviolet-B radiation, mixing and biological activity on photo-bleaching of natural chromophoric DOM: A mesocosm study. Limnology and Oceanography. 45(2), 278-291.

Wiebinga CJ, and De Baar HJW. (1998) Determination of the distribution of DOC in the Indian sector of the southern ocean. Marine Chemistry. 61(3/4)185-201.

Willey J.D., R.J. Kieber, M.S. Eyman and G.B. Avery (2000) Rainwater DOC: Concentration and global flux. Global Biogeochemical Cycles 14(1):139-148

Williams, P. J. le B. (1995) Evidence for the seasonal accumulation of carbon-rich dissolved organic material, its scale in comparison with changes in particulate material and the consequential effect on net C/N assimilation ratios. Marine Chemistry. 51:17-29

Williams, P.J. le B. (2000) Heterotrophic bacteria and the dynamics of DOM. In: *Microbial Ecology of the Oceans*. Ed. D.L. Kirchman. Willey-Liss, Inc. pg.153

Williams P.M. and E.R.M. Druffel (1987) Radiocarbon in DOM in the central North Pacific ocean. Nature. 330:246-248

Williams P.M., Bauer, JE, Robertson, K.J., Wolgast DM., and Ocelli ML. (1993) Report on DOC and DON measurements made at Scripps Institution of Oceanography, 1988-1991 Marine Chemistry. 41:271-281

Williams S.K.R and R.G. Keil (1997) Monitoring the biological and physical reactivity of dextran carbohydrates in seawater incubations using flow field-flow fractionation. Journal of Liquid Chromatography and Related Technologies. 20(16-17):2815-2833

Winter P.E.D., T.A. Schlacher and D. Baird (1996) Carbon flux between an estuary and the ocean: A case for outwelling. Hydrobiologia. 337(1-3)123-132

Wollast R. (1991) The Coastal Organic Carbon Cycle: Fluxes, Sources and Sinks. In: *Ocean margin processes in global change: report of the Dahlem Workshop on Ocean Margin Processes in Global Change*, Berlin, 1990. R.F.C. Mantoura, J.-M. Martin and R. Wollast eds. John Wiley & Sons Ltd. pg.365

Yamanaka, Y. and E. Tajika (1997) Role of dissolved organic matter in the marine biogeochemical cycle: Studies using an ocean biogeochemical general circulation model. Global Biogeochemical Cycles. 11(4):599-612

Ziegler S. and R. Benner (2000) Effects of solar radiation on DOM cycling in a subtropical sea-grass meadow. Limnology and Oceanography. 45(2): 257-266

Zweifel, U.L., B. Norrman and A. Hagstrom (1993) Consumption of DOC by marine bacteria and demand for inorganic nutrients. Marine Ecology Progress Series. 101(1-2) 23-32

Zweifel, U.L., J. Wikner, A. Hagstrom, E. Lundberg, and B. Norrman (1995) Dynamics of DOC in a coastal ecosystem. Limnology and Oceanography. 40(2) 299-305